# Linking tumour susceptibility ESCRT proteins and epithelial cell polarity

Fish, Laura

*Award date:*
2011

*Awarding institution:*
University of Bath

# LINKING TUMOUR SUSCEPTIBILITY, ESCRT PROTEINS AND EPITHELIAL CELL POLARITY

Laura Pamela Fish

A thesis submitted for the degree of Doctor of Philosophy

University of Bath

Department of Biology and Biochemistry

December 2011

# ABSTRACT

The ESCRT machinery has a well established role within the endocytic pathway. Studies conducted in *Drosophila* have identified ESCRT proteins as important regulators of epithelial cell polarity and growth. Consequently ESCRTs have been classified as potential tumour suppressors. Alterations in the expression of various ESCRT components have been observed in human cancers. However, the possible link between ESCRT proteins, mammalian epithelial cell polarity and tumourigenesis has not been investigated.

This thesis demonstrates for the first time that the ESCRT-I protein, Tsg101, is required for maintenance of mammalian epithelial cell organisation and polarity. siRNA knockdown of Tsg101 in the human Caco-2 cell line results in the formation of a multilayered epithelium with compromised apicobasal polarity. In addition, Tsg101 depletion impairs differentiation of the epithelial sheet and formation of polarised 3D Caco-2 cysts.

Depletion of Tsg101 also results in intracellular accumulation of the tight junction protein, claudin-1. This is shown to be constitutively endocytosed and recycled in Caco-2 epithelial monolayers, suggesting that ESCRT-I is required for claudin-1 recycling to tight junctions. Tsg101 knockdown also impairs epithelial barrier formation and enhances Caco-2 migratory ability. This suggests that tight junction integrity is impaired and may contribute to the loss of Caco-2 cell organisation and polarity observed upon Tsg101 depletion.

Finally, Tsg101 depleted Caco-2 cells appear to overproliferate, forming multilayered regions of the epithelial sheet. However, multilayered cells are eventually eliminated via apoptosis. Preliminary results suggest that inhibition of this apoptotic response enhances the aberrant epithelial phenotype, suggesting that the ability to evade apoptosis may be an important factor in determining the tumourigenic potential of ESCRT-I depletion.

Therefore, results presented in this thesis suggest that the role of ESCRT-I as a tumour suppressor is conserved from *Drosophila* to mammals.

# TABLE OF CONTENTS

# List of Figures

# List of Tables

# List of Publications

**Fish, L**.,* Dukes, J.D.,* Richardson, J.D., Blaikley, E., Burns, S., Caunt, C.J., Chalmers, A.D., and Whitley, P. (2011). Functional ESCRT machinery is required for constitutive recycling of claudin-1 and maintenance of polarity in vertebrate epithelial cells. Mol Biol Cell *22*, 3192-3205.
(*Joint First Authors)

# ACKNOWLEDGEMENTS

First and foremost I would like to thank my supervisors, Dr Andrew Chalmers and Dr Paul Whitley, for giving me the opportunity to carry out this research. I am extremely grateful for all the support and guidance they have given me over the course of my PhD. Most importantly, their never-wavering optimism has encouraged me to battle on and eventually produce a thesis of which I am proud.

To all members past and present of the Chalmers, Whitley, Wood, Holman and Williams labs, thank you for making my PhD experience thoroughly enjoyable. In particular, I would like to express my gratitude to Dr Joseph Dukes for all his help and advice over the years and to Lucy Roche, with whom I have found a lifelong friend.

My thanks go to Dr Will Wood, Prof Geoff Holman, Dr Jim Caunt, Dr David Tosh and Dr Rob Williams for use of their laboratory equipment and reagents as well as many helpful discussions about the project. I am also very grateful to Dr Adrian Rogers for his valuable technical assistance with the confocal microscopy.

Finally, I could not have completed my PhD without the support from all my family and friends. I am lucky to have so many wonderful people in my life who never fail to make me smile. In particular, my sisters and closest friend Clair Thomas, but especially my Mum and Dad, whose strength and determination have been my inspiration. Thank you for your unconditional love and belief in me.

# CHAPTER ONE

# 1. INTRODUCTION

## 1.1. Epithelial Cell Polarity

Epithelial or epithelial-derived cells account for approximately 60% of mammalian cell types. The regulated association of these cells into epithelial sheets serves multiple functions, such as control of tissue architecture and barrier formation (Gibson and Perrimon, 2003; Bryant and Mostov, 2008). Epithelial cells are polarised along their apicobasal axis, which is achieved and maintained by asymmetric distribution of membrane proteins, lipids, the cytoskeleton and various other macromolecules within the cell. This results in the formation of apical and basolateral membrane domains with specific protein and lipid compositions (Figure 1.1) (Bryant and Mostov, 2008). Functionally distinct, apical surfaces are important for processes such as absorption and secretion; lateral membranes form cell-cell contacts with adjacent cells and are important for adhesion and diffusion barriers; and the basal surface contacts the underlying basement membrane and extracellular matrix (ECM). There are three key processes which are important for epithelial cell polarisation. These are formation of cell-cell junctions; asymmetrical distribution of polarity complexes; and interaction of cells with the ECM. These combined cues allow individual epithelial cells to establish polarity and coordinate to form a polarised tissue (Bryant and Mostov, 2008).

### 1.1.1. Epithelial Cell-Cell Junctions

Development and function of polarised epithelial tissues depends in part, on the formation of specialised cell-cell junctions. These form between the lateral membranes of adjacent cells and are composed of various transmembrane and membrane-associated proteins. The epithelial junctional complex is composed of tight junctions, adherens junctions and desmosomes (Figure 1.2). In addition, epithelial cells can also form gap junctions. These intercellular junctions play important roles in epithelial polarisation, cell-cell adhesion, barrier formation and signal transduction (Knust and Bossinger, 2002; Miyoshi and Takai, 2005; Balda and Matter, 2008).

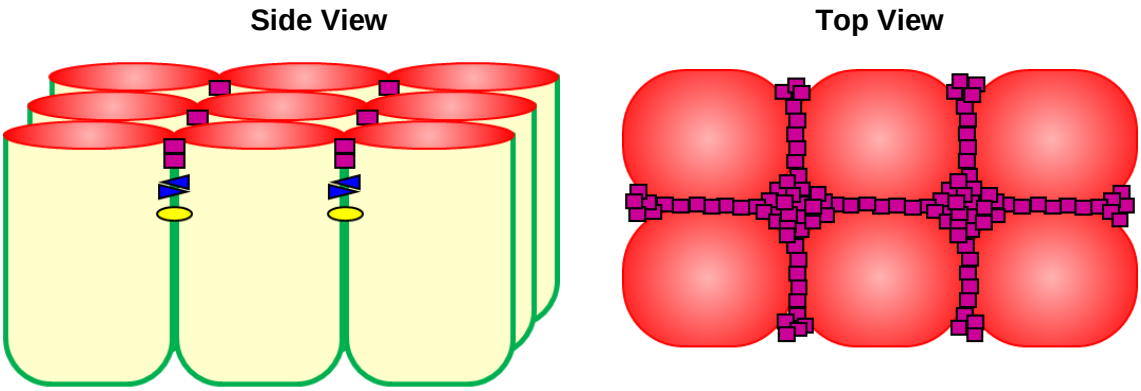


***Figure 1.1* Morphology of polarised epithelial cells.** Most epithelial cells are polarised along their apicobasal axis resulting in distinct apical (red) and basolateral (green) membrane domains. Specialised cell-cell junctions form along lateral membranes of adjacent cells (side view), surrounding the circumference of each cell (top view). These junctions are important to maintain apicobasal polarity, cell-cell adhesion and to control diffusion across the epithelial sheet.

### *Tight Junctions*

Tight junctions (TJs) form at the most apical part of the epithelial lateral membrane and appear as a series of very close membrane contacts between adjacent cells by transmission electron microscopy (Farquhar and Palade, 1963). By freeze-fracture electron microscopy, TJs appear as a continuous network of intramembrane strands that encircle the cells (Staehelin, 1973). TJs define the boundary between the apical and basolateral membrane domains of epithelial cells. Here they serve a fence function to restrict intramembrane diffusion of lipids in the outer leaflet of the plasma membrane (Shin *et al.,* 2006; Matter and Balda, 2007). This is thought to be important to help maintain apicobasal cell polarity although one study has demonstrated that in epithelial cells which mostly lack expression of the cytoplasmic TJ proteins, ZO-1, -2 and -3, apicobasal cell polarity is unperturbed despite a complete lack of TJ formation (Umeda *et al.,* 2006).

TJs also form a barrier to regulate paracellular diffusion across the epithelial sheet, which is crucial for the function of epithelial tissues (Matter and Balda, 2007). This epithelial barrier is semipermeable, allowing selective diffusion of ions and small hydrophilic molecules depending on their charge and size. Paracellular permeability is regulated by various distinct molecular mechanisms.

***Figure 1.2*** **Composition of the epithelial junctional complex.** Polarised epithelial cells form tight junctions (TJs), adherens junctions (AJs) and desmosomes, which collectively form the epithelial junctional complex. TJs are the most apical cell-cell junctions and mark the boundary between the apical (red) and basolateral (green) membrane domains. TJs are composed of three families of transmembrane proteins: claudins, TJ-associated MARVEL protein family (TAMP) occludin, marvelD3 and tricellulin, and JAMs. TJs interact with the actin cytoskeleton via various cytoplasmic adaptor proteins, such as the ZO-1. AJs are localised below TJs and are composed of transmembrane proteins, E-cadherin and nectin, which interact with cytoplasmic adaptor proteins, β-catenin and afadin, respectively. β-catenin binds to α-catenin which interacts with actin. p120-catenin also associates with the cadherin/catenin complex. Afadin binds to actin and can also interact with α-catenin. Lastly desmosomes are composed of transmembrane proteins, desmogleins and desmocollins, which bind to cytoplasmic proteins, plakoglobin and plakophilin. These interact with desmoplakin which associates with intermediate filaments. Epithelial cells also form cell-ECM contacts along the basal membrane (adapted from Miyoshi and Takai, 2005)

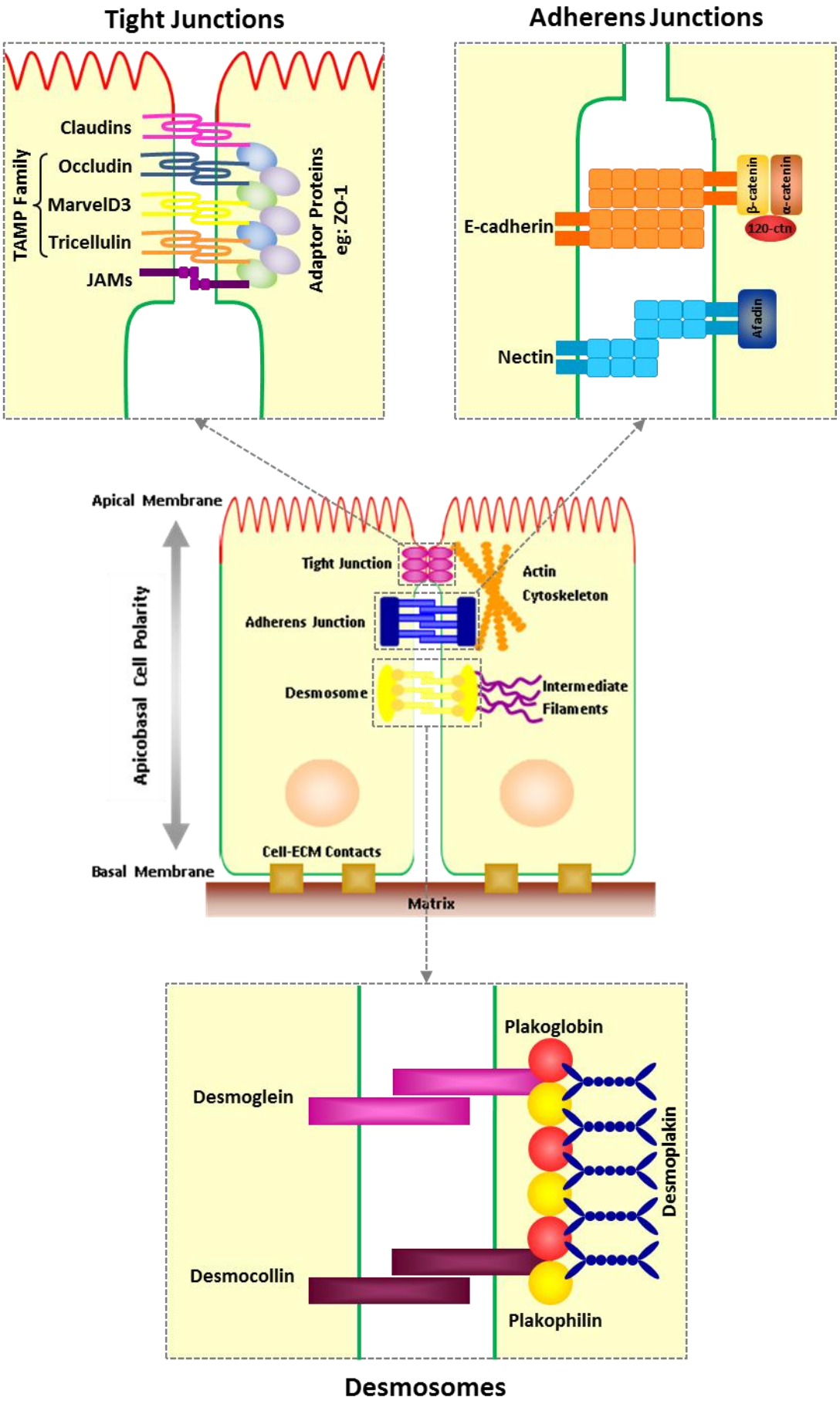
Tight Junctions
Claudins
TAMP Family
Occludin
MarvelD3
Tricellulin
JAMs
Adaptor Proteins
eg: ZO-1
Adherens Junctions
E-cadherin
β-catenin
α-catenin
120-ctn
Nectin
Afadin
Apical Membrane
Apicobasal Cell Polarity
Tight Junction
Actin
Cytoskeleton
Adherens Junction
Desmosome
Intermediate
Filaments
Cell-ECM Contacts
Basal Membrane
Matrix
Plakoglobin
Desmoglein
Desmoplakin
Desmocollin
Plakophilin
Desmosomes

and can differ among epithelia (reviewed in Gonzalez-Mariscal *et al.,* 2008). It is also becoming increasingly apparent that TJs play an important role in establishment of epithelial cell polarity, proliferation, differentiation and gene expression through multiple signalling mechanisms (reviewed in Kohler and Zahraoui, 2005; Shin *et al.,* 2006; Matter and Balda, 2007).

TJs are composed of three main families of transmembrane proteins. Claudins along with the tight junction associated MARVEL (MAL and related proteins for vesicle trafficking and membrane link) protein (TAMP) family, occludin, tricellulin and marvelD3, are all tetraspan transmembrane proteins whereas the junctional adhesion molecules (JAMs) are single-span transmembrane proteins (Shin *et al.,* 2006; Chiba *et al.,* 2008; Balda and Matter, 2008; Mariano *et al.,* 2011).

The claudins, a family of at least 27 proteins, are thought to be the main structural components of the TJ barrier (Mineta *et al.,* 2011). These are expressed in a tissue-specific manner, with most cells expressing at least two claudin family members (Balda and Matter, 2008; Chiba *et al.,* 2008). Various studies have indicated that claudins are important for the barrier function of TJs in epithelial tissues. Furthermore, TJ claudin composition determines the paracellular permeability of an epithelial tissue (reviewed in Van Itallie and Anderson, 2006; Krause *et al.,* 2008). Some claudins are thought to tighten the paracellular barrier, for example a sealing function has been demonstrated for claudin-1 as knockout mice display defective epidermal barrier function and die soon after birth due to transepidermal water loss (Furuse *et al.,* 2002). Similarly, in claudin-5 deficient mice leakage of small tracers across the brain endothelium is observed (Nitta *et al.,* 2003) and claudin-14 knockout is thought to result in deafness due to perturbed barrier function of the inner ear epithelium (Ben-Yosef *et al.,* 2003).

In contrast, other claudins have been shown to increase permeability across the epithelium by forming charge-selective paracellular ion pores (Van Itallie and Anderson, 2006; Krause *et al.,* 2008). For example, claudin-2 overexpression in MDCK cells results in the formation of paracellular cation pores increasing cation permeability across the epithelial sheet (Amasheh *et al.,* 2002). Correlating with this, claudin-2 expression *in vivo* is found in leaky epithelia,

such as proximal renal tubules, where it is required for the cation paracellular permeability properties of the epithelium (Muto *et al.,* 2010).

The TAMP family of TJ transmembrane proteins includes occludin, the first transmembrane TJ protein to be identified (Furuse *et al.,* 1993). However, the function of occludin remains to be fully determined. A role for occludin in the barrier and fence functions of TJs has been demonstrated, for example expression of mutant occludin in MDCK cells increases paracellular flux of small tracers and disrupts polarised distribution of the lipid sphingomyelin to the apical membrane (Balda *et al.,* 1996). In contrast, occludin knockout mice appear to retain normal TJ morphology and barrier formation (Saitou *et al.,* 2000). However, these knockout mice displayed growth retardation and histological abnormalities in various tissues, suggesting that the role of occludin is more complex than TJ barrier formation alone. Indeed occludin has been linked to regulation of various signalling pathways (reviewed in Chiba *et al.,* 2008). Studies have demonstrated that occludin is important for regulation of the actin cytoskeleton in MDCK cells via RhoA signalling (Yu *et al.,* 2005) and inhibition of apoptosis via mitogen-activated protein kinase (MAPK) signalling pathways (Murata *et al.,* 2005). Therefore, further studies will no doubt continue to elucidate mechanisms underlying occludin function in epithelial tissues.

More recently identified components of TJs, tricellulin and marvelD3, also belong to the TAMP family (Ikenouchi *et al.,* 2005; Steed *et al.,* 2009; Raleigh *et al.,* 2010; Mariano *et al.,* 2011). However, similarly to occludin, tricellulin and marvelD3 are unable to form tight junction strands in the absence of claudins (Ikenouchi *et al.,* 2008; Raleigh *et al.,* 2010). Tricellulin is enriched at contacts between three epithelial cells and is thought to play a role in TJ formation as RNAi knockdown impairs epithelial barrier formation (Ikenouchi *et al.,* 2005). However, the only phenotype of mutations in the *tricellulin* gene in humans appears to be deafness (Riazuddin *et al.,* 2006) and therefore, the precise function of tricellulin is still to be elucidated. MarvelD3 has also been shown to colocalise with occludin at TJs (Steed *et al.,* 2009; Raleigh *et al.,* 2010) Although marvelD3 is not required for TJ formation (Steed *et al.,* 2009), studies suggest that this protein is important for permeability properties of epithelial monolayers. However, results from these studies seem to be somewhat

contrasting with one study demonstrating an increase in transepithelial resistance (TER) upon siRNA knockdown of marvelD3 in Caco-2 cells (Steed *et al.,* 2009) whereas a delay in TER development was observed by another study (Raleigh *et al.,* 2010). Therefore, the role of marvelD3 in TJ function remains to be clarified.

Interactions between marvelD3 and both occludin and tricellulin have been observed whereas occludin and tricellulin do not appear to associate directly (Raleigh *et al.,* 2010). It has been suggested that tricellulin and marvelD3 may be able to compensate for occludin loss as siRNA knockdown of occludin in MDCK cells induces redistribution of tricellulin from tricellular to bicellular TJs (Ikenouchi *et al.,* 2008). In addition, increased tricellulin and marvelD3 expression and localisation to TJs have been observed *in vivo* after tumour necrosis factor (TNF) treatment (Raleigh *et al.,* 2010). TNF treatment of mice has previously been shown to disrupt the intestinal epithelial barrier and induce occludin internalisation (Clayburgh *et al.,* 2005). Therefore, the observed increase in expression of tricellulin and marvelD3 may reflect an effort to stabilise the TJ and compensate for occludin loss, although this is not sufficient to restore barrier function (Raleigh *et al.,* 2010). The possibility of overlapping functions of these three TJ proteins may provide an explanation as to why barrier function is not affected in occludin knockout mice (Saitou *et al.,* 2000).

The third transmembrane protein family found at TJs are JAMs. These are members of the immunoglobulin superfamily and are expressed in other cell types as well as epithelial cells, such as leukocytes and endothelial cells (Shin *et al.,* 2006). This means that JAMs can regulate cell-cell adhesion between distinct as well as the same types of cells (Chiba *et al.,* 2008). Four JAMs have been identified: JAM-A, -B, -C and -D and these proteins are thought to be involved in TJ formation and barrier function, although further work is required to understand the role of JAMs in more detail (Shin *et al.,* 2006, Balda and Matter, 2008; Chiba *et al.,* 2008). In addition to JAMs, other types of single-span transmembrane proteins associate with the TJ. These include Crumbs 3 (CRB3), which is important for epithelial polarisation, and blood vessel epicardial substance (Bves), thought to contribute to the establishment and/or maintainence of TJs (Balda and Matter, 2008; Russ *et al.,* 2011).

TJs composition also involves various cytoplasmic adaptor proteins which interact with the intracellular domains of the transmembrane TJ proteins. These cytoplasmic adaptor proteins have key roles in organisation of the transmembrane proteins, attachment to the actin cytoskeleton and initiation of cell signalling (reviewed in Shin *et al.,* 2006). The most studied TJ adaptor protein is zonula occludens (ZO)-1, the first TJ protein to be identified (Stevenson *et al.,* 1986). This is one of three ZO isoforms which belong to the membrane-associated guanylate kinase (MAGUK) family of proteins (Shin *et al.,* 2006). ZO-1 contains several protein-protein interaction domains, allowing it to bind to claudins, ZO-2 or ZO-3, occludin, actin and α-catenin as well as several signalling proteins (Balda and Matter, 2008). ZO proteins play an important role in the assembly and function of TJs, for example simultaneous depletion of ZO-1, -2 and -3 in cultured epithelial cells inhibits claudin polymerisation during TJ formation (Umeda *et al.,* 2006).

Another important cytoplasmic protein which localises to TJs is cingulin (Citi *et al.,* 1989). Cingulin interacts with other TJ proteins, ZO-1, ZO-2, ZO-3 and JAM-A as well as actin and myosin, suggesting that cingulin is important for linking the TJ to the actin cytoskeletan (Cordenonsi *et al.,* 1999; Bazzoni *et al.,* 2000; D'Atri and Citi, 2001; D'Atri *et al.,* 2002). Mutation of cingulin in mouse embryoid bodies does not disrupt TJ formation (Guillemot *et al.,* 2004). This has also been demonstrated in MDCK cells, where depletion of cingulin has no effect on TJ organisation or barrier function (Guillemot and Citi, 2006). However, cingulin disruption results in increased protein and mRNA expression levels of various TJ proteins, including occludin, claudin-2 and ZO-3, suggesting that cingulin plays a role in transcriptional regulation of TJ proteins (Guillemot *et al.,* 2004; Guillemot and Citi, 2006).

Cingulin has also been shown to regulate RhoA signalling, which is important for epithelial proliferation (Aijaz *et al.,* 2005; Guillemot and Citi, 2006). Interaction between cingulin and the RhoA guanine nucleotide exchange factor (GEF) protein, GEF-H1/Lfc, at TJs inactivates GEF-H1/Lfc and therefore, inhibits RhoA signalling (Aijaz *et al.,* 2005). Consistent with this, depletion of cingulin results in increased RhoA activity causing increased cell proliferation and density (Guillemot and Citi, 2006). In addition, RhoA signalling is also

important for TJ assembly and a recent study has identified the RhoA GEF, p114RhoGEF, as an important regulator of RhoA activation specifically at cell-cell junctions (Terry *et al.,* 2011). Interestingly, this study also shows that recruitment of p114RhoGEF to TJs requires cingulin, therefore demonstrating additional roles for this protein in regulation of RhoA signalling and TJ formation.

Epithelial cell proliferation is also regulated by the cytoplasmic TJ protein, ZO-1-associated nucleic acid binding protein (ZONAB), a Y-box transcription factor which is regulated ZO-1 (Balda and Matter, 2000). Overexpression of ZONAB increases epithelial cell proliferation *in vitro* and *in vivo* (Balda *et al.,* 2003; Georgiadis *et al.,* 2010). Proliferation is promoted by nuclear accumulation of ZONAB, resulting in expression of target genes such as ErbB-2 (Balda and Matter, 2000). In addition, ZONAB has been shown to regulate nuclear localisation of cell division kinase (CDK) 4 which is important for G1/S transition (Balda *et al.,* 2003).

***Adherens Junctions***

Localised just below the tight junctions are the adherens junctions (AJs), which form a continuous adhesion belt across the epithelial sheet (reviewed in Niessen and Gottardi, 2008). The key function of AJs is to mediate strong cell-cell adhesion, however, these junctions also have additional important roles and are crucial for establishment of epithelial cell polarity (Nejsum and Nelson, 2007).

AJs are comprised of two basic adhesive units: the cadherin/catenin and nectin/afadin complexes (Niessen and Gottardi, 2008; Coradini *et al.,* 2011). Classic cadherins are type I, single-pass transmembrane glycoproteins which mediate calcium-dependent intercellular adhesion via homophilic binding of their extracellular domains. The cytoplasmic domain of cadherins interact with cytoplasmic adaptor proteins, catenins (Ozawa *et al.,* 1990). This interaction is important for mediating key structural and signalling activities required for adhesion (Miyoshi and Takai, 2005; Niessen and Gottardi, 2008). The primary cadherin expressed in epithelial cells is E-cadherin. This binds to β-catenin, which in turn binds α-catenin, mediating association with the actin cytoskeleton

(Kobielak and Fuchs, 2004). Cadherins also associate with p120 catenin, which seems to play an important role in regulation of cadherin levels and formation of strong, more “compacted” adhesions (Ireton *et al.,* 2002).

Cooperating with the cadherin/catenin complex, the nectin/afadin complex also mediates intercellular adhesion and actin association. Nectins (1-4) are members of the immunoglobulin superfamily of calcium-independent adhesion molecules (Miyoshi and Takai, 2005; Niessen and Gottardi, 2008). Nectins are single-pass transmembrane proteins which can engage in homophilic and heterophilic adhesion with nectins or nectin-like receptors on adjacent cells (Miyoshi and Takai, 2005; Niessen and Gottardi, 2008). Nectins interact with afadin which can bind to the actin cytoskeleton (Takahashi *et al.,* 1999). Afadin can also bind to α-catenin, therefore providing a link between the two adhesive units of AJs (Tachibana *et al.,* 2000).

***Desmosomes***

Desmosomes are the third component of the epithelial junctional complex, together with TJs and AJs (Balda and Matter, 2008). Desmosomes are found below the AJs and function to anchor intermediate filaments (IFs) to sites of strong adhesion, therefore playing a key role in maintenance of epithelial tissue integrity. In addition, desmosomes appear to function in other cellular processes, such as epithelial proliferation and differentiation and are important for epithelial tissue architecture and morphogenesis (reviewed in Yin and Green, 2004; Delva *et al.,* 2009).

Desmosomes consist of single-pass transmembrane glycoproteins of the desmosomal cadherin family, desmogleins (Dsg 1-4) and desmocollins (Dsc 1-3), which mediate calcium-dependent adhesion between adjacent cells via their extracellular domains. The cytoplasmic domains of Dsgs and Dscs bind to the armadillo family proteins, plakoglobin and plakophilins (Witcher *et al.,* 1996; Chen *et al.,* 2002). These proteins associate with desmoplakin, the most abundant component of the desmosome, which anchors the junction to IFs (Kouklis *et al.,* 1994; Yin and Green, 2004; Delva *et al.,* 2009). However, this linear model may be insufficient to describe the complexity of the desmosomal architecture (Yin and Green. 2004). Additional protein-protein interactions have

been observed, for example plakophilin can also bind to plakoglobin and IF proteins, and Dsgs and Dscs can associate with desmoplakin independently of plakoglobin (Smith and Fuchs, 1998; Bonne *et al.,* 2003). These multiple points of contact may result in greater tensile strength of the desmosome (Yin and Green, 2004).

***Gap Junctions***

Epithelial cells can also form a fourth type of intercellular junction called gap junctions. These junctions mediate intercellular signalling and may also contribute to cellular adhesion (reviewed in Nakagawa *et al.,* 2010). Gap junctions are comprised of tens to thousands of intercellular gap junction channels. These allow passage of ions and small molecules up to 1 kDa in size and are gated by multiple mechanisms. Gap junction channels are formed by pairing of two hemichannels on adjacent cells. Each hemichannel is composed of six connexin (Cx) subunits surrounding a central pore and has distinct permeability and selectivity properties.

### 1.1.2. Epithelial Cell-ECM Contacts

In addition to cell-cell contacts, epithelial cells must also form contacts with the ECM to allow complete polarisation of epithelial tissues (Eaton and Simons, 1995; Matlin *et al.,* 2003). The main components of cellular adhesions to the ECM are the cell surface integrin receptors. Integrins are heterodimeric type I transmembrane glycoproteins comprised of α and β chains which, upon binding to ECM ligands such as fibronectin, laminin or collagen, regulate many aspects of cell behaviour (Matlin *et al.,* 2003; Barczyk *et al.,* 2010). In epithelial cells most integrins are β1-containing heterodimers which, together with various other proteins, are important for the formation of focal adhesions, cell-ECM contacts connected to the actin cytoskeleton (Stutzmann *et al.,* 2000; Matlin *et al.,* 2003). Epithelial cells also express the epithelial specific α6β4 integrin. This is found in hemidesmosomes, cell-ECM adhesion sites that associate with intermediate filaments and are important for maintenance of epithelial tissue integrity (Nievers *et al.,* 1999; Stutzmann *et al.,* 2000; Matlin *et al.,* 2003).

Integrin-mediated cell-ECM contacts are important for polarisation of epithelial tissues (Eaton and Simons, 1995; Matlin *et al.,* 2003). This was initially suggested by studies which demonstrated that α6β1 integrin was required for epithelial polarisation and differentiation in the kidney (Klein *et al.,* 1988; Sorokin *et al.,* 1990). Subsequent studies have also shown that orientation of the apicobasal axis in MDCK cells is dependent on $\beta_1$ integrin (Ojakian and Schwimmer, 1994) and polarisation of mammary epithelial cells *in vitro* requires α6β4 integrin (Weaver *et al.,* 2002). Therefore, this demonstrates that orientation of epithelial polarity depends on cell-ECM contacts. It has also been suggested that maintenance of a polarised epithelium may require continued interaction with the ECM to act as a polarising cue along with cell-cell contacts (Bryant and Mostov, 2008).

### 1.1.3. Epithelial Polarity Complexes

Establishment and maintenance of epithelial cell polarity is regulated via three conserved core polarity complexes (Figure 1.3) (Gibson and Perrimon, 2003; Suzuki and Ohno, 2006; Assemat *et al.,* 2008; Bryant and Mostov, 2008). These are the Partitioning-Defective (PAR) complex, the Crumbs (CRB) complex and the Scribble (SCRIB) complex. Originally identified in *Caenorhabditis elegans* and *Drosophila melanogaster*, these complexes have since been identified in vertebrates and are essential for epithelial cell polarity (Assemat *et al.,* 2008).

***The PAR Complex***

The PAR complex consists of two PDZ-domain-containing scaffold proteins, PAR-6 and PAR-3, and an atypical protein kinase C, aPKC. The complex is recruited to the apical membrane where it promotes establishment of apicobasal polarity and development of tight junctions (Suzuki *et al.,* 2001; Suzuki and Ohno, 2006; Assemat *et al.,* 2008; Horikoshi *et al.,* 2009). PAR-6 interacts with aPKC and acts as an adaptor molecule, allowing aPKC to interact with its downstream effectors, such as PAR-3 (Suzuki *et al.,* 2001; Assemat *et al.,* 2008). PAR-3 is thought to localise to sites of forming cell-cell junctions and recruit the aPKC-PAR6 complex. The function of PAR-3 seems to be dependent on its phosphorylation state. This is partially regulated by aPKC, whose kinase

activity is required for the formation of the mature junctional complex (Suzuki *et al.,* 2002; Suzuki and Ohno, 2006; Assemat *et al.,* 2008).

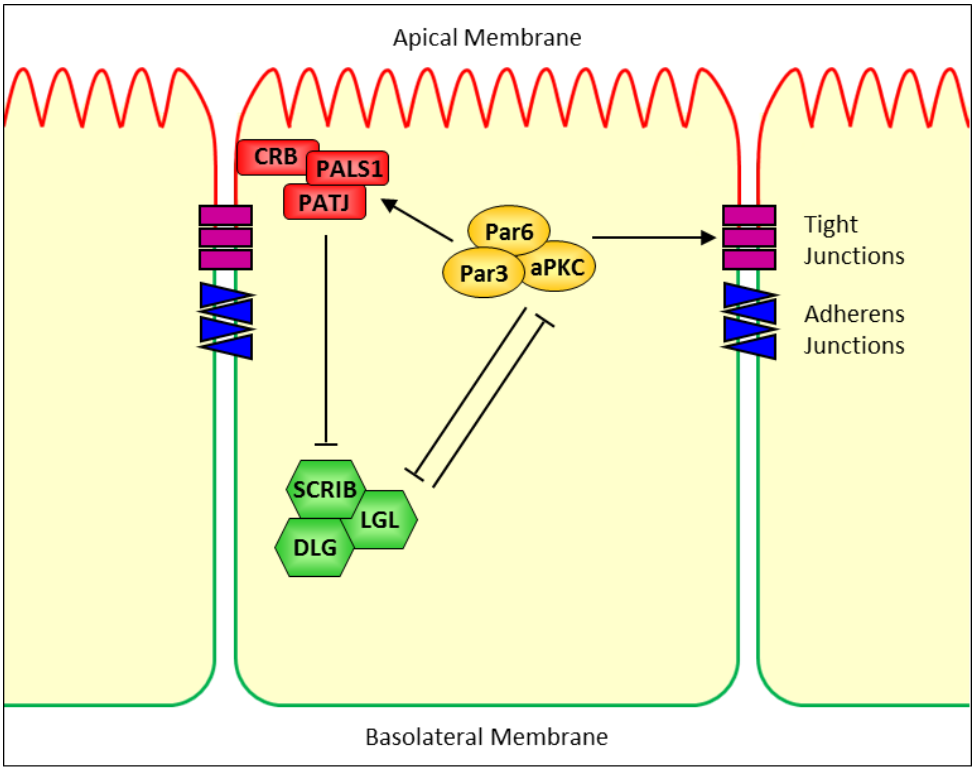


***Figure 1.3* Polarity complexes important for establishment and maintenance of epithelial cell polarity.** Epithelial cell apicobasal polarity is regulated by three core polarity complexes: the PAR complex (Par3/Par6/aPKC; yellow), CRB complex (CRB/PALS1/PATJ; red), and SCRIB complex (SCRIB/LGL/DLG; green). The PAR and CRB complexes localise in the apical region of the cell and promotes formation of the apical membrane (red) and maturation of cell-cell junctions. The SCRIB complex is localised to and maintains the basolateral membrane domain (green). Mutual antagonism between the apical and basolateral polarity complexes ensures maintainance of apicobasal polarity (adapted from Suzuki and Ohno, 2006; Coradini *et al.,* 2011).

### *The CRB Complex*

The CRB complex also localises to the apical membrane and is composed of a transmembrane protein, CRB-3, and two cytoplasmic scaffolding proteins, PALS1 (Proteins Associated with Lin Seven 1) and PATJ (PALS1-Associated Tight Junction protein) (Assemat *et al.,* 2008). CRB-3 and PALS1 directly interact and are important for tight junction formation and epithelial polarity (Roh *et al.,* 2003). In addition, CRB-3 appears to be involved in differentiation of the apical membrane (Assemat *et al.,* 2008). PALS1 also binds to PATJ and is

essential for PATJ expression (Straight *et al.,* 2004). PATJ is important for tight junction formation and polarisation and is thought to stabilise the CRB complex (Shin *et al.,* 2005; Assemat *et al.,* 2008).

### *The SCRIB Complex*

Finally, the SCRIB complex consisting of SCRIB, DLG (Discs Large) and LGL (Lethal Giant Larvae) is basolaterally localised and functions to establish apicobasal polarity by restricting apical membrane identity (Bilder and Perrimon, 2000; Kallay *et al.,* 2006). SCRIB is a large cytoplasmic multidomain protein which is thought to bind to LGL (Kallay *et al.,* 2006). DLG is able to bind to a variety of additional proteins thought to be important for stability of DLG and its distribution to cellular junctions (Assemat *et al.,* 2008).

### *Functional Interactions between Polarity Complexes*

Activities of the three polarity complexes are coordinated in order to establish a polarised epithelium. In addition, further proteins are also implicated within the process of epithelial cell polarisation and interaction with various junctional proteins appears to be important for recruitment and activity of the polarity complexes (reviewed in Suzuki and Ohno, 2006; Assemat *et al.,* 2008). Briefly, during establishment of epithelial cell polarity one of the initial events is the recruitment of PAR-3 to the early junctional complex, thought to be mediated by association with JAMs (Itoh *et al.,* 2001; Rehder *et al.,* 2006). PAR-3 then recruits aPKC-PAR-6. Concurrently, activation of aPKC via phosphorylation must occur. This is thought to be initiated by Cdc42 which is activated upon E-cadherin mediated cell-cell adhesion (Kim, 2000). Active aPKC then phosphorylates PAR-3, resulting in formation of the active PAR complex at the apical junctions. Once phosphorylated, PAR-3 dissociates from aPKC leaving it free to phosphorylate further target proteins and resulting in accumulation of phosphorylated PAR-3 at tight junctions. The CRB complex is then recruited to the apical membrane and evidence suggests that interactions between the PAR and CRB complexes stabilises their localisation to the apical membrane and promotes maturation of cell-cell junctions (Lemmers *et al.,* 2004; Assemat *et al.,* 2008; Krahn *et al.,* 2010).

The SCRIB complex is recruited to the basolateral membrane slightly later and mutual antagonism between this complex and the apical PAR and CRB complexes ensures maintenance of apical and basolateral membrane domain identity (Suzuki and Ohno, 2006). LGL competes with PAR-3 for binding to aPKC–PAR-6, sequestering aPKC–PAR-6 away from PAR-3. Upon aPKC activation, aPKC phosphorylates LGL which then dissociates from aPKC–PAR-6 and can interact with SCRIB and DLG at the lateral membrane. Therefore, aPKC is essential for restricting the SCRIB complex to the basolateral membrane and LGL maintains apical localisation of the active PAR complex (Bilder *et al.,* 2003; Chalmers *et al.,* 2005; Yamanaka *et al.,* 2006; Assemat *et al.,* 2008).

Therefore, establishment and maintenance of epithelial cell polarity is a complex, highly regulated process and ongoing work will continue to elucidate the dynamics of the cell polarity machinery.

## 1.2. Epithelial Cell Polarity and Cancer

Tumour formation and progression is a complex, multi-step process in which tumour cells acquire various physiological alterations including self-sufficiency in growth signalling, insensitivity to growth-inhibitory signals, evasion of apoptosis, and tissue invasion and metastasis (reviewed in Hanahan and Weinberg, 2011). These hallmarks of cancer collectively result in the growth of malignant tumours. Most human cancers originate from epithelial cells and one key step in the process of tumour formation and metastasis is loss of epithelial cell polarity, often termed epithelial-to-mesenchymal transition (EMT) (Yang and Weinberg, 2008). During EMT, epithelial cells lose cell-cell adhesion and progressively redistribute or downregulate apical and basolateral epithelial-specific proteins, acquiring a more mesenchymal phenotype. Consequently cells lose their polarised morphology and are able to migrate from the epithelial sheet, invade the underlying ECM and metastasise to distant sites in the body where they will proliferate and form new tumour cell colonies (Yang and Weinberg, 2008; Coradini *et al.,* 2011). Formation of these metastases accounts for the majority of cancer deaths (Hanahan and Weinberg, 2011; Kopfstein and Christofori, 2006).

Therefore, it is clear that regulation of epithelial cell polarity is crucial to maintain structure and function of epithelial tissues and prevent diseases such as cancer. Indeed, numerous studies have identified a role for many of the proteins involved in maintenance of epithelial cell-cell junctions and apicobasal polarity during tumourigenesis (reviewed in Coradini *et al.,* 2011). Proteins from all three core polarity complexes have been implicated in cancer. Experiments in *Drosophila* have classified *scrib, lgl* and *dlg* as neoplastic tumour suppressor genes, mutations in which disrupt epithelial polarity and result in neoplastic overgrowth of epithelial tissues (Bilder, 2004). The importance of the SCRIB complex in tumour suppression has also been demonstrated in mammals. For example, depletion of SCRIB disrupts cell polarity and promotes transformation of mammary epithelial cells *in vitro* and *in vivo* (Zhan *et al.,* 2008). Decrease in SCRIB expression has also been associated with invasive cervical cancers (Nakagawa *et al.,* 2004). Reduced expression of LGL has been reported in gastric adenocarcinoma (Lisovsky *et al.,* 2009), colorectal cancer (Schimanski *et al.,* 2005) and malignant melanoma (Kuphal *et al.,* 2006). Components of other polarity complexes are also important within the process of tumourigenesis, for example loss of CRB3 has been associated with tumourigenicity of mouse kidney epithelial cells (Karp *et al.,* 2008). In addition, aPKC has been classed as a potential oncogene in ovarian and non-small cell lung cancers where overexpression is associated with poor survival (Eder *et al.,* 2005; Regala *et al.,* 2005).

In addition to the polarity complexes, components of cell-cell and cell-ECM contacts are also often associated with cancer. E-cadherin downregulation is frequently observed in various human cancers and has been shown to correlate with increased metastatic behaviour (Perl *et al.,* 1998; Coradini *et al.,* 2011). Alterations in tight junction structure and function are also often associated with enhanced invasiveness of human carcinomas (Miyoshi and Takai, 2005; Oliveira and Morgado-Diaz, 2007). For example, occludin levels have been found to be reduced in breast and prostate cancer (Busch *et al.,* 2002; Martin *et al.,* 2010) and changes in expression of claudins are frequently observed in human tumours (Morin, 2005). Claudin-1 has been found to be reduced in breast (Kramer *et al.,* 2000; Tokes *et al.,* 2005); lung (Chao *et al.,* 2008); and colon (Resnick *et al.,* 2005) cancers, and upregulation of claudins has also

been associated with carcinogenesis (Oliveira *et al.,* 2005). Cell-ECM interactions are also important for the development of carcinomas and changes in expression of integrin receptors is often observed in neoplastic cells (Bosman *et al.,* 1993).

The incidence of defective epithelial cell polarity during tumour formation and progression highlights the need to fully understand the mechanisms governing polarisation within normal, healthy epithelial tissues. As already discussed, various mechanisms involving polarity complexes and formation of cellular contacts are required to establish epithelial polarity. However, in order to carry out their function these proteins must be delivered and maintained at the correct location. Polarised epithelial cells feature a complex, highly regulated protein trafficking network and it is becoming clear that this is important for the establishment and maintenance of a functional epithelium.

## 1.3. Protein Trafficking and Epithelial Cell Polarity

### 1.3.1. Endocytosis

In general, endocytosis is the process by which cells transport extracellular material or membrane-bound cargo from the plasma membrane to specific intracellular compartments. This process is required for many important cellular functions, including regulation of cell-surface receptors, uptake of extracellular nutrients and maintenance of cell polarity (Mukherjee *et al.,* 1997). Several mechanisms of endocytosis exist but generally, the endocytic pathway begins with internalisation of transmembrane proteins into endocytic vesicles which invaginate and pinch off from the plasma membrane. These are delivered to the early endosome and from here, material can either be recycled back to the cell surface via recycling endosomes, or can be degraded via trafficking to the lysosome (Mukherjee *et al.,* 1997; Stuffers *et al.,* 2009a). In order to sort cargo destined for degradation from that which must be recycled, the formation of multivesicular bodies (MVB) occurs (Mukherjee *et al.,* 1997; Babst, 2005). MVBs are formed by invagination and budding of vesicles from the early endosomal membrane into the lumen. During this process, proteins to be degraded are sorted into these intralumenal vesicles (ILVs), whereas those to

be recycled are retained on the endosomal limiting membrane and sorted towards the recycling pathway. Eventually the MVB will fuse with the lysosome and its contents will be degraded (Figure 1.4) (Mukherjee *et al.,* 1997; Babst, 2005; Stuffers *et al.,* 2009a).

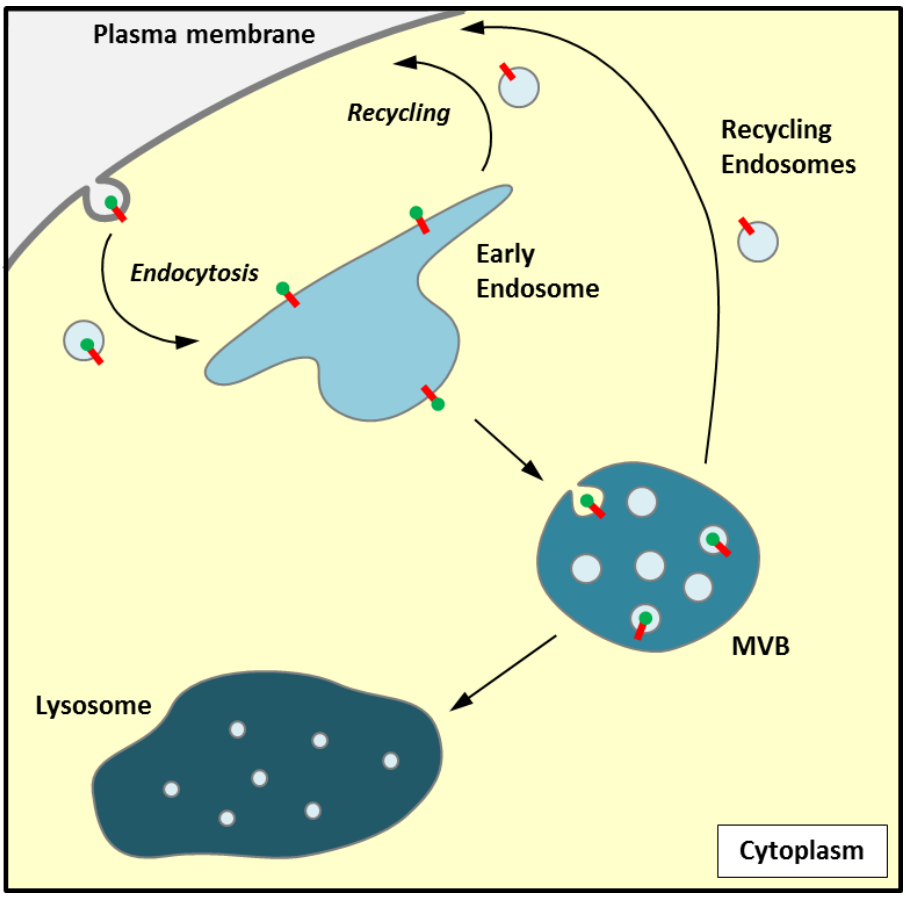


***Figure 1.4* The endocytic pathway.** Generally the endocytic pathway begins with endocytosis of proteins into endocytic vesicles which invaginate and pinch off from the plasma membrane. Upon delivery to the early endosome, proteins can either be recycled back to the cell surface via recycling endosomes, or can be targeted for degradation. Proteins to be degraded are internalised from the endosomal membrane into intraluminal vesicles, forming the multivesicular body (MVB). The MVB will then fuse with the lysosome and its contents will be degraded (adapted from Babst, 2005).

Endocytosis in polarised cells is a complex, highly dynamic process and various signalling and sorting mechanisms are important to regulate transport to and from the distinct apical and basolateral membrane domains in order to maintain apicobasal polarity (Hoekstra *et al.,* 2004; Mellman and Nelson, 2008; Weisz and Rodriguez-Boulan, 2009). In comparison to unpolarised cells, polarised

epithelial cells contain additional populations of endosomal compartments and protein trafficking can occur along multiple endocytic routes (Figure 1.5) (Hoekstra *et al.,* 2004; Golachowska *et al.,* 2010).

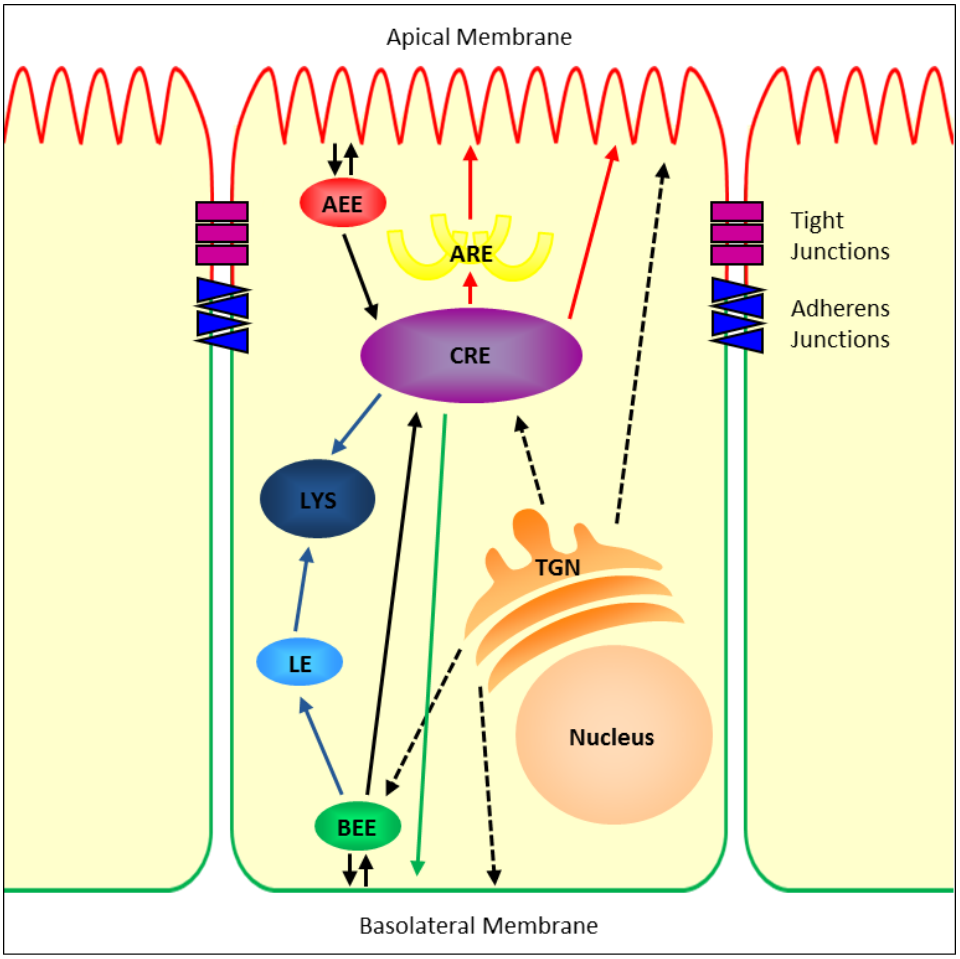


***Figure 1.5*** **Endocytic compartments and trafficking routes in polarised epithelial cells.** Cargo internalised from the apical (red) or basolateral (green) membrane is delivered to apical early endosomes (AEE) or basolateral early endosomes (BEE), respectively. Cargo can then be recycled back to the plasma membrane domain of origin, directed to the degradative pathway (blue arrows) via trafficking to late endosomes (LE) and lysosomes (LYS), or transported to the common recycling endosome (CRE). From the CRE, cargo can be transported to the basolateral (green arrow) or apical (red arrows) membrane, or can be directed to lysosomes for degradation. Apically destined cargo can travel directly from the CRE or via apical recycling endosomes (ARE). Recycling endosomes are also important for the biosynthetic trafficking pathway. Newly synthesised proteins can be delivered from the TGN to their specific membrane domain directly, via the CRE or BEE (broken arrows) (adapted from Hoekstra *et al.,* 2004; Golachowska *et al.,* 2010).

### 1.3.2. Endocytic Trafficking in Polarised Cells

In polarised epithelial cells, cargo endocytosed either from the apical or basolateral membrane is delivered to apical early endosomes (ARE) or basolateral early endosomes (BEE), respectively. From here, cargo can either be recycled back to the plasma membrane domain of origin, directed to the degradative late endosomal (LE)/lysosomal pathway (LYS), or transported to the common recycling endosome (CRE) (Hoekstra *et al.,* 2004; Golachowska *et al.,* 2010). The CRE, which appears to be a ubiquitous feature of epithelial cells, is characterised as a mildly acidic, tubulovesicular network which clusters in the apical region and extends to the cell periphery (Knight *et al.,* 1995; Futter *et al.,* 1998; Wang *et al.,* 2000; Hoekstra *et al.,* 2004). Above the CRE is a population of cup-shaped vesicles termed the apical recycling endosomes (ARE). These localise just below the apical membrane and contain apically destined cargo but not basolaterally recycling cargo (Gibson *et al.,* 1998; Brown *et al.,* 2000). It is not clear whether ARE are separate compartments or sub-domains of the CRE and there is evidence to support both scenarios (reviewed in Hoekstra *et al.,* 2004; Golachowska *et al.,* 2010).

The CRE is, therefore, an important organelle within the polarised endocytic pathway. As endocytosed apical and basolateral cargo merge in this compartment it is suggested that the CRE acts as a sorting centre crucial for establishment and maintenance of membrane polarity (Hoekstra *et al.,* 2004; Golachowska *et al.,* 2010). Data suggests that sorting is carried out after endocytosed apical and basolateral cargo reaches the CRE rather than cargo being transported to distinct regions of entry (Golachowska *et al.,* 2010). This is thought to be achieved through lateral membrane segregation of endocytosed apical and basolateral plasma membrane proteins in the CRE, a process which has been visualised directly in polarised MDCK cells (Thompson *et al.,* 2007). From the CRE cargo can recycle back to the basolateral or apical surface. Transport to the apical surface can occur directly or via the ARE. In addition, cargo can also be directed from the CRE to lysosomes.

Sorting and subsequent trafficking from the CRE is regulated by various mechanisms, the complexities of which are still to be unravelled. Examples of

proteins which appear to be important in this process include clathrin adaptor proteins and Rab proteins. In addition, it appears that cargo can be transported via multiple routes and these can change as cells polarise (Hoekstra *et al.,* 2004; Weisz and Rodriguez-Boulan, 2009; Golachowska *et al.,* 2010).

It should be noted that the CRE also plays an important role in the biosynthetic trafficking pathway (reviewed in Folsch *et al.,* 2009). Newly synthesised proteins can be sorted in the *trans*-Golgi network (TGN) and delivered directly to the apical or basolateral plasma membrane. Alternatively, cargo can be transported from the TGN to the specific membrane domain via recycling endosomes, for which multiple routes exist (Cresawn *et al.,* 2007; Cramm-Behrens, 2008; Farr *et al.,* 2009). It seems that basolaterally destined cargo can travel via the CRE or may avoid this compartment and traffic through BEE instead. Apically destined cargo can travel from the TGN to the plasma membrane via the CRE, ARE or AEE and studies have suggested that multiple pathways exist depending on the cargo involved (Folsch *et al.,* 2009). In addition, cargo can reach the apical surface by transcytosis from the basolateral membrane, a process which also involves trafficking through the CRE (Apodaca *et al.,* 1994; Hoekstra *et al.,* 2004).

### 1.3.3. Endocytosis: Important Regulator of Polarity?

Tightly regulated protein trafficking is key for the maintenance of plasma membrane polarity and it is becoming clear that it is also important for establishment of epithelial cell polarity (Hoekstra *et al.,* 2004; Folsch *et al.,* 2009; Golachowska *et al.,* 2010). For example, knockdown of proteins implicated in apical transport, such as Rab-11 and annexin-13, disrupted establishment of polarity in 3D cell culture cysts (Torkko *et al.,* 2008; Gao and Kaestner, 2010).

Studies to elucidate mechanisms underlying establishment and maintenance of epithelial cell polarity have mainly focused on protein trafficking along the biosynthetic pathway, including transcytosis (Folsch *et al.,* 2009). However, it is becoming clear that endocytosis plays an essential role in establishment and maintenance of a polarised epithelium (Shivas *et al.,* 2010). For example,

endocytosis has been implicated in biogenesis of the apical membrane in MDCK cells. Schluter and colleagues have demonstrated that during the first MDCK cell division, Crumbs is internalised and concentrates in Rab11-positive ARE which are delivered to the site of cytokinesis and thus form the first apical membrane (Schluter *et al.,* 2009). This suggests that endocytosis is important for targeted delivery of proteins required for establishment of epithelial cell polarity. In support of this, during *C.elegans* embryonic development correct polarisation of PAR proteins requires dynamin and Rab-11, important for clathrin-mediated endocytosis and endocytic recycling, respectively (Zhang *et al.,* 2008; Nakayama *et al.,* 2009).

***Dynamics of Cell-Cell Junctions***

A key role of endocytosis within maintenance of epithelial polarity could be through the regulation of cell-cell junctions. Once formed, cell-cell junctions are dynamic structures that are continuously being remodelled, suggesting that the endocytic machinery is important for the regulation of cell-cell junction structure and function (Ivanov *et al.,* 2005; Shen *et al.,* 2008; Yu and Turner, 2008; Steed *et al.,* 2010). Previous studies have demonstrated that occludin and E-cadherin are continuously endocytosed and recycled back to the plasma membrane in mammalian epithelial cells (Le *et al.,* 1999; Morimoto *et al.,* 2005). Constitutive endocytosis of claudin-1 has also been observed (Matsuda *et al.,* 2004) and inhibition of recycling in MDCK cells altered the localisation of claudin-1 and specifically delayed recruitment of claudin-1 to tight junctions (Marzesco *et al.,* 2002). Internalisation of different junctional components appears to be highly specific and may be mediated by ubiquitylation by specific E3 ubiquitin ligases (Fujita *et al.,* 2002; Traweger *et al.,* 2002; Yu and Turner, 2008; Takahashi *et al.,* 2009).

Disruption of cell-cell junctions can often perturb epithelial cell polarity and therefore, endocytic trafficking of cell-cell junction proteins may be important for regulation of epithelial cell polarity (Brennan *et al.,* 2010; Coradini *et al.,* 2011; Turksen and Troy, 2011). For example, the balance of E-cadherin trafficking plays an important role in regulation of epithelial cell adhesion (Bryant and Stow, 2004) and loss of E-cadherin from adherens junctions is associated with loss of polarity and EMT (Perl *et al.,* 1998; Yang and Weinberg, 2008). It is

possible that trafficking of other junctional proteins is also important for the maintenance of epithelial cell polarity.

***Evidence from Drosophila***

Various studies have provided evidence for links between endocytosis, regulation of epithelial junctions (Ivanov *et al.,* 2005) and cell polarity (Shivas *et al.,* 2010). Therefore, it is likely that protein trafficking plays a crucial role in maintaining a polarised epithelium although a direct role for endocytosis in this process is yet to be determined. Studies in *Drosophila,* however, have provided strong evidence for the importance of endocytosis in regulation of epithelial cell polarity. In these studies, mosaic genetic screens were conducted in order to uncover further novel regulators of epithelial cell polarity. Interestingly the majority of these newly isolated genes have been identified as regulators of the endocytic pathway (reviewed in Hariharan and Bilder, 2006, Vaccari and Bilder, 2009; Herz and Bergmann, 2009; Lobert and Stenmark, 2011). Mutation of these genes disrupts epithelial cell polarity and induces overproliferation resulting in formation of neoplastic tumours. These genes have accordingly been classified as endocytic tumour suppressor genes (TSGs) (Vaccari and Bilder, 2009).

The proteins encoded by these endocytic TSGs can be split into two groups: those that regulate cargo entry into the early endosome, and those that regulate cargo sorting within MVBs (Vaccari and Bilder, 2009). The first group include the *Drosophila* homologues of syntaxin 7/12 (Avalanche), required for vesicle fusion to form early endosomes, and the GTPase Rab5, required to regulate traffic to the early endosome. In addition, the syntaxin binding protein Vps45, and the Rab5 effector Rabenosyn-5 (Rbsn) have also been identified as tumour suppressors (Lu and Bilder, 2005; Morrison *et al.,* 2008). The second group of endocytic TSGs encode components of the Endosomal Sorting Complex Required for Transport (ESCRT) machinery. This family of proteins act at a later stage of the endocytic pathway and are required for cargo sorting and MVB formation (Hariharan and Bilder, 2006). The ESCRT proteins are the focus of this thesis and will be discussed in detail below.

## 1.4. ESCRT Proteins

The ESCRT machinery is comprised of four multi-subunit complexes termed ESCRT-0, -I, -II and -III, as well as several accessory components (Table 1.1). Originally identified in yeast as the class E vacuolar protein sorting (Vps) proteins, the ESCRT machinery has since been shown to be highly conserved in eukaryotic cells (Raymond *et al.,* 1992; Babst, 2005; Hurley, 2008). ESCRT proteins have a well established role in the sorting of ubiquitylated proteins for degradation via the formation of MVBs and trafficking to the lysosome (Hurley and Emr, 2006; Hurley, 2008; Raiborg and Stenmark, 2009; Roxrud *et al.,* 2010).

### 1.4.1. The ESCRT Complexes: Structure

The composition of the ESCRT machinery has been studied over several years and detailed structural biology of the ESCRT proteins is described in recent reviews (Hurley and Emr, 2006; Williams and Urbe, 2007). Here I will briefly summarise the components of each ESCRT complex and provide details of the key interactions.

***ESCRT-0***

ESCRT-0 consists of Hrs (hepatocyte growth factor (HGF)-regulated Tyrosine-kinase substrate) and STAM (signal transducing adaptor molecule) and is required for initial selection of ubiquitylated cargo at the endosomal membrane (Williams and Urbe, 2007). ESCRT-0 binds monoubiquitin via ubiquitin-interacting motifs (UIMs) found on both Hrs and STAM. Ubiquitylation provides the signal for sorting into the MVB pathway (Clague and Urbe, 2006) and therefore, ESCRT-0 binding to ubiquitin is the initial step in the sorting process (Urbe *et al.,* 2003). ESCRT-0 is recruited to the early endosomal membrane via the FYVE (Fab1, YOTB, Vac1 and early endosome antigen-1 (EEA1)) zinc finger domain of Hrs which binds to the endosomal lipid, phosphatidylinositol-3-phosphate (PI(3)P) (Katzmann *et al.,* 2003; Hurley and Emr, 2006). ESCRT-0 proteins also bind to the coat protein clathrin and are thought to sequester ubiquitylated cargo into clathrin-coated microdomains which will eventually form ILVs (Sachse *et al.,* 2002; Raiborg *et al.,* 2006; Williams and Urbe, 2007;

Raiborg and Stenmark, 2009). Finally, ESCRT-0 is important for recruitment of downstream ESCRTs via direct interaction of Hrs with ESCRT-I (Bache *et al.,* 2003a; Katzmann *et al.,* 2003).

| Complex | Yeast Protein | Mammalian Protein |
|---|---|---|
| ESCRT-0 | Vps27 | HRS |
| | Hse1 | STAM1, 2 |
| ESCRT-I | Vps23 | Tsg101 |
| | Vps28 | Vps28 |
| | Vps37 | Vps37A, B, C, D |
| | Mvb12 | Mvb12A, B |
| ESCRT-II | Vps22 | Vps22 (EAP30) |
| | Vps25 | Vps25 (EAP20) |
| | Vps36 | Vps36 (EAP45) |
| ESCRT-III | Vps20 | CHMP6 |
| | Vps32 (Snf7) | CHMP4A,B,C |
| | Vps24 | CHMP3 |
| | Vps2 | CHMP2A,B |
| | Vps46 (Did2) | CHMP1A,B |
| | Vps60 | CHMP5 |
| | – | CHMP 7 |
| Vps4 | Vps4 | Vps4A,B |
| | Vta1 | LIP5 |
| Accessory | Bro1 | Alix |
| DUB | Doa4 | UBPY |
| | – | AMSH |

***Table 1.1* Endosomal Sorting Complex Required For Transport (ESCRT) protein subunits and ESCRT-related proteins.** The ESCRT complexes are comprised of several proteins subunits. For each yeast class E Vps protein, one or more mammalian homologues have been identified.

### *ESCRT-I*

ESCRT-I consists of four subunits: Tsg101 (tumour susceptibility gene 101), Vps28, Vps37 and Mvb12 (multivesicular body sorting factor of 12 kDa) (Raiborg and Stenmark, 2009). This ESCRT complex also binds to ubiquitin via the Tsg101 and Mvb12 proteins (Hurley and Emr, 2006; Roxrud *et al.,* 2010).

ESCRT-I binds to ESCRT-0 via Tsg101 (Bache *et al.,* 2003a; Katzmann *et al.,* 2003) and, in yeast, ESCRT-I binds to ESCRT-II via its Vps28 subunit although no direct link has been observed in mammalian cells (Teo *et al.,* 2006; Williams and Urbe, 2007).

***ESCRT-II***

The ESCRT-II complex contains one Vps22 subunit, one Vps36 subunit and two Vps25 subunits (Hierro *et al.,* 2004). The Vps36 subunit has a GLUE (GRAM-like ubiquitin-binding in EAP45) domain at its N-terminus which can bind to PI(3)P, ubiquitin and the ESCRT-I subunit Vps28 (Williams and Urbe, 2007; Raiborg and Stenmark, 2009). ESCRT-II also recruits, and possibly activates, ESCRT-III via its Vps25 subunit (Im *et al.,* 2009; Raiborg and Stenmark, 2009). Therefore, ESCRT-II is thought to provide a link between ubiquitylated cargo, the endosomal membrane, and ESCRT-I and -III (Hurley and Emr, 2006).

***ESCRT-III***

ESCRT-III consists of several small, highly charged subunits, termed CHMPs (charged multivesicular body proteins) in mammalian cells. Seven CHMPs have been identified (CHMP1-7) and each of these, with the exception of CHMP7, correspond to one of the six different ESCRT-III subunits present in yeast (Table 1.1) (Lata *et al.,* 2009). In contrast to ESCRT-0, -I and -II, which exist as soluble complexes in the cytosol, ESCRT-III proteins are thought to assemble into a multimeric complex on endosomal membranes (Lata *et al.,* 2009; Raiborg and Stenmark, 2009).

All of the ESCRT-III proteins have a basic N-terminal and acidic C-terminal region (Williams and Urbe, 2007). Studies into the structure of CHMP3 have revealed that the C-terminal region is autoinhibitory and interacts with the N-terminal core to form a closed, inactive conformation (Lata *et al.,* 2008a). Activation of the ESCRT-III subunits is thought to be triggered by a conformational change which displaces the C-terminal region from the N-terminal core, relieving the autoinhibition and allowing membrane targeting and assembly of the ESCRT-III complex (Lata *et al.,* 2008; Lata *et al.,* 2009; Raiborg and Stemark, 2009). This may occur in a directional manner in that one

ESCRT-III subunit activates the next and so on. Studies in yeast have demonstrated that the core ESCRT-III complex, consisting of Vps20, Vps32, Vps24 and Vps2 (CHMP6, CHMP4, CHMP3 and CHMP2, respectively), assembles sequentially on the endosomal membrane (Teis *et al.,* 2008). Vps20 is N-terminally myristoylated and can interact with the endosomal membrane. In addition, Vps20 also binds to the ESCRT-II subunit Vps25 which is thought to activate Vps20 and initiate assembly of the ESCRT-III complex (Yorikawa *et al.,* 2005; Im *et al.,* 2009; Raiborg and Stenmark, 2009). Vps20 also interacts with Vps32 and triggers the assembly of Vps32 into oligomers which appear to be capped by Vps24. Vps2 then associates with Vps24 and recruits the AAA-ATPase Vps4, which is important for disassembly of the ESCRT-III complex (Teis *et al.,* 2008; Raiborg and Stenmark, 2009). CHMP1 and CHMP5 are thought to regulate the recruitment and activity of the AAA-ATPase Vps4, although the exact mechanism of this is unknown (Raiborg and Stenmark, 2009).

### 1.4.2. The ESCRT Complexes: Function

ESCRTs have been classically characterised for their role in endosomal sorting and degradation of ubiquitylated proteins via MVB formation. It is also becoming increasingly clear that ESCRT proteins have additional functional roles within the endocytic pathway as well as other biological processes (Roxrud *et al.,* 2010).

#### *Targeting Proteins for Degradation via Formation of MVBs*

In the conventional model for ESCRT assembly it is thought that, during MVB formation, the ESCRT complexes are recruited sequentially to the early endosomal membrane (Figure 1.6) (Hurley, 2008). ESCRT-0 is proposed to be responsible for the initial recognition of ubiquitylated cargo. However, the presence of ubiquitin-binding domains in ESCRT-I and -II has led to a model whereby ubiquitylated cargo is handed over sequentially from one ESCRT complex to the other (Hurley, 2008; Raiborg and Stenmark, 2009). In support of this model, studies have demonstrated that the ubiquitin-binding domains of all three ESCRT complexes interact with the same hydrophobic region of ubiquitin at Ile44 (Hurley and Emr, 2006; Raiborg and Stenmark, 2009). However, the

binding sites for ubiquitylated cargo and the ubiquitin-interacting domain of ESCRT-II are at opposite ends of the 25 nm long ESCRT-I complex, therefore arguing against cargo exchange from ESCRT-I to ESCRT-II (Kostelansky *et al.,* 2007; Hurley, 2008; Raiborg and Stenmark, 2009). An alternative model proposes that simultaneous binding of ESCRT-0, -I and -II to multiple ubiquitylated proteins allows clustering of cargo for subsequent packaging into ILVs (Hurley and Emr, 2008).

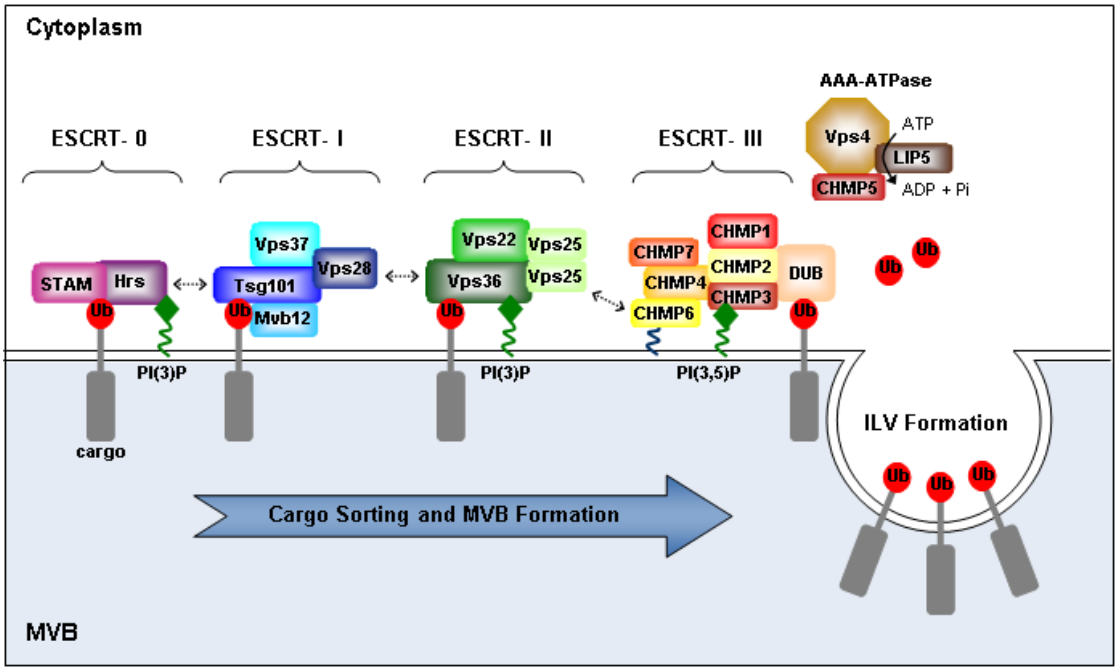


***Figure 1.6*** **Cargo sorting and MVB formation is dependent on the ESCRT protein complexes.** During MVB formation the ESCRT complexes are thought to be recruited sequentially to the endosomal membrane where they recognise ubiquitylated membrane proteins (cargo) and function to package these into intraluminal vesicles (ILV) which bud off into the lumen of the MVB. Both ESCRT-0 components, Hrs and STAM, bind to ubiquitin. Hrs also binds to the endosomal lipid, PI(3)P, and recruits ESCRT-I via interaction with Tsg101. ESCRT-I binds ubiquitin via Tsg101 and Mvb12, and Vps28 is thought to interact with the ESCRT-II subunit, Vps36. Vps36 also binds to ubiquitin and PI(3)P. In contrast to the other ESCRTs, which exist as soluble complexes in the cytosol, assembly of ESCRT-III is thought to occur on the endosomal membrane. CHMP6 binds to the ESCRT-II protein, Vps25, which initiates recruitment of CHMP4, CHMP3 and CHMP2. The ATPase Vps4 complex is then recruited which disassembles the ESCRT-III complex, allowing membrane scission to occur forming the ILV. Prior to ILV budding, ESCRT-III also recruits a deubiquitylating enzyme (DUB) which removes the ubiquitin from the cargo (adapted from Tanaka *et al.,* 2008).

The mechanism responsible for endosomal membrane deformation and scission, which is required to form ILVs, is not fully understood. However, the prime candidate to elicit this process is ESCRT-III. Evidence to support this is provided by a study which demonstrates that overexpressed CHMP4 (Vps32) polymerises into spiral filaments which induce protrusion of buds and tubules from the plasma membrane in mammalian cells (Hanson *et al.,* 2008). Budding of ILVs into the MVB also requires the AAA-ATPase Vps4. Vps4 is recruited by ESCRT-III where it appears to induce disassembly of the ESCRT-III complex in an ATP-dependent manner (Hurley *et al.,* 2008; Raiborg and Stenmark, 2009: Saksena *et al.,* 2009). Experiments which have reconstituted ESCRT-III assembly *in vitro* have shown that C-terminally truncated CHMP2A coassembles with CHMP3 into hollow helical tubules with a diameter of ~40nm. Membrane interaction sites were found on the inside of these tubules where binding of Vps4 also occurred, mediating disassembly of the tube upon ATP hydrolysis (Lata *et al.,* 2008b). These studies suggest that assembly of the ESCRT-III complex deforms the endosomal membrane to form ILVs. Vps4 then enters these forming ILVs and depolymerises the ESCRT-III complex from the inside. The concerted action of these two complexes leads to membrane constriction and scission (Lata *et al.,* 2009; Raiborg and Stenmark, 2009; Saksena *et al.,* 2009; Wollert *et al.,* 2009). It is currently not clear whether Vps4 is directly required to contribute energy for the membrane scission event as well as disassembling the ESCRT-III complex (Lata *et al.,* 2009).

The final process important for the formation of MVBs is deubiquitylation of cargo. This is carried out by deubiquitylating enzymes (DUBs) which are recruited by the ESCRT-III complex and accessory protein Alix (Hurley, 2008; Lata *et al.,* 2009; Raiborg and Stenmark, 2009). The key DUBs associated with the MVB pathway are Doa4 in yeast, and AMSH and UBPY in mammals (Hurley, 2008). Interestingly, in mammalian cells these DUBs are also recruited by the ESCRT-0 subunit STAM (McCullough *et al.,* 2006; Row *et al.,* 2007) and therefore appear to function at both early and late stages of MVB formation. This could allow deubiquitylation of cargo that is not destined for degradation, adding further complexity to the MVB sorting process (Raiborg and Stenmark, 2009; Berlin *et al.,* 2010).

Therefore, ESCRT proteins are required for efficient sorting of proteins along the degradative endosomal pathway. Disruption of the ESCRT machinery generally results in the inhibition of MVB formation and accumulation of endosomal cargo in aberrant endosomes, therefore perturbing endosomal trafficking and degradation (Raymond *et al.,* 1992; Bishop *et al.,* 2002; Bache *et al.,* 2003b; Lu *et al.,* 2003; Doyotte *et al.,* 2005; Bache *et al.,* 2006; Razi and Futter, 2006; Malerod *et al.,* 2007; Williams and Urbe, 2007; Raiborg *et al.,* 2008, Stuffers *et al.,* 2009b).

***Additional Role for ESCRTs in Endosomal Recycling***

Although ESCRT proteins have been classically characterised for their involvement in degradation of membrane proteins (Hurley and Emr, 2006; Raiborg and Stenmark, 2009), it is also reported that ESCRT function is important for recycling. Some studies have demonstrated that depletion of Hrs or Tsg101 increases recycling of epidermal growth factor (EGF) receptor (EGFR) upon stimulation with EGF ligand. However, knockdown of Vps22 and Vps24 has no effect on EGFR and EGF recycling (Razi and Futter, 2006; Raiborg *et al.,* 2008). In contrast, other studies have suggested that knockdown of Tsg101 causes a decrease in recycling resulting in reduced levels of EGFR and transferrin receptor (TfR) at the cell surface (Doyotte *et al.,* 2005). In addition, ESCRT-I and -III are required for recycling of EGFR upon stimulation with amphiregulin (AR) whereas ESCRT-0 and -II are dispensable for this process (Baldys and Raymond, 2009). Vps4 has also been shown to be required for recycling of TfR and low-density lipoprotein receptor (LDLR) back to the cell surface (Yoshimori *et al.,* 2000; Fujita *et al.,* 2003). Further evidence for the importance of ESCRTs in the endosomal recycling pathway is provided by the observation that the ESCRT-0 subunit, STAM can bind the DUB, UBPY (McCullough *et al.,* 2006; Row *et al.,* 2007). Deubiquitylation of EGFR by UBPY protects EGFR from degradation via an Hrs-dependent pathway demonstrating that UBPY and ESCRT-0 play in key role in determining the fate of endocytosed EGFR (Berlin *et al.,* 2010). Therefore, it is becoming apparent that the ESCRT machinery is important for regulating sorting of cargo between degradative and recycling pathways and ESCRT function may be required for efficient trafficking along both these endosomal routes.

### *ESCRTs and Regulation of Signalling*

ESCRT proteins also play a crucial role in regulation of cell signalling (Rodahl *et al.,* 2009a; Wegner *et al.,* 2011). Sequestration of activated membrane receptors into ILVs during MVB formation and subsequent lysosomal degradation terminates ligand-induced signalling (Sorkin and Von Zastrow, 2009). Therefore, this provides one mechanism whereby ESCRTs can negatively regulate receptor signalling (Wegner *et al.,* 2011). This is highlighted through various studies which demonstrate that ESCRTs are required for degradation of activated receptor tyrosine kinases (RTK) (Wegner *et al.,* 2011). For example, disruption of the ESCRT machinery causes reduced degradation of EGF-stimulated EGFR (Bishop *et al.,* 2002; Lu *et al.,* 2003; Bache *et al.,* 2006; Malerod *et al.,* 2007; Raiborg *et al.,* 2008). ESCRTs can also negatively regulate other signalling pathways such as Notch, Toll-like receptor (TLR) and G-protein coupled receptor (GPCR) signalling (Rodahl *et al.,* 2009a; Wegner *et al.,* 2011). Therefore, perturbed ESCRT function can enhance activity of various signalling pathways.

In addition to reduced degradation of activated receptors, there are also other possible mechanisms which could account for the increase in receptor signalling in ESCRT depleted cells. Firstly, receptors may remain active whilst on the limiting membrane of endosomes and therefore, disrupted sequestration into ILVs may prolong the time that the receptor is signal competent (Sorkin and Von Zastrow, 2009; Wegner *et al.,* 2011). This is supported by studies which show that depletion of ESCRT-0 and -I, but not ESCRT-II and -III, results in sustained EGFR activity indicating a requirement for early acting ESCRT proteins in the attenuation of EGFR signalling (Bache *et al.,* 2006; Malerod *et al.,* 2007). In addition, some signalling complexes preferentially assemble on endosomal membranes and therefore, disruption of endosomal trafficking upon ESCRT disruption will enhance their activity (Sorkin and Von Zastrow, 2009). This is observed for the Notch signalling pathway in *Drosophila* whereby ESCRT mutation results in increased endosomal signalling due to accumulation of Notch within early endosomes (Thompson *et al.,* 2005; Vaccari and Bilder, 2005; Herz *et al.,* 2006; Herz *et al.,* 2009; Gilbert *et al.,* 2009; Vaccari *et al.,* 2009).

Alternatively, blocking endosomal degradation by ESCRT depletion may enhance recycling of endocytosed receptors back to the plasma membrane resulting in sustained signalling (Wegner *et al.,* 2011). This is supported by the observation that Hrs or Tsg101 depletion decreases degradation but increases recycling of epidermal growth factor (EGF) receptor (EGFR) upon stimulation with EGF ligand (Razi and Futter, 2006; Raiborg *et al.,* 2008). However, other studies have demonstrated the opposite effect in that ESCRT disruption decreases recycling of other receptors, such as the transferrin receptor (Yoshimori *et al.,* 2000; Fujita *et al.,* 2003; Doyotte *et al.,* 2005). Therefore, there may be a number of mechanisms by which ESCRTs regulate cellular signalling pathways and the importance of these could differ depending on various factors such as receptor type, ligand concentration and cell type (Wegner *et al.,* 2011).

It is also important to note that the ESCRT pathway may play a positive role in the regulation of other signalling pathways (Wegner *et al.,* 2011). For example, ESCRT-dependent sequestration of the inhibitory glycogen synthase kinase 3 (GSK3) within MVBs is required for activation of canonical Wnt signalling (Taelman *et al.,* 2010). Therefore, whilst perturbed ESCRT function can enhance receptor signalling, it could also inhibit signalling through other pathways at the same time.

***ESCRTs and Autophagy***

Autophagy is a degradation pathway for cytoplasmic components, such as protein aggregates, cellular macromolecules, damaged organelles and invading pathogens (Fader and Colombo, 2009; Rusten and Stenmark, 2009). Autophagy is tightly regulated by cellular signalling mechanisms, in particular those activated by nutrient starvation and cellular stress (Mizushima *et al.,* 2008). The protein kinase Tor (target of rapamycin) is central to this regulation by inhibiting the autophagic process under nutrient rich conditions (Rusten and Stenmark, 2009). During the autophagic process a portion of cytoplasm is engulfed by a cup-shaped double membrane structure called the phagophore which will seal the sequestered cytoplasmic contents, forming an autophagosome. These autophagosomes then fuse with lysosomes to form an autolysosome and the contents are degraded. Autophagosomes can also fuse

with endosomes to form amphisomes prior to fusion with lysosomes (Fader and Colombo, 2009; Rusten and Stenmark, 2009).

At least 30 evolutionary conserved Atg (autophagy related) proteins have been identified which make up two ubiquitin-like conjugation systems required for autophagosome formation (Fader and Colombo, 2009; Rusten and Stenmark, 2009). Interestingly various studies have revealed a role for the ESCRT machinery within the process of autophagy and disruption of ESCRT function results in autophagosome accumulation (Nara *et al.,* 2002; Filimonenko *et al.,* 2007; Rusten *et al.,* 2007; Tamai *et al.,* 2007). It is currently not clear why ESCRTs are important for autophagy. It has been suggested that a functional MVB is necessary to allow autophagic degradation and therefore, disruption of MVB formation due to perturbed ESCRT function may consequently inhibit autophagy (Fader and Colombo, 2009). Alternatively, ESCRTs may be required for autophagosome fusion with endosomes and lysosomes (Rusten and Stenmark, 2009). ESCRT disruption would inhibit this fusion resulting in an increase in the number of autophagosomes and a decrease in amphisomes and autolysosomes, an effect which has been reported previously (Rusten *et al.,* 2007; Tamai *et al.,* 2007). There may also be other mechanisms to explain the importance of the ESCRT machinery within the process of autophagy and further work will continue to elucidate the possibility of interplay between autophagy and MVB biogenesis.

***Non Endosomal Functions of ESCRTs***

ESCRT proteins are also involved in other cellular processes in addition to their roles within endocytic trafficking (Roxrud *et al.,* 2010). These include cytokinesis and viral budding, both processes involving membrane fission. Cytokinesis is the final step of cell division whereby the dividing cell is physically cleaved into two daughter cells (Barr and Gruneberg, 2007). Various studies have implicated the ESCRT machinery in this process (Raiborg and Stenmark, 2009; Roxrud *et al.,* 2010). ESCRT-III is recruited to the midbody by ESCRT-I and/or Alix and, as in MVB formation, Vps4 appears to be required for ESCRT-III disassembly and subsequent membrane scission (Carlton and Martin-Serrano, 2007; Morita *et al.,* 2007; Dukes *et al.,* 2008). The role, if any, of ESCRT-II in this process remains to be elucidated.

Budding of enveloped viruses from the plasma membrane of infected cells also requires ESCRT function. During this process viruses hijack the ESCRT machinery by binding to the ESCRT-I subunit Tsg101 and/or Alix. ESCRT-III and Vps4 are then recruited to mediate membrane fission and the viral buds are released from the plasma membrane (Garrus *et al.,* 2001; Martin-Serrano *et al.,* 2003; Fujii *et al.,* 2007; Roxrud *et al.,* 2010). The role of ESCRT-II in viral budding however is unclear. It appears that ESCRT-II is not essential for budding of HIV-1 (Langelier *et al.,* 2006) whereas release of avian sarcoma virus requires the ESCRT-II subunit Vps25 (Pincetic *et al.,* 2008). Therefore, it seems that different viruses can utilise different ESCRT-mediated budding pathways (Roxrud *et al.,* 2010). In addition, ESCRT-independent viral budding has also been demonstrated (Chen and Lamb, 2008).

## 1.5. ESCRTs as Tumour Suppressors

### 1.5.1. Lessons from *Drosophila*

***Loss of Epithelial Cell Polarity and Organisation***

Genetic screens in *Drosophila* have discovered a role for the ESCRT machinery within regulation of epithelial cell polarity and tumourigenesis (Vaccari and Bilder, 2009; Herz and Bergmann, 2009; Lobert and Stenmark, 2011). Two of the first ESCRT proteins to be identified as potential neoplastic tumour suppressors in *Drosophila* were Tsg101, a component of ESCRT-I, and Vps25, a component of ESCRT-II (Moberg *et al.,* 2005; Thompson *et al.,* 2005; Vaccari and Bilder, 2005; Herz *et al.,* 2006). Since these initial studies, other components of the ESCRT machinery have been identified as important regulators of epithelial cell polarity, although the precise roles for each ESCRT protein may differ (Table 1.2) (Rodahl *et al.,* 2009b; Herz *et al.,* 2009; Vaccari *et al.,* 2009).

| Complex | | ESCRT-0 | ESCRT-I | | ESCRT-II | | | ESCRT-III | | | ATPase | References |
|---|---|---|---|---|---|---|---|---|---|---|---|---|
| Component | | Hrs | Tsg101 | Vps28 | Vps25 | Vps22 | Vps36 | Vps20 | Vps32 | Vps2 | Vps4 | |
| Effect of Mutation | Enlarged Endosomes | + *1* | *n/a* | *n/a* | + *4,8* | + *8* | + *8* | *n/a* | *n/a* | *n/a* | + *9* | (1) Jekely & Rorth, 2003<br>(2) Moberg *et al.,* 2005<br>(3) Thompson *et al.,* 2005<br>(4) Vaccari & Bilder, 2005<br>(5) Herz *et al.,* 2006<br>(6) Vaccari *et al.,* 2008<br>(7) Gilbert *et al.,* 2009<br>(8) Herz *et al.,* 2009<br>(9) Rodahl *et al.,* 2009b<br>(10) Vaccari et al, 2009 |
| | Accumulation of Ubiquitin | + *1* | + *2* | + *10* | + *3,5,8,10* | + *8,10* | + *8* | + *10* | + *10* | + *10* | + *9* | |
| | Accumulation of EGFR | + *1* | *n/a* | + *10* | + *10* | + *10* | *n/a* | + *10* | + *10* | + *10* | *n/a* | |
| | Sustained EGFR signalling | *n/a* | *n/a* | + *10* | + *10* | + *10* | *n/a* | + *10* | + *10* | + *10* | *n/a* | |
| | Accumulation of Notch | + *1,6* | + *2,6* | + *10* | + *4,5,6,8,10* | + *8,10* | + *8* | + *6,10* | + *10* | + *10* | + *9* | |
| | Increased Notch activity | - *6* | + *2,6* | + *10* | + *4,5,6,8,10* | + *8,10* | - *8* | + *6,10* | + *10* | + *10* | *n/a* | |
| | Disrupted epithelial organisation | - *1* | + *2,7* | + *10* | + *3,8,10* | + *8,10* | + *8* | + *10* | + *10* | + *10* | + *9* | |
| | Disrupted apicobasal polarity | - *1* | + *2,7* | *n/a* | + *4* | *n/a* | *n/a* | *n/a* | *n/a* | *n/a* | + *9* | |
| | Reduced differentiation | *n/a* | *n/a* | *n/a* | + *3,4,5* | *n/a* | *n/a* | *n/a* | *n/a* | *n/a* | *n/a* | |
| | Increased apoptosis | *n/a* | *n/a* | *n/a* | + *4,5,8* | + *8* | + *8* | *n/a* | *n/a* | *n/a* | + *9* | |
| | Neoplastic growth | - *1,6* | + *2,7* | *n/a* | + *4,8* | + *8* | + *8* | *n/a* | *n/a* | *n/a* | + *9* | |
| | Hyperplastic growth | - *1,6* | + *2,6* | + *10* | + *3,4,5,8,10* | + *8,10* | - *8* | + *10* | + *10* | + *10* | + *9* | |

***Table 1.2*** **Comparison of phenotypes resulting from mutation of ESCRTs in epithelial tissues of *Drosophila.*** The main phenotypes resulting from ESCRT mutation are listed. Positive (+) and negative (-) results and corresponding references are indicated for each ESCRT component studied. For some ESCRT components the effect of mutation on certain phenotypes has not been reported in the literature, indicated by 'n/a'. All results listed are from studies conducted in imaginal discs, the developing epithelial tissues of the *Drosophila* embryo. Phenotypes listed were observed in the ESCRT mutant cells, with the exception of 'Hyperplastic growth' which represents non-cell autonomous overproliferation.

The majority of analysis of ESCRT function has been carried out in *Drosophila* imaginal discs, polarised epithelial tissues found in the larva which will develop to form the eye, leg and wing of the adult fly (Muller, 2000). Mutation of ESCRTs disrupts the endocytic pathway resulting in aberrant endosomes and accumulation of ubiquitylated proteins (Moberg *et al.,* 2005; Thompson *et al.,* 2005; Vaccari and Bilder, 2005; Vaccari *et al.,* 2008). Interestingly, ESCRT mutation also results in a loss of epithelial cell polarity indicating that ESCRTs are important to maintain the polarised architecture of epithelial tissues (Figure 1.7) (Moberg *et al.,* 2005; Thompson *et al.,* 2005; Vaccari and Bilder, 2005; Herz *et al.,* 2006; Rodahl *et al.,* 2009b; Herz *et al.,* 2009; Vaccari *et al.,* 2009). In these mutant cells, aPKC is localised throughout the entire plasma membrane instead of being restricted to the apical membrane domain (Vaccari and Bilder, 2005). The mechanism responsible for this loss of apicobasal polarity is unclear, however, studies have demonstrated that the polarity protein Crumbs may be important. In Tsg101 mutant cells, Crumbs is mislocalised from the apical membrane to aberrant endosomes (Moberg *et al.,* 2005; Gilbert *et al.,* 2009). Overexpression of Crumbs has been shown to disrupt apicobasal polarity and drive neoplastic transformation (Lu and Bilder, 2005) and therefore, it is suggested that the intracellular accumulation of Crumbs may contribute to the polarity defects observed in ESCRT mutant cells (Vaccari and Bilder, 2009).

Mutation of ESCRTs in *Drosophila* also results in overproliferation, although the mechanisms responsible for this appear to differ depending on the context of the mutant tissue. The majority of studies have analysed the mechanism underlying this overproliferation in mosaic imaginal discs whereby ESCRT mutant cells are surrounded by wild type cells. In these tissues the ESCRT mutant cells do not overproliferate. Instead ESCRT mutation results in the overproliferation of surrounding wild type cells, despite these cells displaying a normal epithelial morphology (Figure 1.7B). Consequently, the resulting adult tissue is enlarged but is mainly comprised of wild type cells (Moberg *et al.,* 2005; Thompson *et al.,* 2005; Vaccari and Bilder, 2005; Herz *et al.,* 2006; Herz *et al.,* 2009; Rodahl *et al.,* 2009b; Vaccari *et al.,* 2009).

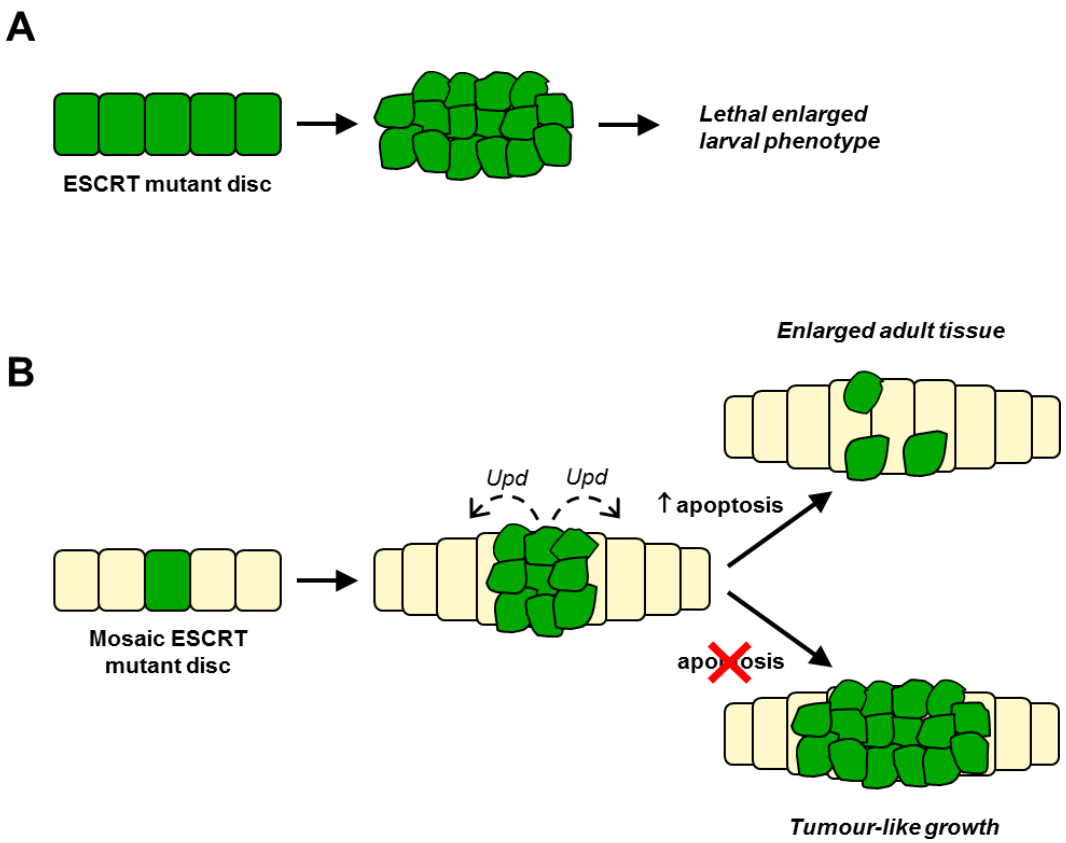


***Figure 1.7*** **ESCRT proteins act as tumour suppressors in *Drosophila*. (A)** *Drosophila* imaginal discs composed almost entirely of ESCRT mutant cells lose polarity and form large masses lacking normal epithelial morphology. Mutants die as enlarged larvae. **(B)** In *Drosophila* mosaic imaginal discs, whereby mutant cells are surrounded by wild type cells, ESCRT mutant cells lose epithelial polarity and organisation. Despite retaining polarity, surrounding wild type cells overproliferate due to increased Notch activation in mutant cells resulting in ectopic production of the secreted growth factor Unpaired (Upd). Eventually mutant cells are eliminated via apoptosis and therefore, the resulting enlarged adult tissue is composed mainly of wild type cells. However, if apoptosis is inhibited mutant cells overproliferate and form tumour-like growths capable of metastasis (Moberg *et al.,* 2005; Thompson *et al.,* 2005; Vaccari and Bilder, 2005; Herz *et al.,* 2006).

This non-cell autonomous proliferation is attributed to endosomal accumulation of Notch in ESCRT mutant cells resulting in increased Notch signalling (Thompson *et al.,* 2005; Vaccari and Bilder, 2005; Herz *et al.,* 2006; Herz *et al.,* 2009; Vaccari *et al.,* 2009). Interestingly Notch can be activated in a ligand-independent manner although the mechanism of this is presently unclear (Thompson *et al.,* 2005; Vaccari *et al.,* 2008; Vaccari and Bilder, 2009). Steady state levels of Notch are maintained by continuous turnover of unliganded

Notch via endocytic trafficking (Sakata *et al.,* 2004). In ESCRT mutant cells it appears that Notch trafficking is blocked and consequently the unliganded receptor accumulates within enlarged endosomes. Notch is activated upon cleavage by γ-secretase, the activity of which is optimal at endosomal pH (Pasternak *et al.,* 2003). Therefore, it is possible that Notch activation is due to γ-secretase-mediated cleavage of unliganded Notch which has accumulated within ESCRT mutant cells (Thompson *et al.,* 2005; Vaccari *et al.,* 2008; Vaccari and Bilder, 2009). The consequence of increased Notch activity in ESCRT mutant cells is ectopic production of the secreted growth factor, Unpaired (Upd). This then induces proliferation of surrounding wild type cells via paracrine activation of the Jak-STAT signalling pathway (Thompson *et al.,* 2005; Vaccari and Bilder, 2005; Herz *et al.,* 2006; Herz *et al.,* 2009; Gilbert *et al.,* 2009; Vaccari *et al.,* 2009).

In contrast, in imaginal discs composed almost entirely of ESCRT mutant cells, mutant cells overproliferate to form large masses lacking normal epithelial morphology which are characteristic of neoplastic tumours (Figure 1.7A). The resulting mutant larvae are enlarged and will eventually die. This neoplastic growth is thought to be due to an extended period of proliferation rather than an increased growth rate and therefore suggests that ESCRT mutant cells are unable to respond to signals which usually sense and restrict organ size (Moberg *et al.,* 2005; Vaccari and Bilder, 2005; Herz *et al.,* 2009; Vaccari *et al.,* 2009). The mechanism responsible for this overproliferation is currently unknown although it has been suggested that increased mitogenic signalling may play a role (Vaccari and Bilder, 2009). For example, EGFR accumulates in ESCRT mutant cells and consequently signalling is sustained (Jekely and Rorth, 2003; Lloyd *et al.,* 2006; Vaccari *et al.,* 2009). EGFR signalling is important for regulation of proliferation and increased signalling can induce overproliferation and is often linked to tumourigenesis (Kim and Choi, 2010). Therefore, sustained EGFR activation may contribute to the overgrowth associated with ESCRT disruption in *Drosophila.*

Another mechanism which may account for the overproliferation of ESCRT mutant cells is increased Notch activity. As in mosaic ESCRT mutant discs, endosomal accumulation and increased activation of Notch is observed when

the disc is almost entirely mutant for ESCRTs (Vaccari *et al.,* 2008). Whether this increase in Notch activity can induce cell-autonomous overproliferation remains to be established. Therefore, ESCRT mutation appears to affect multiple mitogenic signalling pathways and further research will be important to determine the contribution of these pathways and potentially others to the phenotype induced by ESCRT disruption.

***The Importance of Apoptosis***

In mosaic ESCRT mutant imaginal discs studies found that ESCRT mutant cells are eventually eliminated via apoptosis (Thompson *et al.,* 2005; Herz *et al.,* 2006; Rodahl *et al.,* 2009b). Therefore, the mutant cells only seem to contribute to a small proportion of the resulting overgrown tissue. Strikingly, if apoptosis is blocked ESCRT mutant cells undergo extensive overproliferation and form neoplastic tumours capable of metastasis (Thompson *et al.,* 2005; Herz *et al.,* 2006; Rodahl *et al.,* 2009b). This suggests that when ESCRT mutant cells are surrounded by wild type cells, activation of apoptotic pathways overrides any potential increase in mitogenic signalling, therefore, hindering the proliferative capacity of ESCRT mutant cells.

Studies have demonstrated that apoptosis of ESCRT mutant cells is induced by at least two pathways, one mediated by c-Jun N-terminal kinase (JNK) signalling and another mediated by Hid/Diap1/Dronc/Ark (Herz *et al.,* 2006; Rodahl *et al.,* 2009b; Vaccari and Bilder, 2009). Hippo signalling has been suggested to function as an upstream regulator of these two apoptotic pathways as inactivation of Hippo signalling in ESCRT mutant cells completely blocks cell death (Herz *et al.,* 2006). Interestingly, Hippo signalling is important for a wide range of cellular processes including cell proliferation and polarity (Genevet and Tapon, 2011; Halder and Johnson, 2011). JNK, a member of the mitogen-activated protein (MAP) kinase family, is also thought to have roles in cell survival and proliferation in addition to inducing apoptosis (Weston and Davis, 2002; Bode and Dong, 2007). Therefore, these signalling pathways represent potential mechanisms to link the apoptotic, proliferative and polarity defects observed upon disruption of the ESCRT machinery in *Drosophila* (Vaccari and Bilder, 2009).

It is interesting that when the entire imaginal disc is mutant for ESCRTs, mutant cells are not apoptotic. The mechanism which results in this contrasting behaviour of ESCRT mutant cells is unknown, however, it is possible that at the boundaries of wild type and mutant cells signalling discontinuities occur which may influence cell behaviour. For example, activation of JNK-mediated apoptosis has been observed when morphogenic gradients between adjacent cells are disrupted in developing *Drosophila* imaginal discs (Adachi-Yamada and O'Connor, 2002). It is also important to note that Vps25 mutation has been shown to increase levels of Diap1, an inhibitor of apoptosis, in wild type cells surrounding ESCRT mutant clones (Herz *et al.,* 2006). Therefore, loss of ESCRT function may confer apoptotic resistance and enhance the survival of surrounding wild type tissue whilst at the same time, apoptotic pathways are activated in the mutant cells.

Therefore, these studies have demonstrated that disruption of the ESCRT machinery can lead to loss of cell polarity and self-sufficiency in growth signalling, two important hallmarks of cancer (Hanahan and Weinberg, 2011). Data suggests that ESCRT function is required for trafficking of important regulators of epithelial cell polarity and proliferation in *Drosophila* and as a result, ESCRT proteins have been classified as potential tumour suppressors (Vaccari and Bilder, 2009).

### 1.5.2. ESCRTs and Cancer in Vertebrates

Although recent studies have elucidated important roles for the ESCRT proteins within regulation of cell polarity and tumourigenesis in *Drosophila*, the situation in mammalian cells is still unclear. However, there is emerging evidence that genes identified as tumour suppressors in *Drosophila* have similar roles in mammals (Stuffers *et al.,* 2009a).

#### *Tumour Susceptibility Gene 101: True or False?*

The ESCRT-I protein, Tsg101 was originally identified in mice, whereby knockout of the gene resulted in cellular transformation of mouse fibroblasts and formation of metastatic tumours in nude mice (Li and Cohen, 1996). However, subsequent mice knockout studies have failed to support a tumour

suppressor function of Tsg101. Null mutation of the *Tsg101* gene in mice results in early embryonic lethality whereas heterozygous mutation does not affect development (Ruland *et al.,* 2001; Wagner *et al.,* 2003). In conditional knockout mice, whereby *Tsg101* was deleted in mammary epithelial cells, reduced proliferation and increased cell death was observed resulting in impaired mammary development during lactation (Wagner *et al.,* 2003). Despite these effects, tumour formation was not observed in either heterozygous complete or tissue-specific *Tsg101* knockout mice monitored over two years (Wagner *et al.,* 2003). Therefore, these results suggest that Tsg101 is not acting as a tumour suppressor in mice, although it is possible that the full tumourigenic potential of Tsg101 is masked by the high level of cell death, similar to the situation observed in *Drosophila* mosaic ESCRT mutant tissues (Thompson *et al.,* 2005; Herz *et al.,* 2006).

Subsequent to its identification in mice, the human homologue of *Tsg101* was identified and mapped to chromosome 11, subbands p15.1-15.2, a region that often shows loss of heterozygosity in a variety of human cancers (Li *et al.,* 1997). Aberrant *Tsg101* transcripts have been observed in various tumours including breast (Lee and Feinberg, 1997), cervical (O'Boyle *et al.,* 1999) and small cell lung cancer (Oh *et al.,* 1998), although no genomic deletions or mutations have been observed. In addition, reduced expression of Tsg101 protein has been observed in ovarian and endometrial tumours (Bennett *et al.,* 2001). Conversely, overexpression of Tsg101 has been associated with breast (Oh *et al.,* 2007), thyroid (Liu *et al.,* 2002) and ovarian cancers (Young *et al.,* 2007). Furthermore, one study found that reduction of Tsg101 inhibited tumour cell growth in prostate and breast cancer cell lines (Zhu *et al.,* 2004), suggesting that Tsg101 could also exhibit oncogenic properties. Therefore, the role of Tsg101 in human cancers is somewhat controversial and a clear role for this ESCRT protein within the process of tumourigenesis in vertebrates is still to be confirmed.

### *Expression of Other ESCRT Proteins in Human Tumours*

There is evidence to suggest that other components of the ESCRT machinery act as tumour suppressors within human cancer models. Reduced expression of the ESCRT-I component, Vps37A is found in hepatocellular and ovarian

carcinomas. Knockdown of this protein increased cell growth and invasive abilities of both heptatocellular and ovarian cancer cell lines *in vitro* (Xu *et al.,* 2003; Bache *et al.,* 2004; Wittinger *et al.,* 2011). In addition, Vps37A knockdown in an ovarian cancer cell line resulted in increased tumour growth in a mouse xenograft model (Wittinger *et al.,* 2011). Furthermore, a study by Li and colleagues demonstrated that silencing of the ESCRT-III component, CHMP1A, resulted in cellular transformation and tumour formation *in vivo*, as well as increased growth of human pancreatic tumour cells *in vitro* (Li *et al.,* 2008). In contrast with these studies, overexpression of Hrs, an ESCRT-0 component, has been observed in stomach, colon, liver, cervix and melanoma tumour samples. In addition, Hrs was required to maintain tumourigenic properties of HeLa cells, suggesting that Hrs is an oncogenic factor which may play a role in determining the malignancy of cancer cells (Toyoshima *et al.,* 2007).

In summary the role of ESCRTs in human cancer remains unclear. Although various studies have associated reduced ESCRT function with tumourigenesis, increased expression of ESCRT proteins also seems to enhance tumourigenicity. It has been suggested that overexpression of ESCRTs may have a dominant negative effect (Vaccari and Bilder, 2009), however, this is yet to be confirmed.

***Potential Roles of ESCRTs in Tumourigenesis***

In *Drosophila,* studies suggest that ESCRTs act as tumour suppressors by regulating epithelial cell polarity and growth signalling. It is tempting to speculate that this could also be true in mammalian tissues. Indeed, signalling pathways affected by ESCRT mutation in *Drosophila* have been linked to tumour formation in humans. Firstly, EGFR has been shown to play an important role in tumourigenesis with expression observed in the majority of human carcinomas (Normanno *et al.,* 2006; De Luca *et al.,* 2008). Furthermore, mutations in EGFR occur frequently in lung and colorectal cancers and inhibitors of EGFR, such as gefitinib, are used therapeutically for the treatment of non-small cell lung cancer (Paez *et al.,* 2004; Grandal and Madshus, 2008; Kim and Choi, 2010). The Notch signalling pathway has also been implicated in a variety of human cancers (Roy *et al.,* 2007). The best studied example of oncogenic Notch signalling is in T-acute lymphoblastic leukemia/lymphoma (T-

ALL), but Notch upregulation has also been associated with colon and breast cancers (Reedijk *et al.,* 2005; Grabher *et al.,* 2006; Meng *et al.,* 2009).

In addition to its role in apoptosis, JNK signalling has also been implicated in promoting cell survival and proliferation (Davis, 2000; Bode and Dong, 2007). Evidence suggests that JNK plays an important role in tumourigenesis, for example, JNK activity has been reported to be elevated in glioblastomas (Tsuiki *et al.,* 2003; Bode and Dong, 2007). Interestingly, Hrs and Tsg101 have been shown to be required for lysosomal localisation and degradation of the transcription factor Jun (Ikeda and Kerppola, 2008). Jun is a major substrate for JNK and has also been implicated in carcinogenesis (Bode and Dong, 2007), for example the *v-jun* oncogene has a longer half-life that is thought to contribute to cell transformation (Treier *et al.,* 1994). Finally, the possibility of aberrant Hippo signalling in *Drosophila* ESCRT mutants may be relevant to human carcinogenesis as deregulation of various components of the Hippo pathway is expected to cause defects in cell growth, often resulting in tumour formation (reviewed in Zeng and Hong, 2008; Chan *et al.,* 2011).

The other major phenotype routinely observed upon ESCRT disruption in *Drosophila* was a loss of epithelial cell polarity. As discussed previously, endocytosis is thought to be important for regulation of epithelial polarity in mammalian tissues, however, the role of ESCRTs in this process has not been studied. Therefore, it is possible that ESCRT proteins function as tumour suppressors in vertebrates and similar mechanisms of tumourigenesis identified in *Drosophila* may also be important within mammalian tumour formation and progression.

## 1.6. Thesis Aims

The overall aim of this thesis is to determine whether ESCRT proteins function as tumour suppressors in mammalian epithelial tissues. Specifically, the importance of ESCRT proteins in the regulation of mammalian epithelial cell polarity and growth will be investigated. The mechanisms underlying any regulatory functions will also be explored. This study will provide important insight into the role of endocytic trafficking within the maintenance of mammalian epithelial tissues and may implicate impaired endocytosis as a contributing factor to the process of tumour formation, maintenance and progression.

# CHAPTER TWO

# 2. MATERIALS AND METHODS

## 2.1. Materials

### 2.1.1. Reagents

Unless otherwise specified, all chemicals and general laboratory reagents were of molecular biology grade and were purchased from Sigma-Aldrich or ThermoFisher Scientific.

***Cell Culture Buffers:***

Caco-2 Growth Media

Dulbecco's Modified Eagle Medium (DMEM) (4.5g/L glucose, without L-glutamine; BE12-614F) supplemented with 20% (v/v) fetal bovine serum (FBS) (heat inactivated; DE14-801FH), 2mM L-glutamine (BE17-605E), 1X non-essential amino acid solution (NEAA) (BE13-114E), 100U/ml penicillin, 100µg/ml streptomycin (DE17-602F) (all Lonza) and 10mM Hepes, pH 7.4 (in $dH_2O$, sterile filtered; Sigma).

Caco-2 Antibiotic-Free Media

As Caco-2 growth media but lacking penicillin/streptomycin.

Caco-2 Serum-Free Media

As Caco-2 growth media but lacking FBS and penicillin/streptomycin.

Dulbecco's Phosphate Buffered Saline (DPBS)

1X DPBS without calcium and magnesium purchased from Lonza (17-512F).

***Cell Biology Buffers:***

Phosphate Buffered Saline (PBS)

12.5 mM $Na_2HPO_4.12H_2O$, 154 mM NaCl, pH 7.2.

Cell Lysis Buffer

50mM Tris-HCl pH 8, 150mM NaCl, 1% NP40, 0.5% sodium deoxycholate and 10µM protease inhibitor cocktail for mammalian cell extracts (Sigma, P8340).

4% Paraformaldehyde (PFA)

4% PFA (w/v) was dissolved in PBS by heating at 65°C, with stirring. When dissolved and cooled, it was adjusted to pH 7.4 and stored at -20°C until required.

Immunoprecipitation (IP) Buffer

50mM Tris-HCl pH 7.4, 200mM NaCl, 0.5% (w/v) sodium deoxycholic acid, 1% (v/v) Triton X-100, 0.1% (w/v) SDS, 1mM EDTA.

10X Wash Buffer (Caco-2 Cysts)

1.3M NaCl, 70mM dibasic heptahydrate sodium phosphate, 30mM monobasic monohydrate sodium phosphate, 77mM sodium azide, 1% (w/v) BSA, 2% (v/v) Triton-X 100, 0.4% (v/v) Tween-20, pH 7.4.

Mowiol Mounting Medium

2.4g Mowiol 4-88 (Calbiochem, 475904) was mixed with 6g glycerol and 6ml $dH_2O$ and incubated for 2 h at RT, stirring. 12ml 0.2M Tris, pH 8.5 was added and the solution was heated to 53°C until Mowiol 4-88 had dissolved. Solution was centrifuged at 5000g for 20 min to remove any undissolved solid and stored in 1ml aliquots at -20°C until required.

***Western Blotting Buffers:***

Resolving Gel Buffer

1.5M Tris-HCl pH 8.8, 0.4% (w/v) SDS.

Stacking gel buffer

0.5 M Tris-HCl pH 6.8, 0.4% (w/v) SDS.

3X Sample Buffer

187.5mM Tris-HCl pH 6.8, 6% (w/v) SDS, 30% (w/v) glycerol, 0.03% (w/v) bromophenol blue. Prior to use, Dithiothreitol (DTT) was added to a final concentration of 100mM.

SDS Electrophoresis Buffer

25mM Tris-HCl pH 8.3, 0.2M glycine, 0.1% (w/v) SDS.

Transfer Buffer

48mM Tris-HCl pH 8.8, 39mM glycine, 0.0375% (w/v) SDS, 20% (v/v) methanol.

Ponceau S Stain

0.1% (w/v) Ponceau S, 3% (w/v) trichloroacetic acid.

Tris-Buffered Saline containing Tween-20 (TBST)

10mM Tris-HCl pH 7.4, 154mM NaCl, 0.1% (v/v) Tween-20.

Blocking Buffer

5% (w/v) Marvel milk powder in TBST.

Enhanced Chemiluminescence (ECL) Reagent

Solution A: 100mM glycine (pH 10), 0.4mM luminol, 8mM 4-iodophenol.

Solution B: 0.12% (w/v) hydrogen peroxide in water.

***Biotinylation Assay Buffers:***

Phosphate Buffered Saline with Calcium and Magnesium (PBS/CM)

PBS supplemented with 0.9mM calcium chloride and 0.33mM magnesium chloride purchased from Lonza (BE17-513Q).

Tris-Buffered Saline with Calcium (TBS/C)

50mM Tris-HCl pH 8.6, 100mM NaCl, 2.5mM $CaCl_2$.

Wash Buffer

50mM Tris-HCl pH 8.0, 150mM NaCl, 0.5% (v/v) Triton X-100, 0.1% (w/v) SDS, 5mM EDTA.

### 2.1.2. Antibodies

A list of antibodies used, supplier and dilutions for different applications is detailed in Table 2.1.

| | Antibody | Species | Source | Application/Dilution |
|---|---|---|---|---|
| PRIMARY | α-Tsg101 | mouse, monoconal | Abcam ab83 | WB - 1:1000 *(in 5% milk)* |
| | α-Vps25 (serum #6973) | rabbit, polyclonal | Gift (Dr Kate Bowers) | WB - 1:1000 *(in 5% milk)* |
| | α-β tubulin (clone TUB 2.1) | mouse, monoclonal | Sigma T4026 | WB - 1:5000 |
| | α-claudin-1* | rabbit, polyclonal | Zymed 59-9000 | WB - 1:2000 IF - 1:25 |
| | α-claudin-1 | mouse, monoclonal | Zymed 37-4900 | WB - 1:1000 |
| | α-claudin-4* | mouse, monoclonal | Zymed 32-9400 | WB - 1:1000 IF - 1:25 |
| | α-occludin* | mouse, monoclonal | Zymed 33-1500 | WB - 1:1000 IF - 1:25 |
| | α-ZO-1 | mouse, monoclonal | Zymed 33-9100 | IF - 1:25 |
| | α-ZO-1 | rabbit, polyclonal | Zymed 61-7300 | IF - 1:25 |
| | α-E-cadherin | mouse, monoclonal | Zymed 33-4000 | WB - 1:1000 IF - 1:25 |
| | α-desmoglein-2 | mouse, monoclonal | Abcam ab14415 | IF - 1:25 |
| | α-JAM-A | mouse, monoclonal | Zymed 36-1700 | IF - 1:50 |
| | α-PKC-ζ (C-20) | rabbit, polyclonal | Santa Cruz sc-216 | IF - 1:200 |
| | α-DppIV (CD26) | mouse, monoclonal | Abcam ab3154 | IF - 1:50 |
| | α-ubiquitin (mono- & polyubiquitinated conjugates, clone FK2) | mouse, monoclonal | Enzo Life Sciences BML-PW8810 | WB - 1:1000 IF - 1:500 |
| | α-EEA1 | mouse, monoclonal | BD Biosciences 610457 | IF - 1:500 |
| | α-EEA1 | rabbit, polyclonal | Abcam ab2900 | IF - 1:500 |

| | Antibody | Species | Source | Application/Dilution |
|---|---|---|---|---|
| PRIMARY | α-CD63 | mouse, monoclonal | Santa Cruz sc5275 | IF - 1:1000 |
| | α-M6PR | mouse, monoclonal | Abcam ab2733 | IF - 1:200 |
| | α-TfR | mouse, monoclonal | Zymed 13-6800 | IF - 1:50 |
| | α-Lamp 1 | mouse, monoclonal | Gift (Dr Scott Lawrence) | IF - 1:8000 |
| | α-active caspase 3 | rabbit, polyclonal | Abcam ab13847 | IF - 1:100 |
| | α-phospho-histone H3 | mouse, monoclonal | Abcam ab14955 | IF - 1:500 |
| | α-p44/42 MAPK (Erk1/2) | rabbit, monoclonal | Cell Signalling 4695 | WB - 1:1000 |
| | α-phospho-p44/42 MAPK (p-Erk1/2) | mouse, monoclonal | Cell Signalling 9106S | WB - 1:2000<br>IF - 1:200 |
| | α-SAPK/JNK | rabbit, polyclonal | Cell Signalling 9252 | WB - 1:1000 |
| | α-phospho-SAPK/JNK | mouse, monoclonal | Cell Signalling 9255S | WB - 1:2000 |
| | α-BrdU (part of labelling kit) | mouse, monoclonal | Roche 11 296 736 001 | IF - 1:10 |
| SECONDARY | α-mouse IgG (H+L) Alexa Fluor® 488 | goat, polyclonal | Molecular Probes A11001 | IF - 1:100 |
| | α-mouse IgG (H+L) Alexa Fluor® 546 | goat, polyclonal | Molecular Probes A11003 | IF - 1:100 |
| | α-rabbit IgG (H+L) Alexa Fluor® 488 | goat, polyclonal | Molecular Probes A11008 | IF - 1:100 |
| | α-rabbit IgG(H+L) Alexa Fluor® 546 | goat, polyclonal | Molecular Probes A11010 | IF - 1:100 |
| | α-rabbit IgG (H+L)-HRP | goat, polyclonal | Pierce 31460 | WB - 1:5000 |
| | α-mouse IgG (Fc specific)-HRP | goat, polyclonal | Sigma A2554 | WB - 1:5000 |

***Table 2.1*** **List of antibodies used**. Supplier and catalogue number of antibodies are detailed, dilutions are of original supplied stocks. For the conditions of antibody utilisation, refer to main text. For IF, antibodies which required fixation in methanol are indicated by '*', 4% PFA fixation was used for all other antibodies (see section 2.2.8 for details). Abbreviations: WB = Western Blotting, IF = Immunofluorescence.

### 2.1.3. RNA Interference

Tsg101 and Vps25 proteins were depleted using the small interfering RNA (siRNA) oligonucleotides detailed in Table 2.2 and 2.3. All siRNA was purchased from Dharmacon.

| Target Protein | Catalogue Number | Target sequence (5'→3') |
|---|---|---|
| Tsg101 | L-003549-00 | I1: CCGUUUAGAUCAAGAAGUA<br>I2: CUCCAUACCCAUCCGGAUA<br>I3: CCACAACAAGUUCUCAGUA<br>I4: CCAAAUACUUCCUACAUGC |
| Vps25 | L-004699-01 | I1: GAUCAUCACUGUCAGCGAU<br>I2: ACGUCAAGCUACAGCGAAA<br>I3: CAGUCCAGCAUGACGGUGA<br>I4: ACCUCGAGUGGUUGGAUAA |
| Non Targeting Control | D-001810-10 | N/A |

***Table 2.2*** **ON-TARGET*plus* SMARTpool siRNA used for transient knockdown of Tsg101 and Vps25.** Tsg101 and Vps25 were depleted via transfection with ON-TARGET*plus* SMARTpool siRNA, composed of four separate siRNA target sequences. ON-TARGET*plus* Non-Targeting Pool was used as a control.

| Name | Catalogue Number | Target sequence (5'→3') |
|---|---|---|
| Tsg101 | J-003549-06 | (I1) CCGUUUAGAUCAAGAAGUA |
| Tsg101 A1 | J-003549-07 | (I2) CUCCAUACCCAUCCGGAUA |
| Tsg101 A2 | J-003549-07<br>J-003549-08 | (I2) CUCCAUACCCAUCCGGAUA<br>(I3) CCACAACAAGUUCUCAGUA |

***Table 2.3*** **ON-TARGET*plus* siRNA sequences used for Tsg101 knockdown.** Tsg101 knockdown was carried out using a single siRNA oligonucleotide sequence for the majority of experiments. Verification of knockdown phenotype was carried out using an alternate single Tsg101 siRNA oligonucleotide (A1) and a mixture of two Tsg101 siRNA oligonucleotides (A2). All Tsg101 siRNA sequences were part of the original SMARTpool, denoted I1 - I4 in Table 2.2.

## 2.2. Methods

### 2.2.1. Cell Culture

Caco-2 (human colorectal adenocarcinoma; HPA, 86010202) cells were cultured in Caco-2 complete growth media at 37°C in 5% $CO_2$. Cells were maintained in T75 flasks and passaged every 3-4 days, after reaching approximately 80% confluence. Cells were used between passages 40 to 60. Cells were routinely tested for mycoplasma contamination using MycoAlert® Mycoplasma Detection Kit (Lonza, LT07-218). All tissue cultured treated plasticware was purchased from Greiner Bio-One unless otherwise stated.

To plate cells for experimental conditions, cells were washed in DPBS and incubated with 1X trypsin (in DPBS; Lonza, BE02-007E) for approximately 10 min at 37°C, 5% $CO_2$, until detached. Trypsin was neutralised with Caco-2 antibiotic-free media and cell suspension was centrifuged at 200g for 3 min. Cells were resuspended in antibiotic-free media and counted using a haemocytometer (Fisher Scientific). Cells were diluted to the desired concentration in antibiotic-free media, plated to either 35mm dishes or 13mm glass coverslips (Fisher Scientific, MNJ-500-010G) in 24-well plates and incubated at 37°C, 5% $CO_2$.

### 2.2.2. Phase Contrast Microscopy

Caco-2 cell morphology was monitored using a Nikon Eclipse TS100-F Inverted Microscope (10X or 20X objective). Images were obtained using a Nikon CoolPix 5000 digital camera and were processed using Adobe Photoshop.

### 2.2.3. Transfection with small interfering RNA (siRNA)

Caco-2 cells were plated at 7.5 x $10^4$ cells/ml (unless otherwise indicated) onto either 35mm dishes (2ml per well), or 13mm glass coverslips (for immunofluorescence, 1ml per coverslip) and incubated in antibiotic-free media at 37°C, 5% $CO_2$ for approximately 4 h to adhere. 2µM siRNA (in DPBS) and DharmaFECT 1 (Dharmacon, T-2001) were diluted in serum-free media (SFM) as detailed below (Table 2.4) and incubated for 5 min at RT. The two solutions were mixed and incubated for 20 min at RT. The required volume of antibiotic-free media was added and the transfection mixture was added to cells. Cells

were incubated at 37°C, 5% $CO_2$ for the desired time period, changing media to complete growth media after 3 d.

| | Tube 1 (µl) | | | Tube 2 (µl) | | Antibiotic-free media (µl) | Final volume (µl) |
|---|---|---|---|---|---|---|---|
| | 20µM siRNA | DPBS | SFM | Dharma FECT-1 | SFM | | |
| 35mm dish | 10 | 90 | 100 | 4 (5) | 196 (195) | 1600 | 2000 |
| Coverslip | 2.5 | 22.5 | 25 | 1 (1.25) | 49 (48.75) | 400 | 500 |

***Table 2.4*** **Volumes of reagents required for transfection with siRNA oligonucleotides.** Solutions were prepared as detailed in methods using the volumes indicated. Transfection with Vps25 siRNA required an increased volume of DharmaFECT-1, as indicated in brackets.

### 2.2.4. Cell Lysis and Protein Quantification

Cells were washed once in ice-cold PBS and scraped into an appropriate volume of ice-cold cell lysis buffer containing mammalian protease inhibitors. Cell lysates were pulse sonicated on ice, five times for 3 s and incubated for 30 min at 4°C, with rotation. Lysates were centrifuged at 15000g for 15 min at 4°C to remove nuclear debris and stored at -20°C until required for further analysis.

Protein quantification of cell lysates was carried out with the colorimetric BCA (bicinchoninic acid) Protein Assay Kit (Pierce, 23227) using a bovine serum albumin (BSA) standard curve (0, 1, 2, 4, 6, 8, 10µg BSA). BCA solution (reagent A + 1:50 dilution reagent B) was freshly prepared and 200µl was added to each well of a 96-well flat bottom plate (Iwaki) containing standard or test samples (2µl). All samples were carried out in triplicate. The plate was incubated for 30 min at 37°C and absorbance was measured at 565nm using a Spectra Rainbow Thermo microplate spectrophotometer (Tecan). Results were analysed using Microsoft Excel and unknown protein concentrations were calculated.

### 2.2.5. SDS-PAGE and Immunoblotting

Proteins were separated according to size using sodium dodecyl sulfate polyacrylamide gel electrophoresis (SDS-PAGE). Equal amounts of lysate (10-25µg protein) was added to 1X sample buffer (final concentration) containing 100mM DTT and incubated for 5 min at 95°C. Polyacrylamide gels of 1mm thickness were prepared using acrylamide/bis-acrylamide (30% (w/v)

acrylamide: 0.8% (w/v) bis-acrylamide) (ProtoGel; National Diagnostics, EC-890) and gel buffers previously described. Polymerisation of the gels was induced by the addition of 10% (w/v) ammonium persulphate (APS; Sigma) and N,N,N,N'-tetramethylethylenediamine (TEMED; Sigma). The gels were composed of a 12% resolving gel (pH 8.8) and a lower percentage stacking gel (pH 6.8). The composition of the resolving and stacking gels is given in Table 2.5. Gels were assembled into the mini PAGE chamber (ATTO Corporation, model AE-6450) and samples (25µl) were loaded alongside 8µl Broad Range Prestained Protein Marker (New England Biolabs, P77085). Gels were run at 40 mA/gel for approximately 50 min.

| Solution | Resolving Gel (12%) | Stacking Gel |
|---|---|---|
| Protogel | 3 ml | 850 µl |
| Resolving gel buffer | 2.5 ml | - |
| Stacking gel buffer | - | 1.25 ml |
| $dH_20$ | 2 ml | 1.875 ml |
| 10% APS | 50 µl | 20 µl |
| TEMED | 4 µl | 5 µl |

***Table 2.5.*** **Composition of SDS-PAGE gels.** Volumes are for one 90 x 80 x 1mm gel.

Separated proteins were then transferred to Biotrace™ Pure Nitrocellulose Blotting Membrane (Pall Life Sciences, 66485). Filter papers (Extra thick, 7.5x10cm; Bio-Rad, 1703965) and the nitrocellulose membrane were pre-soaked in transfer buffer and assembled onto the HorizBlot semi-dry transfer apparatus (ATTO Corporation, model AE-6675L) in the following order: filter paper, nitrocellulose membrane, gel, filter paper. Air bubbles were carefully removed and transfer of proteins was carried out at 54 mA/gel for 110 min. Following the transfer, nitrocellulose membranes were briefly incubated with Ponceau S stain to confirm the presence of transferred proteins.

Detection of specific proteins transferred to nitrocellulose membrane was performed via immunoblotting. Membranes were rinsed with TBST to remove Ponceau S stain and incubated in blocking buffer for 1 h at RT. Membranes were then incubated with primary antibodies diluted in 1% (w/v) BSA (in TBST) (unless otherwise stated) for either 2 h at RT or overnight at 4°C. The

appropriate species-specific horseradish-peroxide (HRP)-conjugated secondary antibody was diluted in blocking buffer and added to membranes for 1 h at RT. Following all antibody incubations, membranes were washed 6 times in TBST, 5 min per wash. To visualise proteins, membranes were incubated for 5 min at RT with either equal volumes of Solution A and B of the ECL Reagent (homemade), or Luminata™ Forte HRP Substrate (Millipore, WBLUF0500). Proteins were visualised and quantified using an Optichem detector with associated software (Ultra Violet Products).

### 2.2.6. Immunoprecipitation

Caco-2 cells were plated onto 35mm dishes, transfected with siRNA as detailed previously (section 2.2.3) and incubated for 7 d at 37°C, 5% $CO_2$. Cells were lysed in 100µl cell lysis buffer as previously described (section 2.2.4) and 10µl of total lysate was taken from each sample for use as a loading control. The remaining lysate was used for immunoprecipitation of claudin-1. Protein A-coupled Sepharose Beads (Amersham Biosciences, 17-0780-01) were prepared as follows. 0.1g sepharose beads were suspended in 20ml $dH_2O$ and allowed to swell for 30 min. Beads were centrifuged at 1000g for 5 min at RT. Beads were washed three times by resuspension and centrifugation using IP Buffer. A slurry was prepared containing 75% beads and 25% IP Buffer. Prior to immunoprecipitation, a pre-clearing step was performed to reduce non-specific binding. 80µl cell lysate was added to 80µl IP Buffer, 1µg rabbit IgG (Sigma, I5006) and 50µl 75% slurry and the sample was incubated for 2 h at 4°C, with rotation. Concurrently, a coupling reaction was prepared to allow binding of the antibody to the sepharose beads. 1µg rabbit anti-claudin-1 was added to 500µl IP Buffer and 50µl 75% slurry and the sample was incubated for 2 h at 4°C, with rotation. Both samples were then centrifuged at 1000g for 3 min. The supernatant from the pre-clearing sample was added to the sepharose beads from the coupling reaction and the sample was incubated overnight at 4°C, with rotation in order to isolate claudin-1 protein from the cell lysate. Beads were washed 5 times by centrifuging at 1000g for 3 min and resuspending in 1ml cold IP Buffer. Finally, beads were resuspended in 1X sample buffer (final concentration) containing 100mM DTT and incubated for 15 min at 95°C to release isolated proteins from the beads. Samples were centrifuged at 1000g for 3 min and supernatant was collected. Samples were then analysed using

SDS-PAGE and immunoblotting (see section 2.2.5). Antibodies used were mouse anti-claudin-1, to verify that the immunoprecipitation was successful, and mouse anti-ubiquitin, to analyse the amount of ubiquitinated claudin-1 present. Total cell lysates were included alongside immunoprecipitation samples to serve as loading controls.

To ensure the immunoprecipitation was specific for claudin-1, the following controls were also included: a no antibody control and an IgG control, in which the rabbit anti-claudin-1 was replaced with $dH_2O$ or 1µg rabbit IgG, respectively.

### 2.2.7. Biotinylation Trafficking Assays

The biotinylation assay to study endocytosis and recycling of tight junction proteins was modified from a method described previously (Nishimura and Sasaki, 2008). See Figure 2.1 for a schematic of the process.

#### *Endocytosis Assay*

Prior to carrying out the biotinylation assay, Caco-2 cells were plated at 7.5 x $10^4$ cells/ml onto 35 mm dishes and cultured for 7 d at 37°C, 5% $CO_2$. Cells were transferred to ice and washed with PBS supplemented with calcium and magnesium (PBS/CM). Cells were then incubated with 1ml of the cleavable non-membrane permeable sulfo-NHS-SS-biotin (Pierce; in PBS/CM) at a concentration of 0.5mg/ml for 30 min on ice to label all cell surface proteins. Free biotin was quenched with 50mM $NH_4Cl$ (Sigma) (in PBS/CM) for 3 x 5 min washes on ice. For the endocytosis assay, 2ml pre-warmed complete growth medium was added and cells returned to 37°C, 5% $CO_2$ for indicated times. Cells were then transferred to ice to stop endocytosis, and surface (non-endocytosed) biotin was stripped by reduction with 100mM 2-mercaptoethanesulfonate (MESNA; Sigma) (in tris-buffered saline supplemented with calcium; TBS/C) for 3 x 10 min washes on ice. Internalised biotinylated cargo was protected from biotin stripping with MESNA by an intact plasma membrane. Free –SH groups were then quenched by incubating cells with 5 mg/ml iodoacetamide (Sigma) (in PBS/CM) for 3 x 5 min washes on ice. Following the endocytosis assay, cells were either lysed to determine amount of protein endocytosed (‘endocytosis’ sample) or used for the subsequent recycling assay.

Alongside the ‘endocytosis’ sample, a number of controls were also carried out. Firstly, a ‘no biotin’ condition was included to which no sulfo-NHS-SS-biotin was added. This ensured the neutravidin pull down was specific for biotinylated proteins. To ensure the stripping procedure was efficient, a ‘surface strip’ condition was included whereby biotin was stripped from the cell surface immediately after incubation. Lastly, the total amount of biotinylated protein at the cell surface (‘surface label’) was determined by lysing cells after incubation with biotin.

***Recycling Assay***

For the recycling assay, 2ml pre-warmed complete growth medium was added and cells were returned to 37°C, 5% $CO_2$ for 20 min. This allows for potential recycling of internalised biotinylated proteins back to the cell surface. Cells were then transferred to ice, and surface biotin was stripped by reduction with 100mM MESNA (in TBS/C) for 3 x 10 min washes on ice. Free –SH groups were quenched by incubating cells with 5 mg/ml iodoacetamide (in PBS/CM) for 3 x 5 min washes on ice. Therefore, the remaining biotinylated protein is that which has endocytosed and not recycled back to the cell surface (‘recycling’ sample). To control for potential loss of biotinylated cargo via degradation rather than recycling, a ‘degradation control’ was included which lacked the second MESNA treatment. Thus any loss in biotinylated cargo at this step, relative to the ‘endocytosis’ step, would indicate a loss in signal due to degradation of cargo instead of recycling. The amount of recycled cargo is indicated by the difference in signal between the ‘degradation control’ and ‘recycling’ samples.

***Cell Lysis and Isolation of Biotinylated Proteins***

Cells were lysed in 100µl cell lysis buffer and protein concentration determined as previously described (see section 2.2.4). An equal amount of total lysate (10µg protein) was taken from each sample for use as a loading control. Remaining samples were diluted to equal protein concentrations (in 100µl cell lysis buffer) and biotinylated proteins were collected by incubation with 50µl Neutravidin beads (Pierce), rotating overnight at 4$^{o}$C. Beads were washed by centrifuging at 1000g for 2 min, 5 times with 1ml wash buffer and 3 times with 1ml PBS/CM. Sample buffer containing 100mM DTT was then added to beads and samples were incubated for 15 min at 95°C to release biotinylated proteins

from the beads. Samples were centrifuged at 1000g for 3 min and supernatant was collected. The amount of biotinylated proteins present in each sample was analysed using SDS-PAGE and immunoblotting for the protein of interest (see section 2.2.5). Total cell lysates were included alongside Neutravidin pull-downs to serve as a loading control. For quantification of the biotinylated proteins, the amount of protein was normalized to the respective total protein bands determined from total cell lysate samples.

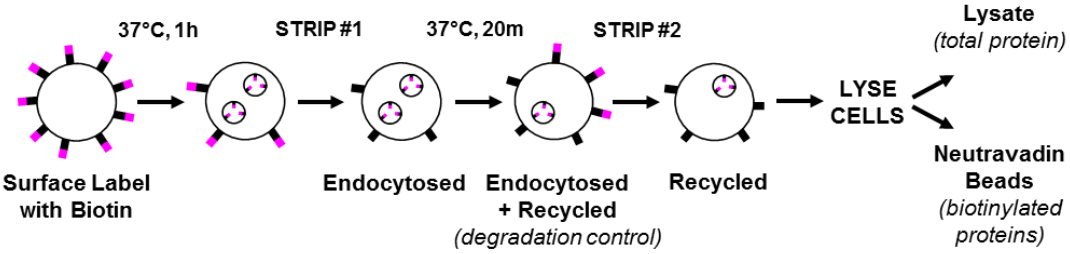


***Figure 2.1*** **Biotinylation Endocytosis and Recycling Assay.** Schematic to illustrate the steps involved. Cells were lysed at each step and levels of biotinylated protein was compared.

### 2.2.8. Cycloheximide Treatment

Caco-2 cells were plated at 7.5 x $10^4$ cells/ml onto 35 mm dishes and cultured for 7 d at 37°C, 5% $CO_2$. Cells were incubated with 2µg/ml cycloheximide (Sigma, C4859) diluted in antibiotic-free media for 20 min, 1 h, 6 h, 16 h or 24 h at 37°C, 5% $CO_2$. DMSO controls were carried out alongside. At each timepoint cells were lysed and processed for SDS-PAGE and immunoblotting to analyse levels of occludin, claudin-1 and connexion-43, which was used as a positive control (sections 2.2.4, 2.2.5).

### 2.2.9. Immunofluorescence

Cells were cultured on 13mm glass coverslips for the desired time. Prior to processing for immunofluorescence, media was removed and cells were washed twice in PBS. Depending on the antibodies used (see Table 2.1 for list of antibodies and conditions required), cells were fixed according to the following protocols. Following fixation, cells were either immediately processed for antibody staining or stored in PBS at 4°C until required.

***Fixation in 4% PFA***

Cells were fixed in 4% (w/v) paraformaldehyde (PFA) for 20 min at RT. Cells were washed twice in PBS and then permeabilised in ice-cold 100% Methanol for 5 min at -20°C, followed by two further PBS washes.

***Fixation in Methanol***

Cells were fixed and permeabilised in ice-cold 100% Methanol for 10 min at -20°C followed by two PBS washes.

***Antibody Staining***

Following fixation, cells were incubated in 10% FBS (v/v in PBS) for 30 min at RT to block non-specific binding sites. Cells were then washed twice in 2% FBS (v/v in PBS) and once in PBS, 3 min per wash. Primary antibodies diluted in 2% FBS were added and cells were either incubated for 2 h at RT or overnight at 4°C. Cells were incubated with species specific fluorophore-conjugated secondary antibodies for 1 h at RT, in the dark. After all antibody incubations cells were washed 3 x 5 min in 2% FBS and 3 x 5 min in PBS. Nuclei were stained using 1µg/ml DAPI (4',6-diamidino-2-phenylindole) (Sigma, D9564) for 10 min at RT, in the dark. Following a quick wash in PBS, cells were mounted onto glass slides using Mowiol Mounting Medium and allowed to dry at RT overnight, protected from light. Stained cells were examined on a Zeiss LSM510META laser-scanning confocal microscope (Plan-ApoChromat 63x/1.4 Oil DIC objective). Images were taken and processed using the LSM Image Browser Software (Zeiss) and Adobe Photoshop.

### 2.2.10. EGF Stimulation

Cells were serum starved overnight prior to EGF treatment. For immunofluorescence studies, cells were incubated in 500ng/ml EGF (Calbiochem, 324831) or EGF-Alexa Fluor® 555 diluted in SFM for 4 h at 37°C, 5% $CO_2$. Cells were washed in PBS and then processed as detailed previously (section 2.2.9). For pulse-chase experiments, cells were incubated in 500ng/ml EGF in SFM for 10 min on ice. Media was replaced with SFM and cells were incubated in SFM for 15 min, 1 h or 4 h at 37°C, 5% $CO_2$. Cells were then lysed and processed for SDS-PAGE and immunoblotting to analyse levels of p-Erk1/2 and total Erk1/2 (sections 2.2.4, 2.2.5).

### 2.2.11. Cysts

Caco-2 cells were plated at 1 x $10^5$ cells/ml into 35mm dishes, transfected with siRNA as detailed previously (section 2.2.3), incubated at 37°C, 5% $CO_2$ for 3 d. Cells were washed in DPBS, trypsinised and centrifuged at 200g for 3 min. Cells were resuspended in 300µl complete growth media and counted using a haemocytometer, including 0.2% (v/v) Trypan Blue (Sigma, T8154) to exclude dead cells. Cells were diluted to 3.5 x $10^5$ cells/ml in complete growth media. A cell:matrix mix was prepared on ice containing 5.8 x $10^4$ cells/ml, 0.02 M HEPES, pH 7.4, 1 mg/ml Collagen I (Inamed Biomaterials, 5409) and 40% Growth Factor Reduced BD Matrigel™ Matrix (BD Biosciences, 356230) (see Table 2.6). All solutions were kept on ice and tubes and pipette tips were pre-cooled to prevent the matrigel from solidifying. The cell:matrix mix was plated into an 8 chamber slide (BD Biosciences, 354108), 100µl per chamber, incubated at 37°C, 5% $CO_2$ for 1 h to solidify and overlaid with 300µl complete growth media. Cysts were allowed to develop for 7 d at 37°C, 5% $CO_2$, changing media every 3-4 d.

| Component | Volume (µl) | Final Concentration |
|---|---|---|
| 3.5 x $10^5$ cells/ml Caco-2 cell suspension | 41.4 | 5.8 x $10^4$ cells/ml |
| Caco-2 complete growth media | 20.3 | N/A |
| 1M HEPES, pH 7.4 | 5 | 0.02 M |
| Collagen I, 3 mg/ml | 83.3 | 1 mg/ml |
| Growth Factor Reduced BD Matrigel™ Matrix | 100 | 40 % |

***Table 2.6.*** **Composition of cell:matrix mix for culture of Caco-2 cell cysts.** Volumes given are sufficient for 2 wells of an 8 chamber slide, plating 100µl per well.

After 7 d culture, cysts were washed 3 x 5 min in PBS and treated with 5U/ml Collagenase VII (in PBS) (Sigma, C0773) for 15 min at RT. Cysts were washed in PBS then fixed in 4% (w/v) PFA for 30 min at RT. Cysts were washed 3 x 10 min with 1X wash buffer (in $dH_2O$) and incubated with blocking buffer (10% (v/v) FBS in 1X wash buffer) for 1 h at RT. Cysts were then incubated with primary antibodies diluted in blocking buffer overnight at 4°C, followed by incubation with species specific fluorophore-conjugated secondary antibodies diluted in blocking buffer for 1 h at RT, in the dark. Following all antibody incubations cysts were washed 3 x 20 min in 1X wash buffer. Cysts were rinsed 2 x 5 min in

PBS and post-fixed in 4% (w/v) PFA for 30 min at RT. Following a further 3 x 5 min washes with PBS, nuclei were stained with 1µg/ml DAPI for 30 min at RT. After a final rinse in PBS, cysts were mounted in Mowiol Mounting Medium and examined on a Zeiss LSM510 META laser-scanning confocal microscope (Plan-ApoChromat 63x/1.4 Oil DIC objective). Images were taken and processed using the LSM Image Browser Software (Zeiss) and Adobe Photoshop.

### 2.2.12. Transepithelial Resistance (TER) Measurements

Caco-2 cells were plated at 1 x $10^5$ cells/ml into 35mm dishes, transfected with siRNA as detailed previously (section 2.2.3) and incubated at 37°C, 5% $CO_2$ for 3 d. To plate onto filters, cells were washed in DPBS, trypsinised and centrifuged at 200g for 3 min. Cells were resuspended in 300µl complete growth media and counted using a haemocytometer, including 0.2% (v/v) Trypan Blue to exclude dead cells. Cells were diluted to 1.25 x $10^6$ cells/ml in complete growth media. Cells were plated in triplicate on Transwell® (Corning; 3470) permeable polyester filters (0.4µm pore size, 0.33$cm^2$ surface area), 200µl per filter (2.5 x $10^5$ cells/filter final density). Filter inserts were placed in a 24-well plate and 1ml complete growth media was added to each basal compartment. Cells were incubated at 37°C, 5% $CO_2$. TER was measured every 24 h for 4 d using a EVOM TER machine with an Endohm-6$^{TM}$ chamber (World Precision Instruments), changing media after every reading.

#### *Calcium Switch*

To induce disassembly followed by reassembly of cell-cell junctions, a calcium switch method was carried out. Following culture of Caco-2 cells on filters for 4 d, cells were washed in DPBS and incubated in calcium-free media (EMEM with Earle's BSS, with NEAA and L-glutamine, without calcium; Lonza, 06-174G) for 90 min at 37°C, 5% $CO_2$ to induce internalisation of cell-cell junction proteins. Following measurement of TER, media was replaced with complete growth media and cells were incubated at 37°C, 5% $CO_2$ to allow cell-cell junctions to reform. Recovery of TER was measured every hour for 5 h.

### 2.2.13. MTT Assay

Caco-2 cells were plated at 7.5 x $10^4$ cells/ml into 35mm dishes, transfected with siRNA as detailed previously (section 2.2.3) and incubated at 37°C, 5% $CO_2$ for the desired time period. To carry out the MTT assay, cells were washed

briefly in DPBS and incubated with 2ml 2.5mg/ml MTT (3-(4,5-Dimethyl-2-thiazolyl)-2,5-diphenyltetrazolium bromide) (Alfa Aesar, L11939) in phenol red-free media (DMEM with 4.5 g/L glucose, without L-glutamine or phenol red; Lonza, BE12-917F) for 1 h at 37°C, 5% $CO_2$. A control was included containing no cells. MTT solution was removed and cells were incubated with 1ml of isopropanol for 20 min at RT in the dark. The isopropanol solution was transferred to a 96-well flat bottomed clear plate, 100µl per well and absorbance was measured at 570nm using a Spectra Rainbow Thermo microplate spectrophotometer (Tecan). Results were analysed using Microsoft Excel, calculating mean absorbance for each condition and subtracting background absorbance obtained from no cell control.

### 2.2.14. Quantification of Cell Number

Caco-2 cells were stained with appropriate antibodies and nuclei stained with DAPI as detailed previously (section 2.2.8). Stained cells were examined on a Zeiss LSM510META laser-scanning confocal microscope (Plan-ApoChromat 63x/1.4 Oil DIC objective). Z-stack images were taken at random and cell number was quantified using Image J software. Six images were taken per condition and, for Tsg101 knockdown cells, regions were distinguished as either monolayerd or multilayered.

### 2.2.15. BrdU Incorporation

Caco-2 cells were plated onto 13mm glass coverslips, transfected with siRNA as detailed previously (section 2.2.3) and incubated at 37°C, 5% $CO_2$ for 6 d. BrdU (5-Bromo-2'-deoxy-uridine) labelling reagent (BrdU Labelling and Detection Kit; Roche, 11 296 736 001) was added at 1:1000 dilution directly to media in each well and cells were incubated for 24 h at 37°C, 5% $CO_2$. Cells were washed twice in PBS and fixed in cold 100% Ethanol for 20 min at -20°C. After 2 x 5 min washes in PBS, cells were incubated in 10% (v/v) FBS (in PBS) for 30 min at RT, followed by three further PBS washes. Anti-BrdU (included in the labelling kit) was diluted 1:10 in Incubation Buffer and added to cells for 30 min at 37°C. Cells were then incubated with anti-mouse Alexa Fluor® 488 secondary antibody (in PBS) for 1 h at RT, in the dark. Following both antibody incubations, cells were washed 6 x 5 min in PBS. Nuclei were stained using 1µg/ml DAPI for 10 min at RT, in the dark. Following a quick wash in PBS, cells

were mounted onto glass slides using Mowiol Mounting Medium and allowed to dry at RT overnight, protected from light. Stained cells were examined on a Zeiss LSM510META laser-scanning confocal microscope (Plan-ApoChromat 63x/1.4 Oil DIC objective). Z-stack images were taken at random and BrdU incorporation was quantified using Image J software. Six images were taken per condition and, for Tsg101 knockdown cells, regions were distinguished as either monolayerd or multilayered.

### 2.2.16. Caspase Inhibition

Caco-2 cells were plated onto 13mm glass coverslips, transfected with siRNA as detailed previously (section 2.2.3) and incubated at 37°C, 5% $CO_2$ for a total of 7 or 10 d. The General Caspase Inhibitor (Q-VD-OPh; R&D Systems, OPH001) was added to cells on day 4 and day 7 (for 10 d knockdowns) at 25µM in Caco-2 growth media and cells were incubated at 37°C, 5% $CO_2$ for the remainder of the incubation period. DMSO controls were carried out alongside. After 7 d and 10 d knockdown, cells were fixed in 4% (w/v) PFA and processed for immunofluorescence (see section 2.2.8) to stain for active Caspase-3. Stained cells were examined on a Zeiss LSM510META laser-scanning confocal microscope (Plan-ApoChromat 63x/1.4 Oil DIC objective). Six z-stack images per condition were taken at random and caspase-positive and -negative cell numbers were quantified using Image J software.

### 2.2.17. Migration Assay

Caco-2 cells were plated at 1 x $10^5$ cells/ml into 35mm dishes, transfected with siRNA as detailed previously (section 2.2.3) and incubated at 37°C, 5% $CO_2$ for 3 d. To perform the migration assay, Caco-2 cells were replated into both wells of Culture-Inserts (Ibidi, 80209) placed into 35mm dishes. Cells were washed in DPBS, trypsinised and centrifuged at 200g for 3 min. Cells were resuspended in 200µl complete growth media and counted using a haemocytometer, including 0.2% (v/v) Trypan Blue to exclude dead cells. Cells were diluted to 6.5 x $10^5$ cells/ml in complete growth media and 70µl cell suspension was added to each well of the Culture-Insert. Cells were incubated for 3 d at 37°C, 5% $CO_2$. To initiate migration, Culture-Inserts were removed using sterile forceps, leaving a 500µm cell-free gap. Cells were washed carefully in DPBS and incubated in SFM for 24 h at 37°C, 5% $CO_2$. Migration was monitored at 0, 12 and 24 h

using phase contrast microscopy and images were obtained (section 2.2.2). Quantification of the cell-free area was conducted using Image J Software.

### 2.2.18. Statistical Analysis

Mean and standard error were calculated using Microsoft Excel and results were plotted graphically using GraphPad (Prism). Each experiment was repeated in triplicate unless otherwise stated. Statistical analysis was carried out using either a one-way ANOVA with a Dunnett's post test or a two-way ANOVA with a Bonferroni post test for comparison of data sets over time. Significance level was graded as * $p < 0.05$, ** $p < 0.01$, *** $p < 0.001$.

# CHAPTER THREE

# 3. ESCRT proteins are required for mammalian epithelial cell organisation and polarity

## 3.1. Introduction

### 3.1.1. ESCRTs and Mammalian Epithelial Cell Polarity

Previous work conducted in *Drosophila* has revealed a close link between ESCRT proteins, epithelial cell polarity and tumour formation (reviewed in Vaccari and Bilder, 2009; Herz and Bergmann, 2009; Lobert and Stenmark, 2011). Mutation of ESCRT proteins in *Drosophila* results in loss of epithelial cell polarity and overproliferation. Upon inhibition of apoptosis, this effect is exacerbated and tumour-like growths capable of metastasis are formed. As a result ESCRT proteins have been classified as potential tumour suppressors (Moberg *et al.,* 2005; Thompson *et al.,* 2005; Vaccari and Bilder, 2005; Herz *et al.,* 2006; Herz *et al.,* 2009; Rodahl *et al.,* 2009b; Vaccari *et al.,* 2009).

In mammalian cells, the potential relationship between ESCRTs and epithelial cell polarity has not been investigated. Both reduced expression (Xu *et al.,* 2003; Li *et al.,* 2008) and overexpression (Liu *et al.,* 2002; Oh *et al.,* 2007; Toyoshima *et al.,* 2007; Young *et al.,* 2007) of ESCRT proteins have been associated with various human cancers, however, evidence for a direct role of ESCRTs in mammalian tumourigenesis is inconclusive. The ESCRT-I protein, Tsg101 was originally identified in mice, whereby knockout of the gene resulted in cellular transformation of mouse fibroblasts and acquired ability to form metastatic tumours when injected into nude mice (Li and Cohen, 1996). However, subsequent mice knockout studies have failed to support a tumour suppressor function of Tsg101. Null mutation of the *Tsg101* gene in mice results in early embryonic lethality (Ruland *et al.,* 2001; Wagner *et al.,* 2003). *Tsg101*-deficient embryos are reduced in size, displaying a decrease in cellular proliferation but no increase in apoptosis, and fail to develop past day 6.5 of embryogenesis. This was attributed to an accumulation of p53 via a posttranscriptional mechanism, causing cell cycle arrest and embryonic death (Ruland *et al.,* 2001). Conditional knockout mice, whereby *Tsg101* was deleted

in mammary epithelial cells, showed impaired mammary development during lactation due to an increase in apoptosis of Tsg101-deficient cells. In addition, *Tsg101* knockout resulted in reduced proliferation and increased cell death of mammary epithelial cells *in vitro*. Despite these effects, tumour formation was not observed in either heterozygous complete or tissue-specific *Tsg101* knockout mice monitored over two years (Wagner *et al.,* 2003). Therefore, these results suggest that Tsg101 is not a tumour suppressor gene for initiation of sporadic forms of breast cancer, contradicting previous studies (Li and Cohen, 1996; Li *et al.,* 1997). This discrepancy may be explained by the high level of cell death observed in these *Tsg101* deficient mice as it is possible that this masks the full tumourigenic potential of Tsg101. Indeed, in *Drosophila* ESCRT mutants, tumourous masses are only formed when apoptosis is inhibited (Thompson *et al.,* 2005; Herz *et al.,* 2006). Therefore, an alternative model may be required to fully investigate the importance of ESCRT function in maintenance of epithelial cell polarity and tumour suppression.

### 3.1.2. Caco-2 Cells as a Model System for Studying Mammalian Epithelial Cell Polarity

The human Caco-2 colon adenocarcinoma cell line provides a good *in vitro* model to study the potential relationship between ESCRT proteins and mammalian epithelial cell polarity. Caco-2 cells are a well characterised epithelial cell line. In culture they form cell-cell junctions with neighbouring cells and polarise to establish distinct apical and basolateral membrane domains (Grasset *et al.,* 1984; Sambuy *et al.,* 2005; Volpe, 2008). Caco-2 cells are a heterogeneous population and, upon reaching confluency, spontaneously differentiate to resemble mature enterocytes (Chantret *et al.,* 1988; Engle *et al.,* 1998). During differentiation cell-cell junctions mature, lateral height increases and a brush border of microvilli forms with expression of small intestine hydrolase enzymes, including sucrose-isomerase and dipetidylpeptidase IV (DppIV), at the apical membrane (Chantret *et al.,* 1988; Sambuy *et al.,* 2005; Volpe, 2008).

In addition, when cultured in a matrigel suspension, Caco-2 cells form 3D polarised cysts whereby a single layer of cells surrounds a central lumen. These

cells polarise so that their apical membranes are orientated to the luminal side and the basal membranes are in contact with the matrigel. These 3D cultures are an additional method of investigating cell polarity *in vitro* and are often considered more physiologically relevant than conventional 2D cell culture methods (Martin-Belmonte and Mostov, 2008).

### 3.1.3. Depletion of ESCRTs via siRNA knockdown

RNA interference (RNAi) is a powerful tool for functional analysis of mammalian genes. It offers a simple, cost-effective approach for sequence-specific gene silencing at the posttranscriptional level (Sandy *et al.,* 2005). Two RNAi approaches can be used for knockdown of mammalian genes, the first of which utilises synthetic small interfering RNAs (siRNAs). These are ~21-nucleotide-long double-stranded RNA (dsRNA) molecules composed of a 19-bp core sequence specific for the mRNA of interest along with two unpaired nucleotides at each 3' end (Sandy *et al.,* 2005; Shan, 2010). Once introduced into the cell via transfection, one strand of the siRNA duplex is integrated into RNA-induced silencing complex (RISC), with Ago2 as its core component, whereas the other 'passenger' strand is degraded (Shan, 2010). Inside the RISC, the siRNA guide strand associates with its complementary mRNA sequence and induces mRNA degradation. Consequently, translation of the targeted mRNA is inhibited and levels of the encoded protein are reduced (Sandy *et al.,* 2005; Shan, 2010). An alternative RNAi approach is to use short hairpin RNAs (shRNAs) expressed from plasmids or viral-based vectors. These are useful when longer lasting gene silencing is required or when cells are particularly hard to transfect (Sandy *et al.,* 2005). However, over time cells may adapt to the knockdown and therefore this may result in a different phenotype compared with a transient siRNA knockdown.

Efficient siRNA knockdown of ESCRT proteins has been demonstrated previously in mammalian cell culture (Bishop *et al.,* 2002; Lu *et al.,* 2003; Doyotte *et al.,* 2005; Bache *et al.,* 2006; Raiborg *et al.,* 2008) and, therefore, offers an attractive method to study the function of ESCRT proteins *in vitro*. In addition, due to their relatively simple design and synthesis, siRNAs are often commercially available in a ready-to-transfect format. Another important

consideration when performing siRNA knockdown experiments is the incorporation of appropriate controls. Firstly, a negative control should be employed, typically an RNA duplex with a sequence that has no perfect match within the genome (Shan, 2010). Secondly, any phenotypic effect elicited by knockdown of a particular gene should be confirmed using alternative siRNA duplexes against the same gene in order to exclude off-target effects (Sandy *et al.,* 2005).

### 3.1.4. Domain Structure of Tsg101 and Vps25 Proteins

As studies in *Drosophila* identified a role for Tsg101 (ESCRT-I) and Vps25 (ESCRT-II) within the maintenance of epithelial cell polarity, it is of interest to determine the effect of disrupting the mammalian homologues of these proteins. Tsg101 is approximately 44 KDa with a catalytically inactive N-terminal ubiquitin E2 variant (UEV) domain which binds directly to ubiquitin and mediates interaction of the ESCRT-I complex with ubiquitylated cargo (Figure 3.1A). This UEV domain also mediates binding of ESCRT-I to the Hrs subunit of ESCRT-0 (Hurley and Emr, 2006; Williams and Urbe, 2007). In addition, Tsg101 contains a proline-rich domain (PRD), a coiled-coil (CC) domain and a C-terminal steadiness box (SB) domain, which is thought to be important for autoregulation of protein expression (Pornillos *et al.*, 2002; Hurley and Emr, 2006; Williams and Urbe, 2007; McDonald and Martin-Serrano, 2008).

The ESCRT-II complex contains two Vps25 protein subunits of approximately 21 KDa (Figure 3.1B). Vps25 contains two repeats of the PPXY sequence at its N-terminus which interact with the other two subunits of the ESCRT-II complex, Vps22 and Vps36 (Hurley and Emr, 2006). At the C-terminus of Vps25, two tandem repeats of a winged helix (WH) domain are found. This is a common type of protein-protein and protein-DNA interaction domain and provides a direct link to the ESCRT-III subunit, CHMP6 (Williams and Urbe, 2007).

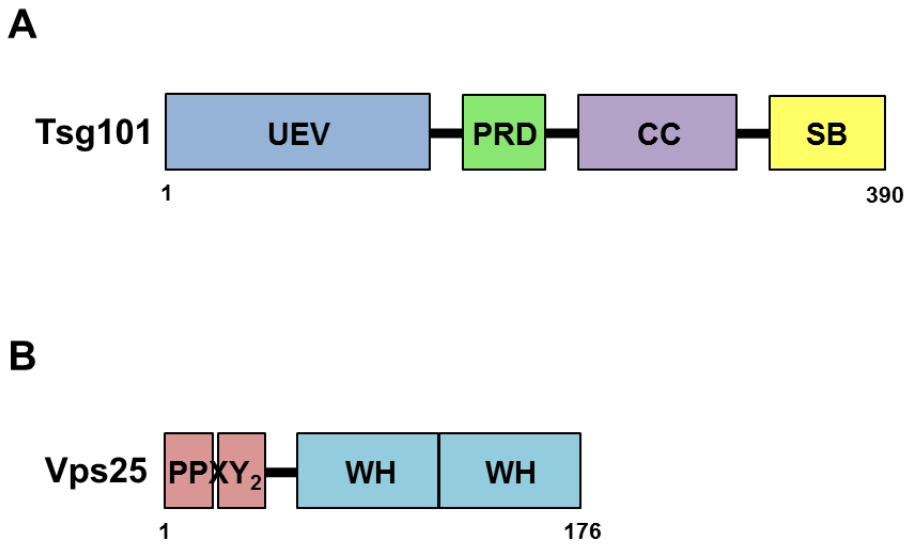


***Figure 3.1*** **Domain structures of Tsg101 and Vps25. (A)** Tsg101 is a 390 amino acid protein containing a ubiquitin E2 variant (UEV) domain, a proline rich (PRD) domain, a coiled-coil (CC) domain and a steadiness box (SB) domain. **(B)** Vps25 is a 176 amino acid protein containing two repeats of the PPXY sequence at the N-terminus and two tandem repeats of a winged helix (WH) domain at the C-terminus (adapted from Pornillos *et al.*, 2002; Hurley and Emr, 2006).

### 3.1.5. Aims

The primary aim of this study is to evaluate whether depletion of Tsg101 and Vps25 results in an alteration in mammalian epithelial cell polarity. Tsg101 and Vps25 will be depleted in Caco-2 cells using siRNA knockdown and the resulting endocytic phenotype will be analysed. The effect of ESCRT depletion on Caco-2 cell morphology will then be investigated. Lastly, characterisation of epithelial organisation and polarity will be conducted upon ESCRT knockdown in both 2D and 3D cell culture systems.

## 3.2. Results

### 3.2.1. Depletion of ESCRTs via siRNA knockdown

In order to assess whether ESCRT proteins are important for the establishment and maintenance of epithelial cell polarity, siRNA was used to knockdown Tsg101, a component of ESCRT-I, and Vps25, a component of ESCRT-II, in Caco-2 cells, a human epithelial colorectal adenocarcinoma cell line. These proteins were chosen as the first studies conducted in *Drosophila* reported that mutations in either Tsg101 or Vps25 resulted in a loss of cell polarity (Moberg *et al.,* 2005, Thompson *et al.,* 2005, Vaccari and Bilder, 2005).

Tsg101 siRNA knockdown was optimised initially using a SMARTpool of four oligonucleotide sequences. After 3 days, Tsg101 protein was reduced by approximately 75% (Figure 3.2A). These siRNA sequences were then tested individually and the oligonucleotide which resulted in the most efficient knockdown (I1) was chosen for all further experiments throughout this thesis (Figure 3.2B + C). Vps25 siRNA knockdown was optimised using a SMARTpool only and after 3 days, protein level was reduced by approximately 50% (Figure 3.2D). To achieve this level of Vps25 knockdown, an increased volume of transfection reagent was required compared with Tsg101 siRNA. Optimal knockdown of approximately 80% depletion in the amount of Tsg101 or Vps25 protein was obtained 7 days after transfection, with the knockdown persisting for at least 10 days (Figure 3.3). Therefore, for the majority of further experiments a 7 day knockdown was used.

### 3.2.2. Depletion of ESCRTs affects endosomal morphology

The ESCRT machinery has a well established role within the process of endosomal cargo sorting and MVB formation (Raiborg and Stenmark, 2009). Disruption of the ESCRT machinery in mammalian cells has been shown to affect endocytic compartments, resulting in accumulation and enlargement of both early and late endosomes (Doyotte *et al.,* 2005; Razi and Futter, 2006; Stuffers *et al.,* 2009b). Therefore, the effects of Tsg101 and Vps25 depletion on

***Figure 3.2*** **Optimisation of Tsg101 and Vps25 knockdown in Caco-2 cells. (A)** Caco-2 cells were either untreated (U), mock transfected (M), transfected with Non-Targeting Control siRNA (C) or Tsg101 SMARTpool siRNA (P) and incubated for 3 d. Lysates were immunoblotted for Tsg101 and β-tubulin as a loading control. **(B)** Tsg101 SMARTpool siRNA was split into four individual Tsg101 siRNA oligonucleotides (I1-I4). Cells were transfected with Non-Targeting Control siRNA (C), Tsg101 SMARTpool siRNA (P) or individual Tsg101 siRNA oligonucleotides (I1-I4) and incubated for 3 d. Lysates were immunoblotted for Tsg101 and β-tubulin as a loading control. **(C)** Quantification of Tsg101 protein levels, normalised to β-tubulin and expressed as a percentage of the Non-Targeting Control. Data shown are the means ± standard error from three independent experiments. **(D)** Caco-2 cells were either untreated (U), mock transfected (M), transfected with Non-Targeting Control siRNA (C) or Vps25 SMARTpool siRNA (V) and incubated for 3 d. Lysates were immunoblotted for Vps25 and β-tubulin, used as a loading control. Transfection was carried out with an increased volume of transfection reagent compared to Tsg101 siRNA.

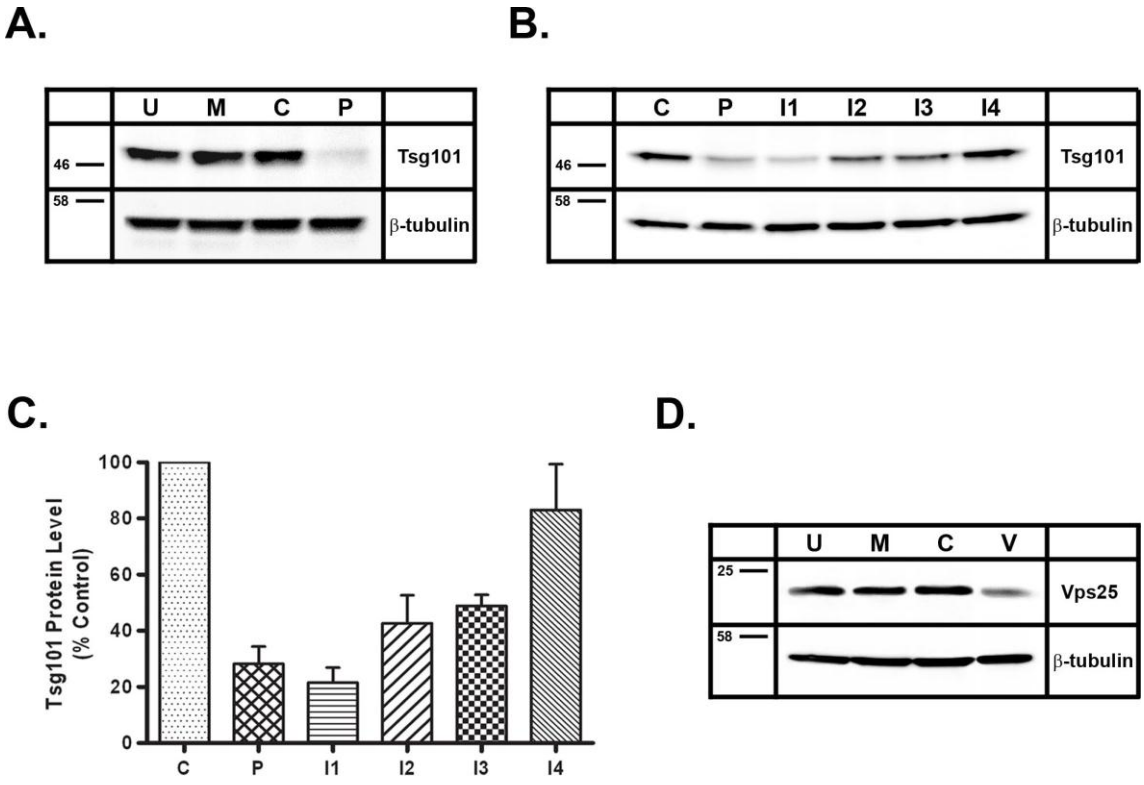
A.
U
M
C
P
46
58
Tsg101
β-tubulin
B.
C
P
I1
I2
I3
I4
46
58
Tsg101
β-tubulin
C.
Tsg101 Protein Level
(% Control)
100
80
60
40
20
0
C
P
I1
I2
I3
I4
D.
U
M
C
V
25
58
Vps25
β-tubulin

***Figure 3.3*** **Tsg101 and Vps25 knockdown in Caco-2 cells persists over time. (A)** Caco-2 cells were transfected with either Non-Targeting Control siRNA (C), Tsg101 siRNA (T) or Vps25 siRNA (V) and incubated for 3, 7 or 10 d. Lysates were immunoblotted for Tsg101, Vps25 and β-tubulin as a loading control. **(B)** Protein levels were quantified, normalised to β-tubulin levels, and expressed as a percentage of the Non-Targeting Control for each timepoint. Data shown is the mean ± standard error from three independent experiments. Results were analysed using a one-way ANOVA and Dunnett's post test, **p<0.01, ***p<0.001.

**A.**

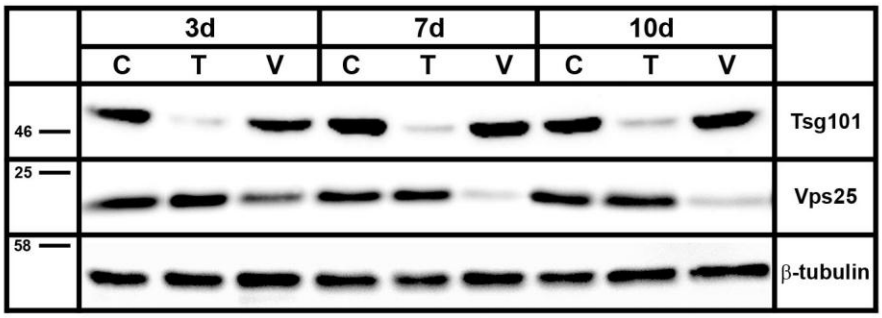
3d
7d
10d
C T V C T V C T V
46
25
58
Tsg101
Vps25
β-tubulin

**B.**

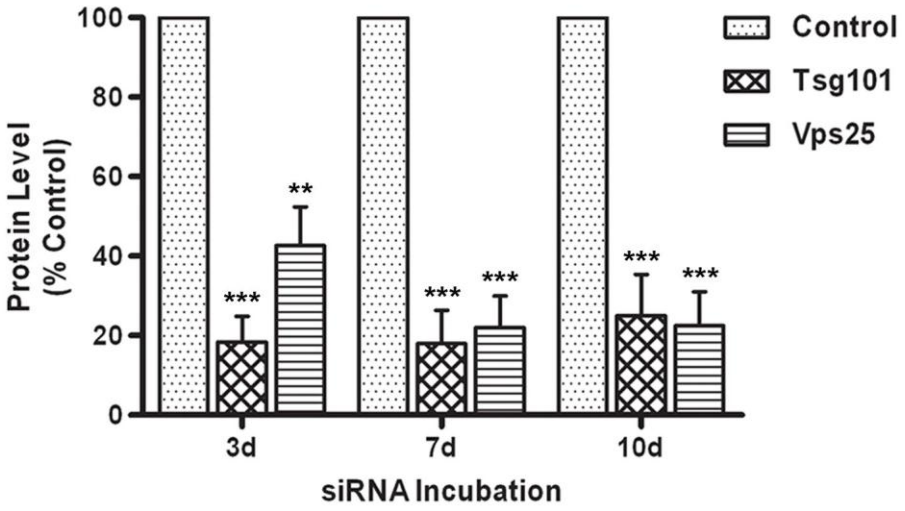
Control
Tsg101
Vps25
Protein Level (% Control)
100
80
60
40
20
0
**
***
***
***
***
***
3d
7d
10d
siRNA Incubation

Caco-2 cell endosomal morphology were investigated in order to confirm that the siRNA knockdown was having the expected effect. Knockdown of Tsg101 or Vps25 resulted in enlargement and accumulation of both early and late endosomes after incubation with EGF, indicated by EEA1 and CD63 staining respectively (Figure 3.4). Despite this enlargement, the two endosomal compartments seemed to remain morphologically distinct, indicated by the lack of colocalisation of EEA1 and CD63. In the absence of EGF the endosomal effects were less pronounced (data not shown).

Trafficking of EGF was also investigated after Tsg101 and Vps25 knockdown (Figure 3.5). Binding of EGF to the EGF receptor (EGFR) at the plasma membrane induces internalisation and delivery of the EGF-EGFR complex to early endosomes. The EGF-EGFR complex is then usually targeted for degradation via internalisation into MVBs and trafficking to the lysosome (Wiley and Burke, 2001). EGFR degradation is often reduced in ESCRT depleted cells (Bishop *et al.,* 2002; Lu *et al.,* 2003; Bache *et al.,* 2006; Malerod *et al.,* 2007; Raiborg *et al.,* 2008) and consequently, EGF-induced signalling may be sustained (Bache *et al.,* 2006; Malerod *et al.,* 2007). However, in Tsg101 or Vsp25 depleted Caco-2 cells, EGF trafficking did not appear to be significantly altered, although a slightly increased amount of EGF remained in some Tsg101 knockdown cells after a 4 hour incubation compared with control (Figure 3.5A). In line with this observation, sustained phosphorylation of ERK1/2, a downstream component of the EGF signalling pathway, was not observed in either Tsg101 or Vps25 knockdown cells (Figure 3.5B). Levels of phosphorylated ERK1/2 varied between experiments and no significant increase could be concluded after Tsg101 and Vps25 knockdown. Therefore, despite the effects on early endosomal morphology, these results suggest that EGF trafficking is not significantly altered upon Tsg101 or Vps25 depletion.

### 3.2.3. Caco-2 cell morphology is altered upon ESCRT knockdown, with Tsg101 knockdown cells forming multilayered epithelial sheets

To begin to characterise the effects of Tsg101 and Vps25 knockdown, Caco-2 cell morphology was monitored over time (Figure 3.6). After 3 days culture, knockdown cells appeared similar to control. However, after 7 day Tsg101

***Figure 3.4*** **Depletion of Tsg101 and Vps25 causes enlargement of both early and late endosomes in EGF treated Caco-2 cells.** Caco-2 cells were transfected with either Non-Targeting Control siRNA, Tsg101 siRNA, or Vps25 siRNA and incubated for 7 d. Cells were allowed to internalise EGF for 4 h, fixed and examined by confocal fluorescence microscopy for CD63 (green) and EEA1 (red). Nuclei were stained with DAPI (blue), shown in merged images. Bar, 10μm.

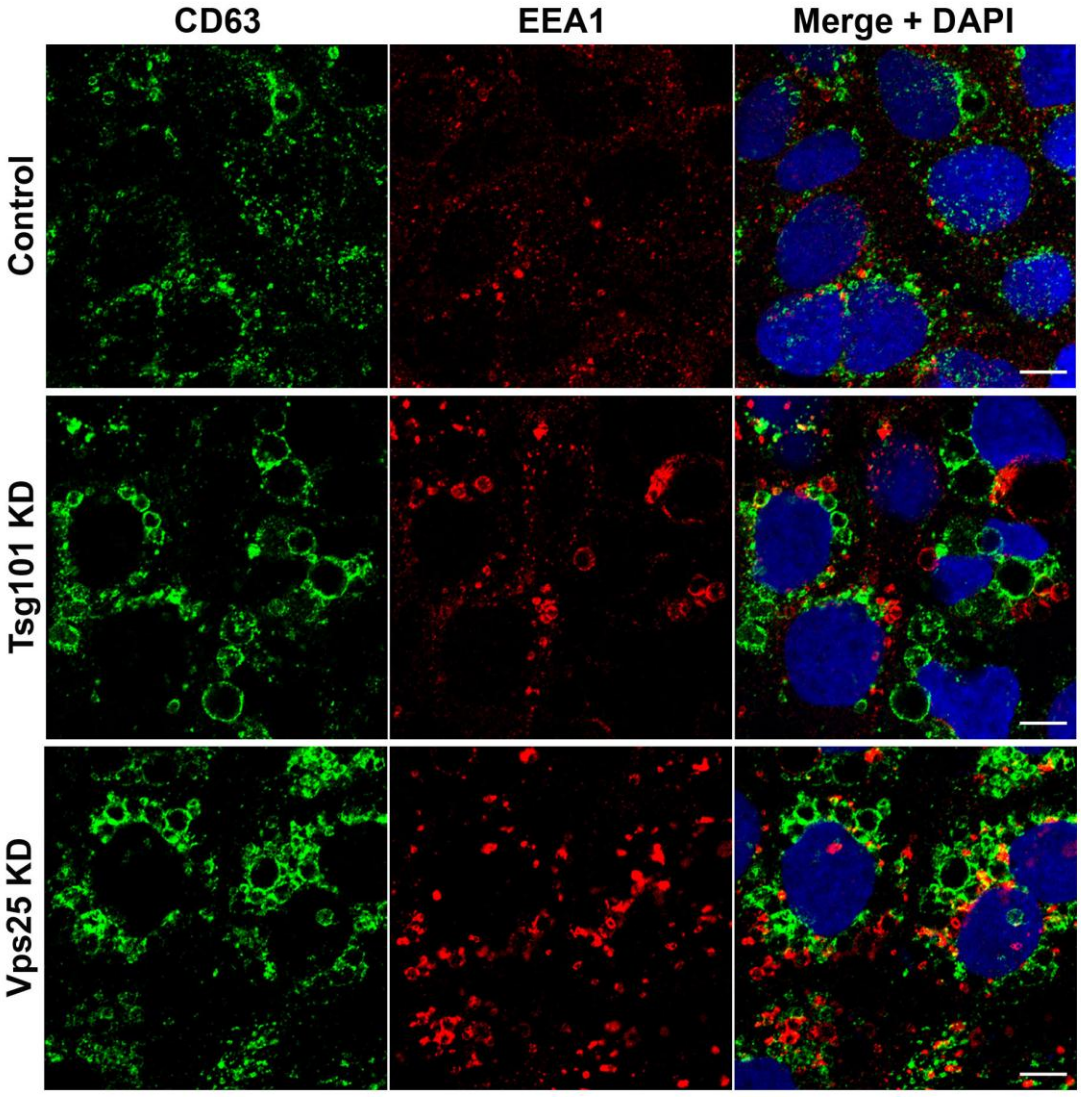
CD63
EEA1
Merge + DAPI
Control
Tsg101 KD
Vps25 KD

***Figure 3.5*** **Tsg101 or Vps25 knockdown in Caco-2 cells does not impair degradation of EGF and MAPK phosphorylation is not sustained.** Caco-2 cells were transfected with Non-Targeting Control siRNA, Tsg101 siRNA, or Vps25 siRNA and incubated for 7 d. Cells were serum starved overnight prior to EGF treatment. **(A)** Caco-2 cells were allowed to internalise Alexa Fluor® 555-conjugated EGF for 4 h, fixed and examined by confocal fluorescence microscopy for EEA1 (green) and EGF (red). Nuclei were stained with DAPI (blue), shown in merged images. Note that although EEA1 staining is increased in Tsg101 and Vps25 knockdown cells, residual EGF levels are similar to control. Bar, 10μm. **(B)** Caco-2 cells were pulse-labelled with EGF for 10 min, followed by a chase in SFM for indicated times. Lysates were immunoblotted for phosphorylated Erk1/2 (p-Erk1/2) and total Erk1/2. Immunoblotting for Tsg101 and Vps25 was carried out to confirm knockdown levels. Levels of p-Erk1/2 increase directly after EGF treatment and decrease over time at a similar rate in both control and knockdown cells.

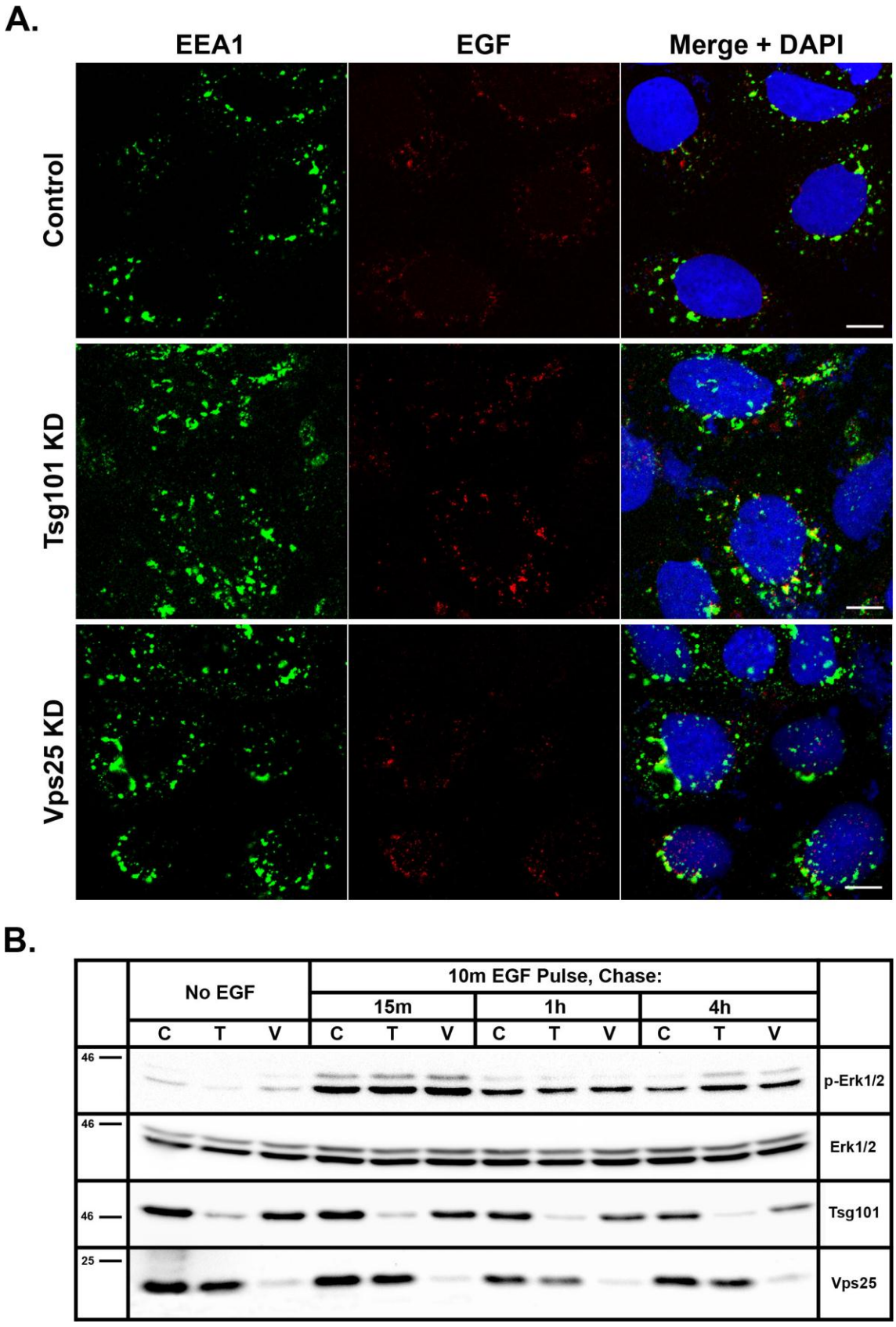
A.
EEA1
EGF
Merge + DAPI
Control
Tsg101 KD
Vps25 KD
B.
No EGF
10m EGF Pulse, Chase:
15m
1h
4h
C T V C T V C T V C T V
46
46
46
25
p-Erk1/2
Erk1/2
Tsg101
Vps25

knockdown, large areas of the epithelial sheet appeared disrupted and cells seemed to be growing in clumps (Figure 3.6, arrows). This aberrant morphology was also observed on day 10, although to a slightly lesser extent. In other areas, the organisation of the epithelial sheet appeared to be retained (Figure 3.6, arrowheads) however, morphology of these cells did not resemble the typical cobblestone effect observed in control cells at day 10 (Figure 3.6, asterisk). Instead cells appeared flatter and less differentiated (Figure 3.6, hash). Vps25 knockdown did not disrupt the organisation of the epithelial sheet although, after 10 days culture, there was a reduction in the areas of cells showing the typical cobblestone morphology (Figure 3.6, asterisk) with cells appearing less differentiated than control (Figure 3.6, hash).

Further analysis of the disrupted areas of the epithelial sheet formed upon Tsg101 knockdown indicated that the cells were stacking on top of one another to form multilayers (Figure 3.7). In addition, nuclear morphology of Tsg101 knockdown cells was more irregular and nuclei often appeared flatter compared to control. In order to confirm that this phenotype was due to depletion of Tsg101 and not off-target effects, siRNA knockdown was performed using two alternative oligonucleotides. Tsg101 protein levels were significantly reduced to approximately 20-30% compared with control after 3 days (Figure 3.8A). However, persistence of the knockdown was not as efficient and after 7 days Tsg101 protein was approximately 30-50% of control levels. In addition, Tsg101 siRNA 2 resulted in a higher level of knockdown compared with siRNA 1 at both timepoints. Morphology of the Tsg101 knockdown cells was similar to that seen previously. Organisation of the epithelial sheet was disrupted (Figure 3.8B) and cells formed multilayered regions (Figure 3.9). Interestingly, the level of knockdown appeared to correspond to the severity of the phenotype. The original Tsg101 siRNA resulted in the most pronounced effect whereas siRNA 1, which gave the least efficient knockdown approach, resulted in a lesser effect. However, overall the multilayered phenotype was observed with all three Tsg101 siRNA oligonucleotides, confirming that the observed effects were caused by Tsg101 depletion. Therefore, Tsg101 is required in order to retain correct organisation of the Caco-2 epithelial monolayer.

***Figure 3.6*** **Caco-2 cell morphology is altered after Tsg101 and Vps25 depletion, with Tsg101 knockdown disrupting organisation of the whole epithelial sheet.** Caco-2 cells were transfected with either Non-Targeting Control siRNA, Tsg101 siRNA or Vps25 siRNA and analysed via phase-contrast microscopy after 3, 7 and 10 d. Tsg101 knockdown cells form monolayers in some areas (arrowheads) but many regions are observed where organisation of the epithelial sheet appears disrupted (arrows). Epithelial organisation is not disrupted after Vps25 knockdown. In addition, after 10 d culture there is a decrease in areas showing the characteristic cobblestone morphology (*) in monolayered regions of Tsg101 knockdown cells and Vps25 knockdown cells. Instead cell morphology appears similar to that observed at 7 d (#).

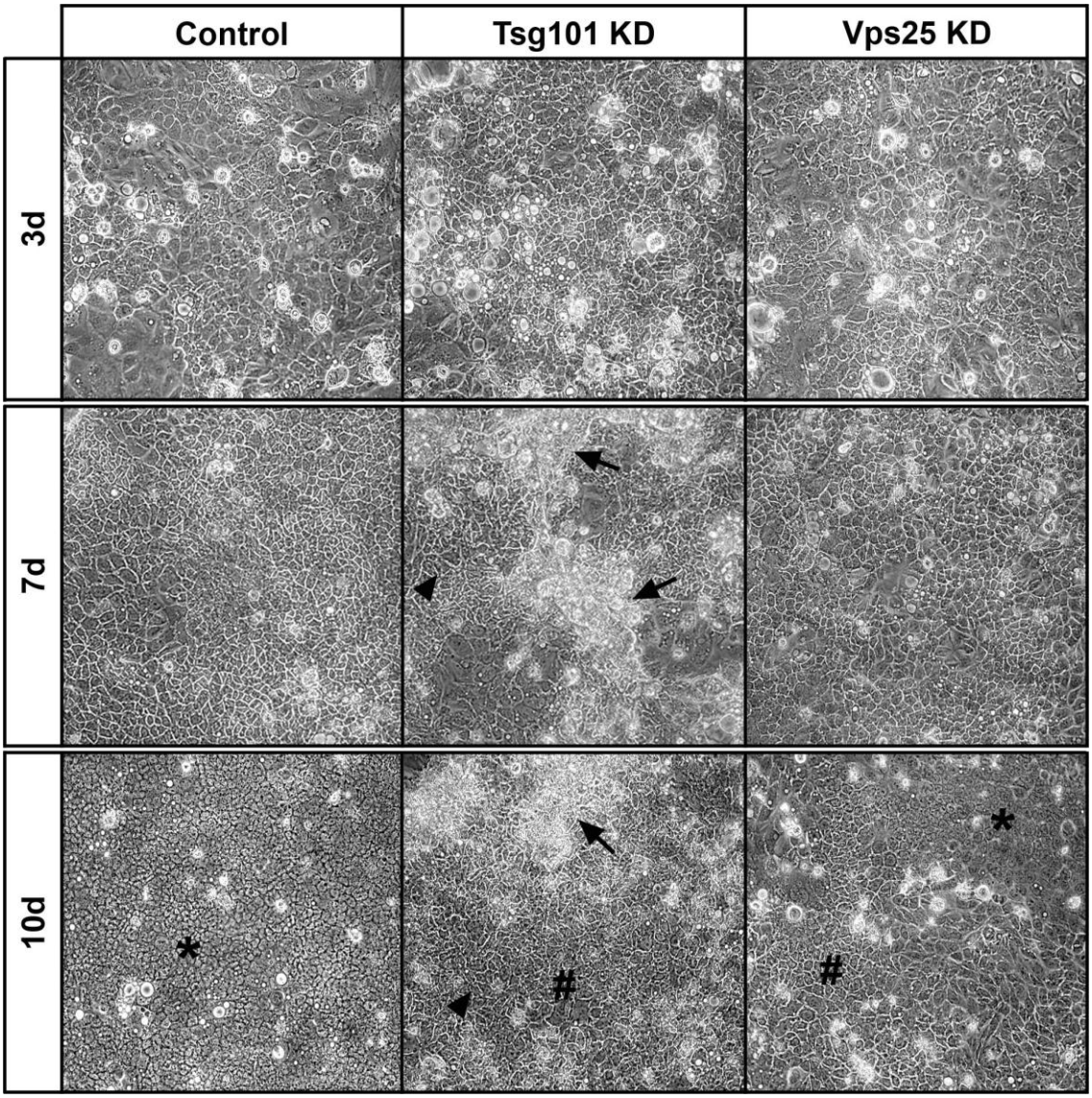
Control
Tsg101 KD
Vps25 KD
3d
7d
10d
*
#
*
#
*
#

***Figure 3.7*** **Caco-2 cells form multilayers upon Tsg101 knockdown.** Caco-2 cells were transfected with either Non-Targeting Control siRNA or Tsg101 siRNA and incubated for 7 d. Nuclei were stained with DAPI and cells were examined via confocal fluorescence microscopy. Tsg101 knockdown disrupts nuclear morphology and regions of cells show a multilayered organisation. Confocal projections and corresponding z-sections (indicated by dotted line) are displayed. Bar, 10µm.

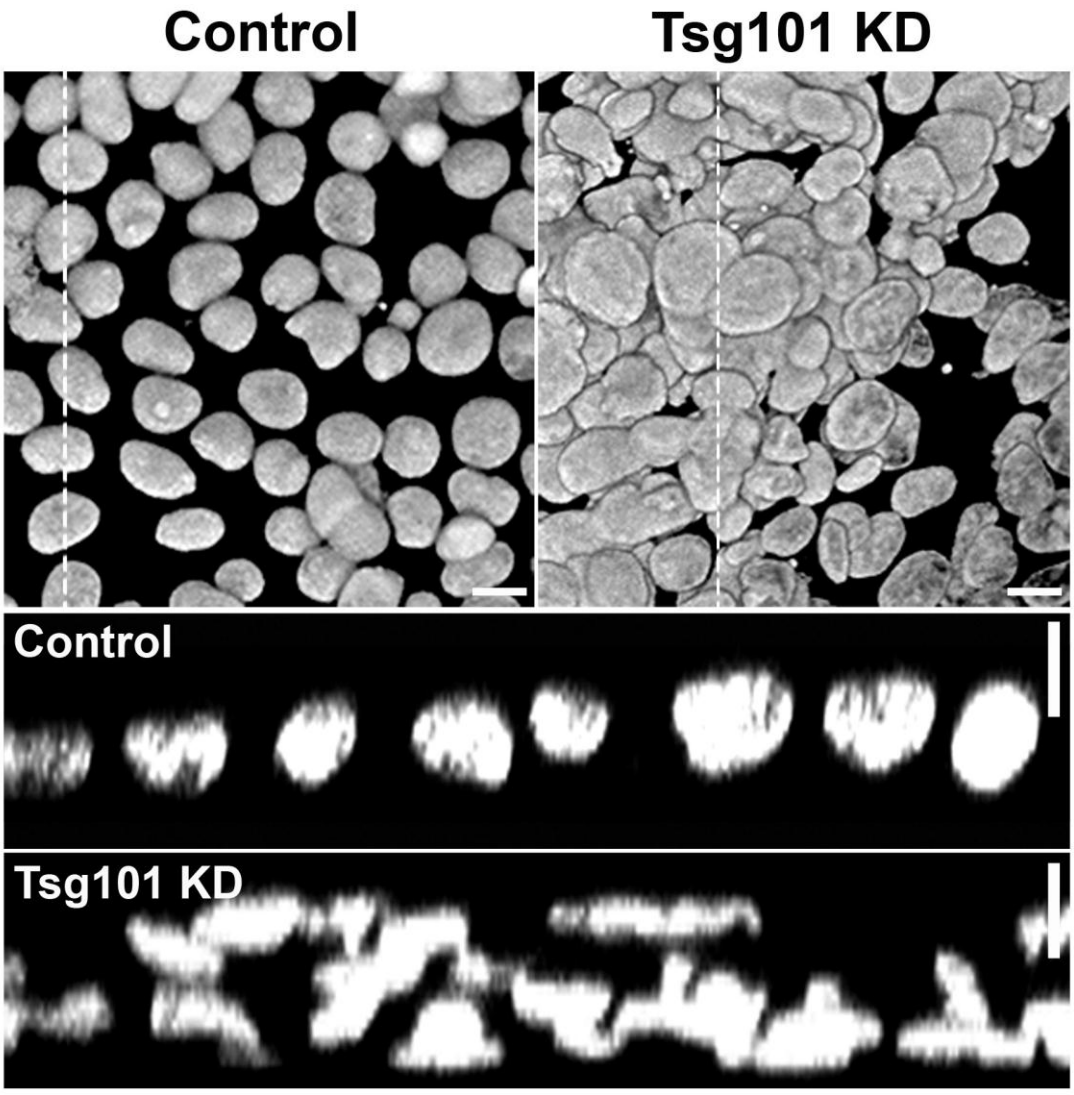
Control
Tsg101 KD
Control
Tsg101 KD

***Figure 3.8*** **Knockdown of Tsg101 using alternative siRNA oligonucleotides results in a similar disruption to Caco-2 epithelial organisation.** Caco-2 cells were transfected with either Non-Targeting Control siRNA (C) or Tsg101 siRNA (T). Tsg101 knockdown was also achieved using a different single siRNA oligonucleotide (1) or a combination of two different siRNA oligonucleotides (2). **(A)** Cells were incubated for 3 d and 7 d and lysates were immunoblotted for Tsg101 and β-tubulin as a loading control (i). Protein levels were quantified, normalised to β-tubulin and expressed as a percentage of the Non-Targeting Control for each timepoint (ii). Data shown is the mean ± standard error from three independent experiments. Results were analysed using a one-way ANOVA and Dunnett's post test, *$p<0.05$, **$p<0.01$, ***$p<0.001$. **(B)** Cells were analysed via phase-contrast microscopy after 7 d knockdown. A similar disruption to the epithelial sheet is observed after knockdown of Tsg101 using alternative siRNA oligonucleotides (1 and 2) (arrows).

A.

i.

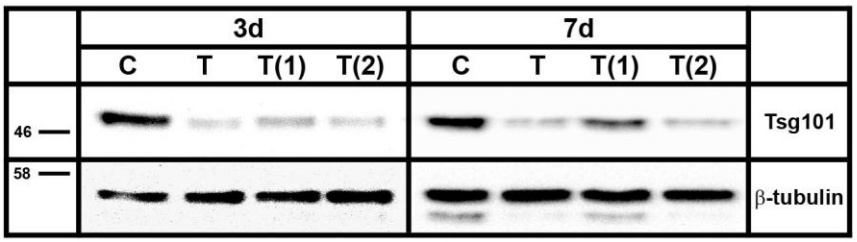
3d
7d
C
T
T(1)
T(2)
C
T
T(1)
T(2)
46
58
Tsg101
β-tubulin

ii.

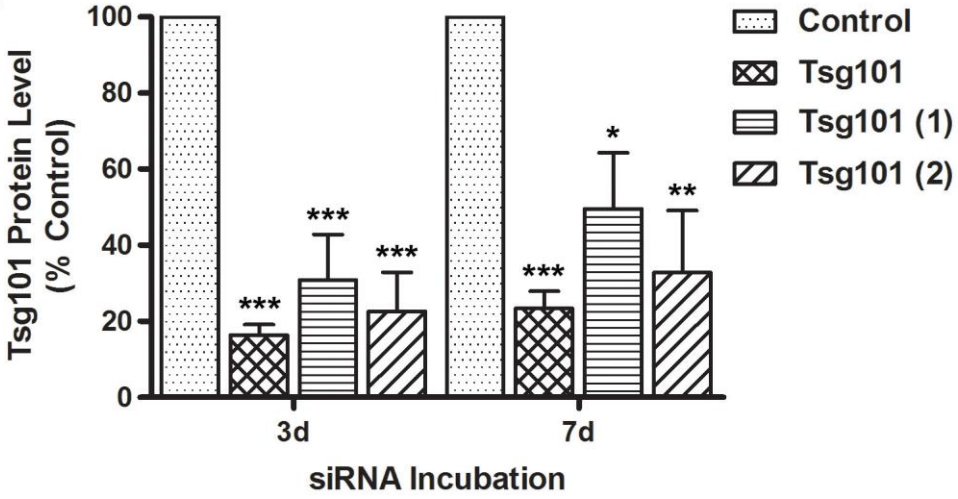
Tsg101 Protein Level (% Control)
100
80
60
40
20
0
***
***
***
***
*
**
3d
7d
siRNA Incubation
Control
Tsg101
Tsg101 (1)
Tsg101 (2)

B.

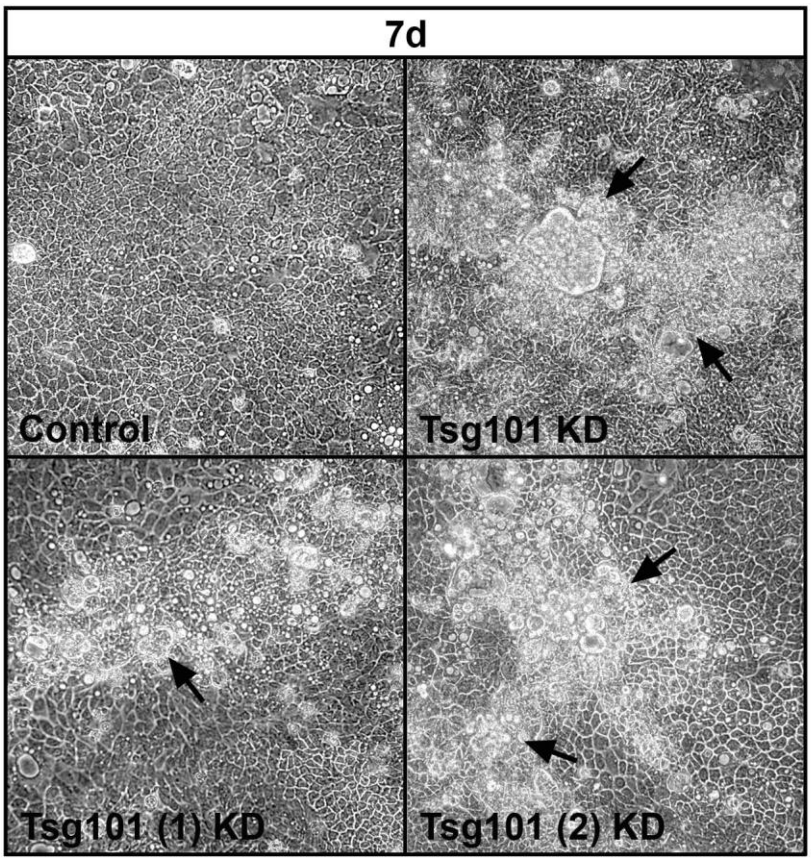
7d
Control
Tsg101 KD
Tsg101 (1) KD
Tsg101 (2) KD

***Figure 3.9*** **A similar multilayered phenotype is observed upon knockdown of Tsg101 using different siRNA oligonucleotides.** Caco-2 cells were transfected with either Non-Targeting Control siRNA (C), or two alternative Tsg101 siRNA combinations (1 and 2) and incubated for 7 d. Nuclei were stained with DAPI and cells were examined via confocal fluorescence microscopy. Tsg101 knockdown cells display a similar phenotype as observed previously (compare with Figure 3.6). Nuclear morphology is disrupted and multilayered regions of cells are formed. Confocal projections and corresponding z-sections (indicated by dotted line) are displayed. Bar, 10µm.

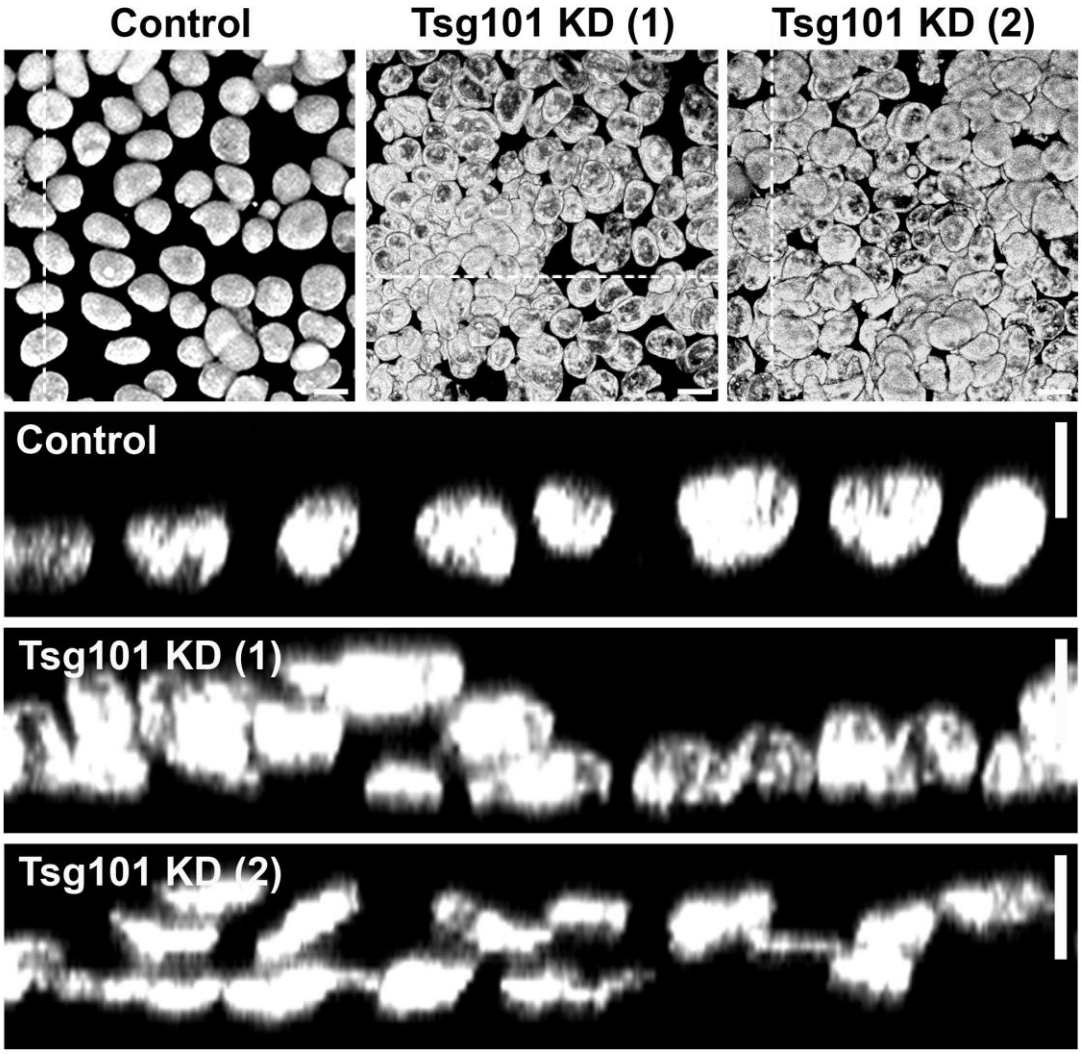
Control
Tsg101 KD (1)
Tsg101 KD (2)
Control
Tsg101 KD (1)
Tsg101 KD (2)

### 3.2.4. ESCRT depletion prevents differentiation of Caco-2 cells

Caco-2 cells are a well characterised polarised human epithelial cell line. In culture they form cell-cell junctions with neighbouring cells and will polarise to establish distinct apical and basolateral membrane domains (Sambuy *et al.,* 2005). Upon reaching confluency, cells will begin to spontaneously differentiate to resemble mature enterocytes. During this process cell-cell junctions mature, lateral height increases and cells develop a brush border of microvilli at the apical membrane (Chantret *et al.,* 1988; Sambuy *et al.,* 2005; Volpe, 2008). This can be observed by comparing Caco-2 cell morphology over time (Figures 3.10 and 3.11). Cell-cell junctions, including tight junctions indicated by occludin localisation (Figure 3.11, arrowheads) and adherens junctions indicated by E-cadherin localisation (Figure 3.10), form between adjacent cells and mature over time. When confluent, Caco-2 cells establish apicobasal polarity demonstrated by localisation of aPKC and E-cadherin to apical and basolateral membranes, respectively (Figure 3.10). Four days after reaching confluency, cells display a more differentiated phenotype whereby intensity of apical staining and lateral height has increased. Localisation of the brush border protein, Dipeptidyl peptidase-IV (DppIV) to the apical membrane increases as cells reach confluency and begin to differentiate (Figure 3.11). The classic 'cauliflower' pattern is displayed four days post-confluence, indicative of a mature brush border (Baricault *et al.,* 1995).

Upon depletion of Tsg101, some areas of the Caco-2 epithelial sheet retained a normal monolayered organisation whereas other areas displayed a more striking multilayered phenotype. Therefore, the morphology of these two different populations of Tsg101 knockdown cells were characterised independently. Firstly, the phenotype of the monolayered regions will be discussed (below) followed by the multilayered regions (Section 3.2.5).

In the monolayered regions of Tsg101 knockdown cells, apicobasal polarity was retained demonstrated by correct localisation of aPKC and E-cadherin to the apical and basolateral membrane domains, respectively (Figure 3.12A). This was also observed after Vps25 knockdown. However, lateral height of the knockdown cells was reduced to approximately 7µm compared to 10µm for

***Figure 3.10*** **Caco-2 cells polarise and differentiate over time.** As Caco-2 cells proliferate cell-cell junctions are formed and apical and basolateral membrane domains are defined. After reaching confluency, lateral height increases and junctions mature as cells differentiate. Caco-2 cells were fixed either prior to reaching confluency, when confluent, or 4 d post-confluency. Cells were then examined by confocal fluorescence microscopy for E-cadherin (green) and aPKC (red) to indicate basolateral and apical membranes, respectively. Nuclei were stained with DAPI (blue), shown in merged images. Apical confocal slices and corresponding z-sections (indicated by dotted line) are displayed. Bar, 10µm.

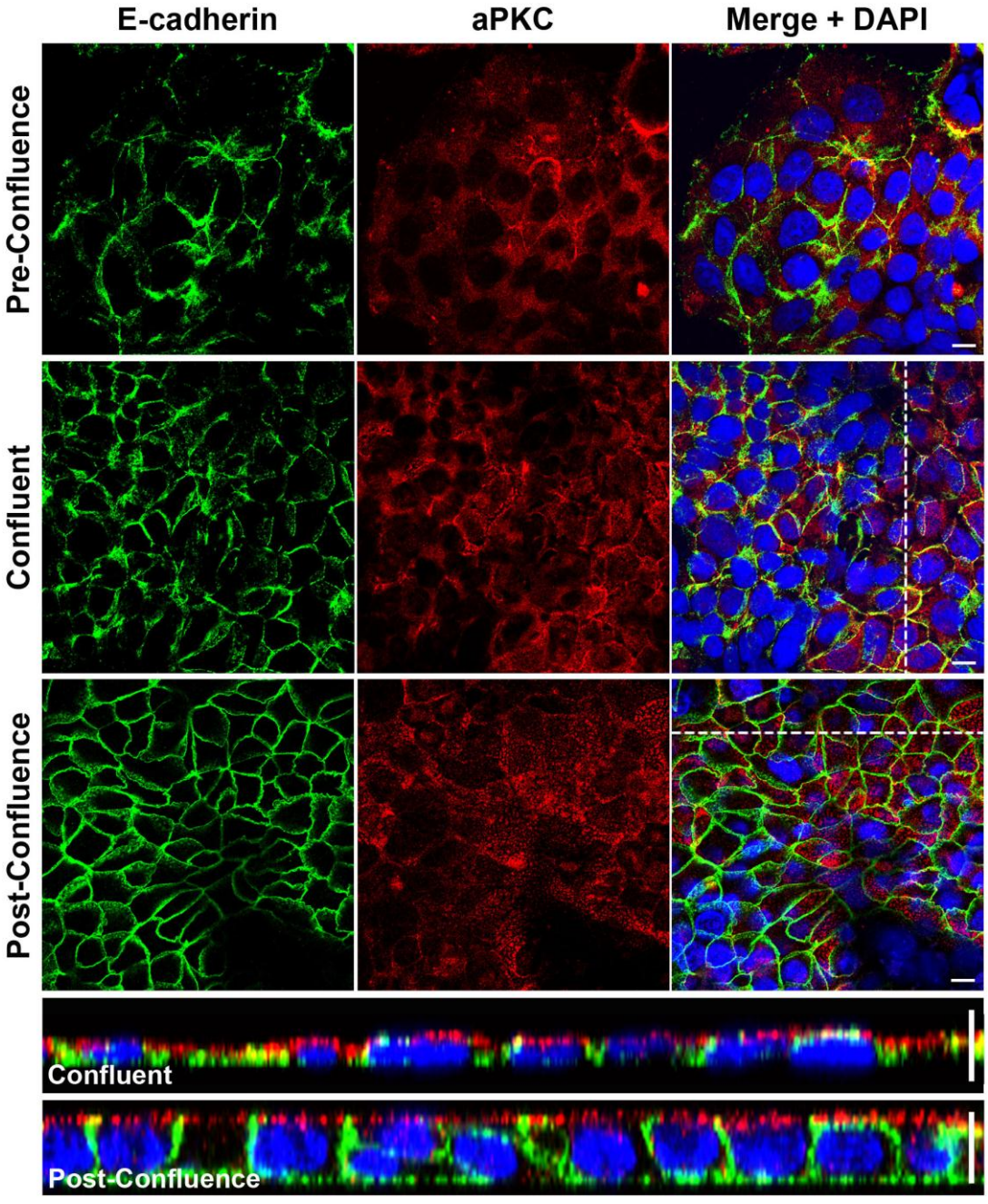
E-cadherin
aPKC
Merge + DAPI
Pre-Confluence
Confluent
Post-Confluence
Confluent
Post-Confluence

***Figure 3.11*** **Caco-2 cells form a brush border at the apical membrane.** Upon reaching confluency, Caco-2 cells begin to develop a brush border at the apical membrane. Caco-2 cells were fixed either prior to reaching confluency, when confluent, or 4 d post-confluency and non-permeabilised cells were immunostained for DppIV (brush border marker; green). Cells were then permeabilised and immunostained for occludin (tight junctions; red). Nuclei were stained with DAPI (blue) and cells were examined by confocal fluorescence microscopy. Confocal slices and corresponding z-sections (indicated by dotted line) are displayed. Arrowheads indicate tight junctions. Bar, 10µm.

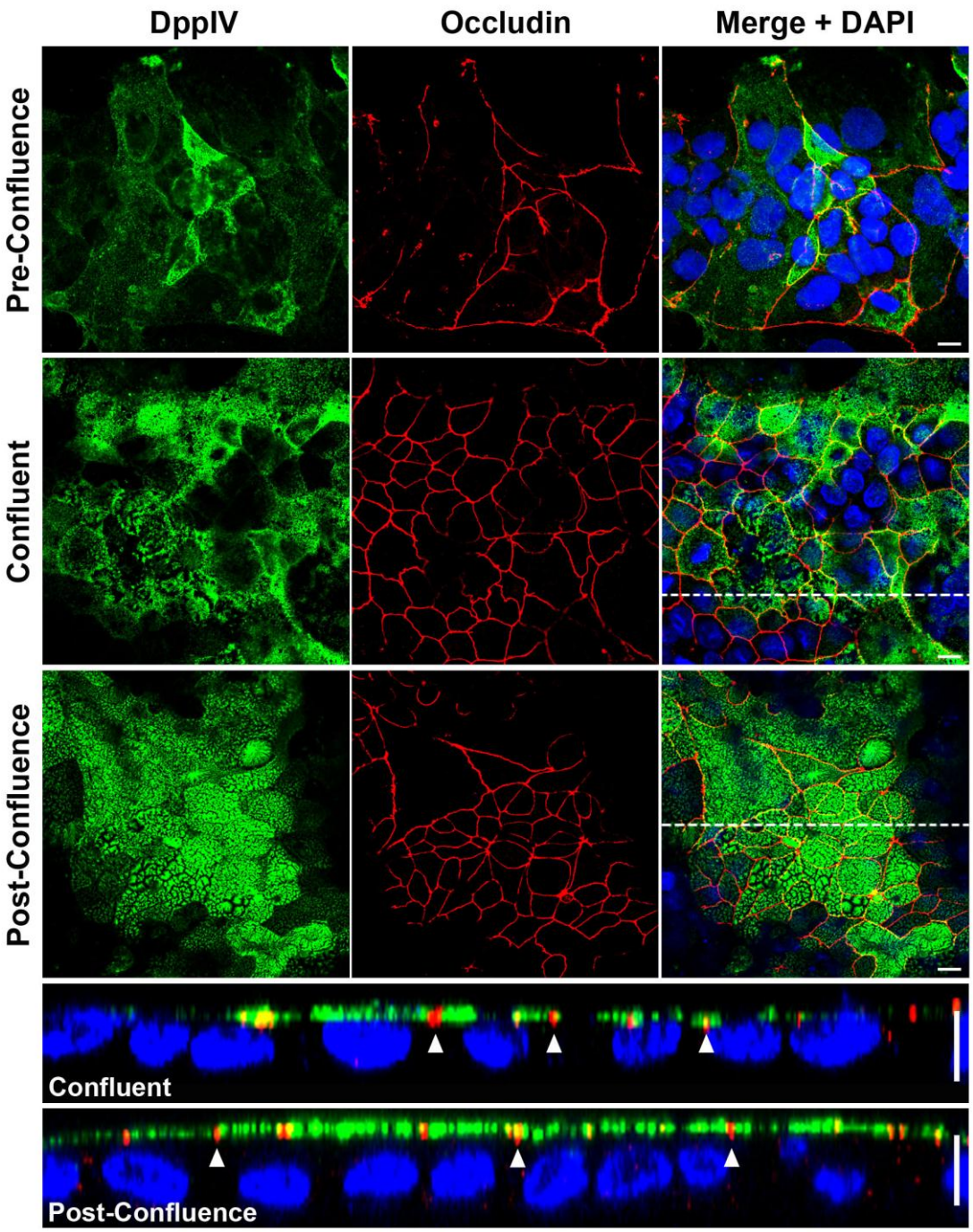
DppIV
Occludin
Merge + DAPI
Pre-Confluence
Confluent
Post-Confluence
Confluent
Post-Confluence

control cells (Figure 3.12B). In addition, a reduction in DppIV localisation to the apical membrane was observed suggesting that brush border development is impaired upon Tsg101 and Vps25 knockdown (Figure 3.13). Therefore, although ESCRT proteins are not required for the initial establishment of distinct apical and basolateral membrane domains, Tsg101 and Vps25 knockdown appears to impede differentiation of Caco-2 cells.

### 3.2.5. Tsg101 depletion disrupts epithelial cell organisation and polarity

Upon Tsg101 knockdown, regions of the Caco-2 epithelial sheet were disrupted and cells displayed a multilayered phenotype. In these areas apicobasal polarity was compromised (Figure 3.14). Some cells appeared to lack a defined apical membrane indicated by absence of aPKC staining (Figure 3.14, asterisk) whereas, in other cells expansion of apical membrane is observed (Figure 3.14, hash). It is also important to note that some cells appeared to retain distinct apical and basolateral membrane domains, indicated by aPKC and E-cadherin staining, respectively however, due to these cells being stacked on top of each other apical staining appeared along what should be the basal surface of the epithelial sheet (Figure 3.14, arrowheads). This suggests that these cells are incorrectly orientated within the multilayered epithelial sheet.

Multilayered regions of Tsg101 knockdown cells also displayed brush border defects (Figure 3.15, asterisks). Often multilayered areas lacked DppIV staining (Figure 3.15, arrowheads) however, in some cases cells displayed DppIV staining localised to the apical membrane (Figure 3.15, arrows). This suggests that the ability of Tg101 knockdown cells to form a brush border is compromised but not lost entirely. This effect also appears different to that seen in Tsg101 knockdown cells which retained their monolayered organisation (Figure 3.13). Instead of a general reduction in DppIV localisation to the apical membrane observed in Tsg101 monolayered regions, multilayered cells seem to either display strong DppIV staining or very little/no staining at all, although this effect is difficult to quantify.

***Figure 3.12*** **Tsg101 and Vps25 depleted Caco-2 cells establish distinct apical and basolateral membrane domains but lateral height is reduced. (A)** Caco-2 cells were transfected with either Non-Targeting Control siRNA, Tsg101 siRNA or Vps25 siRNA, incubated for 7 d and stained for E-cadherin (green) and aPKC (red) to visualise basolateral and apical surfaces, respectively. Nuclei were stained with DAPI (blue). Apical confocal slices and corresponding z-sections (indicated by dotted line) are displayed. Bar 10µm. **(B)** Lateral height was quantified using ImageJ. For each condition, lateral height was quantified for at least two images per experiment. Ten z-sections were analysed per image, taking three measurements per z-section, and average lateral height was calculated. Data shown are means ± standard error from three independent experiments. Results were analysed using a One-Way ANOVA and Dunnett's post-test, *$p<0.05$. Note that for Tsg101 knockdown cells, analysis was carried out on areas where monolayered organisation was maintained, a more striking polarity phenotype is seen in the multilayered regions (Figure 3.14).

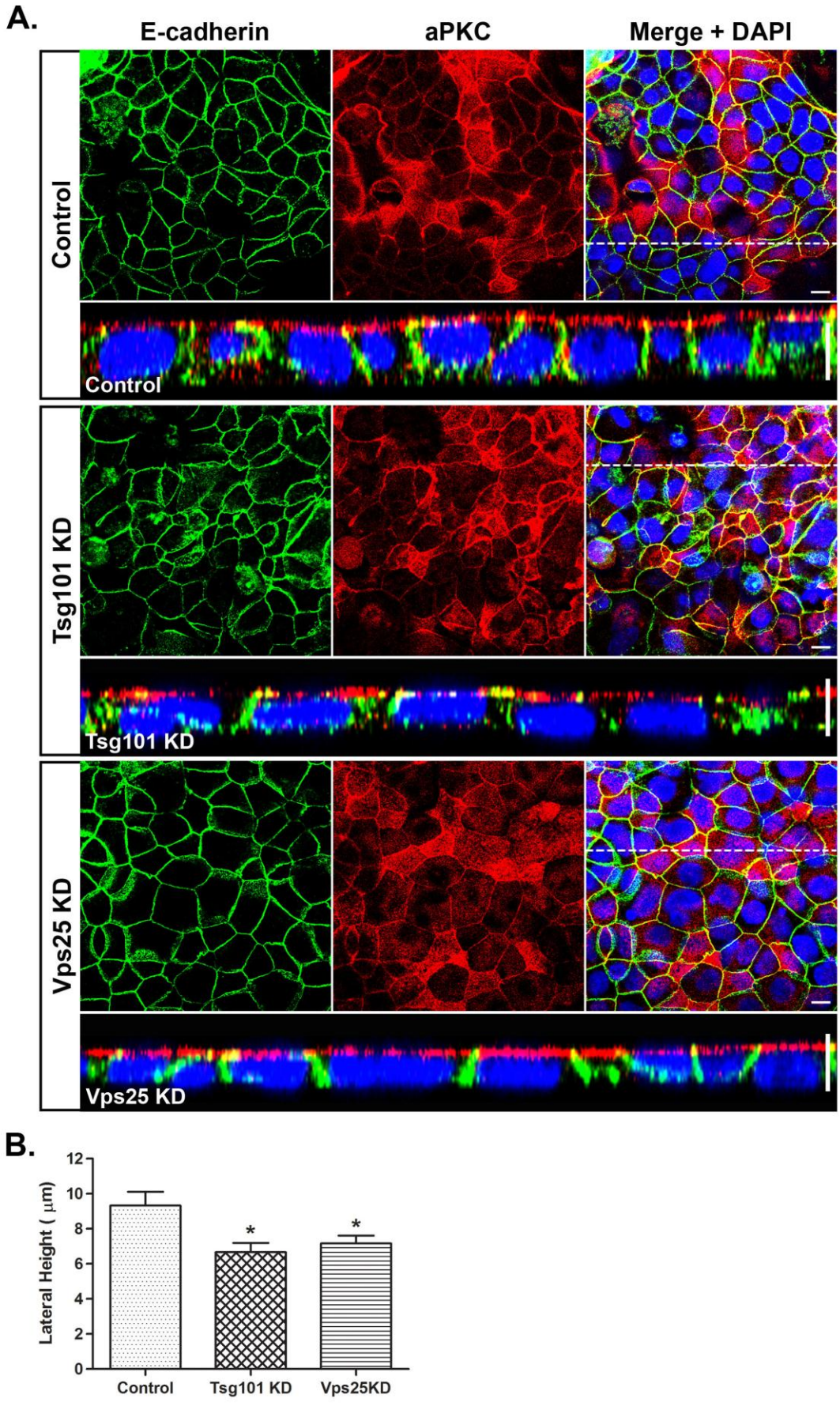
A.
E-cadherin
aPKC
Merge + DAPI
Control
Control
Tsg101 KD
Tsg101 KD
Vps25 KD
Vps25 KD
B.
Lateral Height ( μm)
12
10
8
6
4
2
0
*
*
Control
Tsg101 KD
Vps25KD

***Figure 3.13*** **Knockdown of Tsg101 and Vps25 impairs brush border formation. (A)** Localisation of the brush border protein DppIV to the apical membrane is reduced in Tsg101 and Vps25 depleted cells. Caco-2 cells were transfected with either Non-Targeting Control siRNA, Tsg101 siRNA or Vps25 siRNA and incubated for 7 d. Non-permeabilised cells were immunostained for DppIV (green), followed by permeabilisation and staining for the tight junction protein, occludin (red). Nuclei were stained with DAPI (blue). Confocal projections and corresponding z-sections (indicated by dotted line) are displayed. Bar 10µm. **(B)** Quantification of DppIV fluorescence was carried out using ImageJ. For each condition, DppIV fluorescence was quantified for at least three images per experiment. Random projections were obtained and average fluorescence intensity in the green channel was quantified for each field of view and expressed as a ratio over corresponding cell number. Data shown are means ± standard error from four independent experiments. Results were analysed using a One-Way ANOVA and Dunnett's post-test, *$p<0.05$. Note that for Tsg101 knockdown cells, analysis was carried out on areas where monolayered organisation was maintained.

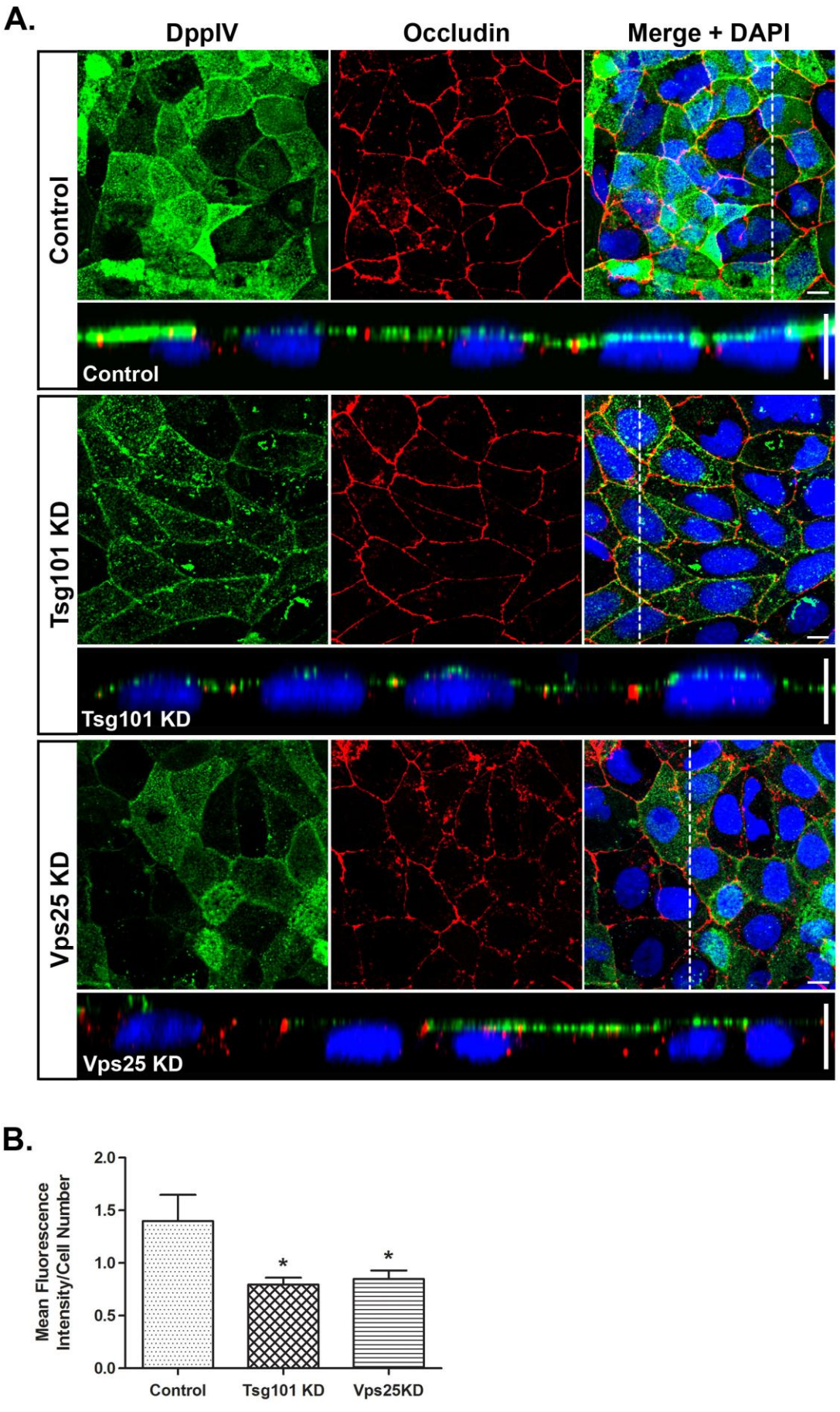
A.
DppIV
Occludin
Merge + DAPI
Control
Control
Tsg101 KD
Tsg101 KD
Vps25 KD
Vps25 KD
B.
Mean Fluorescence Intensity/Cell Number
2.0
1.5
1.0
0.5
0.0
*
*
Control
Tsg101 KD
Vps25KD

***Figure 3.14*** **Tsg101 is required to maintain a polarised epithelial monolayer in Caco-2 cells.** Tsg101 knockdown cells form multilayered regions with compromised apicobasal polarity. Caco-2 cells were transfected with either Non-Targeting Control siRNA or Tsg101 siRNA, incubated for 7 d and stained for E-cadherin (green) and aPKC (red) to visualise basolateral and apical surfaces, respectively. Nuclei were stained with DAPI (blue). Note that some Tsg101 knockdown cells lack aPKC staining (*), whereas other cells show an expanded apical membrane (#). In addition, some cells retain distinct aPKC and E-cadherin staining, however, aPKC staining appears along the basal surface of the epithelial sheet (arrowheads). Apical confocal slices and corresponding z-sections (indicated by dotted line) are displayed. Bar 10µm.

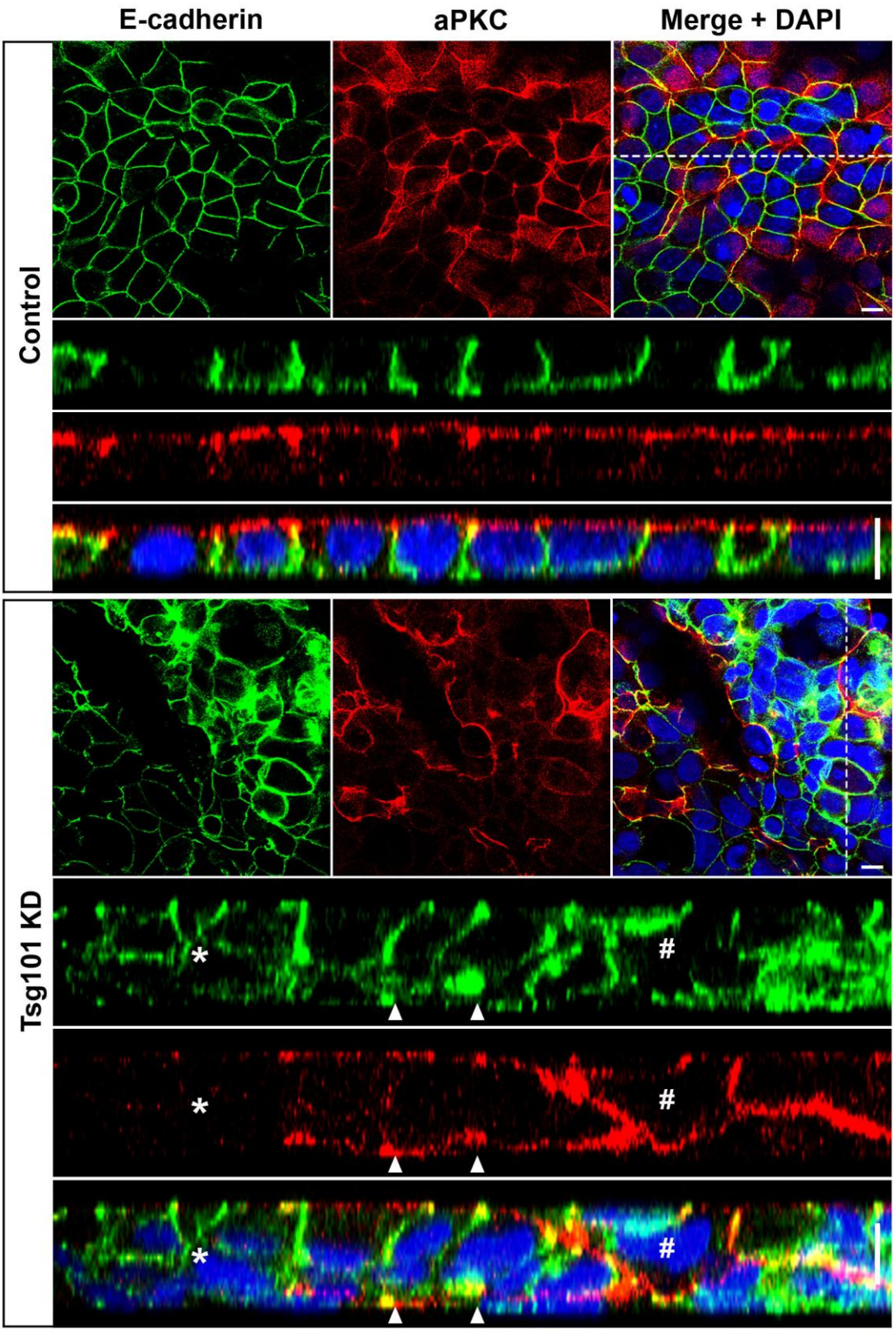
E-cadherin
aPKC
Merge + DAPI
Control
Tsg101 KD
*
#
*
#
*
#

***Figure 3.15*** **Brush border formation is compromised in multilayered regions of Tsg101 depleted Caco-2 cells.** Caco-2 cells were transfected with either Non-Targeting Control siRNA or Tsg101 siRNA, incubated for 7 d and stained for the brush border protein, DppIV (green). Nuclei were stained with DAPI (blue). Multilayered regions are indicated by an asterisk. Note that some multilayered Tsg101 knockdown cells show an absence of DppIV staining (i, arrowheads) whereas, for other cells, DppIV staining is apparent (ii, arrows). Confocal projections and corresponding z-sections (indicated by dotted line) are displayed. Bar 10µm.

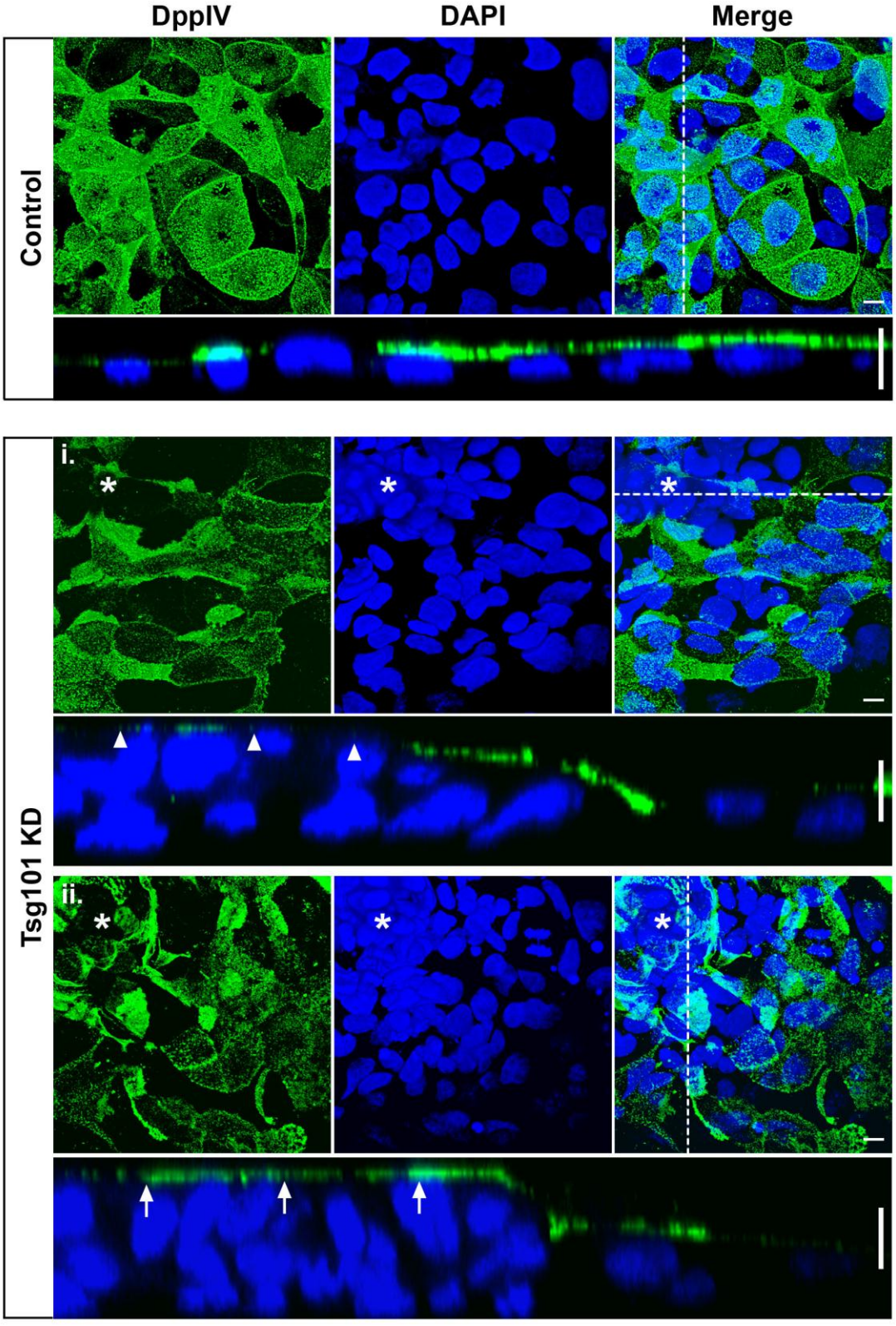
DppIV
DAPI
Merge
Control
Tsg101 KD
i.
ii.

### 3.2.6. Formation of Caco-2 cysts is compromised upon ESCRT knockdown

Finally, in order to further investigate the role of ESCRT proteins in regulation of epithelial cell polarity, a three-dimensional (3D) epithelial cyst formation assay was performed. When cultured in a matrigel suspension, Caco-2 cells form 3D cysts whereby a single layer of cells surrounds a central lumen. These cells polarise so that their apical membranes are orientated to the luminal side and the basal membranes are in contact with the matrigel. Therefore, these 3D cultures are an additional method of investigating cell polarity *in vitro* and are considered more physiologically relevant (Martin-Belmonte and Mostov, 2008). When transfected with non-targeting control siRNA, 64% of Caco-2 cysts displayed a single central lumen (Figure 3.16). The remainder of cysts either failed to form an extended lumen or displayed multiple small cavities. Knockdown of Tsg101 or Vps25 resulted in a significant reduction in the number of cysts formed with a central lumen, instead the proportion of multi-lumen cysts approximately doubled from 20% in control to 40% upon ESCRT knockdown. This observation is indicative of a defect in epithelial cell polarity and therefore suggests that Tsg101 is required for establishment and/or maintenance of Caco-2 cell polarity in both 2D and 3D cultures. Although Vps25 knockdown did not appear to affect cell polarity in 2D cultures, this 3D cyst formation assay suggests that Vps25 is required for correct polarisation of Caco-2 cells.

***Figure 3.16*** **Tsg101 and Vps25 knockdown impairs formation of Caco-2 3D cysts. (A)** Caco-2 cells were transfected with either Non-Targeting Control siRNA, Tsg101 siRNA or Vps25 siRNA, incubated for 3 d and then replated into a Matrigel suspension. Following incubation for 7 d, cysts were stained for aPKC (red) and E-cadherin (green) to mark the apical and basolateral membranes respectively. Nuclei were stained with DAPI (blue). Cysts displayed either a single lumen, multiple lumen or no lumen. Representative images are shown for each phenotype. Z-sections are displayed for each cyst along with a confocal plane through the centre. Bar, 10µm. **(B)** The number of cysts showing either single, multiple or no lumen was quantified. Data shown are the means ± standard error from three independent experiments, >100 cysts were analysed per condition for each experiment. Results were analysed using a One-Way ANOVA and Dunnett's post-test, ** p=< 0.01 * p=< 0.05.

**A.**

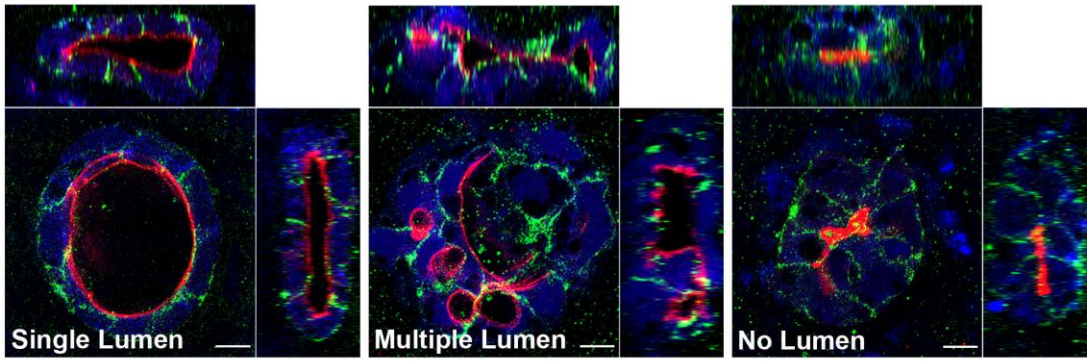
Single Lumen
Multiple Lumen
No Lumen

**B.**

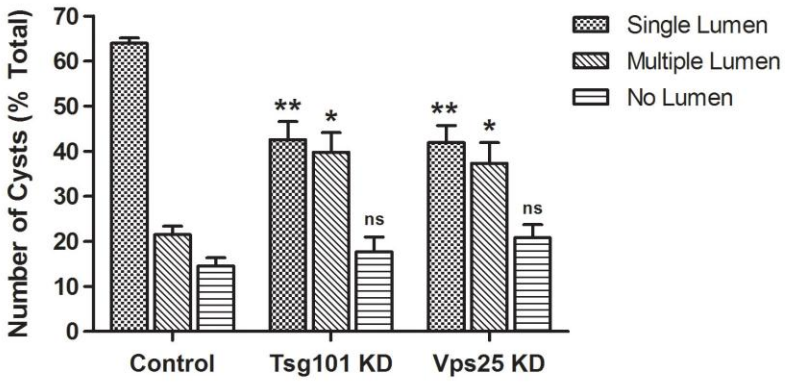
Number of Cysts (% Total)
70
60
50
40
30
20
10
0
**
*
ns
**
*
ns
Control
Tsg101 KD
Vps25 KD
Single Lumen
Multiple Lumen
No Lumen

## 3.3. Discussion

This study sought to establish whether ESCRT proteins are required for maintenance of mammalian epithelial cell polarity. Although studies in *Drosophila* have demonstrated an important link between ESCRT proteins and epithelial cell polarity (Moberg *et al.,* 2005; Thompson *et al.,* 2005; Vaccari and Bilder, 2005; Rodahl *et al.,* 2009b; Vaccari and Bilder, 2009), no similar definitive link has been identified in mammalian cells. My results demonstrate that depletion of Tsg101 and Vps25 can be achieved in the polarised human epithelial Caco-2 cell line via siRNA knockdown, and that this induces an enlarged endosomal phenotype characteristic of ESCRT disruption. Differentiation of Caco-2 cells is impaired upon knockdown of both Tsg101 and Vps25. In addition, Tsg101 depletion compromises organisation and polarity of the Caco-2 epithelial sheet. Finally ESCRT-I and -II are required for the formation of 3D Caco-2 polarised cysts. Therefore, these results begin to elucidate a role for ESCRT proteins within the maintenance of mammalian epithelial cell organisation and polarity.

### 3.3.1. ESCRT depletion in Caco-2 cells via siRNA knockdown

Disruption of ESCRT-I or -II was achieved in the human epithelial Caco-2 cell line via efficient siRNA knockdown of Tsg101 or Vps25, respectively. Tsg101 depletion was achieved using an individual siRNA duplex. This was identified as providing the most efficient knockdown from a SMARTpool of four siRNA oligonucleotides designed to target Tsg101 mRNA. However, Vps25 knockdown was performed using a siRNA SMARTpool only. Due to the lack of an effective commercial Vps25 antibody, the Vps25 siRNA oligonucleotides contained within the SMARTpool were not tested individually and therefore, further studies may require additional optimisation and verification of the Vps25 knockdown phenotype.

### 3.3.2. Endosomal effects upon ESCRT depletion

Depletion of ESCRT-I and -II resulted in an accumulation and enlargement of both early and late endosomes after EGF internalisation. However, despite the

similar effects on morphology, these compartments remained clearly differentiated. Previous studies have shown a similar endocytic phenotype upon ESCRT depletion in a variety of cell lines (Bishop *et al.,* 2002; Doyotte *et al.,* 2005; Razi and Futter, 2006; Stuffers *et al.,* 2009b), therefore, demonstrating that ESCRT knockdown in Caco-2 cells results in the characteristic changes to endosomal morphology. In the absence of EGF, however, endosomal morphology was not significantly altered. This has been observed previously (Razi and Futter, 2006) and indeed, most studies into alterations in endosomal morphology after ESCRT disruption are carried out after EGF stimulation (Doyotte *et al.,* 2005; Stuffers *et al.,* 2009b). It is possible that the burst of endocytosis induced by EGF stimulation results in the endosomal effects induced by ESCRT disruption becoming more pronounced.

Previous studies have also demonstrated a requirement for the ESCRT machinery in the degradation of both EGF and EGFR (Bishop *et al.,* 2002; Lu *et al.,* 2003; Bache *et al.,* 2006; Malerod *et al.,* 2007; Raiborg *et al.,* 2008). In addition, depletion of ESCRTs has been reported to affect EGF signalling. Sustained phosphorylation and activation of extracellular-signal-regulated kinase 1/2 (ERK1/2) which, upon EGF stimulation, becomes phosphorylated, translocates to the nucleus and is involved in regulation of various transcription factors (Murphy and Blenis, 2006), has been observed upon disruption of ESCRT-0 and -I, but not ESCRT-II and -III (Bache *et al.,* 2006; Malerod *et al.,* 2007). This suggests that the early ESCRT complexes are required for silencing of EGF signalling whereas ESCRT-II and -III are not. However, no significant accumulation of EGF or sustained phosphorylation of ERK1/2 was observed in Caco-2 cells after Tsg101 or Vps25 knockdown, despite the characteristic endosomal enlargement. This suggests that EGF degradation is not perturbed in ESCRT depleted Caco-2 cells.

It could be speculated that alternative ESCRT-independent mechanisms of EGF trafficking and degradation exist and that, upon ESCRT depletion, these pathways may be upregulated or preferentially selected. A recent study which depleted subunits of all four ESCRT complexes demonstrated that, upon disruption of the entire ESCRT machinery, MVBs can still form, although the resulting compartment was considerably enlarged (Stuffers *et al.,* 2009b). This

suggests that ESCRT-independent mechanisms of MVB formation exist and is supported by additional studies which demonstrate ESCRT-independent cargo sorting into intraluminel vesicles of MVBs (Theos *et al.,* 2006; Trajkovic *et al.,* 2008).

The relevance of these possible alternative mechanisms may also be dependent on cell type. This could explain the discrepancies between my results and those published by other groups as the effect of ESCRT disruption has not previously been studied in polarised epithelial cells, with the majority of studies undertaken in the HeLa cell line (Bishop *et al.,* 2002; Lu *et al.,* 2003; Doyotte *et al.,* 2005; Bache *et al.,* 2006; Raiborg *et al.,* 2008). Polarised epithelial cells have a more complex endosomal system with a number of additional endocytic compartments (Hoekstra *et al.,* 2004; Mellman and Nelson, 2008; Folsch *et al.,* 2009; Weisz and Rodriguez-Boulan, 2009) therefore, it is likely that additional and/or different trafficking routes exist compared with unpolarised cells. The kinetics of EGF-EGFR trafficking upon ESCRT disruption could be studied in more detail, for example using radiolabelled $^{125}$I-EGF to study its' degradation and recycling.

### 3.3.3. ESCRT depletion alters Caco-2 cell morphology

Caco-2 cells are a well characterised polarised human epithelial cell line. In culture they form a functional polarised monolayer with established cell-cell junctions and distinct apical and basolateral membrane domains. Upon reaching confluency, cells spontaneously differentiate during which cell-cell junctions mature, lateral height increases and a brush border of microvilli forms at the apical membrane (Grasset *et al.,* 1984; Chantret *et al.,* 1988; Sambuy *et al.,* 2005; Volpe, 2008). At this stage, Caco-2 cells exhibit the characteristic cobblestone morphology via phase contrast microscopy, which is typical of a differentiated epithelial monolayer. However, upon knockdown of Tsg101 and Vps25, Caco-2 cell differentiation was inhibited. Although ESCRT depleted cells were still able to establish apicobasal polarity if monolayered epithelial organisation was retained, lateral height and brush border formation were reduced. This suggests that establishment of distinct apical and basolateral membrane domains does not require a functional ESCRT machinery, however,

differentiation to a fully polarised epithelial monolayer is directly or indirectly ESCRT-dependent.

In support of this observation, ESCRT mutant cells also fail to differentiate in *Drosophila* (Vaccari and Bilder, 2005; Herz *et al.,* 2006). In mammalian epithelial cells, several studies have demonstrated a requirement for phosphatidylinositol 3-kinase (PI3K) signalling for differentiation (Laprise *et al.,* 2002; Gassama-Diagne *et al.,* 2006; Jeanes *et al.,* 2009). Inhibition of PI3K impaired differentiation of epithelial cells, shown by a reduction in cell height and brush border formation. This was accompanied by a reduction in phosphatidylinositol-3,4,5-triphosphate ($PIP_3$), a key regulator of basolateral membrane formation in epithelial cells (Gassama-Diagne *et al.,* 2006). Interestingly, although PI3K has been shown to be important for adherens junction assembly (Laprise *et al.,* 2002), surface expression of E-cadherin and apicobasal polarity of established epithelial monolayers was not affected by PI3K inhibition (Laprise *et al.,* 2002; Jeanes *et al.,* 2009). Therefore, this phenotype is similar to that observed upon ESCRT depletion in Caco-2 cells. The ESCRT machinery is important for regulation of various receptor signalling pathways (Wegner *et al.,* 2011) although a role within the PI3K pathway has not been documented. As PI3K activity is important for epithelial cell differentiation, it would be of interest to establish whether the effects seen on Caco-2 cell height and brush border formation are accompanied by alterations in PI3K signalling.

### 3.3.4. ESCRT-I is required for maintenance of a polarised Caco-2 epithelial monolayer

In addition to defects in differentiation of Caco-2 cells upon Tsg101 knockdown, large areas of the epithelial sheet lost the normal monolayered organisation and multilayered stacks of cells were formed. These multilayers displayed compromised apicobasal polarity and brush border formation. This phenotype was confirmed using two different Tsg101 siRNA oligonucleotides and therefore is specific for Tsg101 depletion. The loss of epithelial polarity and organisation is similar to that observed in *Drosophila* upon mutation of Tsg101 (Moberg *et al.,* 2005) and suggests that the requirement for a functional ESCRT machinery

is conserved in mammalian cells. Studies in *Drosophila* also demonstrated a similar disruption in epithelial cell polarity upon Vps25 mutation as well as other components of the ESCRT machinery (Thompson *et al.,* 2005; Vaccari and Bilder, 2005; Herz *et al.,* 2006; Rodahl *et al.,* 2009b; Vaccari *et al.,* 2009). This is in contrast to my data in which Vps25 knockdown does not cause a disruption in apicobasal polarity or organisation of the epithelial sheet. The role of ESCRT-II in mammalian cells is unclear as it has been demonstrated that Vps25 is dispensable for MVB protein sorting (Bowers *et al.,* 2006). It is possible that the requirement for ESCRT-II varies from *Drosophila* to mammals and therefore, this may explain why Vps25 knockdown does not affect apicobasal polarity in Caco-2 cells.

Alternatively, this difference in phenotype between Tsg101 and Vps25 depletion may be due to the level of knockdown achieved over time. After 3 days approximately 80% Tsg101 knockdown was achieved whereas only 60% of Vps25 protein was depleted. After 7 days, Vps25 knockdown reached a similar level to Tsg101, however, by this timepoint cells will have been subjected to an extended period of Tsg101 depletion compared with Vps25. Therefore, this may result in a stronger phenotype for Tsg101 knockdown cells. It would be of interest to optimise Vps25 knockdown to the same level as Tsg101 knockdown in order to investigate whether a defect in epithelial cell polarity and organisation is observed. One approach to accomplish this would be to split the Vps25 siRNA SMARTpool into the four individual oligonucleotides and determine whether a more efficient knockdown could be achieved at an earlier timepoint. In addition, other ESCRT-II components could be depleted, either individually or in combination.

The disruption in apicobasal polarity and formation of multilayers after Tsg101 knockdown in Caco-2 cells could be due to a number of possible mechanisms. Firstly, disruption of ESCRT-I may affect the trafficking of various proteins important for the maintenance of epithelial cell polarity. For example, in *Drosophila* ESCRT mutants, loss of cell polarity was attributed to mislocalisation of Crumbs from the apical membrane to a subapical compartment (Moberg *et al.,* 2005). It is clear that localisation of polarity complexes to specific membrane domains is also crucial for establishment and maintenance of mammalian

epithelial cell polarity. The PAR and CRB complexes are important for apical membrane identity and the SCRIB complex for basolateral membrane identity (Roh *et al.,* 2003; Kallay *et al.,* 2006; Suzuki and Ohno, 2006; Yamanaka *et al.,* 2006; Horikoshi *et al.,* 2009). In addition, maintenance of cell-cell junctions is also important to retain a polarised phenotype. Tight junctions provide a fence function to prevent diffusion of lipids between the apical and basolateral membrane domains (Matter and Balda, 2003; Shin *et al.,* 2006) and loss of E-cadherin from the adherens junctions is often associated with epithelial to mesenchymal transition (Perl *et al.,* 1998; Yang and Weinberg, 2008). In fact, it is becoming increasingly apparent that cell-cell junctions function as a platform for many regulatory and signalling proteins important for establishing the epithelial phenotype (Ivanov *et al.,* 2005). Cell-cell junctions are dynamic structures that are constantly being remodelled (Shen *et al.,* 2008; Steed *et al.,* 2010) and there is growing evidence of links between endocytosis, regulation of epithelial junctions (Ivanov *et al.,* 2005) and cell polarity (Shivas *et al.,* 2010). Thus, it is likely that protein trafficking plays a crucial role in maintaining epithelial cell polarity. ESCRT-I depletion has been shown to disrupt the endocytic pathway (Bishop *et al.,* 2002; Doyotte *et al.,* 2005; Razi and Futter, 2006; Stuffers *et al.,* 2009b) and therefore, compromised Caco-2 cell polarity observed upon Tsg101 knockdown may be due to perturbed trafficking of proteins important for maintenance of apicobasal polarity and cell-cell junctions. As a result of this defect in polarity cells may be unable to retain the correct organisation within the epithelial sheet and begin to form multilayers. The effects of ESCRT depletion on cell-cell junctions will be analysed in more detail in Chapter Four.

Conversely, Tsg101 knockdown cells may lose correct epithelial organisation, form multilayers and, as a consequence, apicobasal polarity of the epithelial sheet cannot be retained. Some cells within the multilayered regions do seem to retain distinct apical and basolateral membrane domains suggesting that individually apicobasal polarity may be maintained however, due to loss of the monolayered organisation, cells are incorrectly orientated within the multilayered epithelial sheet. Multilayering of cells may be due to an increased rate of proliferation whereby cells divide too rapidly to maintain epithelial organisation. Alternatively, Tsg101 knockdown may result in a defect in contact

inhibition. Upon reaching confluency, Caco-2 cells will reduce rate of cell division as a result of contact inhibition (Nelson and Daniel, 2002) and begin to differentiate (Volpe, 2008). If Tsg101 knockdown somehow interferes with this process, cells may continue to proliferate and as a result begin to pile on top of one another, disrupting the normal epithelial monolayer. Studies in *Drosophila* support this hypothesis as the overgrowth observed in epithelial tissues composed almost entirely of ESCRT mutant cells was attributed to a failure of cells to exit the cell cycle rather than an increased rate of proliferation (Moberg *et al.,* 2005; Vaccari and Bilder, 2005). Chapter Five will begin to investigate the effects of ESCRT knockdown on Caco-2 cell proliferation.

Finally, Tsg101 knockdown may destabilise cellular contacts with the ECM resulting in a loss of basal adhesion. Cells may then detach and migrate out of the epithelial monolayer, leading to the formation of multilayers. The main components of cellular adhesions to the ECM are the cell surface integrin receptors (Bosman *et al.,* 1993; Matlin *et al.,* 2003; Lobert *et al.,* 2010). Integrins are heterodimeric type I transmembrane glycoproteins comprised of α and β chains which, upon binding to ECM ligands such as fibronectin, laminin or collagen, regulate many aspects of cell behaviour (Matlin *et al.,* 2003; Lobert *et al.,* 2010). In epithelial cells, integrins are important for the maintenance of apicobasal polarity (Eaton and Simons, 1995; Matlin *et al.,* 2003). Orientation of the apicobasal axis in MDCK cells is dependent on $\beta_1$ integrin (Ojakian and Schwimmer, 1994) and loss of apical polarity and formation of multilayers in MDCK cells transformed with viral K-*ras* (Schoenenberger *et al.,* 1991) has been attributed to a reduction in $\beta_1$ integrin (Schoenenberger *et al.,* 1994). A role for ESCRT proteins in the regulation of integrins has been suggested by a recent study which demonstrated that in fibroblasts, ESCRT-I binds to $\alpha_5\beta_1$ integrin after fibronectin-induced activation and subsequent ubiquitination. Furthermore, ESCRT-I was required for degradation of $\alpha_5\beta_1$ integrin via sorting into MVBs and this in turn, was required for efficient cell migration (Lobert *et al.,* 2010). Therefore, it is possible that ESCRT proteins may function to regulate integrin levels in epithelial cells. It would be interesting to investigate whether the multilayering of Caco-2 cells induced by Tsg101 knockdown was accompanied by alterations in integrin protein levels and localisation.

### 3.3.5. ESCRTs are required for epithelial cell polarity in 3D cultures

ESCRT depletion resulted in an increase in the proportion of Caco-2 cysts displaying multiple small lumen. This phenotype is indicative of a defect in epithelial cell polarity (Schluter and Margolis, 2009) and provides additional evidence for a role of ESCRT proteins in the establishment and maintenance of cell polarity. Interestingly, whilst Vps25 knockdown did not appear to disrupt formation of a polarised Caco-2 cell monolayer in 2D cultures, formation of 3D cysts was perturbed by Vps25 depletion. 3D cell cultures may provide a more sensitive assay for detecting defects in epithelial cell polarity, providing a possible explanation for this disparity. This has been observed in previous studies whereby defects in epithelial cell polarity were only apparent upon growth of cells in 3D cultures (Roh *et al.,* 2003; Martin-Belmonte *et al.,* 2007; Torkko *et al.,* 2008). It has been suggested that polarisation and formation of the apical membrane is extremely robust and can be executed despite defects in epithelial architecture and therefore, polarity defects are not observed upon formation of a simple 2D epithelial monolayer (Torkko *et al.,* 2008). Epithelial cyst formation is also considered to be a more physiologically relevant method of investigating epithelial cell polarity *in vitro* (Martin-Belmonte and Mostov, 2008). This, therefore, highlights the necessity to utilise a variety of methods to fully characterise a knockdown phenotype in polarised epithelial cells.

Formation of 3D polarised epithelial cysts requires individual cells to generate apical, lateral and basal membrane surfaces in a coordinated manner in order to establish a polarised multicellular structure (O'Brien *et al.,* 2002). Formation of a central lumen is thought to occur via two mechanisms: hollowing and cavitation (Martin-Belmonte and Mostov, 2008). During hollowing, separation of opposing membranes results in the formation of an intercellular lumen, whereas cavitation involves apoptosis of cells in the centre of the structure to create luminal space (O'Brien *et al.,* 2002; Martin-Belmonte and Mostov, 2008; Schluter and Margolis, 2009). Separation of membranes is thought to be induced by the delivery of lumen formation factors, such as anti-adhesive large transmembrane glycoproteins, to the nascent luminal surface. In addition, exocytosis of a specialised fluid-filled organelle, the vacuolar apical compartment (VAC) to the centre of the forming cyst aids in lumen formation

(O'Brien *et al.,* 2002; Martin-Belmonte and Mostov, 2008; Schluter and Margolis, 2009).

The mechanism of lumen formation can shift between hollowing and cavitation and this has been shown to be dependent on efficiency of apicobasal polarisation (Martin-Belmonte *et al.,* 2008). In the absence of apicobasal polarity, lumen formation does not occur (Martin-Belmonte and Mostov, 2008; Schluter and Margolis, 2009). For example, interference with the key polarity proteins, such as CRB3, during cyst formation results in an abnormal lumen phenotype (Roh *et al.,* 2003; Straight *et al.,* 2004; Shin *et al.,* 2005; Martin-Belomonte *et al.,* 2007; Schluter *et al.,* 2009). In addition, formation of tight junctions and correct localisation of apical and basolateral proteins is also important for formation of polarised epithelial cysts (Schluter and Margolis, 2009). Depletion of JAM-A, a tight junction component, (Rehder *et al.,* 2006) and abnormal segregation of membrane phosphoinositides (Martin-Belmonte *et al.,* 2007) resulted in defective cyst formation.

It has been proposed that defective trafficking of proteins involved in epithelial cyst formation could result in abnormal lumen phenotypes (Schluter and Margolis, 2009). In support of this, depletion of various proteins implicated in apical transport perturbed polarised epithelial cyst formation (Torkko *et al.,* 2008). Therefore, the increase in Caco-2 cysts displaying multiple lumen after ESCRT depletion may reflect a defect in trafficking of proteins important for maintenance of apicobasal polarity and/or cell-cell junctions. Interestingly, abnormal lumen formation is also observed in epithelial glandular cancers such as breast cancer, and thus proteins important for epithelial cyst formation may be implicated in the process of tumourigenesis (Debnath and Brugge, 2005). Therefore, this provides further evidence for a potential role of the ESCRT proteins as tumour suppressors in vertebrates.

## 3.4. Conclusion

This study demonstrates for the first time that ESCRT proteins have an important role within the maintenance of mammalian epithelial cell polarity. Depletion of Tsg101 in the human Caco-2 cell line results in loss of epithelial organisation and the formation of a multilayered epithelium with compromised apicobasal polarity. In addition both ESCRT-I and -II are required for differentiation of a mature Caco-2 epithelial sheet and formation of polarised 3D Caco-2 cysts. These results are very similar to findings in *Drosophila* whereby disruption of the ESCRT machinery resulted in a loss of epithelial cell polarity, reduced differentiation and the formation of tumour-like tissue overgrowths (Moberg *et al.,* 2005; Thompson *et al.,* 2005; Vaccari and Bilder, 2005; Herz *et al.,* 2006; ; Herz *et al.,* 2009; Rodahl *et al.,* 2009b; Vaccari *et al.,*, 2009). Therefore, these results demonstrate that ESCRT proteins are required for the maintenance of mammalian epithelial cell organisation and polarity, suggesting that the role of ESCRTs as tumour suppressors may be conserved from *Drosophila* to mammals.

# CHAPTER FOUR

# 4. Claudin localisation to tight junctions and epithelial barrier formation is dependent on ESCRT-I

## 4.1. Introduction

### 4.1.1. Cell-Cell Junctions and Epithelial Cell Polarity

Establishment and maintenance of epithelial cell polarity is regulated, in part, through the formation of specialised cell-cell junctions. These form between the lateral membranes of adjacent cells and are composed of various transmembrane and membrane-associated proteins (Bryant and Mostov, 2008; Coradini *et al.,* 2011). At the most apical part of the lateral membrane, tight junctions define the boundary between the apical and basolateral membrane domains where they provide a fence function to restrict intramembrane diffusion of lipids (Matter and Balda, 2003). Tight junctions also form a barrier to control paracellular diffusion across the epithelial sheet (Matter and Balda, 2003; Shin *et al.,* 2006). Localised below tight junctions are adherens junctions, desmosomes and gap junctions, important for cell-cell adhesion, anchoring the cytoskeleton to the plasma membrane and intercellular signalling (Yin and Green, 2004; Niessen and Gottardi, 2008; Nakagawa *et al.,* 2010).

Disruption of cell-cell junctions can often perturb epithelial cell polarity (Brennan *et al.,* 2010; Coradini *et al.,* 2011; Turksen and Troy, 2011). For example, loss of E-cadherin from adherens junctions is associated with epithelial to mesenchymal transition (Perl *et al.,* 1998; Yang and Weinberg, 2008) and alterations in tight junction structure and function are often associated with enhanced invasiveness of human carcinomas (Miyoshi and Takai, 2005; Oliveira and Morgado-Diaz, 2007). In addition, cell-cell junctions are thought to function as a platform for many regulatory and signalling proteins important for establishing the epithelial phenotype (Ivanov *et al.,* 2005).

### 4.1.2. ESCRT Proteins and Cell-Cell Junctions

Once formed, cell-cell junctions are dynamic structures that are continuously being remodelled (Shen *et al.,* 2008; Steed *et al.,* 2010). Previous studies have demonstrated that the tight junction proteins, claudin and occludin, and adherens junction protein, E-cadherin, are endocytosed in epithelial cells (Le *et al.,* 1999; Marzesco *et al.,* 2002; Matsuda *et al.,* 2004; Morimoto *et al.,* 2005). Internalisation of different junctional components appears to be highly specific and may be mediated by ubiquitylation by specific E3 ubiquitin ligases (Fujita *et al.,* 2002; Traweger *et al.,* 2002; Yu and Turner, 2008; Takahashi *et al.,* 2009).

Due to growing evidence of links between endocytosis, regulation of epithelial junctions (Ivanov *et al.,* 2005) and cell polarity (Shivas *et al.,* 2010), it is likely that protein trafficking plays a crucial role in maintaining a polarised epithelium. Previously I have demonstrated that ESCRT-I depletion compromises epithelial organisation and polarity of Caco-2 cells in both 2D and 3D cultures. As ESCRT-I depletion has been shown to disrupt the endocytic pathway (Bishop *et al.,* 2002; Doyotte *et al.,* 2005; Razi and Futter, 2006; Stuffers *et al.,* 2009b), it is possible that the compromised Caco-2 cell polarity observed upon Tsg101 knockdown is due to perturbed trafficking of junctional proteins. As a result, cell-cell junctions may be destabilised and this could in turn disrupt epithelial cell polarity.

### 4.1.3. Aims

The work described in this chapter aims to establish whether depletion of Tsg101 or Vps25 affects cell-cell junctions in Caco-2 epithelial cells. Localisation of various junctional proteins will be investigated followed by analysis of the functional consequences of knockdown on epithelial barrier formation and migratory ability. In addition, the dynamics of cell-cell junction proteins in Caco-2 cells will be characterised.

## 4.2. Results

### 4.2.1. Tsg101 depletion affects localisation of claudin-1 and -4 to tight junctions

In order to investigate whether ESCRT depletion affected cell-cell junctions, the localisation of various junction proteins was analysed following Tsg101 and Vps25 knockdown in Caco-2 cells. Note that characterisation of Tsg101 knockdown cells was carried out in areas where the epithelial monolayered organisation was retained. Multilayered areas of Tsg101 knockdown cells display compromised epithelial cell polarity which may have indirect effects on cell-cell junctions. In addition, these multilayered regions were difficult to image in detail using confocal fluorescence microscopy. Upon knockdown of Tsg101 or Vps25, the tight junction proteins, occludin and ZO-1, desmosomal protein, desmoglein-2, and adherens junction protein, E-cadherin, all localised to cell-cell junctions as in control cells (Figure 4.1A+B). However, localisation of claudin-1 and claudin-4 was disrupted in Tsg101 knockdown cells compared with control (Figure 4.2A). Claudin-1 and -4 appeared to accumulate within the same intracellular compartment (Figure 4.2A, arrowheads). In addition, localisation of these proteins to tight junctions was reduced but not completely lost. This intracellular claudin accumulation was not accompanied by significant changes in total claudin levels (Figure 4.2B). In contrast, Vps25 knockdown did not appear to significantly affect claudin-1 or -4 localisation or protein levels and these cells appeared similar to control (Figure 4.2A+B).

The effect of Tsg101 knockdown on claudin-1 localisation was confirmed using two alternative siRNA oligonucleotides which were optimised previously (Chapter 3, section 3.2.3). Intracellular accumulation of claudin-1 was observed after Tsg101 knockdown using these alternative siRNA oligonucleotides indicating that the effect is specific to Tsg101 depletion rather than any off-target effects (Figure 4.3). Therefore, this demonstrates that ESCRT-I is required for the correct localisation of claudin-1 and -4 to tight junctions in Caco-2 cells. Interestingly, other cell-cell junction proteins analysed were not affected.

***Figure 4.1*** **Depletion of Tsg101 and Vps25 does not alter the localisation of a number of cell-cell junction proteins in Caco-2 cells.** Caco-2 cells were transfected with either Non-Targeting Control siRNA, Tsg101 siRNA or Vps25 siRNA and incubated for 7 d. Cells were fixed and examined by confocal fluorescence microscopy for **(A)** occludin (red) and desmoglein-2 (green) or **(B)** ZO-1 (red) and E-cadherin (green). Nuclei were stained with DAPI (blue). Bar, 10μm.

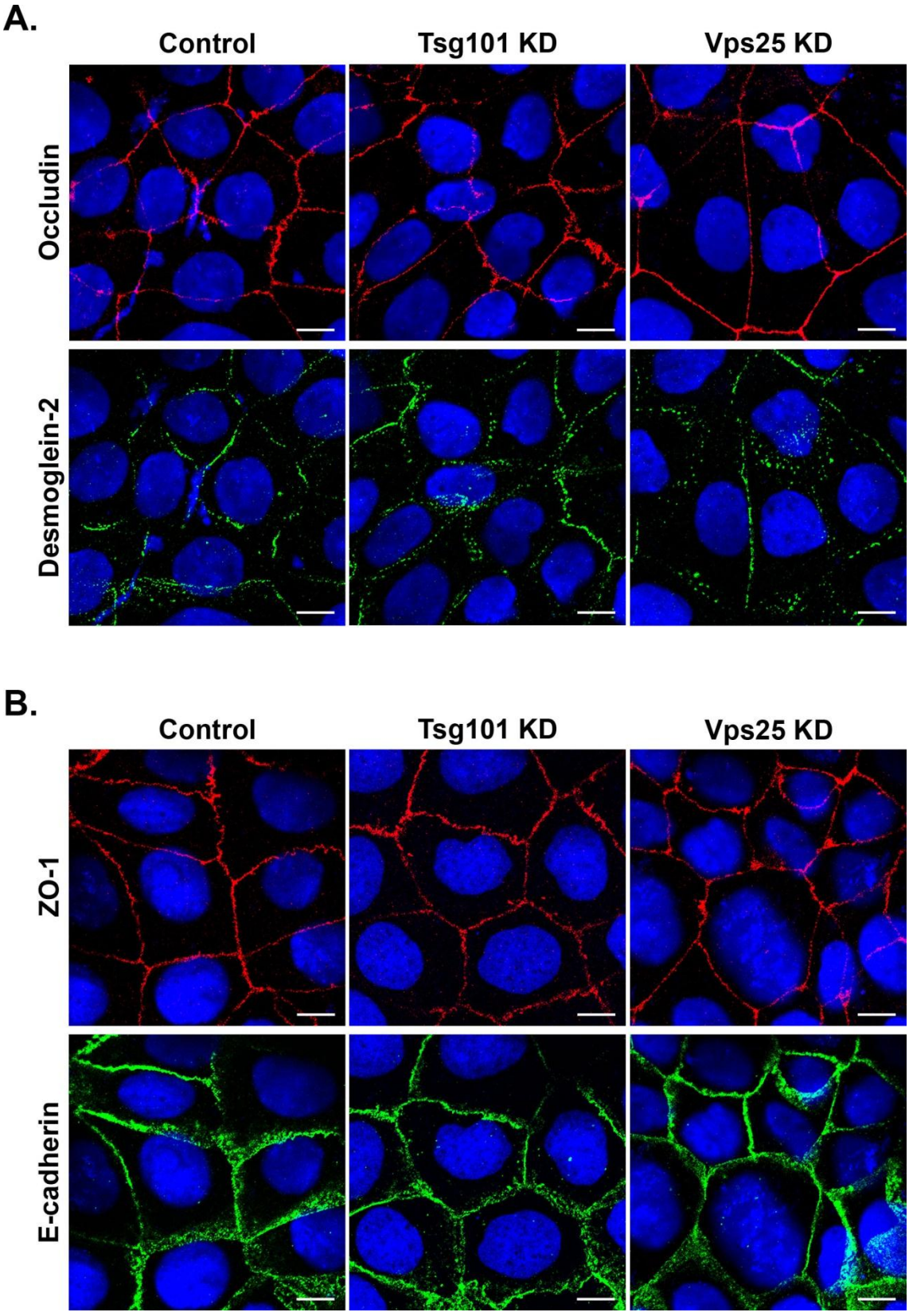
A.
Control
Tsg101 KD
Vps25 KD
Occludin
Desmoglein-2
B.
Control
Tsg101 KD
Vps25 KD
ZO-1
E-cadherin

***Figure 4.2*** **Tsg101 knockdown results in intracellular accumulation of claudins in Caco-2 cells. (A)** Caco-2 cells were transfected with either Non-Targeting Control siRNA, Tsg101 siRNA or Vps25 siRNA and incubated for 7 d. Cells were fixed and examined by confocal fluorescence microscopy for claudin-1 (green) and claudin-4 (red). Nuclei were stained with DAPI (blue) shown in merged images. Claudin-1 and -4 accumulate in a similar intracellular compartment after Tsg101 knockdown (arrowheads) whereas Vps25 knockdown cells appear similar to control. Bar, 10μm. **(B)** Caco-2 cells were transfected with either Non-Targeting Control siRNA (C), Tsg101 siRNA (T) or Vps25 siRNA (V) and incubated for 7 d. Lysates were immunoblotted for claudin-1 and claudin-4. β-tubulin is shown as a loading control. Total claudin-1 and claudin-4 protein levels do not appear to be altered in Tsg101 or Vps25 knockdown cells compared to control.

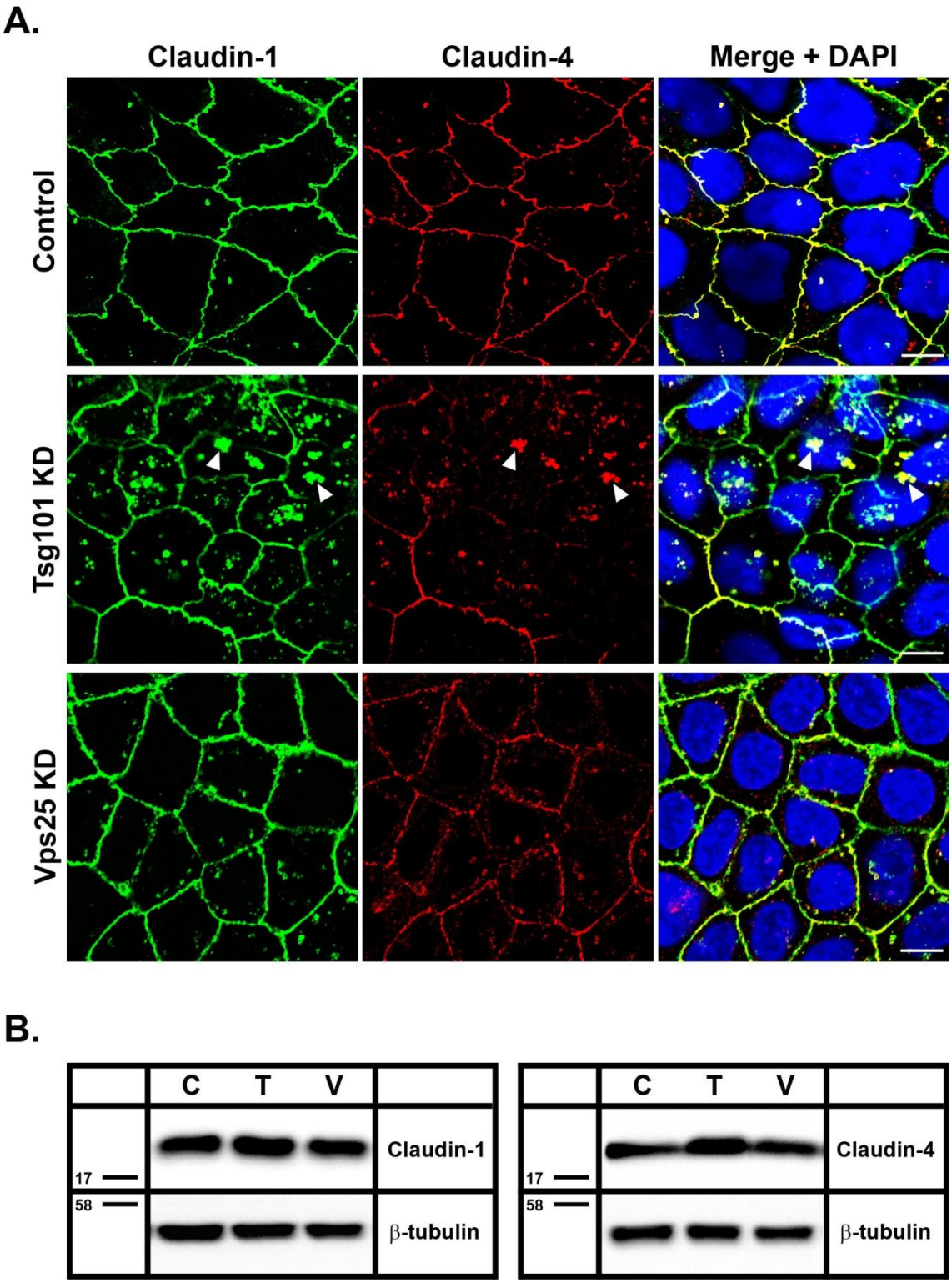
A.
Claudin-1
Claudin-4
Merge + DAPI
Control
Tsg101 KD
Vps25 KD
B.
C
T
V
Claudin-1
β-tubulin
17
58
C
T
V
Claudin-4
β-tubulin
17
58

***Figure 4.3*** **Knockdown of Tsg101 using alternative siRNA oligonucleotides results in a similar intracellular accumulation of claudin-1 in Caco-2 cells.** Caco-2 cells were transfected with either Non-Targeting Control siRNA or Tsg101 siRNA. Tsg101 knockdown was also achieved using a different single siRNA oligonucleotide (1) or a combination of two different siRNA oligonucleotides (2). After 7 d incubation, cells were fixed and examined by confocal fluorescence microscopy for claudin-1 (green). Nuclei were stained with DAPI (blue) shown in merged images. A similar intracellular accumulation of claudin-1 is observed after knockdown of Tsg101 using alternative siRNA oligonucleotides (1 and 2). Bar, 10µm.

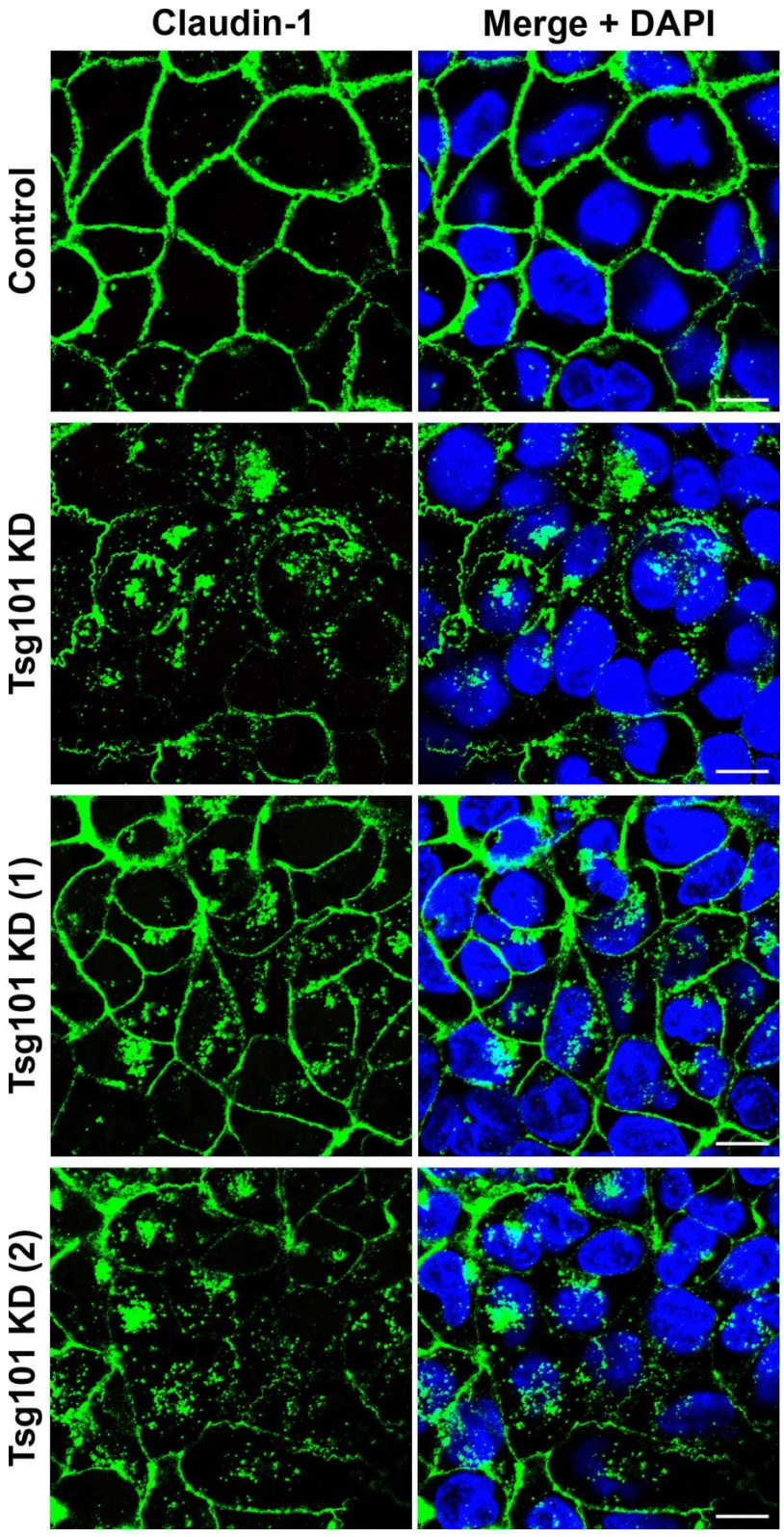
Claudin-1
Merge + DAPI
Control
Tsg101 KD
Tsg101 KD (1)
Tsg101 KD (2)

### 4.2.2. Tsg101 depleted Caco-2 cells accumulate ubiquitylated cargo

In addition to intracellular accumulation of claudin-1, Tsg101 knockdown cells show a dramatic increase in ubiquitin staining, compared to low levels in control cells (Figure 4.4A). This demonstrates that ubiquitylated proteins are accumulating in Tsg101 depleted cells. This has been reported in other studies analysing the effects of ESCRT disruption (Bishop *et al.,* 2002; Dukes *et al.,* 2008; Stuffers *et al.,* 2009b) and suggests that Tsg101 knockdown alters the flux of ubiquitylated proteins along the endocytic pathway. The internal pool of claudin-1 observed upon Tsg101 knockdown partially colocalises with this ubiquitin, indicating that at least some of the mislocalised claudin-1 is accumulating within a similar intracellular compartment (Figure 4.4A, arrowheads). In contrast, Vps25 knockdown had no effect on ubiquitin staining (data not shown).

Ubiquitylation of claudin-1 by the ubiquitin ligase, LNXp180, has previously been shown to induce internalisation (Takahashi *et al.,* 2009). To analyse whether ubiquitylation of claudin-1 was increased in Tsg101 knockdown cells, claudin-1 was immunoprecipitated following Tsg101 knockdown and in control cells. Analysis was carried out for any associated ubiquitin using an antibody which recognises mono- and poly-ubiquitylated proteins but not free ubiquitin (Figure 4.4B). Although ubiquitin was observed in the whole cell lysate, shown by the characteristic smear after immunoblotting (Figure 4.4B, Total Lysate), ubiquitin was not detected in claudin-1 pull downs (Figure 4.4B, IP: CL-1; IB: Ub). Bands showing on the blot are likely to be antibody heavy chain as these are absent from the no IgG control sample (Figure 4.4B, arrowhead). Results demonstrate that claudin-1 immunoprecipitation was successful and specific as claudin-1 was detected in all samples except those which did not include a claudin-1 antibody (Figure 4.4B, no IgG and Rb IgG). Therefore, this demonstrates that claudin-1 ubiquitylation is not observably increased after Tsg101 or Vps25 knockdown. Although the internal pool of claudin-1 often colocalised with ubiquitin in Tsg101 depleted cells, these results suggest that claudin-1 accumulates in a similar compartment to ubiquitylated cargo rather than being directly modified with ubiquitin.

***Figure 4.4*** **Ubiquitin accumulates in Caco-2 cells upon Tsg101 knockdown in a similar intracellular compartment to claudin-1. (A)** Caco-2 cells were transfected with either Non-Targeting Control siRNA or Tsg101 siRNA and incubated for 7 d. Cells were fixed and examined by confocal fluorescence microscopy for claudin-1 (green) and ubiquitin (red). Nuclei were stained with DAPI (blue) shown in merged images. Right panels are zoomed images of areas indicated by dotted lines. Ubiquitin also accumulates in Tsg101 knockdown cells and often localises to a similar intracellular compartment as claudin-1 (arrowhead). However, some claudin-1 and ubiquitin localise to separate compartments (arrows). Bar, 10µm. **(B)** Caco-2 cells were transfected with either Non-Targeting Control siRNA (C), Tsg101 siRNA (T) or Vps25 siRNA (V) and incubated for 3, 7 or 10 d. Claudin-1 was immunoprecipitated from cell lysates at each timepoint and samples were immunoblotted for ubiquitin, arrowhead indicates non-specific (ns) bands. Claudin-1 is shown to confirm efficiency of immunoprecipitation. Controls were performed on untransfected cells and show specific pull down of claudin-1 (compare No IgG/Rb IgG with CL-1 IgG). Total lysates are shown as loading controls. Claudin-1 ubiquitylation does not appear to increase after Tsg101 or Vps25 knockdown.

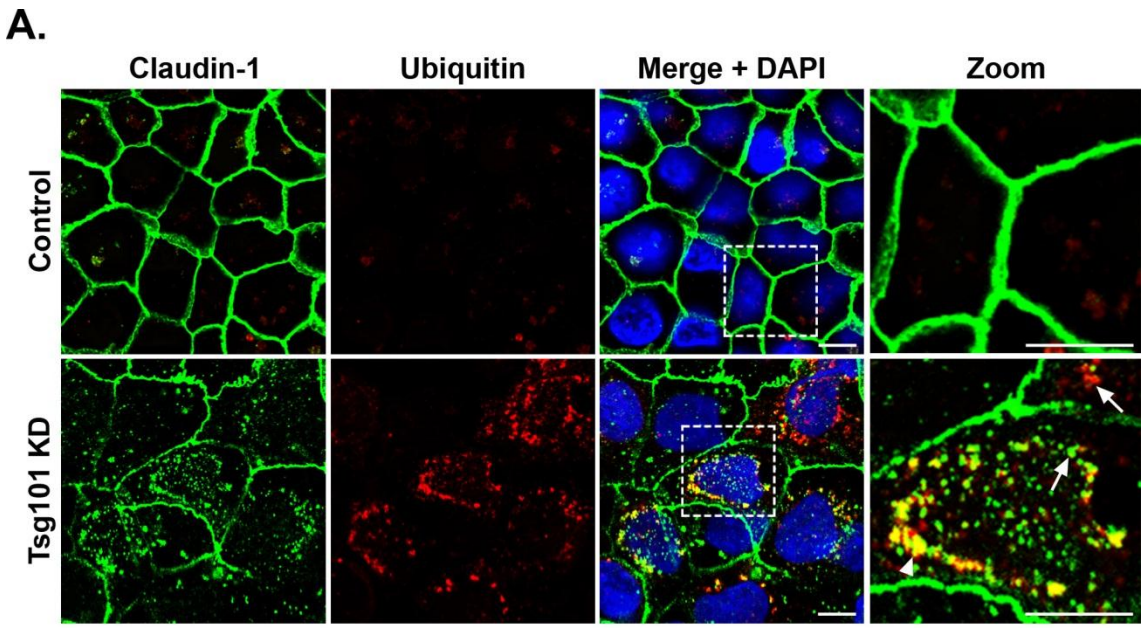
A.
Claudin-1
Ubiquitin
Merge + DAPI
Zoom
Control
Tsg101 KD

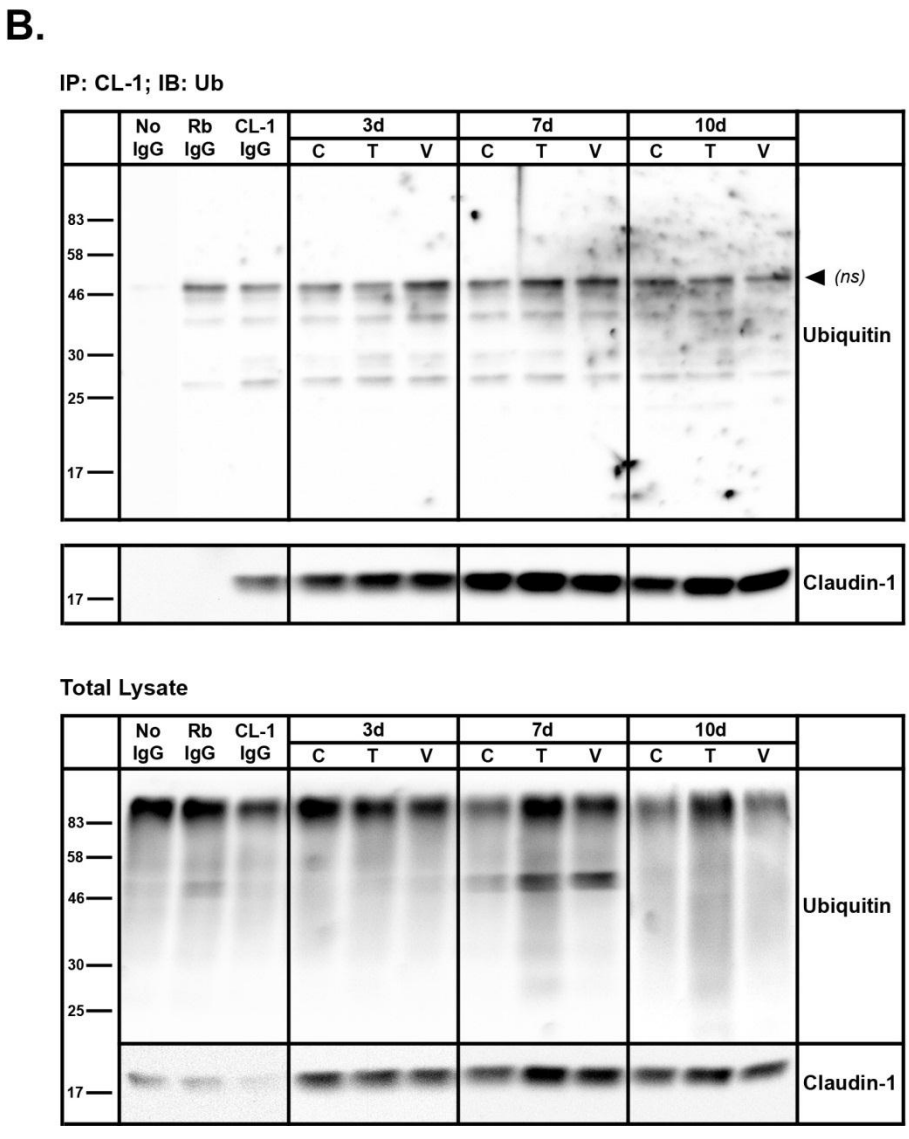
B.
IP: CL-1; IB: Ub
No IgG
Rb IgG
CL-1 IgG
3d
7d
10d
C T V C T V C T V
83
58
46
30
25
17
(ns)
Ubiquitin
Claudin-1
Total Lysate
No IgG
Rb IgG
CL-1 IgG
3d
7d
10d
C T V C T V C T V
83
58
46
30
25
17
Ubiquitin
Claudin-1

### 4.2.3. Characterisation of the internal claudin-1 positive compartment in Tsg101 depleted Caco-2 cells

To further characterise the claudin-1 positive internal compartment observed in Tsg101 knockdown cells, co-staining with various endosomal markers was performed (Figure 4.5 and 4.6). Claudin-1 does not colocalise completely with any of the markers analysed (Figure 4.5 and 4.6, arrows), however, partial colocalisation was demonstrated with the early endosome marker, EEA1, and with transferrin receptor (TfR) as a marker of recycling endosomes (Figure 4.5, arrowheads). Partial colocalisation was also observed with the late endosome markers, mannose-6-phosphate receptor (M6PR) and CD63, and with the lysosome marker, Lamp-1, although this was to a slightly lesser extent (Figure 4.6, arrowheads). These results show that the intracellular pool of claudin-1 observed upon Tsg101 knockdown localises to multiple endosomal compartments, suggesting that claudin-1 trafficking through the endocytic system is perturbed.

### 4.2.4. ESCRT-I depletion impairs Caco-2 epithelial barrier formation

Claudins are important for producing a tight junction permeability barrier (Van Itallie and Anderson, 2006) and therefore, reduced localisation of claudin-1 and -4 to tight junctions may affect their barrier function. To establish whether ESCRT depletion had an impact on epithelial barrier formation, transepithelial resistance (TER) was monitored after Tsg101 and Vps25 knockdown. TER is a measure of resistance to an electrical current passed from the apical to the basal surface of an epithelial sheet and can be used to indicate the integrity of cell-cell junctions. As junctions mature TER will increase and, conversely, disruption of junctions is often accompanied with a reduction in TER (Cereijido *et al.,* 1978). Establishment of TER was monitored over 4 days after plating siRNA transfected Caco-2 cells onto Transwell filters. Tsg101 knockdown significantly reduced TER compared to control at all timepoints measured whereas Vps25 knockdown had no effect (Figure 4.7A).

In addition, TER recovery after calcium switch was measured (Figure 4.7B). Removal of calcium from the cell culture growth media induces internalisation of

***Figure 4.5*** **The internal pool of claudin-1 in Tsg101 knockdown localises to both early and recycling endosomes.** Caco-2 cells were transfected with either Non-Targeting Control siRNA or Tsg101 siRNA and incubated for 7 d. Cells were fixed and examined by confocal fluorescence microscopy for claudin-1 (green) and either EEA1 or TfR (red). Nuclei were stained with DAPI (blue) shown in merged images. Right panels are zoomed images of areas indicated by dotted lines. Intracellular claudin-1 partially colocalises with the early endosome marker, EEA1 (top panels) and the recycling endosome marker, TfR (bottom panels). Colocalisation is shown as yellow in zoomed images (arrowheads). Note that for each marker, some claudin-1 localises to an unlabelled compartment (arrows). Bar, 10µm.

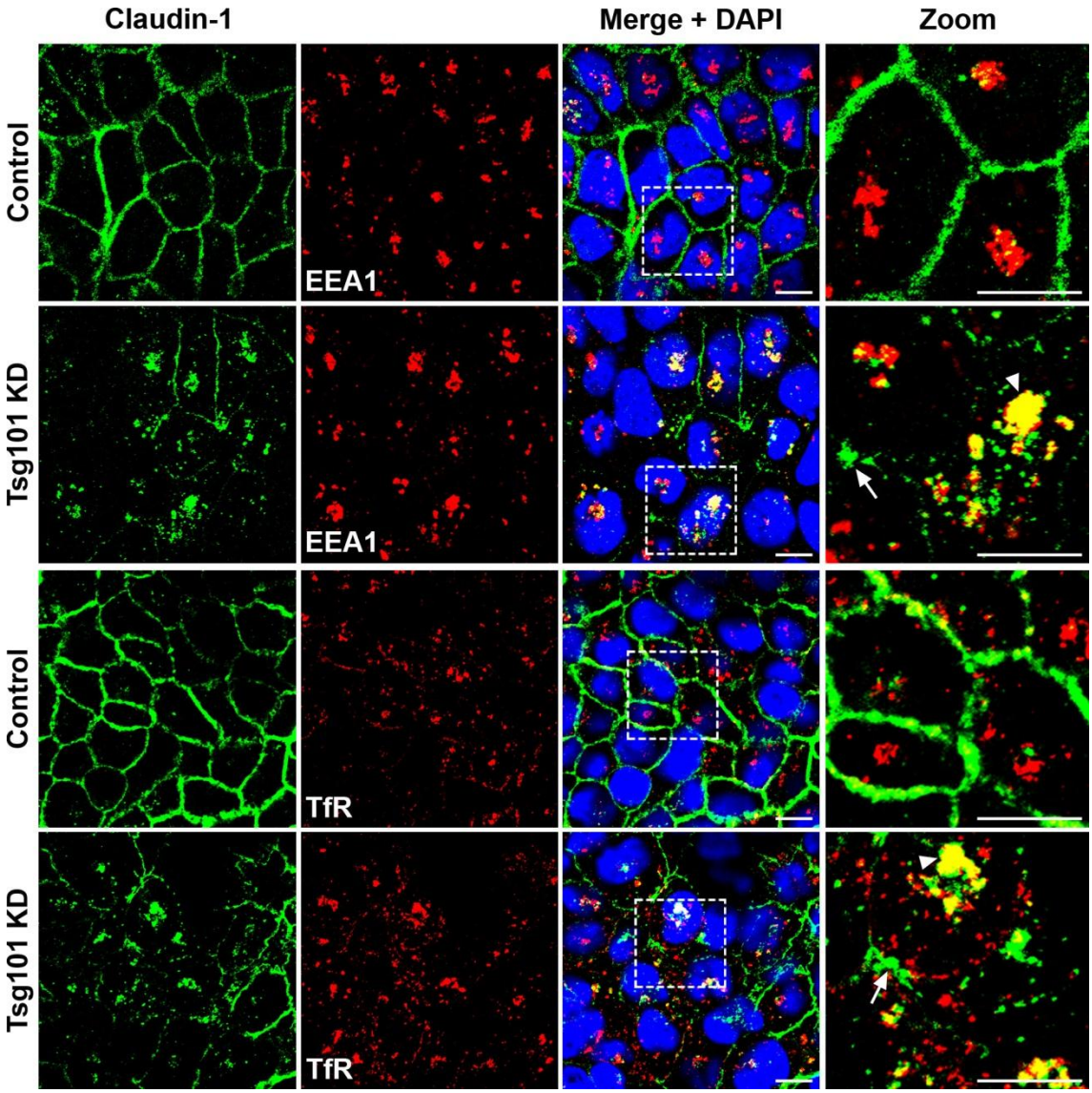
Claudin-1
Merge + DAPI
Zoom
Control
EEA1
Tsg101 KD
EEA1
Control
TfR
Tsg101 KD
TfR

***Figure 4.6*** **Intracellular claudin-1 partially colocalises with late endosomal markers in Tsg101 depleted Caco-2 cells.** Caco-2 cells were transfected with either Non-Targeting Control siRNA or Tsg101 siRNA and incubated for 7 d. Cells were fixed and examined by confocal fluorescence microscopy for claudin-1 (green) and either M6PR, CD63 or Lamp-1 (red). Nuclei were stained with DAPI (blue) shown in merged images. Right panels are zoomed images of areas indicated by dotted lines. The internal pool of claudin-1 partially colocalises with late endosomal markers, M6PR (top panels) and CD63 (middle panels) and less so with the lysosome marker, Lamp-1 (bottom panels). Colocalisation is shown as yellow in zoomed images (arrowheads). Note that for each marker, some claudin-1 localises to an unlabelled compartment (arrows). Bar, 10µm.

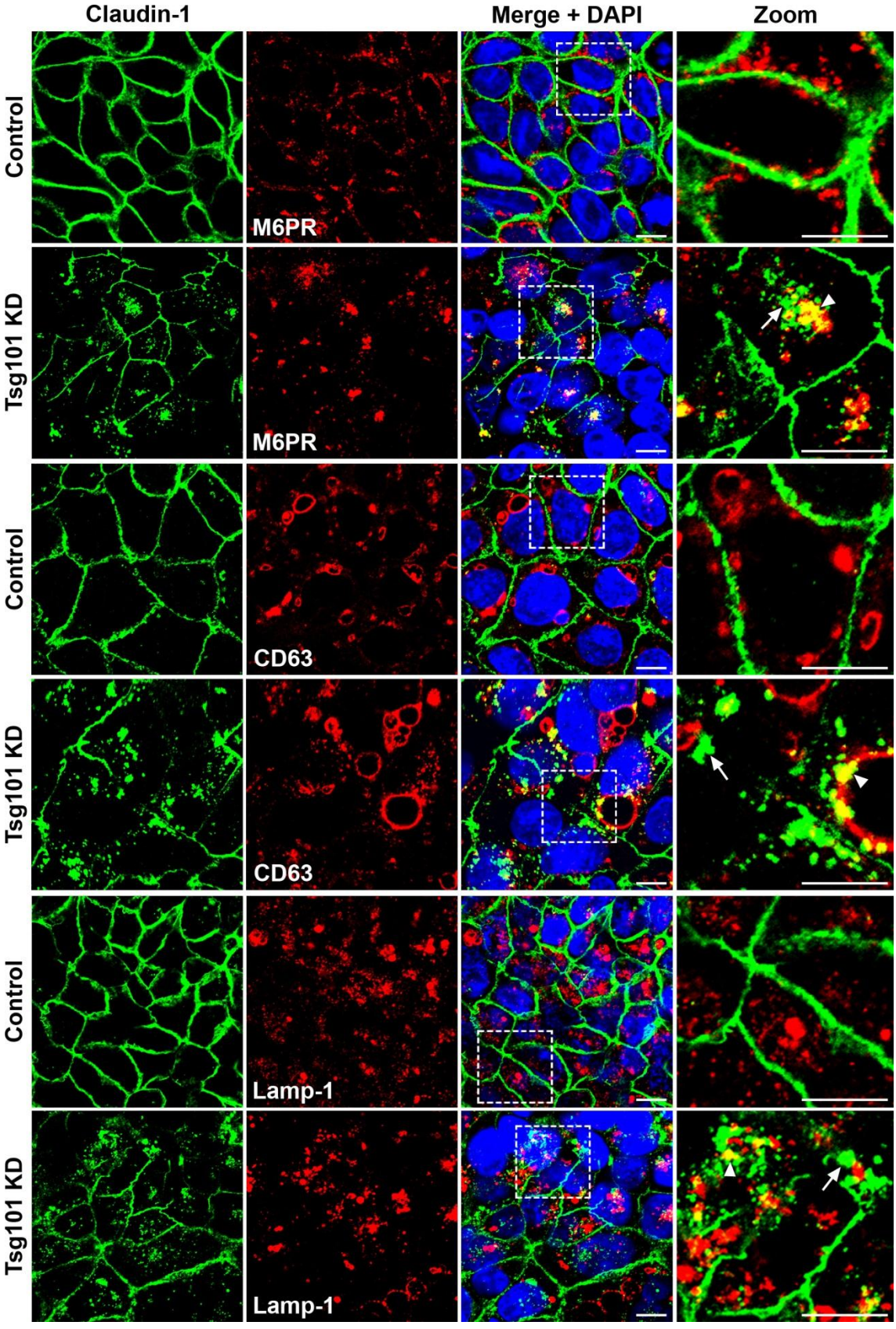
Claudin-1
Merge + DAPI
Zoom
Control
M6PR
Tsg101 KD
M6PR
Control
CD63
Tsg101 KD
CD63
Control
Lamp-1
Tsg101 KD
Lamp-1

***Figure 4.7*** **Transepithelial resistance (TER) is reduced following Tsg101 siRNA knockdown in Caco-2 cells.** Caco-2 cells were transfected with either Non-Targeting Control siRNA, Tsg101 siRNA or Vps25 siRNA, replated on day 3 to transwell filters and incubated for a further 4 days **(A)** TER was measured between day 4 and day 7. Tsg101 depletion reduces TER at all time points compared to control whereas Vps25 knockdown has no effect. **(B)** On day 7 cells were incubated in calcium-free media for 2 h to destabilise cell-cell junctions. Incubation in calcium-containing media then allowed junctions to reform and TER was measured at the indicated timepoints. TER recovers after calcium switch in ESCRT depleted cells however Tsg101 knockdown cells consistently display a reduced TER compared to control. Data shown are the means ± standard error of three independent experiments. Results were analysed using a two-way ANOVA and Bonferroni post test, *** $p<0.001$ * $p<0.05$.

**A.**

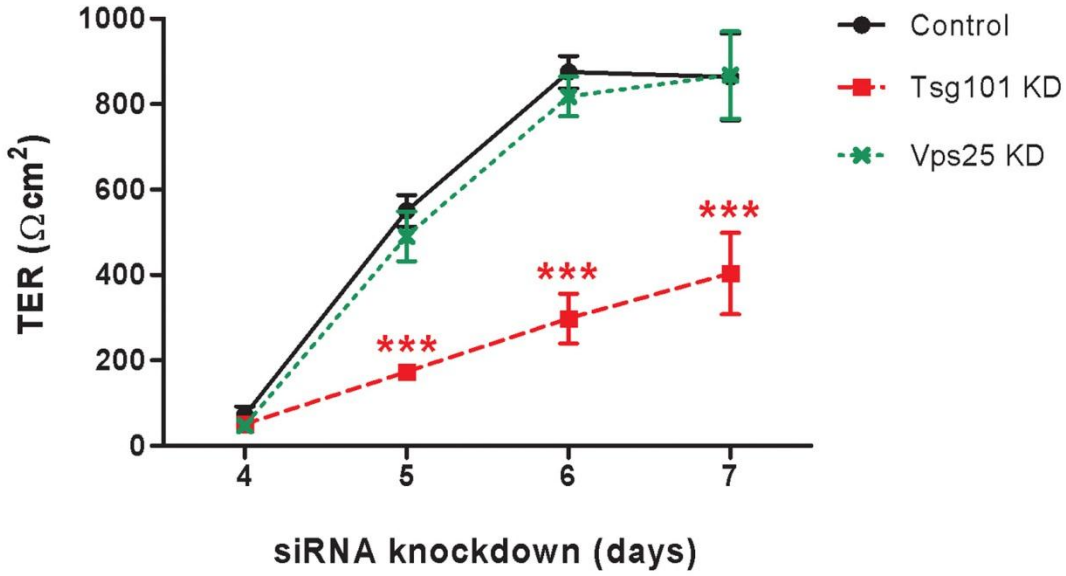
1000
800
600
400
200
0
TER (Ωcm²)
4
5
6
7
siRNA knockdown (days)
***
***
***
Control
Tsg101 KD
Vps25 KD

**B.**

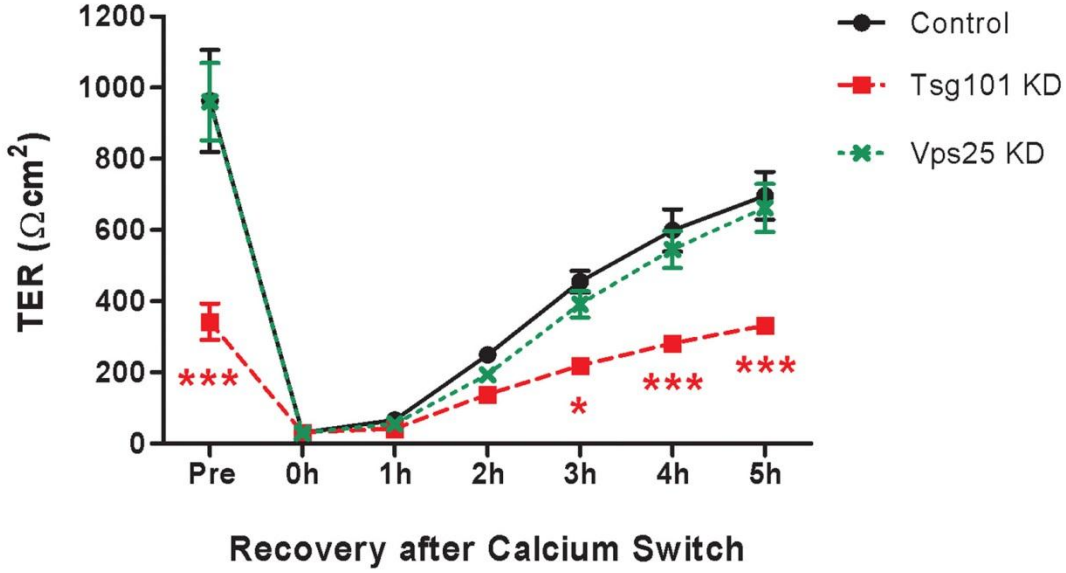
1200
1000
800
600
400
200
0
TER (Ωcm²)
Pre
0h
1h
2h
3h
4h
5h
Recovery after Calcium Switch
***
*
***
***
Control
Tsg101 KD
Vps25 KD

cell-cell junction proteins and as a result TER dropped to almost zero (Figure 4.7B, 0 h timepoint). Calcium was then added back into the media, allowing cell-cell junctions to reform. In control cells, a gradual increase of TER was observed over a 5 hour period. A similar increase was seen after Vps25 knockdown, however TER was consistently lower in Tsg101 depleted cells (Figure 4.7B). Therefore, establishment of TER as well as recovery after a calcium switch requires Tsg101 indicating that depletion of ESCRT-I results in impaired barrier formation of the Caco-2 epithelial sheet. In contrast, Vps25 knockdown does not appear to have a significant effect on TER.

### 4.2.5. Tsg101 knockdown enhances Caco-2 cell migratory ability

Loss of apicobasal polarity and cell-cell adhesion can promote migration of epithelial cells and is often observed during metastasis of cancer cells (Hanahan and Weinberg, 2011). As tight junctions play an important role in maintenance of the polarised epithelial phenotype, alterations in tight junction structure and function are often associated with enhanced invasiveness of human carcinomas (Miyoshi and Takai, 2005; Oliveira and Morgado-Diaz, 2007). In addition, changes in expression of claudins are frequently observed in various human tumours (reviewed in Morin, 2005; Oliveira and Morgado-Diaz, 2007; Turksen and Troy, 2011). For example claudin-1 has been found to be reduced in breast (Kramer *et al.,* 2000; Tokes *et al.,* 2005), lung (Chao *et al.,* 2008) and colon (Resnick *et al.,* 2005) cancer. Conversely, upregulation of claudins has also been associated with carcinogenesis (Oliveira *et al.,* 2005). As Tsg101 depletion compromised apicobasal polarity and altered claudin-1 and -4 localisation, the effect of knockdown on the migratory ability of Caco-2 cells was investigated.

After siRNA knockdown, a scratch assay was performed on confluent Caco-2 cells and migration of cells into the wound area was monitored over time (Figure 4.8). After 24 h, approximately 35% of the original scratch area was covered by Tsg101 knockdown cells compared to 12% in control (Figure 4.8B). Therefore, ESCRT-I depletion significantly enhances migration of Caco-2 cells.

***Figure 4.8*** **Tsg101 depleted Caco-2 cells display enhanced migratory ability.** Caco-2 cells were transfected with Non-Targeting Control siRNA or Tsg101 siRNA and replated on day 3 to cell culture inserts used to assess cell migration. Migration was initiated on day 6 by removal of the cell culture insert to reveal a cell-free area of approximately 500µm. Images were obtained using phase contrast microscopy 0, 12 and 24 h after initiation of migration. **(A)** Representative images for 0 and 24 h migration are shown. The migratory front of the epithelial sheet was detected using ImageJ at each timepoint and can be overlaid to show cell migration after 24 h (overlay, black lines) compared to 0 h (overlay, red lines). **(B)** Scratch area was quantified using ImageJ and expressed as an inverse percentage of 0 h. After 24 h, migration of Tsg101 depleted cells is increased compared to control. Data shown are the means ± standard error of three independent experiments. Results were analysed using a two-way ANOVA and Bonferroni post test, * $p<0.05$.

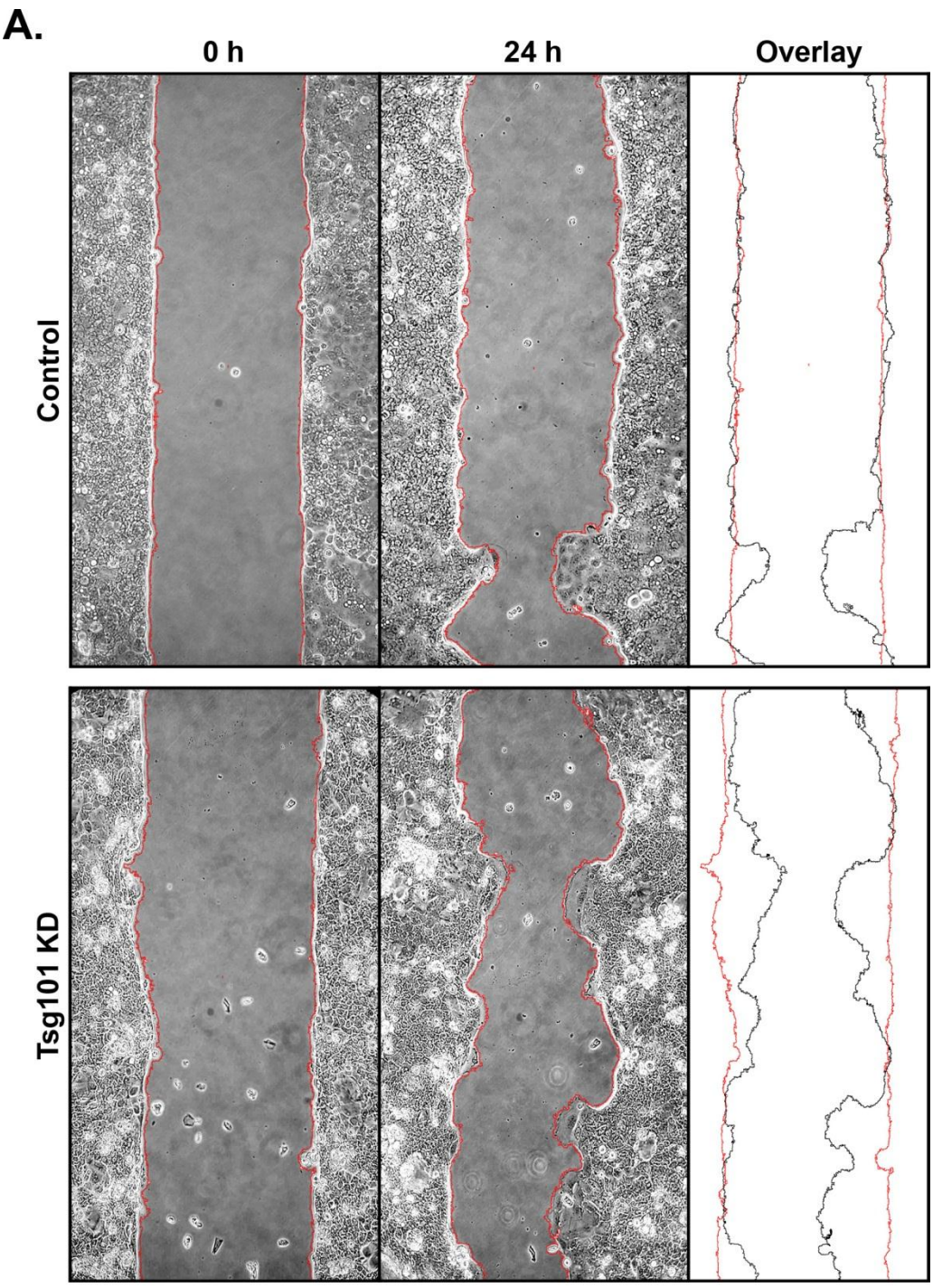
A.
0 h
24 h
Overlay
Control
Tsg101 KD

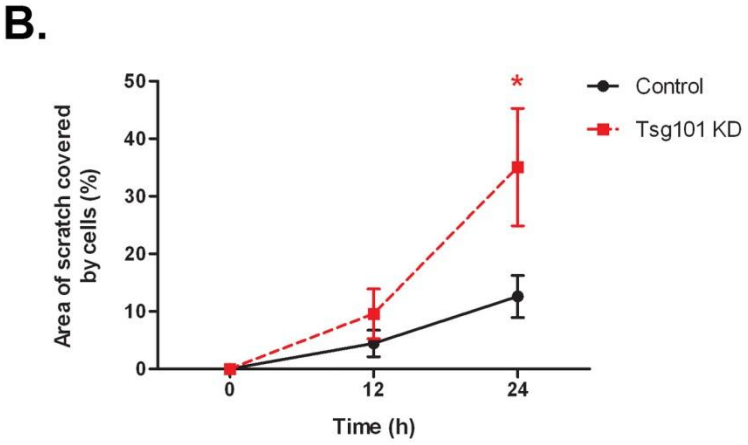
B.
Area of scratch covered by cells (%)
50
40
30
20
10
0
0
12
24
Time (h)
*
Control
Tsg101 KD

### 4.2.6. Caco-2 cell tight junctions are dynamic structures

Tsg101 depletion results in intracellular accumulation of claudin-1 which localises to multiple endosomal compartments, suggesting that claudin-1 trafficking is perturbed. A functional ESCRT machinery is required for the degradation of various membrane proteins (Raiborg and Stenmark, 2009) and so disruption of claudin-1 trafficking to lysosomes for degradation may explain its intracellular accumulation. However, ESCRT proteins have also been shown to be important for protein recycling (Yoshimori *et al.,* 2000; Fujita *et al.,* 2003; Doyotte *et al.,* 2005; Baldys and Raymond, 2009). Therefore, the internal pool of claudin-1 could also arise due to inhibition of endocytic recycling. Although previous studies have begun to analyse the dynamic behaviour of cell-cell junction proteins (Le *et al.,* 1999; Marzesco *et al.,* 2002; Matsuda *et al.,* 2004; Morimoto *et al.,* 2005), trafficking of tight junction components has not been studied in Caco-2 cells.

In order to investigate whether tight junction proteins constitutively traffic through the endosomal system in Caco-2 cells, a surface biotinylation assay was used. This assay employs a membrane-impermeant biotin molecule to label cell surface proteins. Trafficking of biotinylated proteins can then be followed over time, using various incubation and stripping procedures, followed by neutravidin pull down and immunoblotting for the protein of interest (for schematic, see Chapter 2: Materials and Methods, Figure 2.1). Surface claudin-1 and occludin could be labelled with biotin and were successfully detected after neutravidin pull down (Figure 4.9A, 'Surface Biotinylated'). No detection was observed in mock treated cells, indicating that the pull down was specific to biotinylated proteins (Figure 4.9A, 'Non Specific'). In addition, the biotin could be efficiently removed from labelled proteins by a surface stripping procedure (Figure 4.9A, 'Strip Control'). Endocytosis of claudin-1 and occludin was then analysed over time (Figure 4.9B). After labelling surface proteins with biotin at 4°C, Caco-2 cells were incubated at 37°C for the indicated timepoints to allow trafficking. Following this, biotin was stripped from surface proteins and analysis of the remaining biotinylated claudin-1 and occludin was performed. This therefore indicated the amount of biotinylated claudin-1 and occludin endocytosed within each time period. Following a 60 min incubation,

***Figure 4.9*** **Claudin-1 and occludin are endocytosed in Caco-2 cells.** Surface biotinylation and endocytosis assays were performed on Caco-2 cells. **(A)** Caco-2 cells were incubated at 4°C with non-membrane permeable biotin to label surface proteins. Biotinylated proteins were isolated using neutravidin pull down and samples were immunoblotted for claudin-1 and occludin. Surface claudin-1 and occludin was successfully labelled with biotin ('Surface Biotinylated'). No signal was observed after mock treatment ('Non-specific') or after stripping with MESNA ('Strip Control). Total cell lysate is shown as a loading control. **(B)** After surface biotinylation, Caco-2 cells were incubated at 37°C for indicated timepoints to allow endocytosis. Remaining biotin at the cell surface was stripped with MESNA and biotinylated proteins were isolated using neutravidin pull down. Samples were immunoblotted for claudin-1 and occludin to indicate the amount of protein endocytosed within each time period. Total cell lysate immunoblotted for claudin-1 is shown as a representative loading control. **(C)** Protein levels were quantified, normalised to total protein and expressed as a percentage of the corresponding amount of surface biotinylated protein. Claudin-1 and occludin are endocytosed in Caco-2 cells. This endocytosis is rapid and a steady state is reached after approximately 30 min. Data shown are the means ± standard error of three independent experiments.

A.

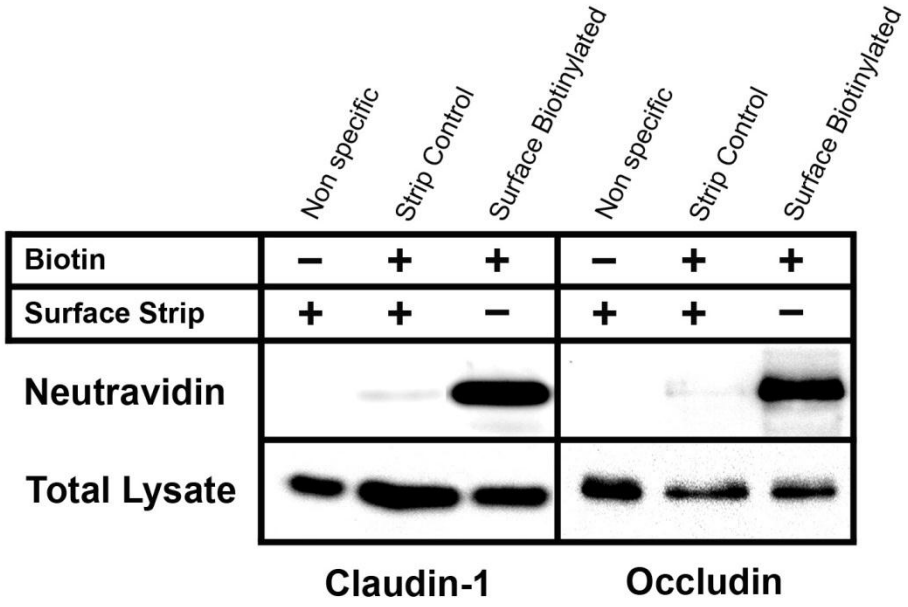
Non specific
Strip Control
Surface Biotinylated
Non specific
Strip Control
Surface Biotinylated
Biotin
Surface Strip
Neutravidin
Total Lysate
Claudin-1
Occludin

B.

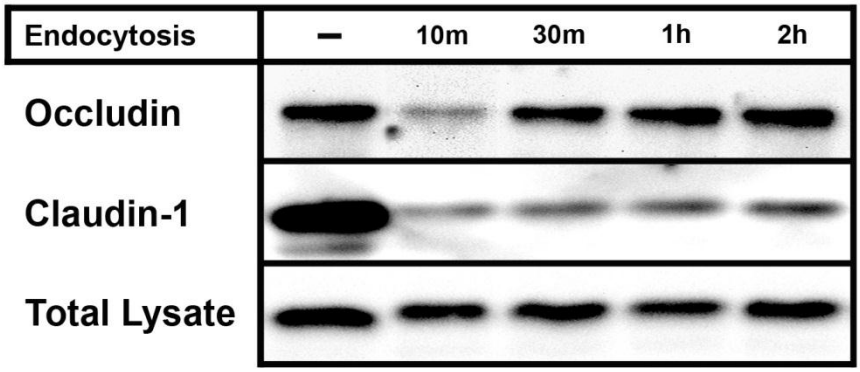
Endocytosis
10m
30m
1h
2h
Occludin
Claudin-1
Total Lysate

C.

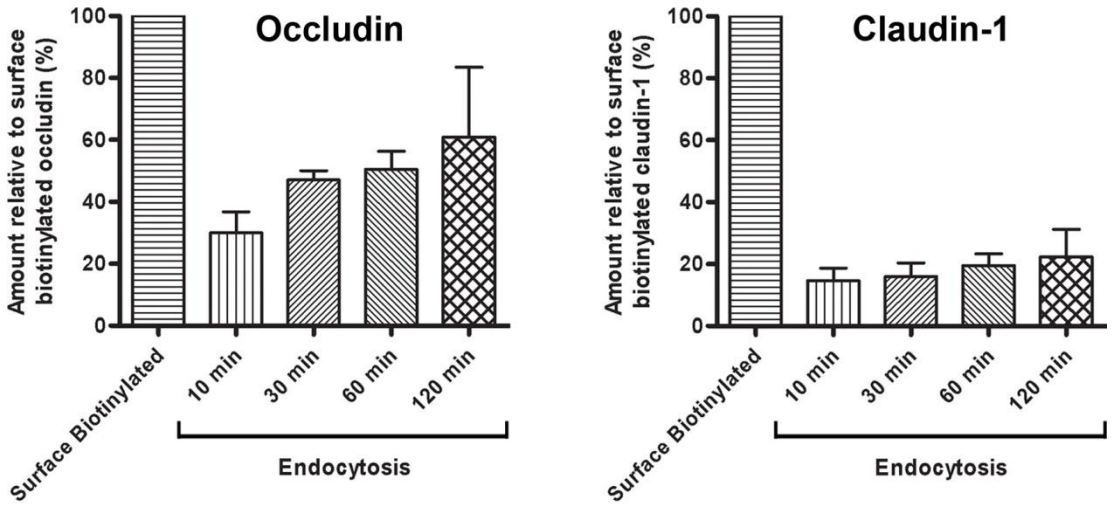
Occludin
Amount relative to surface biotinylated occludin (%)
100
80
60
40
20
0
Surface Biotinylated
10 min
30 min
60 min
120 min
Endocytosis
Claudin-1
Amount relative to surface biotinylated claudin-1 (%)
100
80
60
40
20
0
Surface Biotinylated
10 min
30 min
60 min
120 min
Endocytosis

approximately 50% of biotinylated occludin and 20% of biotinylated claudin-1 was endocytosed (Figure 4.9B + C). The amount of internal biotinylated claudin-1 and occludin only increased slightly between 30 min and 2 h suggesting that the level of endocytosis reaches an approximate plateau after 30 min.

The fate of the endocytosed claudin-1 and occludin was then investigated. Caco-2 cells were labelled with biotin and incubated at 37°C for 1 h to allow endocytosis (Figure 4.10A+B, 'Endocytosis 60 min'). Surface biotin was stripped and cells were incubated for a further 20 min at 37°C. Following this, cells were surface stripped for a second time or mock treated. This second stripping procedure removes biotin from endocytosed proteins which have returned to the cell surface and therefore allows the fate of the endocytosed proteins to be studied. A reduction in the amount of biotinylated protein detected after mock treatment compared to the endocytosis condition indicates that some of the endocytosed protein has been targeted for degradation (Figure 4.10A+B, 'Degradation Control'). Levels of recycled proteins are indicated by a reduction in the amount of biotinylated protein pulled down after a second surface strip compared with the degradation control (Figure 4.10A+B, 'Recycling 20 min). This procedure revealed that approximately 40% of endocytosed claudin-1 is recycled with very little being targeted for degradation (Figure 4.10A+B). In contrast, the fate of endocytosed occludin was split between degradation and recycling with approximately 40% degraded and 30% of the remaining internal occludin recycled (Figure 4.10A+B). Therefore, in Caco-2 cells claudin-1 is constitutively endocytosed and recycled and occludin is endocytosed then either degraded or recycled.

### 4.2.7. Turnover of tight junction proteins occurs over time

The biotinylation assay studied the degradation and recycling of endocytosed claudin-1 and occludin over a short time period of 20 min. Analysis of claudin-1 and occludin turnover over a longer time period was performed by monitoring protein levels after varying lengths of cycloheximide treatment (Figure 4.11). Effective inhibition of protein synthesis via cycloheximide treatment was demonstrated after 6 h by a reduction in the levels of connexin-43, a gap junction protein known to undergo rapid turnover (Fallon and Goodenough,

***Figure 4.10*** **Claudin-1 and occludin are constitutively endocytosed and recycled in Caco-2 cells.** The surface biotinylation, endocytosis and recycling assay was performed on Caco-2 cells. **(A)** After surface biotinylation, Caco-2 cells were incubated at 37°C for 60 min to allow endocytosis. Remaining biotin at the cell surface was stripped with MESNA and cells were incubated at 4°C for 20 min to allow recycling. Cells were surface stripped to indicate recycling or mock treated to control for degradation. After each step cells were lysed, biotinylated proteins were isolated using neutravidin pull down and samples were immunoblotted for claudin-1 and occludin. Total cell lysate is shown as a loading control. Lanes marked 'Surface biotinylated' represent the initial biotinylated protein at the cell surface and 'Endocytosis 60 min' is the internal biotinylated protein that is resistant to surface stripping. Degradation is shown by a reduction of signal in the 'Degradation control' lane in comparison to the 'Endocytosis 60 min' lane. Recycling is the reduction of signal in the 'Recycling 20 min' lane relative to the 'Degradation control' lane. **(B)** Protein levels were quantified, normalised to total protein and expressed as a percentage of the corresponding amount of surface biotinylated protein. Claudin-1 is endocytosed and recycled in Caco-2 cells whereas occludin is endocytosed and then either recycled or degraded. Data shown are the means ± standard error of three independent experiments.

A.

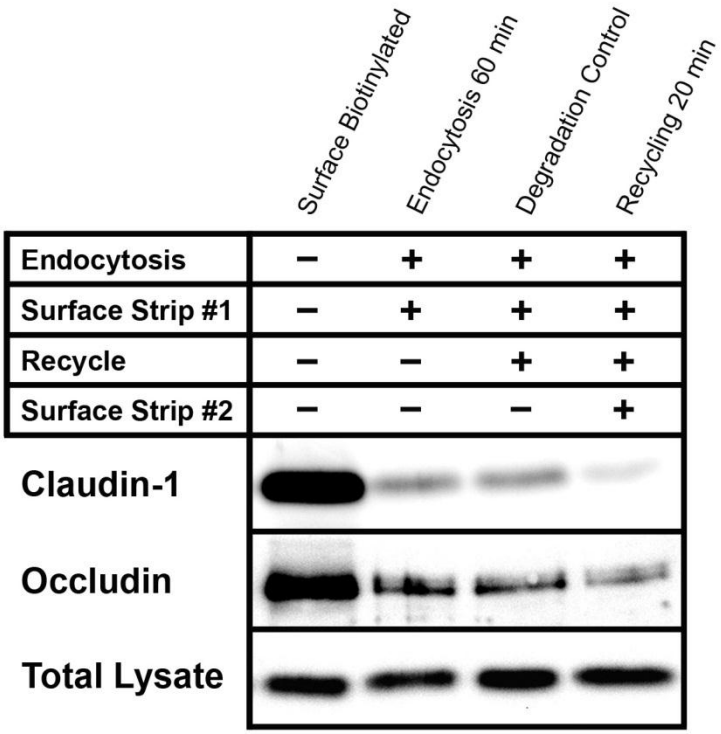
Surface Biotinylated
Endocytosis 60 min
Degradation Control
Recycling 20 min
Endocytosis
Surface Strip #1
Recycle
Surface Strip #2
Claudin-1
Occludin
Total Lysate

B.

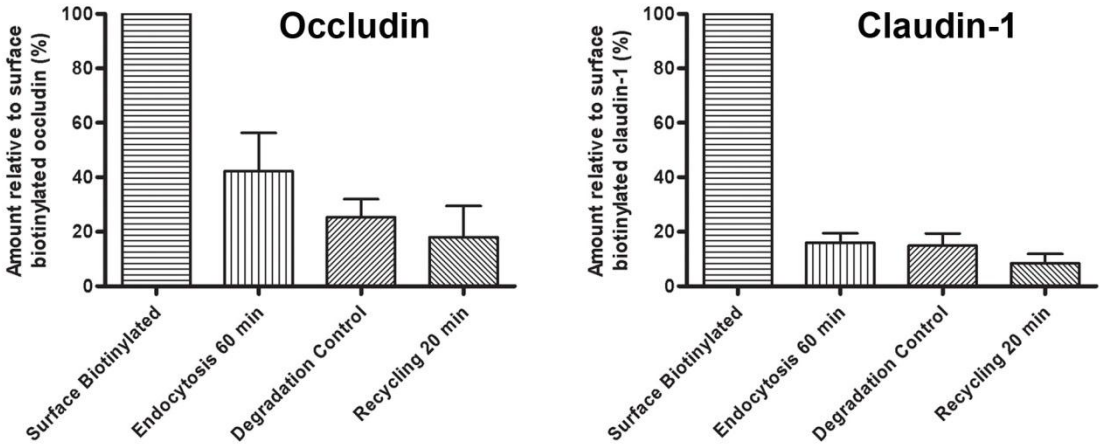
Occludin
Amount relative to surface biotinylated occludin (%)
100
80
60
40
20
0
Surface Biotinylated
Endocytosis 60 min
Degradation Control
Recycling 20 min
Claudin-1
Amount relative to surface biotinylated claudin-1 (%)
100
80
60
40
20
0
Surface Biotinylated
Endocytosis 60 min
Degradation Control
Recycling 20 min

1981). Importantly, up to 24 h treatment with cycloheximide had no effect on Caco-2 cell viability (data not shown). After 6 h cycloheximide treatment, total occludin and claudin-1 levels remained stable. However, 16 h and 24 h treatment reduced total protein levels (Figure 4.11), suggesting that over time tight junction proteins are turned over in Caco-2 cells.

***Figure 4.11*** **Claudin-1 and occludin are turned over in Caco-2 cells.** Caco-2 cells were incubated at 37°C with 2µg/ml cycloheximide (CHX) for the indicated time periods and lysates were immunoblotted for occludin and claudin-1. Connexin-43 is shown as a positive control for CHX treatment and β-tubulin is shown as a loading control. Turnover of claudin-1 and occludin is demonstrated after 24 h CHX treatment.

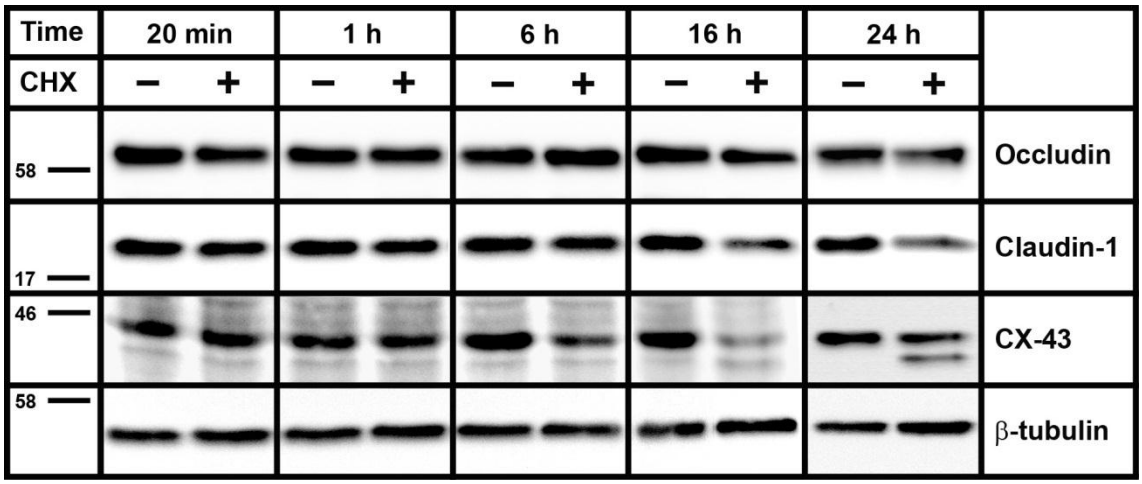
Time
20 min
1 h
6 h
16 h
24 h
CHX
– + – + – + – + – +
58
Occludin
17
Claudin-1
46
CX-43
58
β-tubulin

## 4.3. Discussion

This work aimed to investigate whether ESCRT proteins are required for the formation and/or maintenance of epithelial cell-cell junctions in Caco-2 cells. Functional cell-cell junctions are important to maintain a polarised epithelium and therefore defective epithelial junctions could provide a mechanism for the compromised Caco-2 cell polarity and organisation observed upon ESCRT-I depletion (discussed in Chapter 3). My results demonstrate that Tsg101 knockdown causes an internal accumulation of claudins whereas the localisation of various other cell-cell junction proteins is unaffected. In addition, Tsg101 depletion impairs Caco-2 epithelial barrier formation and enhances migratory ability, providing further support for a tumour suppressor role of ESCRT-I in mammalian epithelial cells. I have shown that claudin-1 and occludin are continuously trafficked through the endosomal system in Caco-2 epithelial cells. Therefore, the intracellular accumulation of claudin-1 in ESCRT deficient cells is likely to be due to defective claudin-1 endosomal trafficking.

### 4.3.1. Claudin localisation to tight junctions and Caco-2 epithelial barrier formation is dependent on ESCRT-I

Depletion of Tsg101 in Caco-2 cells caused an intracellular accumulation of claudin-1 and -4 whereas localisation of various other cell-cell junction proteins was unaffected. Knockdown of Vps25 however had no significant effect on localisation of claudin-1 and -4 or any of the other junctional proteins studied. Additional data from our laboratory has demonstrated a similar internal accumulation of claudin-1 in MDCK cells, a canine kidney cell line, after disruption of ESCRT-III and inactivation of the AAA-ATPase Vps4 using dominant negative constructs (Dukes *et al.,* 2011). This suggests that ESCRT function is required for junctional localisation of claudin-1 in at least two different epithelial cell types. Analysis of other cell lines would indicate whether this requirement is a common feature of vertebrate epithelial cells.

Ubiquitylated proteins also accumulated within Tsg101 depleted Caco-2 cells, a phenotype which has been observed in other cell lines after ESCRT disruption and is indicative of a defect in trafficking through the endocytic pathway (Bishop

*et al.,* 2002; Dukes *et al.,* 2008; Stuffers *et al.,* 2009b). Claudin-1 often localised to the same internal compartment as these ubiquitylated proteins although modification of claudin-1 with ubiquitin was not observed. Further characterisation of the claudin-1 positive compartment revealed that the internal pool of claudin-1 partially colocalised with markers for both early and recycling endosomes, and to a lesser extent with markers for late endosomes and lysosomes. This suggests that endosomal trafficking of claudin-1 is perturbed in ESCRT-I depleted Caco-2 cells and, as a result, claudin-1 accumulates within numerous endocytic compartments. In addition, identity of individual endosomal domains may be disrupted upon ESCRT depletion (Woodman, 2009). Therefore, claudin-1 may accumulate within a hybrid compartment which is positive for multiple endosomal markers. Previous results demonstrated that although early and late endosomes are enlarged in EGF treated Caco-2 Tsg101 knockdown cells, these two compartments remained morphologically distinct (Chapter 3, section 3.2.2). However, co-staining with multiple endosomal markers has not been carried out and therefore, this could be investigated further by studying the localisation of various markers for recycling, early and late endosomes after Tsg101 knockdown.

ESCRT-I depletion also resulted in a reduction in Caco-2 transepithelial resistance (TER) whereas ESCRT-II depletion had no effect. This is consistent with results demonstrating that Tsg101 knockdown, but not Vps25 knockdown, causes an intracellular accumulation of claudin-1 and -4. Despite this internal accumulation, claudin-1 and -4 are not completely lost from tight junctions in Tsg101 knockdown cells. However, as claudins are crucial for producing a tight junction permeability barrier (Van Itallie and Anderson, 2006), reduced localisation of claudin-1 and -4 to tight junctions may affect their barrier function. The sensitivity of tight junction structure and function to claudin composition has been demonstrated previously (reviewed in Krause *et al.,* 2007; Lal-Nag and Morin, 2009). Therefore, this suggests that mislocalisation of claudin-1 and -4 disrupts tight junction integrity and has a functional impact on Caco-2 epithelial barrier formation. The claudin family consists of least 27 different proteins (Mineta *et al.,* 2011) and therefore, it is possible that ESCRT depletion affects the localisation of other claudins. This may contribute to the defective barrier formation and it would be interesting to analyse the localisation of other claudin

proteins after Tsg101 depletion. In addition, it would be of interest to investigate the impact of ESCRT depletion on tight junction structure further, for example using electron microscopy to analyse the integrity of the tight junction strands in detail.

Alternatively, the reduction in TER following Tsg101 knockdown could be due to loss of a polarised Caco-2 epithelial monolayer. Previous results demonstrated that ESCRT-I depleted cells formed multilayered regions lacking normal epithelial organisation and apicobasal polarity (discussed in Chapter 3). Barrier function may also be perturbed in these areas and therefore this could account for the reduction in TER rather than mislocalisation of claudins. This could be investigated in more detail using dominant negative ESCRT-III constructs which cause a similar internal accumulation of claudins but do not disrupt epithelial cell polarity (Dukes *et al.,* 2011).

Therefore, these results demonstrate that ESCRT-I is required to maintain localisation of claudin-1 and -4 to tight junctions in Caco-2 cells. In addition, epithelial barrier formation is also dependent on ESCRT-I function. This could be a consequence of claudin-1 and -4 mislocalisation but there may also be additional effects of ESCRT-I depletion on other junctional proteins which were not analysed in this study. It can be speculated that mislocalisation of claudins, and possibly other junction proteins, destabilises Caco-2 tight junctions and, as a result, epithelial cell polarity is disrupted. Cells may then lose correct epithelial organisation and this may lead to the multilayered sheets observed upon Tsg101 knockdown.

### 4.3.2. ESCRT-I depletion enhances Caco-2 migratory ability

ESCRT-I depletion was also shown to increase Caco-2 cell migration. This could be due to the mislocalisation of claudin-1 and -4 from tight junctions as alterations in tight junction structure and function are often associated with enhanced invasiveness of human carcinomas (Miyoshi and Takai, 2005; Oliveira and Morgado-Diaz, 2007; Turksen and Troy, 2011). Furthermore, changes in expression of claudins are frequently observed in various human tumours (reviewed in Morin, 2005; Oliveira and Morgado-Diaz, 2007). Claudin-1

has been found to be reduced in breast (Kramer *et al.,* 2000; Tokes *et al.,* 2005); lung (Chao *et al.,* 2008); and colon (Resnick *et al.,* 2005) cancer, and upregulation of claudins has also been associated with carcinogenesis (Oliveira *et al.,* 2005). In addition, tight junctions play an important role in maintenance of the polarised epithelial phenotype (Miyoshi and Takai, 2005) and loss of apicobasal polarity is often observed during metastasis of cancer cells (Hanahan and Weinberg, 2011). Therefore, the disruption of claudin localisation to tight junctions caused by ESCRT-I depletion may perturb apicobasal polarity which, in turn, promotes migration of epithelial cells.

Deregulated matrix metalloproteinases (MMP) activity may provide one potential mechanism for the enhanced migratory ability of Caco-2 cells upon Tsg101 knockdown. MMPs are a family of zinc-dependent endopeptidases which function in various different physiological processes such as tissue remodelling, development and inflammation (Kessenbrock *et al.,* 2010). They are also important in pathological processes such as cancer and MMPs are upregulated in almost every type of human cancer (Egeblad and Werb, 2002; Kessenbrock *et al.,* 2010). The role of MMPs in cancer cell invasion and metastasis has been well documented and is due to their ability to degrade a diverse group of substrates. These include structural components of the extracellular matrix (ECM), growth factor receptors and cell adhesion molecules which results in an alteration in cellular adhesion and signalling, therefore promoting cell migration and invasion (Egeblad and Werb, 2002).

Several studies have identified a role for claudins in the regulation of MMP activity (Miyamori *et al.,* 2001). Claudin-4 overexpression increases activity of MMP-2 and -9 which is accompanied by an increase in migration of Caco-2 cells (Takehara *et al.,* 2009). Overexpression of claudin-1 has also been shown to increase MMP activity and metastasis (Dhawan *et al.,* 2005). In addition, decreased expression of claudins has been shown to promote cell migration and invasion via an increase in MMP activity (Osanai *et al.,* 2007; Ikari *et al.,* 2011). Interestingly, in *Drosophila* ESCRT mutants, increased expression of MMP-1 was observed (Rodahl *et al.,* 2009b; Vaccari *et al.,* 2009; Lobert and Stenmark, 2011). Therefore, ESCRT depletion may increase MMP activity, possibly via disruption of claudin localisation, and this could then enhance the

migratory ability of Caco-2 cells. To investigate this further, it would be interesting to analyse MMP expression and activity in Caco-2 cells after ESCRT knockdown.

It is also important to note that the increased rate of scratch closure observed for Tsg101 knockdown Caco-2 cells may be due to increased proliferation rather than enhanced migration. The assay was carried out in serum-free media in order to reduce cell proliferation, however, the migration assay could also be carried out in the presence of mitomycin c. This inhibits cell proliferation (Lee and Kay, 2006) and therefore, would confirm whether ESCRT-I depletion is enhancing migratory ability of Caco-2 cells independently of cell proliferation.

### 4.3.3. Constitutive trafficking of tight junction proteins is a feature of Caco-2 cells

The structure and function of tight junctions may contribute to the maintenance of a polarised epithelium (Brennan *et al.,* 2010; Coradini *et al.,* 2011). Therefore, it is crucial to understand the processes that regulate the maintenance of tight junctions in epithelial cells. Cell-cell junctions are thought to be dynamic structures that are constantly being remodelled (Shen *et al.,* 2008; Steed *et al.,* 2010). My data demonstrates that claudin-1 and occludin are constitutively endocytosed in unstimulated Caco-2 epithelial monolayers. Internalised claudin-1 is rapidly recycled back to the plasma membrane whereas the fate of occludin is split between recycling and degradation. This was also observed in 16-HBE cells, a human lung epithelial cell line (data shown in Dukes *et al.,* 2011).

Endocytosis of claudins and occludin has been demonstrated previously in vertebrate epithelial cells (Marzesco *et al.,* 2002; Matsuda *et al.,* 2004; Morimoto *et al.,* 2005; Takahashi *et al.,* 2009). Trafficking of tight junction proteins appears to be highly specific for each individual junctional component. For example, claudin-3 is selectively segregated and internalised independently from other tight junction proteins (Matsuda *et al.,* 2004). Ubiquitylation of claudin-1 and occludin has been shown to be promoted by the specific E3 ubiquitin ligases, LNX1p80 (Takahashi *et al.,* 2009) and Itch (Traweger *et al.,*

2002), respectively and, therefore, this may provide a mechanism for selective internalisation. In addition, the dynamics of tight junctions appear dependent on cell type. Inhibition of recycling altered the localisation of occludin in MTD-1A epithelial cells (Morimoto *et al.,* 2005) whereas in MDCK cells, claudin-1 localisation was affected (Marzesco *et al.,* 2002).

Therefore, my data provides further insight into our understanding of tight junction biology, supporting a model whereby stability of cell-cell junctions in epithelial monolayers is maintained by a balance between assembly and disassembly of junctions (Shen and Turner, 2008). This analysis could be widened to include other tight junction transmembrane proteins, such as different claudin family members, JAMs and marvelD3, as well as proteins present in adherens junctions and desmosomes. Regulation of cell-cell junction assembly and disassembly could also be studied in detail. EGF stimulation has been shown to regulate expression and localisation of specific junction proteins (Singh and Harris, 2004; Ikari *et al.,* 2010) and ERK1/2 signalling has been shown to influence tight junction integrity and assembly (Aggarwal *et al.,* 2011). In addition, phosphorylation of junctional proteins such as occludin appears to be important for tight junction assembly (Sakakibara *et al.,* 1997). Therefore, it would be interesting to establish the mechanisms that regulate trafficking of junctional proteins and the importance of these pathways for assembly and disassembly of cell-cell junctions in vertebrate epithelial cells.

### 4.3.4. ESCRT-I is required for continuous claudin-1 trafficking in Caco-2 cells

This study has identified a role for ESCRT-I in maintaining localisation of claudins to tight junctions in Caco-2 epithelial cells. However, the question still remains as to why this internal pool of claudin-1 and -4 accumulates in Tsg101 depleted cells. It can be hypothesised that ESCRT-I is required for constitutive claudin-1 trafficking in Caco-2 cells. Depletion of ESCRT-I may specifically perturb claudin-1 trafficking to tight junctions and as a result an internal pool of claudin-1 accumulates. This intracellular accumulation could be due to an inhibition of claudin-1 recycling and/or degradation. Although ESCRT proteins have been classically characterised for their involvement in degradation of

membrane proteins (Hurley and Emr, 2006; Raiborg and Stenmark, 2009), it is also reported that ESCRT function is important for recycling (Yoshimori *et al.,* 2000; Fujita *et al.,* 2003; Doyotte *et al.,* 2005; Baldys and Raymond, 2009). Therefore, disruption of either of these pathways could explain the accumulation of claudin-1 observed upon Tsg101 knockdown.

The majority of endocytosed claudin-1 was shown to be continuously recycled in Caco-2 epithelial monolayers, therefore, it is possible that depletion of ESCRT-I inhibits claudin-1 recycling. Endocytosis continues and so internalised claudin-1 accumulates over time. This has been demonstrated by additional data from our laboratory whereby disruption of ESCRT-III was shown to inhibit claudin-1 recycling in MDCK cells (Dukes *et al.,* 2011). A similar inhibition of claudin-1 recycling in Caco-2 cells upon ESCRT-I depletion is difficult to show directly due to the experimental approach employed. ESCRT-III disruption in MDCK cells was achieved using adenoviral expression of a dominant negative ESCRT-III protein, $CHMP3^{1-179}$. This system resulted in expression in virtually all cells and caused disruption to the ESCRT machinery within a short time period of approximately 16 hours. In contrast, ESCRT-I depletion via siRNA knockdown of Tsg101 was achieved after 7 days. Claudin-1 accumulation presumably occurs steadily during this time and, therefore, a reduction in recycling over a 20 min period will be difficult to detect using the biotinylation assay. In addition, cells may adapt their trafficking pathways to compensate for the effects of ESCRT-I depletion. Therefore, an alternative approach to disrupt ESCRT-I in Caco-2 cells would be required in order to demonstrate a direct involvement of ESCRT-I in claudin-1 recycling.

Conversely, the internal pool of claudin-1 observed upon ESCRT-I depletion in Caco-2 cells may be due to a block in lysosomal degradation. Using the biotinylation assay, significant degradation of endocytosed biotinylated claudin-1 was not detected within 20 minutes. However, over a longer time period of 16 - 24 hours, claudin-1 turnover was demonstrated. This has also been shown previously (Takahashi *et al.,* 2009) and therefore it is possible that, while the majority of endocytosed claudin-1 is recycled, a small percentage is directed for degradation resulting in a gradual turnover of claudin-1 in Caco-2 cells. Perturbation of the degradative pathway via ESCRT disruption is well

documented (Doyotte *et al.,* 2005; Razi and Futter, 2006; Raiborg and Stenmark, 2009; Stuffers *et al.,* 2009b; Woodman, 2009), thus it is possible that Tsg101 knockdown inhibits degradation of claudin-1 and leads to intracellular accumulation over time. However, my results suggest that a block in claudin degradation is not the major cause of intracellular accumulation as total claudin-1 levels were not increased following Tsg101 knockdown. Furthermore, claudin-1 ubiquitylation, which targets proteins for degradation, was not observed. Therefore, this suggests that a block in claudin-1 degradation is not responsible for the majority of intracellular claudin-1 accumulation.

To analyse this further, treatment with a lysosomal inhibitor, such as chloroquine, could be carried out to establish whether a similar effect on claudin-1 localisation is observed when lysosomal degradation is blocked. This may provide further insight into whether claudin-1 accumulation is likely to arise due to a block in its degradation. However, the time frame may not be comparable with that used to efficiently knockdown Tsg101 as prolonged lysosomal inhibition is likely to be cytotoxic. In addition, cycloheximide treatment could be carried out on ESCRT-I depleted cells to block protein synthesis. Comparison of claudin-1 levels between control and Tsg101 knockdown cells would then indicate whether claudin-1 turnover can occur after ESCRT-I depletion.

In summary, it is likely that the intracellular accumulation of claudin-1 observed upon ESCRT-I depletion is due to inhibition of both claudin-1 recycling and degradation. In support of this, the intracellular pool of claudin-1 in Tsg101 knockdown cells localises to a compartment/s positive for markers of recycling, early and late endosomes as well as lysosomes. My results, along with additional data generated in our laboratory, strongly suggest that ESCRT-I function is required for the constitutive recycling of claudin-1 in Caco-2 cells. Therefore, it is hypothesised that the majority of claudin-1 accumulation in ESCRT-I depleted cells is due to a block in claudin-1 recycling. However, long term turnover of claudin-1 may also be dependent on a functional ESCRT machinery.

### 4.3.5. Variation between claudin-1 and occludin trafficking in Caco-2 cells

The intracellular accumulation of claudin-1 caused by ESCRT-I depletion can be explained by an inhibition of claudin-1 trafficking through the endocytic system. However, occludin is also continuously endocytosed in Caco-2 cells but does not accumulate after Tsg101 knockdown. This may indicate that occludin and claudin-1 are following independent endocytic trafficking routes. In support of this, the dynamics of claudin-1 and occludin trafficking in Caco-2 cells are different. The majority of endocytosed claudin-1 is recycled, whereas the fate of endocytosed occludin is split between recycling and degradation, suggesting that these two proteins are following distinct endosomal pathways. Trafficking of claudin-1 requires ESCRT function whereas occludin may follow an ESCRT-independent trafficking pathway. There are a number of independent recycling pathways (Grant and Donaldson, 2009; Golachowska *et al.,* 2010) and polarised epithelial cells contain a number of distinct recycling compartments (Hoekstra *et al.,* 2004; Weisz and Rodriguez-Boulan, 2009). Therefore, it is possible that claudin-1 is returned to the plasma membrane by a pathway requiring ESCRT function and this is distinct from that used to recycle occludin.

It is interesting that occludin accumulation is not observed upon ESCRT-I depletion despite the fact that some of the endocytosed occludin is directed for degradation. ESCRT proteins have an established role within the endosomal degradative pathway (Doyotte *et al.,* 2005; Razi and Futter, 2006; Raiborg and Stenmark, 2009; Stuffers *et al.,* 2009b; Woodman, 2009), however, the majority of studies into ESCRT function are conducted in non-polarised cells. Polarised epithelial cells contain additional endosomal compartments and endocytic trafficking is thought to be more complex (Hoekstra *et al.,* 2004; Mellman and Nelson, 2008; Farr *et al.,* 2009; Folsch *et al.,* 2009; Weisz and Rodriguez-Boulan, 2009). Therefore, there may be additional degradative routes in Caco-2 cells which are independent of ESCRT function. This is supported by my previous results demonstrating that EGF degradation is not significantly inhibited in ESCRT depleted Caco-2 cells (Chapter 3, section 3.2.2), suggesting that trafficking to lysosomes can occur independently of ESCRTs.

## 4.4. Conclusion

Altered epithelial junctions are associated with a wide range of pathological conditions, such as cancer and inflammatory bowel diseases (Yang and Weinberg, 2008; Yu and Turner, 2008; Capaldo and Nusrat, 2009; Brennan *et al.,* 2010). Therefore, a thorough understanding of cell-cell junction formation, maintenance and remodelling is crucial. My data begins to elucidate some of the mechanisms important for regulation of epithelial junctions and suggests a role for ESCRT-I in this process. The tight junction proteins, claudin-1 and occludin, are constitutively endocytosed and recycled in Caco-2 epithelial monolayers. Depletion of ESCRT-I in Caco-2 cells results in mislocalisation of claudins from tight junctions to an intracellular endocytic compartment/s. Therefore, I propose that claudin-1 recycling is dependent on ESCRT-I function and that this provides a mechanism for the intracellular accumulation of claudin-1 observed upon ESCRT-I depletion in Caco-2 cells.

In addition, ESCRT-I is required for Caco-2 epithelial barrier formation. This may be an effect of claudin mislocalisation and suggests that tight junction integrity is impaired. Tight junctions are thought to be important for maintenance of a polarised epithelium (Brennan *et al.,* 2010; Coradini *et al.,* 2011) and therefore destabilisation may contribute to the loss of Caco-2 cell organisation and polarity observed upon ESCRT-I depletion. Finally, ESCRT-I depletion enhances Caco-2 cell migratory ability. This data, together with previous results demonstrating a requirement of ESCRTs in maintenance of epithelial cell polarity, provides further support for a role of ESCRT proteins as tumour suppressors in vertebrates.

# CHAPTER FIVE

# 5. Multilayered Tsg101 depleted Caco-2 cells are eliminated by apoptosis

## 5.1. Introduction

### 5.1.1. ESCRTs and Epithelial Cell Proliferation

Cell proliferation is a tightly regulated process (King and Cidlowski, 1998). Disruption to any number of important regulatory pathways can trigger uncontrolled cell growth, a hallmark of tumourigenesis (Hanahan and Weinberg, 2011). A role for ESCRT proteins in epithelial cell proliferation has been demonstrated previously in *Drosophila.* Mutation of various components of the ESCRT machinery in epithelial tissues results in increased proliferation (Moberg *et al.,* 2005; Thompson *et al.,* 2005; Vaccari and Bilder, 2005; Herz *et al.,* 2006; Herz *et al.,* 2009; Rodahl *et al.,* 2009b; Vaccari and Bilder, 2009; Vaccari *et al.,* 2009). When epithelial tissues are predominantly mutant for ESCRT components, mutant cells lose polarity and overgrow to form large masses lacking normal epithelial morphology. The resulting mutant larvae are enlarged and eventually die. This neoplastic growth is thought to be due to an extended period of proliferation rather than an increased growth rate and suggests that ESCRT mutant cells are unable to respond to signals which usually sense and restrict organ size (Moberg *et al.,* 2005; Vaccari and Bilder, 2005; Herz *et al.,* 2009; Vaccari *et al.,* 2009).

However, in mosaic epithelial tissues where mutant cells are surrounded by wild type cells, the situation is somewhat different. ESCRT mutant cells still lose epithelial polarity and organisation but do not overproliferate. Instead increased proliferation of surrounding wild type cells is observed, despite these cells displaying a normal epithelial morphology (Moberg *et al.,* 2005; Thompson *et al.,* 2005; Vaccari and Bilder, 2005; Herz *et al.,* 2006; Herz *et al.,* 2009; Rodahl *et al.,* 2009b; Vaccari and Bilder, 2009; Vaccari *et al.,* 2009). This hyperplastic growth is attributed to a block in Notch trafficking within ESCRT mutant cells. Consequently Notch accumulates within large aberrant endosomes, is activated and results in ectopic production of the secreted growth factor, Unpaired (Upd).

This then induces proliferation of surrounding wild type cells via activation of the Jak-STAT signalling pathway (Thompson *et al.,* 2005; Vaccari and Bilder, 2005; Herz *et al.,* 2006; Herz *et al.,* 2009; Gilbert *et al.,* 2009; Vaccari *et al.,* 2009).

Another mechanism by which ESCRT disruption could influence cell growth is through aberrant receptor tyrosine kinase (RTK) signalling. For example, ESCRTs have been identified as important regulators of epidermal growth factor receptor (EGFR) signalling (Vaccari and Bilder, 2009; Woodman, 2009). In both *Drosophila* and vertebrates, ESCRT proteins are required for the degradation of EGFR and attenuation of EGF-induced signalling (Jekely and Rorth, 2003; Bache *et al.,* 2006; Lloyd *et al.,* 2006; Malerod *et al.,* 2007; Raiborg *et al.,* 2008; Vaccari *et al.,* 2009). Increased RTK signalling can induce overproliferation and is often linked to tumourigenesis (Kim and Choi, 2010) and therefore this may contribute to the overgrowth associated with ESCRT disruption in *Drosophila.*

In contrast to the studies conducted in *Drosophila*, mouse models have demonstrated a reduction in proliferation upon ESCRT disruption (Ruland *et al.,* 2001; Wagner *et al.,* 2003). However, the role of ESCRT proteins in growth of vertebrate epithelial tissues has not been analysed in detail. Therefore, it is of interest to determine if ESCRTs are important for the regulation of epithelial cell proliferation in mammalian cells and whether this could contribute to their role as tumour suppressors.

### 5.1.2. ESCRTs and Cell Death

In addition to the role of ESCRTs proteins in cell proliferation, ESCRTs have also been implicated in the process of apoptosis. Apoptosis is a highly regulated mechanism of programmed cell death, important for many physiological processes and often deregulated in cancer (Pettigrew and Cotter, 2009; Ola *et al.,* 2011). In *Drosophila*, Vps25 mutation has been shown to increase levels of Diap1, an inhibitor of apoptosis, in wild type cells surrounding ESCRT mutant clones (Herz *et al.,* 2006). Therefore, loss of ESCRT function may confer apoptotic resistance and enhance the survival of surrounding wild type tissue.

However, a more commonly reported consequence of ESCRT mutation is the proapoptotic response. Loss of ESCRT-I function has been shown to induce cell death of mouse mammary epithelial cells, both *in vivo* and *in vitro* (Wagner *et al.,* 2003). Consistent with this, in *Drosophila*, if ESCRT mutant cells are surrounded by wild type cells, the mutant cells are eventually eliminated from the epithelium via an increase in apoptosis (Thompson *et al.,* 2005; Herz *et al.,* 2006; Rodahl *et al.,* 2009b). This means that the resulting enlarged tissue is mainly comprised of wild type cells. Studies have demonstrated that this apoptosis is induced by at least two pathways, one mediated by JNK signalling and another mediated by Hid/Diap1/Dronc/Ark (Herz *et al.,* 2006; Rodahl *et al.,* 2009b; Vaccari and Bilder, 2009). In addition, Hippo signalling has been suggested to function as an upstream regulator of the overall proapoptotic response observed in ESCRT mutant cells (Herz *et al.,* 2006). Interestingly, if apoptosis of ESCRT mutant cells is inhibited a dramatic overproliferation of mutant tissue is observed resulting in the formation of neoplastic tumours capable of metastasis (Thompson *et al.,* 2005; Herz *et al.,* 2006; Rodahl *et al.,* 2009b).

### 5.1.3. A Role for ESCRT Proteins as Tumour Suppressors

Previous studies suggest that the ESCRT machinery is required for trafficking of important regulators of epithelial cell polarity and proliferation in *Drosophila* (Vaccari and Bilder, 2009). In this model system, disruption of the ESCRT machinery can lead to loss of cell polarity and self-sufficiency in growth signalling, two important hallmarks of cancer (Hanahan and Weinberg, 2011). Therefore, ESCRT proteins have been classified as potential tumour suppressors. Consistent with these studies, I have shown that ESCRT-I is required for maintenance of mammalian epithelial cell polarity and organisation. I have demonstrated that this phenotype may be due to disruption in trafficking of cell-cell junction proteins which may be important for maintaining a polarised epithelium. Therefore, the tumour suppressor role of ESCRTs may be conserved from *Drosophila* to vertebrates. However, it is likely that further alterations in cell physiology, such as evasion of apoptosis, are required in order to exert the full tumourigenic potential of the ESCRT machinery.

### 5.1.4. Aims

In addition to the defects in epithelial cell-cell junctions, it is also possible that alterations in proliferation and/or cell death contribute to the aberrant epithelial morphology observed upon ESCRT-I depletion. Therefore, the aims of this chapter are to determine whether Tsg101 and Vps25 siRNA knockdown affects Caco-2 cell proliferation and apoptosis. In addition, the effect of inhibiting apoptosis in Tsg101 depleted Caco-2 cells will be investigated.

## 5.2. Results

### 5.2.1. ESCRT-I depletion results in overproliferation of Caco-2 cells

The effect of ESCRT depletion on Caco-2 cell number was assessed using a MTT assay. This assay measures the metabolic conversion of MTT to formazan. Absorbance of the resulting formazan solution has a linear relationship to cell number and therefore can be used to indicate changes in cell number over time (data not shown). Results demonstrated that absorbance increased over time in control and ESCRT knockdown cell cultures, suggesting that Caco-2 cell number increased over time in culture. However, the absorbance measurements for Tsg101 knockdown cells appeared to increase at a faster rate and, after 7 days, absorbance was significantly increased compared to control (Figure 5.1A). This suggests that Tsg101 depletion results in an increase in Caco-2 cell number. Caco-2 cell number was also analysed by counting cells using confocal fluorescence microscopy (Figure 5.1B). This demonstrated that increased cell number was only found in multilayered regions of Tsg101 knockdown cells. In monolayered regions of Tsg101 depleted cells, there seemed to be a slight decrease in cell number although this difference was not statistically significant. This may correspond to the reduced differentiation of Tsg101 knockdown cells shown previously (Chapter 3, section 3.2.4) as cells may not be as tightly packed as in control. In contrast, Vps25 knockdown had no effect on cell number, demonstrated by both the MTT assay and fluorescence microscopy cell counting (Figure 5.1A+B).

Despite this significant increase in cell number after Tsg101 knockdown, there was no significant increase in the proportion of phosphorylated Histone H3-positive Tsg101 knockdown cells (Figure 5.2A). Histone H3 is phosphorylated during mitosis and therefore this suggests that after 7 days culture, proliferation of Tsg101 knockdown cells was similar to control. This was also demonstrated by quantifying BrdU (Bromodeoxyuridine) incorporation in Tsg101 depleted cells (Figure 5.2B). BrdU is a synthetic analogue of thymidine which can be incorporated into newly synthesised DNA during S phase of the cell cycle. It is therefore used to indicate the proportion of cells which have divided during a set time period. Results indicated that after Tsg101 knockdown, BrdU incorporation

***Figure 5.1*** **Caco-2 cell number increases upon Tsg101 knockdown. (A)** Caco-2 cells were transfected with either Non-Targeting Control siRNA, Tsg101 siRNA, or Vps25 siRNA and incubated for 1, 3, 7 and 10 d. At each timepoint the MTT assay was carried out, used as a measure of cell number. Cells were incubated with MTT and metabolic conversion of MTT to formazan was measured by reading absorbance at 570nm. After 7 d Tsg101 knockdown Caco-2 absorbance is significantly increased compared with control. Vps25 knockdown has no effect. **(B)** Caco-2 cells were transfected with either Non-Targeting Control siRNA, Tsg101 siRNA, or Vps25 siRNA and incubated for 7 d. Cells were fixed and nuclei were stained using DAPI. Cells were examined by confocal fluorescence microscopy and z-stack images were taken at random. Cell number was quantified by counting individual nuclei in each image using ImageJ. Six images were taken per condition and, for Tsg101 knockdown cells regions were distinguished as either monolayerd or multilayered. Tsg101 knockdown increases Caco-2 cell number due to regions of multilayered cells. Vps25 knockdown has no effect. Data shown are the means ± standard error of at least three independent experiments. Results were analysed using a one-way ANOVA and Dunnett's post test, *** $p<0.001$.

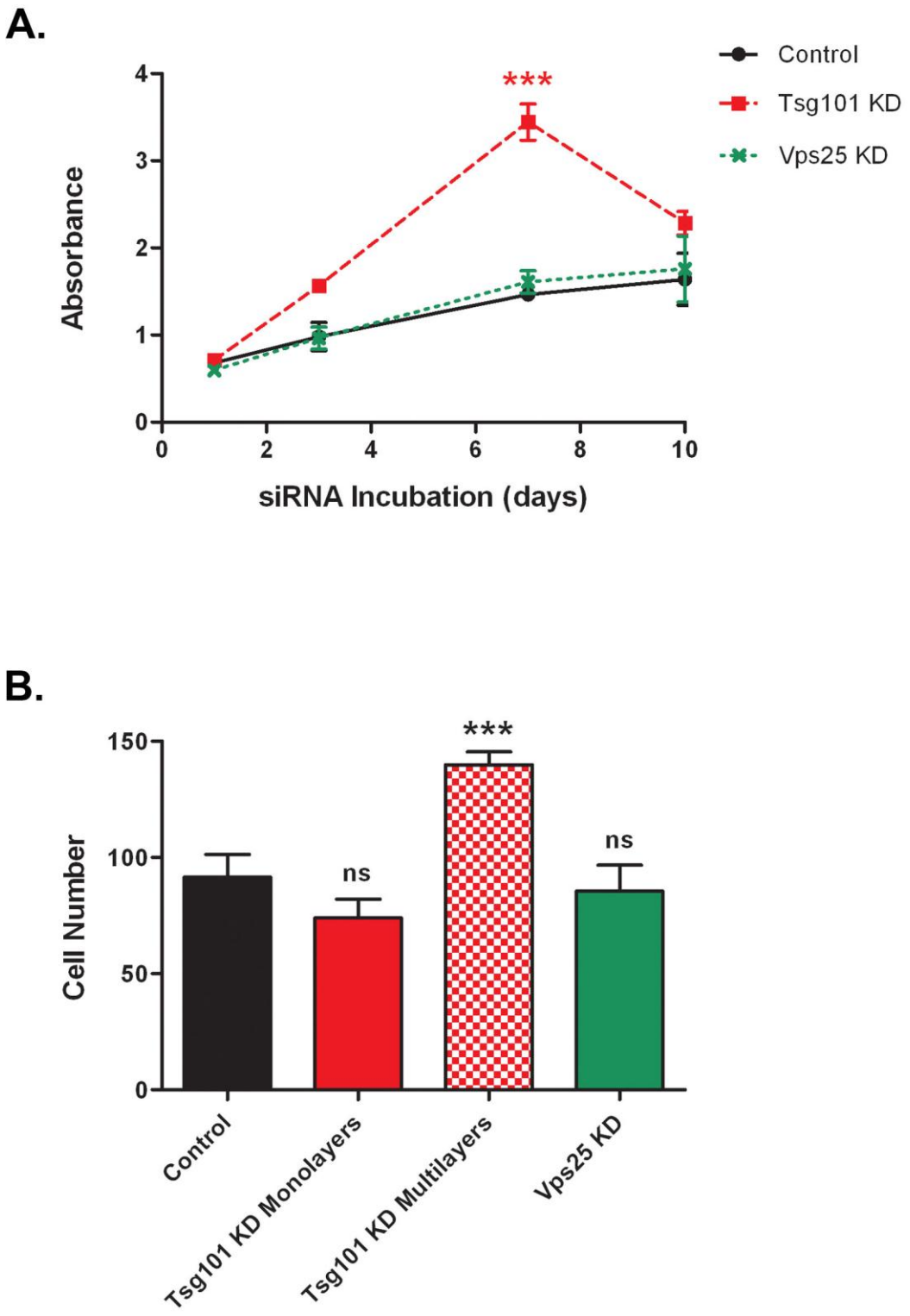
A.
Absorbance
siRNA Incubation (days)
***
Control
Tsg101 KD
Vps25 KD
B.
Cell Number
***
ns
ns
Control
Tsg101 KD Monolayers
Tsg101 KD Multilayers
Vps25 KD

***Figure 5.2*** **Rate of Caco-2 cell proliferation is not increased after 7 day Tsg101 knockdown. (A)** Caco-2 cells were transfected with Non-Targeting Control siRNA or Tsg101 siRNA and incubated for 7 d. Cells were fixed and examined by confocal fluorescence microscopy for phosphorylated Histone H3 (red). Nuclei were stained using DAPI. Number of p-Histone H3-positive cells was quantified using ImageJ and represented as a percentage of total cell number. The proportion of dividing Caco-2 cells is not affected by Tsg101 knockdown. **(B)** Caco-2 cells were transfected with Non-Targeting Control siRNA or Tsg101 siRNA and incubated for 7 d. BrdU was added to the media on day 6 for 24 h. Cells were fixed and examined by confocal fluorescence microscopy for BrdU (green). Nuclei were stained using DAPI. Number of BrdU-positive cells was quantified using ImageJ and represented as a percentage of total cell number. BrdU incorporation is not significantly altered in monolayered regions of Tsg101 knockdown cells whereas multilayered regions show a reduction in BrdU labelling. For each experiment, six images were taken at random per condition and, for Tsg101 knockdown cells regions were distinguished as either monolayerd or multilayered. An example image is shown with the graphical representation of the data. Bar, 10µm. Data shown are the means ± standard error of at least three independent experiments. Results were analysed using a one-way ANOVA and Dunnett's post test, * $p<0.05$.

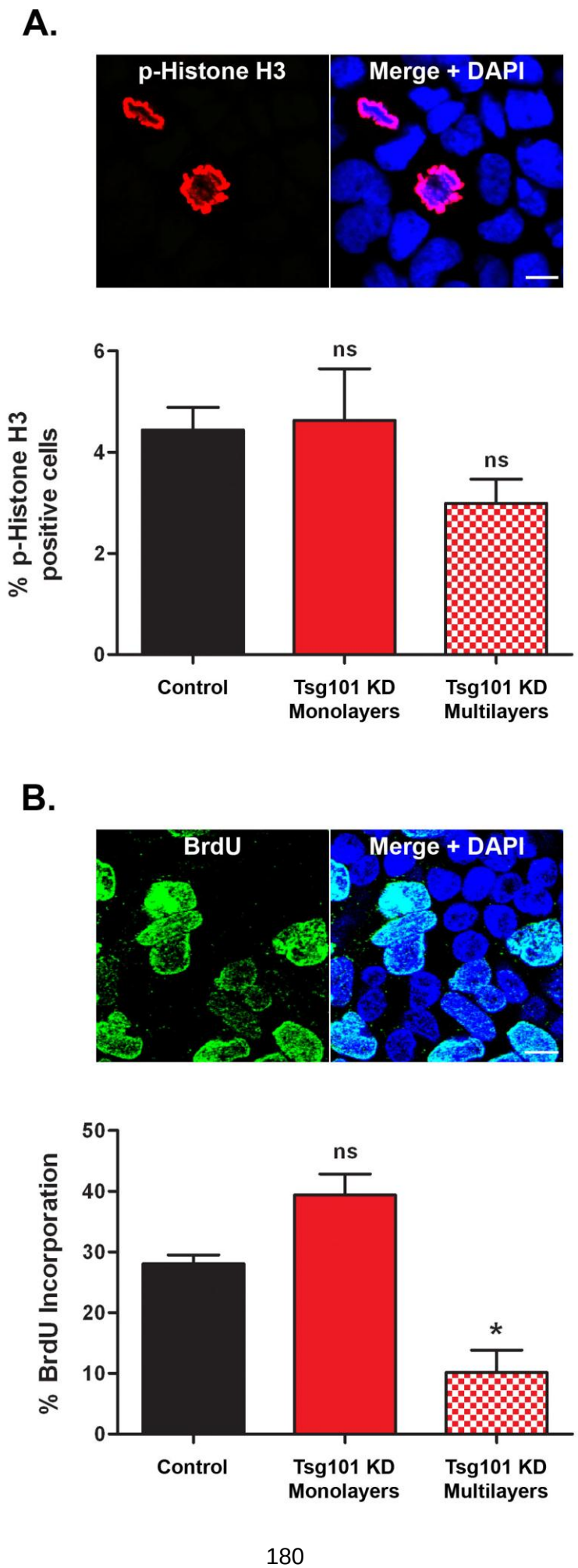
A.
p-Histone H3
Merge + DAPI
% p-Histone H3 positive cells
6
4
2
0
ns
ns
Control
Tsg101 KD Monolayers
Tsg101 KD Multilayers
B.
BrdU
Merge + DAPI
% BrdU Incorporation
50
40
30
20
10
0
ns
*
Control
Tsg101 KD Monolayers
Tsg101 KD Multilayers

was not significantly increased between 6 and 7 days cell culture (Figure 5.2B). However, the proportion of BrdU-positive cells did show a slight increase in monolayered regions of Tsg101 knockdown cells suggesting that a slightly higher proportion of these cells divided over 24 h compared with control.

In contrast, multilayered regions of Tsg101 knockdown cells displayed a significant reduction in BrdU incorporation (Figure 5.2B). In addition, Histone H3 phosphorylation appeared slightly reduced, although this was not statistically significant (Figure 5.2A). This demonstrates that after 7 days culture, proliferation is reduced in multilayered areas of Tsg101 depleted cells. It is also important to note that between 7 and 10 days of Tsg101 knockdown cell culture, there was a reduction in cell number (Figure 5.1A). As a result, after 10 days the number of Tsg101 knockdown cells was similar to control. This may be due to an increase in cell death and will be analysed later.

### 5.2.2. ERK1/2 signalling is not increased after ESCRT-I depletion

Cell proliferation can be regulated by various mitogenic signalling pathways, such as the extracellular signal-regulated kinase (ERK) pathway. The ERK signal transduction pathway is a mitogen-activated protein kinase (MAPK) pathway which functions in proliferation, differentiation and survival and is often deregulated during tumourigenesis (Kim and Choi, 2010). ERK signalling can be mediated by EGFR activation and ESCRTs have been identified as important regulators of this signalling pathway (Jekely and Rorth, 2003; Bache *et al.,* 2006; Lloyd *et al.,* 2006; Malerod *et al.,* 2007; Raiborg *et al.,* 2008; Vaccari *et al.,* 2009). Therefore, it is possible that the increased numbers of Tsg101 knockdown cells is due to altered ERK signalling. The ERK pathway can be stimulated by EGF which results in the phosphorylation of ERK1/2. This was detected via immunofluorescence confocal microscopy using an antibody specific to the phosphorylated form of ERK1/2 (p-ERK1/2) (Figure 5.3A). However, levels of p-ERK1/2 were similar in control and Tsg101 knockdown Caco-2 cells (Figure 5.3B). This suggests that the ERK pathway was not perturbed in Tsg101 knockdown cells after 7 days culture and argues that the overproliferation is not due to altered ERK signalling.

***Figure 5.3*** **Tsg101 knockdown does not appear to alter ERK1/2 activation in Caco-2 cells.** **(A)** To test the efficiency of the phosphorylated Erk1/2 (p-Erk1/2) antibody, Caco-2 cells were incubated with 500ng/ml EGF for 10 min or mock treated. Cells were fixed and examined by confocal fluorescence microscopy for p-Erk1/2 (green). Nuclei were stained using DAPI. p-Erk1/2 levels increase after EGF treatment. **(B)** Caco-2 cells were transfected with Non-Targeting Control siRNA or Tsg101 siRNA and incubated for 7 d. Cells were fixed and examined by confocal fluorescence microscopy for p-Erk1/2 (green). Nuclei were stained using DAPI. Tsg101 knockdown has no discernible effect on activation of Erk1/2. Bar, 10µm.

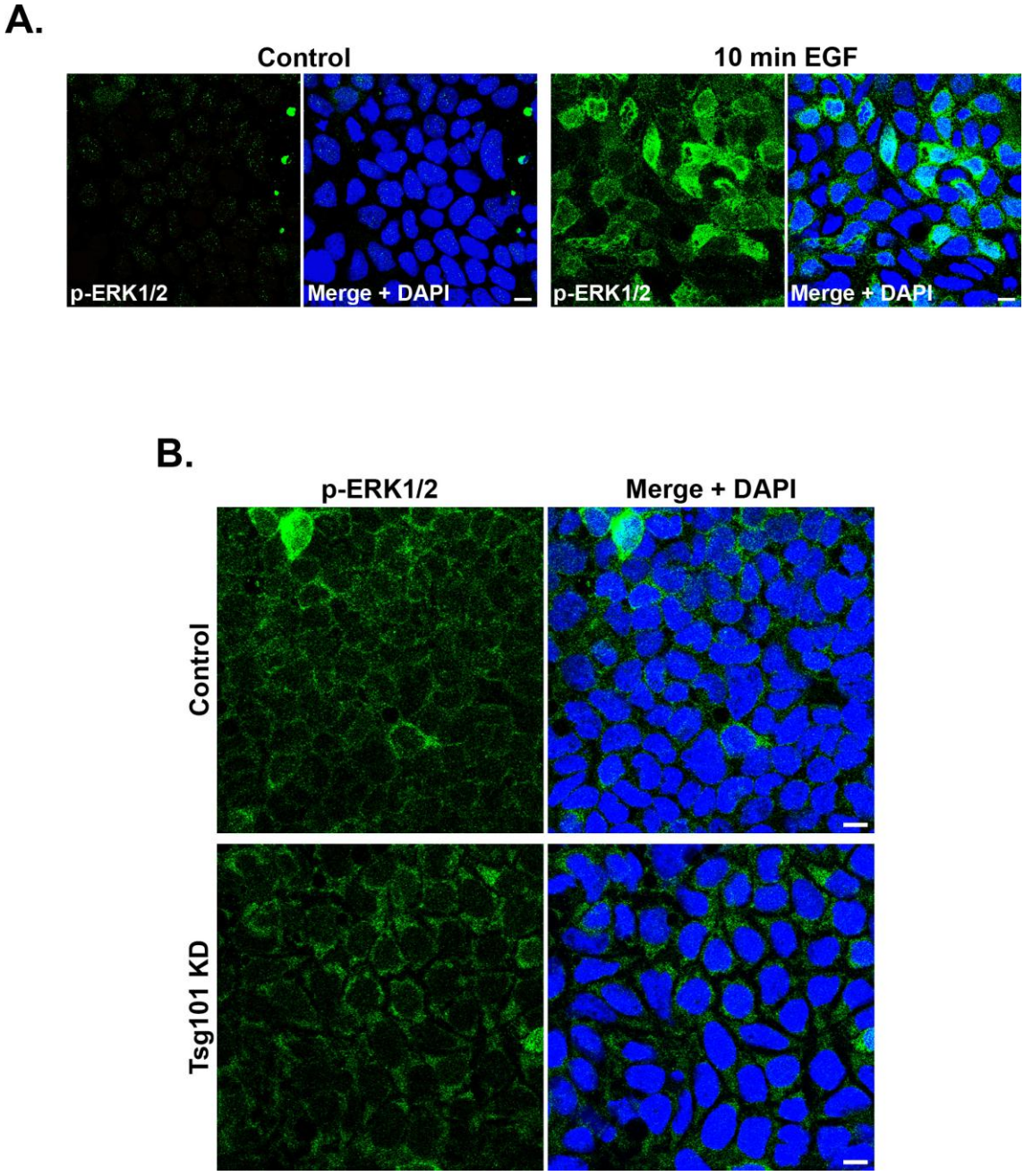
A.
Control
10 min EGF
p-ERK1/2
Merge + DAPI
p-ERK1/2
Merge + DAPI
B.
p-ERK1/2
Merge + DAPI
Control
Tsg101 KD

### 5.2.3. Tsg101 depleted Caco-2 cells are eliminated by apoptosis

As cell number appeared to decrease when Tsg101 depleted cells were cultured for longer than 7 days (Figure 5.1A), the level of cell death after ESCRT knockdown was investigated. Active caspase-3 was used as a marker of apoptotic cells and cells were analysed via immunofluorescence confocal microscopy. The proportion of apoptotic cells was significantly increased in multilayered regions of Tsg101 knockdown Caco-2 cells (Figure 5.4A). Tsg101 knockdown cells which retained their monolayered organisation and Vps25 knockdown cells displayed a similar level of active caspase-3 staining to control. Further analysis of Tsg101 knockdown cells demonstrated that the apoptotic cells were mostly located at the apical side of the multilayered epithelial sheet (Figure 5.4B).

An increase in cell death was also observed in *Drosophila* ESCRT mutants and this was attributed to an increase in JNK signalling (Herz *et al.,* 2006; Rodahl *et al.,* 2009b). However, JNK activation was not observed 3, 7 or 10 days after Tsg101 knockdown in Caco-2 cells (Figure 5.4C).

### 5.2.4. Inhibition of apoptosis may enhance the multilayered phenotype of Tsg101 depleted Caco-2 cells

In *Drosophila* ESCRT mutants, inhibition of apoptosis resulted in a dramatic overproliferation of ESCRT mutant cells to form neoplastic tumours (Thompson *et al.,* 2005; Herz *et al.,* 2006; Rodahl *et al.,* 2009b). As a similar increase in apoptosis was observed in Caco-2 cells after Tsg101 depletion, the effect of inhibiting cell death was investigated. A general caspase inhibitor was used which effectively reduced the number of caspase-3 positive cells after 7 and 10 days culture (Figure 5.5A). Initial results demonstrated that caspase inhibition had no effect on the number of Tsg101 knockdown cells after 7 days culture (Figure 5.5B, '7d Knockdown'). However, after 10 days culture the number of Tsg101 knockdown cells dramatically increased after caspase inhibition (Figure 5.5B, '10d Knockdown'). In addition, caspase inhibition appeared to enhance the degree of multilayering observed upon Tsg101 knockdown after 10 days culture (Figure 5.5C).

***Figure 5.4*** **Cell death is increased in multilayered regions of Tsg101 knockdown Caco-2 cells. (A)** Caco-2 cells were transfected with either Non-Targeting Control siRNA, Tsg101 siRNA or Vps25 siRNA and incubated for 7 d. Cells were fixed and examined by confocal fluorescence microscopy for active caspase-3. Nuclei were stained using DAPI. Number of caspase-3 positive cells was quantified using ImageJ and represented as a percentage of total cell number. Six images were taken at random per condition and, for Tsg101 knockdown cells regions were distinguished as either monolayerd or multilayered. Cell death is increased in multilayered regions of Tsg101 knockdown cells whereas in monolayered regions and Vps25 knockdown cells, the level of cell death is similar to control. Data shown are the means ± standard error of at least three independent experiments. Results were analysed using a one-way ANOVA and Dunnett's post test, * $p<0.05$. **(B)** A representative image of active caspase-3 (green) staining in a multilayered region of Tsg101 knockdown Caco-2 cells. Nuclei were stained with DAPI (blue). A confocal projection is displayed in the xy plane (top) and z plane (bottom). Active caspase-3 positive cells are found apically in the multilayered Caco-2 epithelial sheet. Bar, 10µm. **(C)** Caco-2 cells were transfected with either Non-Targeting Control siRNA (C), Tsg101 siRNA (T), or Vps25 siRNA (V) and incubated for 3, 7 or 10 d. Lysates were immunoblotted for phosphorylated JNK (p-JNK) and total JNK as a loading control. A lysate from UV treated Caco-2 cells was used as a positive control for JNK activation. Tsg101 and Vps25 knockdown does not result in an increase in p-JNK in Caco-2 cells.

A.

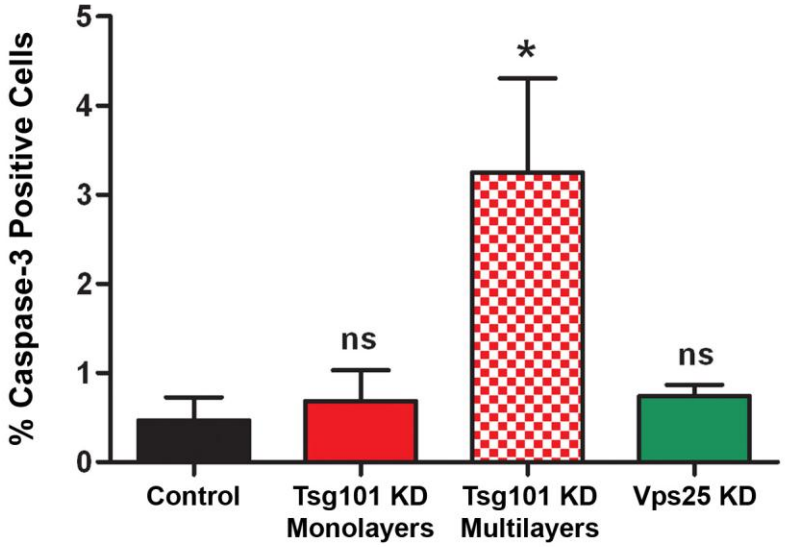
% Caspase-3 Positive Cells
5
4
3
2
1
0
*
ns
ns
Control
Tsg101 KD Monolayers
Tsg101 KD Multilayers
Vps25 KD

B.

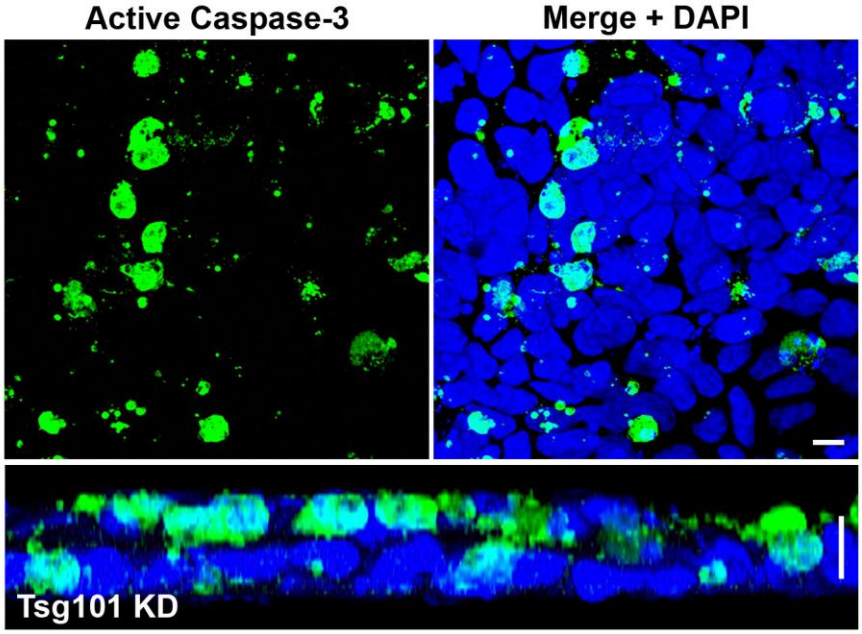
Active Caspase-3
Merge + DAPI
Tsg101 KD

C.

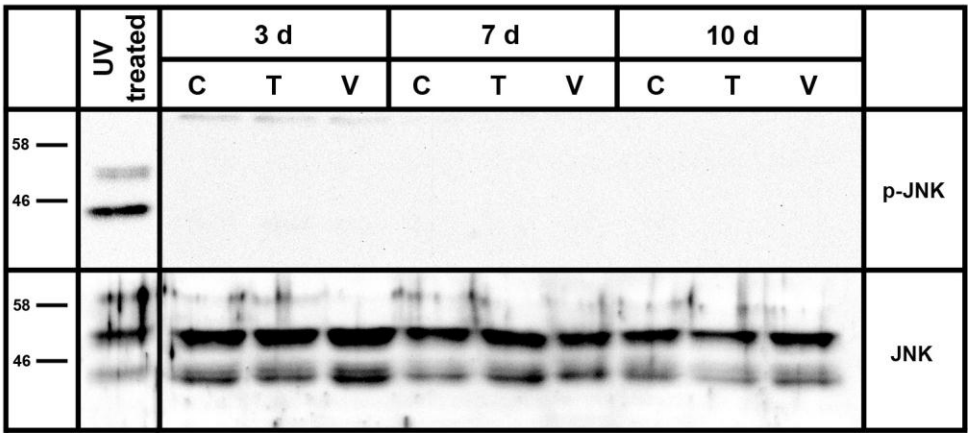
UV treated
3 d
7 d
10 d
C T V C T V C T V
58
46
p-JNK
58
46
JNK

In the absence of caspase inhibition, after 10 days Tsg101 knockdown total cell number was similar to control (Figure 5.5B, ‘10d Knockdown’) and the extent of multilayering was reduced (Figure 5.5C, top panels) compared with the phenotype observed after 7 days (see previous results, Chapter 3, Figure 3.7). This indicates that after extended culture, cells in multilayered regions are eliminated via apoptosis and may explain results from the MTT assay shown previously (Figure 5.1A). If apoptosis is inhibited it seems that Caco-2 cells continue to proliferate and multilayering is enhanced. It is important to note that these results were generated from one initial experiment and therefore, will need to be confirmed with further work.

***Figure 5.5*** **Caspase inhibition enhances the multilayering of Tsg101 knockdown Caco-2 cells.** Caco-2 cells were transfected with Non-Targeting Control siRNA or Tsg101 siRNA and incubated for total of 7 or 10 d. The pan-caspase inhibitor (Q-VD-OPh) was added to cells on day 4 and day 7. DMSO controls were carried out alongside. Cells were fixed and examined by confocal fluorescence microscopy for active caspase-3. Nuclei were stained using DAPI. **(A)** The number of caspase-3 positive cells was quantified using ImageJ and represented as a percentage of total cell number. Caspase-3 activation is reduced upon addition of the general caspase inhibitor. **(B)** Total cell number was quantified using ImageJ. Caspase inhibition dramatically increases the number of Tsg101 knockdown Caco-2 cells after 10 d culture. For quantification, six images were taken at random per condition. Note that separation of Tsg101 knockdown cells into monolayered and multilayered regions was not carried out. Data shown are the means from one preliminary experiment. **(C)** Representative images of Caco-2 cells with and without caspase inhibition 10 d after knockdown with Non-Targeting Control or Tsg101 siRNA. The multilayered phenotype of Tsg101 knockdown Caco-2 cells is enhanced upon caspase inhibition. Confocal projections and corresponding z-sections (indicated by dotted line) are displayed. Bar, 10μm.

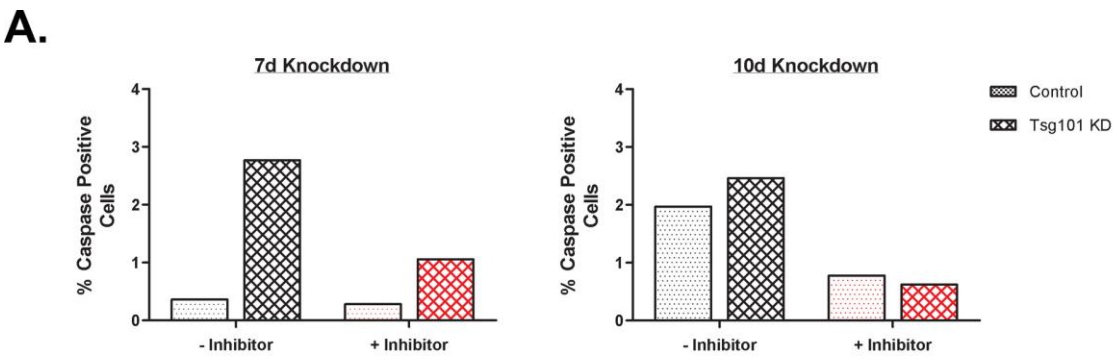
A.
7d Knockdown
10d Knockdown
% Caspase Positive Cells
0
1
2
3
4
- Inhibitor
+ Inhibitor
Control
Tsg101 KD

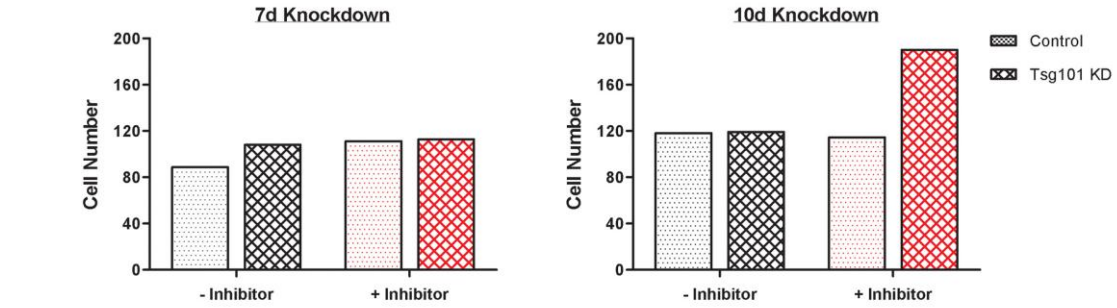
B.
7d Knockdown
10d Knockdown
Cell Number
0
40
80
120
160
200
- Inhibitor
+ Inhibitor
Control
Tsg101 KD

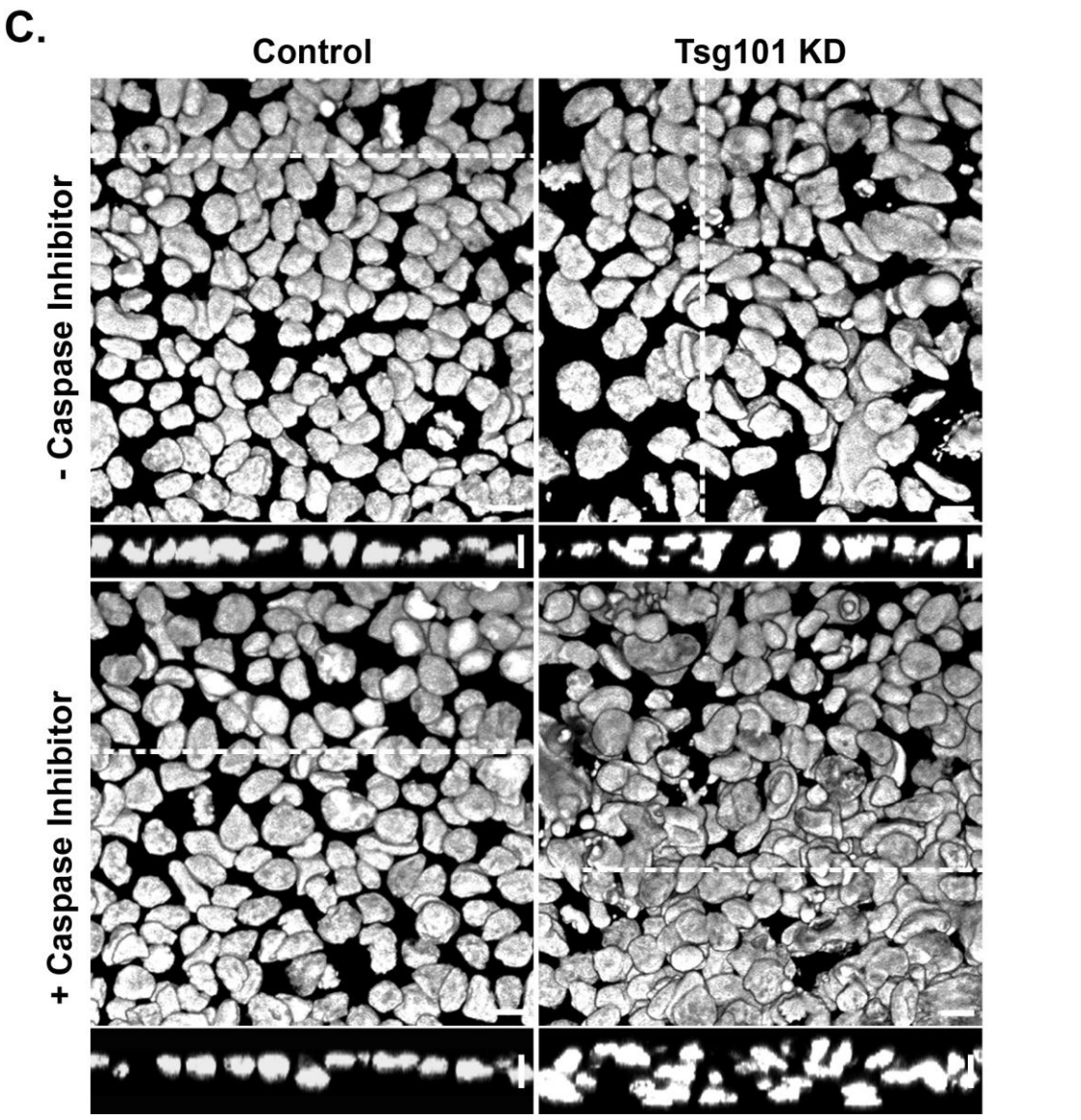
C.
Control
Tsg101 KD
- Caspase Inhibitor
+ Caspase Inhibitor

## 5.3. Discussion

This study sought to investigate the effect of ESCRT depletion on Caco-2 cell growth. I have previously demonstrated that ESCRT-I depleted Caco-2 cells form multilayered epithelial sheets (discussed in Chapter 3). Disruption of ESCRT function has been shown to cause overproliferation in *Drosophila* (Moberg *et al.,* 2005; Thompson *et al.,* 2005; Vaccari and Bilder, 2005; Herz *et al.,* 2006; Herz *et al.,* 2009; Rodahl *et al.,* 2009b; Vaccari *et al.,* 2009). Therefore, it is possible that formation of Caco-2 cell multilayers is due to an increase in proliferation. In addition, studies in *Drosophila* found that in mosaic epithelial tissues, ESCRT mutant cells were eventually eliminated via apoptosis and if this was inhibited neoplastic tumours formed (Thompson *et al.,* 2005; Herz *et al.,* 2006; Rodahl *et al.,* 2009b). Thus, the effect of ESCRT depletion on apoptosis was also analysed in Caco-2 cells. My results demonstrate that Caco-2 cell number increases after Tsg101 depletion. There is also an increase in apoptosis of Tsg10 depleted Caco-2 cells, however this is observed within multilayered regions only. Finally, inhibition of apoptosis appears to enhance the multilayered phenotype of Tsg101 depleted Caco-2 cells suggesting that inhibition of cell death is required in order to demonstrate the full tumourigenic potential of ESCRT-I depletion.

### 5.3.1. Caco-2 cells overproliferate upon ESCRT-I depletion

ESCRT-I depletion appeared to result in overproliferation of Caco-2 cells. After 7 days culture of Tsg101 knockdown cells, there was a significant increase in the metabolic conversion of MTT suggesting that cell number was increased. Counting cells manually using immunofluorescence confocal microscopy indicated that an increase cell number was observed in the multilayered regions of Tsg101 knockdown cells only. In contrast, a reduction in BrdU incorporation was observed in these multilayered regions of Tsg101 knockdown cells suggesting that cell division in these areas is reduced. However, at this timepoint apoptosis of multilayered cells is increased and therefore, this may inhibit any further proliferation. Therefore, analysis of Tsg101 knockdown cells at earlier timepoints is required in order to investigate whether proliferation is enhanced in certain areas of the epithelial sheet. This may then suggest that

increased proliferation of ESCRT-I depleted cells results in the formation of multilayered regions of the Caco-2 epithelial sheet.

Interestingly, in Tsg101 knockdown cells which retained their monolayered organisation there was also no significant increase in the proportion of dividing cells 7 days after knockdown. However, the largest increase in cell number appears to occur between 3 and 7 days after Tsg101 knockdown and therefore, it is possible that the most substantial increase in cell division occurs at an earlier timepoint. It is also possible that the MTT assay is misleading as the metabolic activity of Caco-2 cells may be affected by the differentiation status of the cell culture. I have previously shown that Tsg101 knockdown results in reduced Caco-2 cell differentiation. Undifferentiated cells may have higher metabolic activity and therefore, the large increase in metabolic conversion of MTT may not accurately represent a proportional increase in cell number. Therefore, a thorough analysis of Caco-2 cell division is required in order to establish whether Tsg101 knockdown causes a significant increase in Caco-2 cell proliferation. Fluorescence-activated cell sorting (FACS) analysis could be conducted at various timepoints after Tsg101 knockdown in order to quantify the proportion of cells undergoing cell division.

Studies in *Drosophila* have demonstrated that ESCRT mutation results in overproliferation of epithelial cells. However, the mechanism behind this overproliferation varies depending on the tissue context surrounding the ESCRT mutant cells. When epithelial tissues are predominantly mutant for ESCRT components, mutant cells lose polarity and overgrow to form large masses lacking normal epithelial morphology. This neoplastic growth is thought to be due to an extended period of proliferation rather than an increased growth rate (Moberg *et al.,* 2005; Vaccari and Bilder, 2005; Herz *et al.,* 2009; Vaccari *et al.,* 2009). Caco-2 cells are known to undergo contact inhibition whereby when cells reach confluency they reduce proliferation rate and begin to differentiate (Nelson and Daniel, 2002; Volpe, 2008). It is possible that ESCRT-I depletion inhibits contact inhibition and, as a result, cells continue proliferating for an extended period of time. In support of this, I have previously demonstrated that differentiation of Caco-2 cells is reduced upon Tsg101 knockdown. This may suggest that cells cannot sense their environment correctly and continue to

divide instead of initiating the differentiation process. One mechanism which is important for the regulation of cell contact inhibition and organ size control is the Hippo signalling pathway (Zeng and Hong, 2008). Hippo signalling is deregulated in *Drosophila* Vps25 mutants (Herz *et al.,* 2006) suggesting that ESCRTs are important for regulation of this pathway. The core components of the Hippo pathway are conserved in mammals (Dong *et al.,* 2007; Zeng and Hong, 2008), and therefore aberrant Hippo signalling may provide a mechanism for the overproliferation of Tsg101 depleted Caco-2 cells and warrants further investigation.

On the other hand, if *Drosophila* ESCRT mutant cells are surrounded by wild type cells, mutant cells still lose epithelial polarity and organisation but do not overproliferate. Instead increased proliferation of surrounding wild type cells is observed which has been attributed to an increase in Notch induced signalling (Thompson *et al.,* 2005; Vaccari and Bilder, 2005; Herz *et al.,* 2006; Herz *et al.,* 2009; Gilbert *et al.,* 2009; Vaccari *et al.,* 2009). Using a siRNA knockdown approach, Tsg101 depletion should be induced in almost all Caco-2 cells. However, it is impossible to know whether the extent of knockdown is uniform across all transfected cells or whether some cells show a higher level of knockdown compared to others. Therefore, overproliferation of ESCRT-I depleted Caco-2 cells may be induced via multiple mechanisms and the effect on the regulation of cell proliferation may depend on the extent of Tsg101 knockdown. Further work could be carried out to establish whether the Notch signalling pathway is affected by ESCRT-I depletion. Notch protein levels and localisation could be analysed using immunoblotting and immunofluorescence microscopy, respectively. Notch activity could be investigated by analysing downstream effectors of the Notch signalling pathway, such as activation of Jak-STAT signalling. In addition, a Notch inhibitor could be applied to ESCRT depleted cells in order to investigate whether this prevents the formation of multilayered regions.

Finally, aberrant receptor tyrosine kinase (RTK) signalling could result in overproliferation of Tsg101 depleted Caco-2 cells. ESCRTs have been identified as important regulators of epidermal growth factor receptor (EGFR) signalling in both *Drosophila* and vertebrates (Jekely and Rorth, 2003; Bache *et*

*al.,* 2006; Lloyd *et al.,* 2006; Malerod *et al.,* 2007; Raiborg *et al.,* 2008; Vaccari *et al.,* 2009). Activation of EGFR can induce signalling via various MAPK pathways, including the ERK signalling pathway. No increase in ERK1/2 activation was detected 7 days after Tsg101 knockdown suggesting that the ERK1/2 signalling pathway is not upregulated in ESCRT-I depleted cells. This could be confirmed by immunoblotting, using additional timepoints. Analysis of other signalling pathways important for cell proliferation could also be conducted using additional timepoints after Tsg101 knockdown in order to establish the mechanism of overproliferation.

### 5.3.2. ESCRT-I depleted Caco-2 cells are eventually eliminated via apoptosis

Apoptosis of ESCRT-I depleted Caco-2 cells is increased 7 days after siRNA knockdown. This supports previous studies in both *Drosophila* and mice models which demonstrate an increase in cell death upon disruption of the ESCRT machinery (Wagner *et al.,* 2003; Thompson *et al.,* 2005; Herz *et al.,* 2006; Rodahl *et al.,* 2009b). In *Drosophila*, this was attributed in part to an increase in JNK signalling (Herz *et al.,* 2006; Rodahl *et al.,* 2009b), however in this study apoptosis of Tsg101 depleted Caco-2 cells appears to be JNK-independent. This could be confirmed by analysing active JNK levels via immunofluorescence as a small increase in activity in multilayered cells may not be detected using immunoblotting. It is possible that in Caco-2 cells ESCRT-I depletion triggers apoptosis via another mechanism. Activation of the Hid/Diap1/Dronc/Ark proapoptotic pathway has also been demonstrated in *Drosophila* ESCRT mutants (Herz *et al.,* 2006). This pathway is similar to the intrinsic (or mitochondrial) pathway of apoptosis in vertebrates and Diap1, Dronc and Ark are homologues of vertebrate inhibitor of apoptosis proteins (IAPs), initiator caspase-9 and APAF-1, respectively (Oberst *et al.,* 2008; Steller, 2008). The intrinsic pathway is extremely important for regulation of cell death in mammalian cells (Kroemer *et al.,* 2007; Martinou and Youle, 2001) and therefore it would be of interest to determine whether this pathway plays a role in the apoptosis of ESCRT-I depleted Caco-2 cells. Mitochondrial outer membrane permeabilisation (MOMP) could be investigated as this is often

considered to be the point-of-no-return for the intrinsic pathway of apoptosis as well as other models of programmed cell death (Galluzzi *et al.,* 2007).

In addition, Hippo signalling has been suggested to control the overall apoptotic response in *Drosophila* ESCRT mutants (Herz *et al.,* 2006; Vaccari and Bilder, 2009). Therefore, this pathway may also be activated in ESCRT depleted Caco-2 cells and it would be interesting to investigate this further in future studies. In addition to cell death, Hippo signalling is important for a wide range of cellular processes including cell proliferation and polarity (Genevet and Tapon, 2011; Halder and Johnson, 2011). Therefore, this represents a potential mechanism to link the apoptotic, proliferative and polarity defects observed upon disruption of the ESCRT machinery in epithelial cells (Vaccari and Bilder, 2009).

Alternatively, apoptosis of Caco-2 cells may be induced by loss of cellular contacts. Caspase-3 activation was only detected in multilayered areas of Tsg101 knockdown cells where cell-cell adhesion and cellular contact with the extracellular matrix (ECM) may be perturbed. Loss of or inappropriate cell adhesion can induce a specific type of apoptosis termed anoikis (Gilmore, 2005; Chiarugi and Giannoni, 2008). ECM receptors of the integrin family play an important role in the process of anoikis. Not only do they provide a physical attachment to the ECM but they also activate several pro-survival signalling pathways (Gilmore, 2005; Chiarugi and Giannoni, 2008). In addition, growth factor receptors and cadherin-mediated cell-cell contacts also promote cell survival (Chiarugi and Giannoni, 2008). Lack of ECM or cell-cell contacts removes pro-survival signalling activation thereby inducing anoikis. Anoikis can be triggered by both the intrinsic apoptotic pathway and the extrinsic apoptotic pathway, involving activation of cell surface death receptors, such as the Fas receptor. Both pathways eventually converge with the activation of caspase-3, initiating a proteolytic cascade key to the apoptotic process (Gilmore, 2005; Chiarugi and Giannoni, 2008). Inhibition of anoikis is often observed in malignant cancers. Epithelial cells which acquire resistance to anoikis are able to survive after detachment from their primary site and metastasise to a secondary location (Simpson *et al.,* 2008; Coates *et al.,* 2010).

Therefore, it would be interesting to investigate whether cell death observed after ESCRT-I depletion in Caco-2 cells represents activation of the anoikis pathway. ESCRT proteins have been implicated in the regulation of integrins (Lobert *et al.,* 2010) and therefore Tsg101 depletion may affect integrin levels in Caco-2 cells resulting in destabilisation of cell-ECM contacts. Initially, this may allow cells to detach from the ECM and migrate out of the epithelial monolayer, resulting in the formation of a multilayered epithelial sheet. However, detachment of cells may also induce cell death via anoikis which may account for the increase in caspase-3 activation observed in multilayered regions of Tsg101 knockdown cells. Alternatively, ESCRT depletion may cause multilayering of Caco-2 cells via a separate mechanism and in turn, these multilayered cells could then activate anoikis. Therefore, it is also possible that cell death is an indirect effect of ESCRT-I depletion.

### 5.3.3. Inhibition of apoptosis may enhance the tumourigenic potential of ESCRT-I

After extended culture of Tsg101 depleted Caco-2 cells, an increase in apoptosis results in cell number returning to a similar level as control. In addition, multilayering is reduced as the majority of cell death occurs in the multilayered areas of the epithelial sheet. However, initial results demonstrate that inhibition of caspases increases the number of ESCRT-I depleted Caco-2 cells after 10 days culture. Furthermore, organisation of the epithelial sheet was extensively disrupted and multilayering of cells was enhanced. This supports previous work in *Drosophila* which demonstrates that inhibition of apoptosis causes dramatic overgrowth of ESCRT mutant cells to form tumourous growths capable of metastasis (Thompson *et al.,* 2005; Herz *et al.,* 2006; Rodahl *et al.,* 2009b). Although these experiments must be repeated to ensure the results are reproducible, it can be speculated that inhibition of apoptosis enhances the tumourigenic potential of ESCRT-I depletion in mammalian epithelial cells. Activation of caspases is a critical step in the apoptotic pathway, however, there are upstream events which may still occur, such as MOMP, and could result in caspase-independent apoptosis or other types of cell death such as necrosis (Dussmann *et al.,* 2003). Therefore, it is possible that ESCRT depleted cells will eventually still die by another mechanism. This could be analysed further using

a general marker of cell viability such as propidium iodide. It would also be interesting to investigate whether Tsg101 knockdown increases the invasiveness of Caco-2 cells and if caspase inhibition enhanced this behaviour. This would provide further support for a tumour suppressor role of ESCRT-I.

## 5.4. Conclusion

This study demonstrates that ESCRT-I depletion results in overproliferation of Caco-2 epithelial cells. Together with my previous data this highlights a role for ESCRT-I in regulation of epithelial cell proliferation and polarity, supporting previous observations in *Drosophila* (Vaccari and Bilder, 2009). Loss of cell polarity and self-sufficiency in growth signalling are two important hallmarks of cancer (Hanahan and Weinberg, 2011) and, therefore, ESCRT-I may function as a tumour suppressor in mammalian epithelial tissues. However, ESCRT-I depleted Caco-2 cells are eventually eliminated via apoptosis, although it is currently unclear whether this is a direct effect of Tsg101 knockdown. This suggests that the full tumourigenic potential of ESCRT proteins may not be exerted unless further alterations occur to allow epithelial cells to evade apoptosis. Considering the multi-step process of tumourigenesis this is a substantial possibility, especially as apoptosis is often inhibited in many human cancers (Lowe *et al.,* 2004; Cotter, 2009; Hanahan and Weinberg, 2011).

# CHAPTER SIX

# 6. FINAL DISCUSSION

## 6.1. ESCRTs and Maintenance of Epithelial Cell Polarity

### 6.1.1. ESCRT-I is required for epithelial organisation and polarity

Since ESCRT proteins were classified as tumour suppressors in *Drosophila*, much effort has been made to elucidate the crucial role of the ESCRT machinery within the maintenance of epithelial tissue architecture in this species. Disruption of the ESCRT machinery in *Drosophila* results in loss of epithelial cell polarity and overproliferation, two hallmarks of cancer (Vaccari and Bilder, 2009; Hanahan and Weinberg, 2011). This phenotype is attributed to a disruption in the trafficking of various proteins important for the regulation of polarity and growth in epithelial tissues.

In vertebrates, ESCRTs are well characterised for their role within the endocytic pathway (Raiborg and Stenmark, 2009). Their importance within the regulation of receptor signalling pathways has been demonstrated and alterations in the expression of various ESCRT components have been observed in human cancers (Stuffers *et al.,* 2009a; Wegner *et al.,* 2011). However, a definitive link between the ESCRT proteins, mammalian epithelial cell polarity and tumourigenesis has not been investigated.

This thesis demonstrates for the first time that the ESCRT-I component, Tsg101 is required for the maintenance of mammalian epithelial cell polarity and organisation (Figure 6.1). Depletion of Tsg101 results in an aberrant epithelial phenotype with cells displaying impaired cell-cell junctions, reduced differentiation and enhanced migratory ability. In addition, in some regions of the epithelial sheet organisation and polarity are lost and cell proliferation is increased. Overall, these results suggest that the function of ESCRT-I as a tumour suppressor is conserved from *Drosophila* to vertebrates.

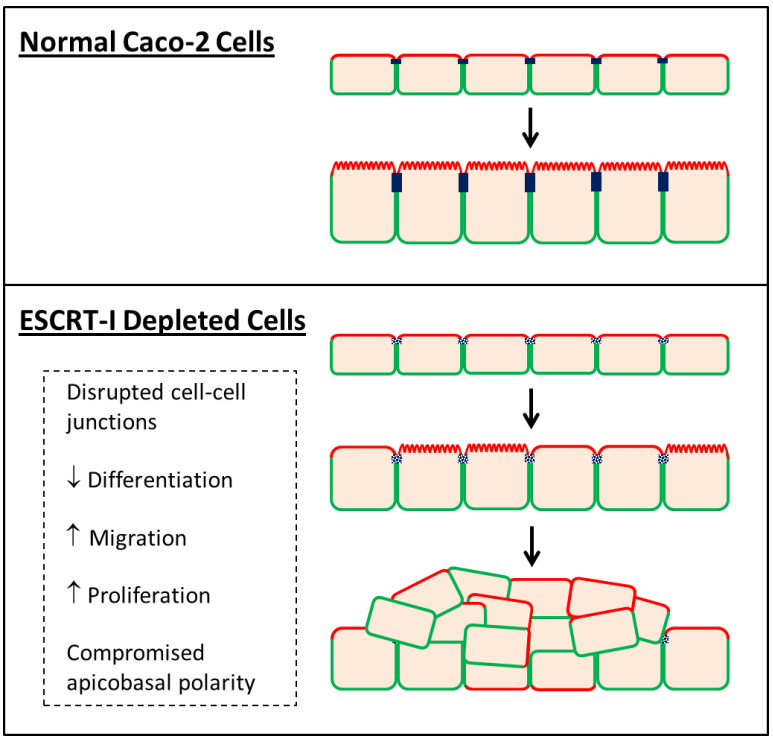


***Figure 6.1* Tsg101 is required for maintenance of mammalian epithelial cell polarity and organisation.** Caco-2 cells form a polarised epithelial monolayer with cell-cell junctions (blue) and distinct apical (red) and basolateral (green) membrane domains. When cells reach confluency differentiation occurs whereby junctions mature, lateral height increases and a brush border forms at the apical membrane. When Tsg101 is depleted via siRNA knockdown, Caco-2 cells initially maintain apicobasal polarity however cell-cell junctions are disrupted and migratory ability is enhanced. In addition, Tsg101 depletion inhibits differentiation so lateral height and brush border formation are reduced. In some areas, Tsg101 depleted cells overproliferate and lose epithelial polarity and organisation forming a multilayered epithelial sheet with compromised apicobasal polarity.

Loss of epithelial cell polarity and organisation following Tsg101 depletion demonstrated in chapter three of this thesis can be attributed to at least three possible mechanisms, discussed in detail below (Figure 6.2). Tsg101 depletion may perturb trafficking of proteins important for the maintenance of cell polarity, resulting in loss of polarised epithelial morphology and organisation. Alternatively, cellular overproliferation or destabilisation of cell-ECM contacts could disrupt organisation of the epithelial sheet and consequently polarised morphology is lost. It is currently unclear whether loss of epithelial cell polarity precedes loss of epithelial organisation or vice versa. It is also possible that these events occur simultaneously and therefore, a combination of the mechanisms detailed below may account for the effects of ESCRT depletion on epithelial morphology.

***Figure 6.2*** **Three possible mechanisms for loss for epithelial cell polarity and organisation following ESCRT-I depletion in Caco-2 cells. (A)** Maintenance of a polarised epithelium is a tightly regulated process. Localisation of various polarity complexes and formation of cell-cell junctions is crucial for establishment and maintenance of epithelial cell polarity. Protein trafficking appears to play an important role in this process and at least two tight junction components, claudin-1 and occludin, are constitutively endocytosed and recycled back to the plasma membrane in Caco-2 cells. In addition, lysosomal degradation may be important for maintenance of polarity. Epithelial cell proliferation is controlled through regulation of mitogenic signalling and contact inhibition. Lastly, cellular contacts with the ECM are required to retain a polarised epithelial monolayer. **(B)** ESCRT-I depletion results in the loss of epithelial polarity and organisation in Caco-2 cells. This may be attributed to at least three mechanisms. (i) Disrupted trafficking of proteins important for maintenance of polarity. ESCRT-I is required for localisation of claudin-1 and -4 to tight junctions. Trafficking of other junctional components and polarity complexes may also be affected by ESCRT-I depletion. (ii) Increased cell proliferation. ESCRT depletion may increase mitogenic signalling and inhibit contact inhibition. (iii) Loss of cell-ECM adhesion. ESCRT depletion may destabilise cellular contacts with the ECM. One or a combination of all three of these mechanisms could disrupt cell-cell adhesion, apicobasal polarity and signalling resulting in the aberrant epithelial phenotype associated with ESCRT-I depletion.

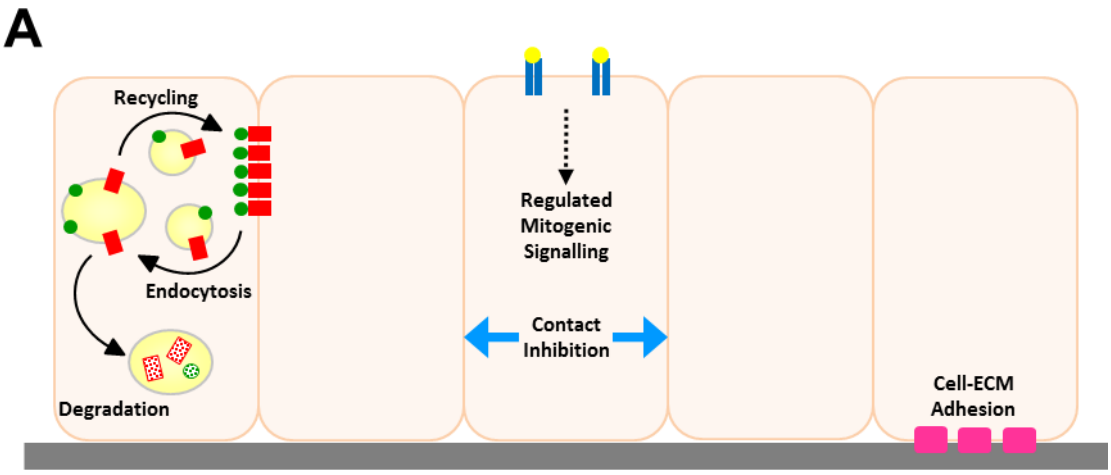


Polarised Epithelial Monolayer

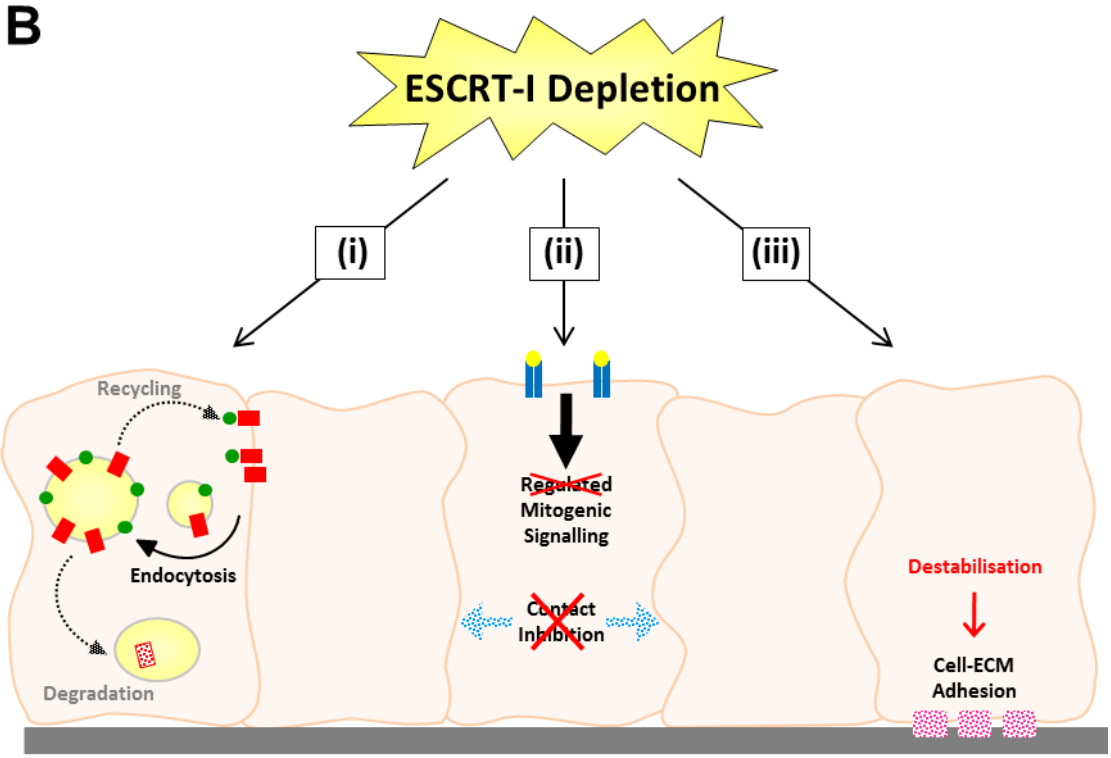


***Loss of Epithelial Polarity and Organisation***

### *(i) ESCRT-I depletion affects trafficking of proteins important for maintenance of epithelial cell polarity*

Cell-cell junctions are important to retain a polarised epithelium, functioning to maintain apicobasal polarity and cell-cell adhesion (Shin *et al.,* 2006; Bryant and Mostov, 2008; Coradini *et al.,* 2011). In addition, it is becoming increasingly apparent that cell-cell junctions function as a platform for many regulatory and signalling proteins important for establishing the epithelial phenotype (Ivanov *et al.,* 2005). Chapter four of this thesis demonstrates that the localisation of claudin-1 and -4 to tight junctions is dependent on ESCRT-I. Depletion of Tsg101 results in an intracellular accumulation of claudin-1 and -4 and is thought to be due to a block in the recycling of these junctional components back to the plasma membrane.

Mislocalisation of claudin-1 and -4 alone is unlikely to explain the loss of polarity phenotype as claudin-1 knockout mice have an epidermal defect but do not appear to display a large scale loss of epithelial polarity (Furuse *et al.,* 2002). However, epithelial cells contain many junctional proteins and it is possible that ESCRT function is required for their recycling. In addition, as ESCRTs are known to be important for endo-lysosomal trafficking, perturbations in the degradation of junction proteins may also affect cell-cell junction integrity. Destabilisation of cell-cell junctions could affect apicobasal polarity, cell-cell adhesion and signalling, all of which may contribute to the loss of epithelial cell polarity following Tsg101 depletion. Therefore, thorough analysis of the endosomal trafficking of additional junctional components should be conducted in the future using the biotinylation endocytosis and recycling assay. The effect of Tsg101 knockdown on these cell-cell junction proteins could then also be investigated.

Localisation of various polarity complexes is also crucial for establishment and maintenance of epithelial cell polarity (Gibson and Perrimon, 2003; Suzuki and Ohno, 2006; Bryant and Mostov, 2008). In *Drosophila*, ESCRT function is required for the correct localisation of Crb, which is important for apical membrane identity (Moberg *et al.,* 2005; Gilbert *et al.,* 2009). Therefore, ESCRTs may also be required for the trafficking of polarity complexes in mammalian epithelial cells and disruption in these trafficking pathways may

contribute to the loss of polarity phenotype in Tsg101 depleted cells. It would be of interest to investigate the effect of Tsg101 knockdown on the localisation of CRB3, the mammalian homologue of Crb, in Caco-2 cells. This could be analysed in the first instance using confocal fluorescence microscopy. However, in *Drosophila* ESCRT mutant cells, Crb is mislocalised from the apical membrane to a sub-apical compartment (Moberg *et al.,* 2005; Gilbert *et al.,* 2009). This may be difficult to determine using fluorescence microscopy, especially within multilayered regions of Tsg101 depleted cells, and therefore immuno-electron microscopy could also be used to identify any small changes in CRB3 localisation.

***(ii) ESCRT-I depletion causes overproliferation of epithelial cells***

Overproliferation may cause cells to stack up on top of one another, disrupting organisation of the epithelial monolayer and consequently perturbing apicobasal polarity. Chapter five of this thesis begins to investigate this, demonstrating that Tsg101 depleted cells overproliferate to form multilayered regions of the epithelial sheet which display compromised apicobasal polarity.

There are at least two possible mechanisms to explain this overproliferation. Firstly, it may be due to an increase in mitogenic signalling. The ESCRT machinery has been identified as important for attenuation of receptor-mediated signalling and so ESCRT depletion may result in sustained mitogenic signalling and consequently cell proliferation may increase (Wegner *et al.,* 2011). One signalling pathway which is enhanced in *Drosophila* ESCRT mutants is the EGFR pathway (Jekely and Rorth, 2003; Lloyd *et al.,* 2006; Vaccari *et al.,* 2009). Reduced EGFR degradation and sustained signalling in response to EGF has also been demonstrated in cultured mammalian cells deficient in ESCRT function (Bache *et al.,* 2006; Malerod *et al.,* 2007; Raiborg *et al.,* 2008). However, my results indicate that Tsg101 is not required for EGF degradation or attenuation of ERK signalling upon EGF treatment in polarised Caco-2 cells (Chapter 3). In addition, no alterations in constitutive ERK1/2 activation were observed 7 days after Tsg101 knockdown (Chapter 5). This suggests that overproliferation of Tsg101 depleted Caco-2 cells may not be due to a significant increase in the EGFR signalling pathway. To confirm this ERK1/2 activation should be analysed at additional timepoints, using both

immunofluorescence microscopy and immunoblotting. In addition, protein levels and localisation of EGFR could also be investigated in order to establish whether Tsg101 knockdown affects trafficking of this receptor in Caco-2 cells.

Another mitogenic signalling pathway which is deregulated in *Drosophila* ESCRT mutants is Notch signalling. Endosomal accumulation of Notch in ESCRT mutant cells results in increased Notch activation (Thompson *et al.,* 2005; Vaccari and Bilder, 2005; Herz *et al.,* 2006; Vaccari *et al.,* 2008; Herz *et al.,* 2009; Vaccari *et al.,* 2009). This has been shown to induce overproliferation in a non-cell autonomous manner via ectopic production of the secreted growth factor Upd and paracrine activation of the Jak-STAT signalling pathway (Thompson *et al.,* 2005; Vaccari and Bilder, 2005; Herz *et al.,* 2006; Herz *et al.,* 2009; Gilbert *et al.,* 2009; Vaccari *et al.,* 2009). Whether Notch accumulation is also responsible for the cell-autonomous overproliferation observed in *Drosophila* ESCRT mutants remains to be established. Therefore, it would be of interest to establish whether the Notch signalling pathway is affected by Tsg101 depletion in Caco-2 cells. Notch protein levels and localisation could be analysed using immunoblotting and immunofluorescence microscopy, respectively. Notch activity could be investigated by analysing downstream effectors of the Notch signalling pathway, such as activation of Jak-STAT signalling. In addition, a Notch inhibitor could be applied to ESCRT depleted cells in order to investigate whether this stops the formation of multilayered regions.

Alternatively, overproliferation of ESCRT-I depleted Caco-2 cells may be due to a loss of contact inhibition. Usually upon reaching confluency, Caco-2 cell proliferation will reduce as a result of contact inhibition and cells will begin to differentiate (Nelson and Daniel, 2002; Volpe, 2008). It is possible that ESCRT-I depletion inhibits contact inhibition and, as a result, cells continue proliferating for an extended period of time. This is supported by studies in *Drosophila* demonstrating that when epithelial tissues are predominantly mutant for ESCRT components, cells lose polarity, fail to differentiate and overgrow to form large masses lacking normal epithelial morphology. Interestingly, this overgrowth is thought to be due to an extended period of proliferation rather than an increased growth rate although the mechanism responsible for this is currently

unknown (Moberg *et al.,* 2005; Vaccari and Bilder, 2005; Herz *et al.,* 2009; Vaccari *et al.,* 2009).

In line with this, my results demonstrate that differentiation of Caco-2 cells is reduced upon Tsg101 depletion (Chapter 3). Therefore, this may suggest that Tsg101 depleted cells cannot sense their environment correctly and continue to divide instead of initiating the differentiation process. It is possible that ESCRT-I may be required for trafficking of proteins important for regulation of the contact inhibition process, such as components of the Hippo signalling pathway (Zeng and Hong, 2008). Indeed, Hippo signalling is deregulated in *Drosophila* Vps25 mutants (Herz *et al.,* 2006) suggesting that ESCRTs are important for regulation of this pathway. Therefore if, and how, ESCRT proteins regulate contact inhibition are questions worth considering for the future.

***(iii) ESCRT-I depletion destabilises cellular contacts with the ECM***

Destabilisation of cellular contacts with the ECM can result in loss of basal adhesion. Consequently, cells may detach and lose epithelial organisation and polarity. The main components of cellular adhesions to the ECM are the cell surface transmembrane integrin receptors (Bosman *et al.,* 1993; Matlin *et al.,* 2003; Lobert *et al.,* 2010). Integrins regulate many aspects of cell behaviour and, in epithelial cells, are important for the maintenance of apicobasal polarity (Eaton and Simons, 1995; Matlin *et al.,* 2003). A role for ESCRT proteins in the regulation of integrins has been recently suggested in fibroblasts (Lobert *et al.,* 2010). It is possible that ESCRT proteins function to regulate integrins in epithelial cells and therefore, the effect of Tsg101 depletion on integrin expression and localisation warrants further investigation.

### 6.1.2. Importance of other ESCRT proteins

This thesis reveals a requirement for Tsg101, an ESCRT-I component, within the maintenance of mammalian epithelial organisation and polarity. This study also investigated the role of the ESCRT-II component, Vps25, and results demonstrate that epithelial organisation and polarity are not perturbed in 2D cultures. However, depletion of Vps25 significantly reduced formation of polarised 3D epithelial cysts suggesting that Vps25 may also be important for

epithelial polarisation. Incidences whereby defects in epithelial cell polarity were only apparent upon growth of cells in 3D cultures have also been observed in other studies (Roh *et al.,* 2003; Martin-Belmonte *et al.,* 2007; Torkko *et al.,* 2008), suggesting that 3D cell cultures may provide a more sensitive assay for detecting defects in epithelial cell polarity. Epithelial cyst formation is often considered to be a more physiologically relevant method of investigating epithelial cell polarity *in vitro* (Martin-Belmonte and Mostov, 2008) and therefore this highlights the necessity to utilise a variety of methods to fully characterise a knockdown phenotype in polarised epithelial cells. The level of Vps25 knockdown may also affect the severity of the phenotype observed in 2D cell cultures. Therefore, it would be of interest to try and increase efficiency of Vps25 knockdown and determine whether this results in a stronger loss of polarity phenotype.

In the future it would also be important to extend this investigation in order to analyse the role of other components of the ESCRT machinery. The effect of siRNA knockdown of ESCRT-0, -I, -II and -III proteins on mammalian epithelial cell polarity could be investigated, using both 2D and 3D cell culture systems. Reduced expression of the ESCRT-I component, Vps37A, and ESCRT-III component, CHMP1A, have been associated with human tumours (Xu *et al.,* 2003; Bache *et al.,* 2004; Li *et al.,* 2008). Therefore, it would be interesting to begin by investigating how siRNA knockdown of these proteins affects Caco-2 epithelial cell polarity. In addition, the ESCRT-I protein, Vps28, ESCRT-II proteins, Vps22 and Vps36, and ESCRT-III proteins, Vps20 (CHMP6), Vps32 (CHMP4), Vps2 (CHMP2), have been identified as important for regulation of epithelial cell polarity in *Drosophila* (Herz *et al.,* 2009; Vaccari *et al.,* 2009). Therefore, thorough analysis of other ESCRT components would expand our knowledge on the importance of the ESCRT machinery within the maintenance of mammalian epithelial cell polarity.

## 6.2. ESCRTs: Tumour Suppressors in Vertebrates?

Results presented in this thesis demonstrate that ESCRT-I is required for the maintenance of epithelial cell polarity and organisation in both 2D and 3D mammalian cell culture models. In addition, regulation of epithelial cell

proliferation is dependent on ESCRT-I function. This phenotype is extremely similar to that observed in *Drosophila* (reviewed in Vaccari and Bilder, 2009) and suggests that ESCRT-I acts as a tumour suppressor in mammalian epithelial tissues. Loss of epithelial polarity and self-sufficiency in growth signalling are two important hallmarks of human cancers. In addition to this, my results also demonstrate that loss of ESCRT-I function results in reduced cellular differentiation and enhanced migratory ability, characteristics often attributed to tumourigenic cells (Hanahan and Weinberg, 2011).

Links between ESCRT proteins and human cancers have been documented previously with aberrant *Tsg101* transcripts observed in various tumours including breast (Lee and Feinberg, 1997), cervical (O'Boyle *et al.,* 1999) and small cell lung cancer (Oh *et al.,* 1998). In addition, reduced expression of Tsg101 (Bennett *et al.,* 2001), Vps37A (Xu *et al.,* 2003; Bache *et al.,* 2004) and CHMP1A (Li *et al.,* 2008) has been associated with various human tumours. In the future it would be interesting to investigate expression levels of ESCRT proteins in different human tumour samples. This would provide more clinical relevance for the involvement of ESCRTs in carcinogenesis. It is also important to note that overexpression of ESCRTs has been associated with various human cancers (Liu *et al.,* 2002; Oh *et al.,* 2007; Toyoshima *et al.,* 2007; Young *et al.,* 2007). This implies that ESCRT proteins can also exhibit oncogenic properties, although it has also been suggested that overexpressed protein may be acting as a dominant negative (Vaccari *et al.,* 2009). The effect of ESCRT protein overexpression on epithelial cell organisation and polarity may therefore be worth considering in the future.

Importantly, this study also demonstrates that ESCRT depleted cells are more susceptible to cell death via apoptosis. Inhibition of this apoptotic response enhances the aberrant epithelial phenotype, as demonstrated by my preliminary results (Chapter 5) and those conducted in *Drosophila* (Thompson *et al.,* 2005; Herz *et al.,* 2006; Rodahl *et al.,* 2009b). Therefore, it seems that the ability to evade apoptosis is an important factor in determining the tumourigenic potential of ESCRT protein depletion. It is possible that disruption of the ESCRT machinery will only result in tumour formation when cell death is inhibited. Tumourigenesis is a multi-step process and there is mounting evidence that

apoptosis is blocked in most human cancers (Hanahan and Weinberg, 2000; Lowe *et al.,* 2004; Cotter, 2009; Hanahan and Weinberg, 2011). Therefore, the possibility of epithelial cells acquiring the ability to evade cell death in addition to loss of ESCRT function is feasible.

In conclusion, this thesis along with previous data generated in the field, suggests that ESCRT proteins are important tumour suppressors, a role which is conserved from *Drosophila* to vertebrates.

# CHAPTER SEVEN

# 7. REFERENCES


Adachi-Yamada, T., and O'Connor, M.B. (2002). Morphogenetic apoptosis: a mechanism for correcting discontinuities in morphogen gradients. Dev Biol *251*, 74-90.

Aggarwal, S., Suzuki, T., Taylor, W.L., Bhargava, A., and Rao, R.K. (2011). Contrasting effects of ERK on tight junction integrity in differentiated and under-differentiated Caco-2 cell monolayers. Biochem J *433*, 51-63.

Aijaz, S., D'Atri, F., Citi, S., Balda, M.S., and Matter, K. (2005). Binding of GEF-H1 to the tight junction-associated adaptor cingulin results in inhibition of Rho signaling and G1/S phase transition. Dev Cell *8*, 777-786.

Amasheh, S., Meiri, N., Gitter, A.H., Schoneberg, T., Mankertz, J., Schulzke, J.D., and Fromm, M. (2002). Claudin-2 expression induces cation-selective channels in tight junctions of epithelial cells. J Cell Sci *115*, 4969-4976.

Apodaca, G., Katz, L.A., and Mostov, K.E. (1994). Receptor-mediated transcytosis of IgA in MDCK cells is via apical recycling endosomes. J Cell Biol *125*, 67-86.

Assemat, E., Bazellieres, E., Pallesi-Pocachard, E., Le Bivic, A., and Massey-Harroche, D. (2008). Polarity complex proteins. Biochim Biophys Acta *1778*, 614-630.

Babst, M. (2005). A protein's final ESCRT. Traffic *6*, 2-9.

Bache, K.G., Brech, A., Mehlum, A., and Stenmark, H. (2003). Hrs regulates multivesicular body formation via ESCRT recruitment to endosomes. J Cell Biol *162*, 435-442.

Bache, K.G., Slagsvold, T., Cabezas, A., Rosendal, K.R., Raiborg, C., and Stenmark, H. (2004). The growth-regulatory protein HCRP1/hVps37A is a subunit of mammalian ESCRT-I and mediates receptor down-regulation. Mol Biol Cell *15*, 4337-4346.

Bache, K.G., Stuffers, S., Malerod, L., Slagsvold, T., Raiborg, C., Lechardeur, D., Walchli, S., Lukacs, G.L., Brech, A., and Stenmark, H. (2006). The ESCRT-III subunit hVps24 is required for degradation but not silencing of the epidermal growth factor receptor. Mol Biol Cell *17*, 2513-2523.

Balda, M.S., Garrett, M.D., and Matter, K. (2003). The ZO-1-associated Y-box factor ZONAB regulates epithelial cell proliferation and cell density. J Cell Biol *160*, 423-432.

Balda, M.S., and Matter, K. (2008). Tight junctions at a glance. J Cell Sci *121*, 3677-3682.

Balda, M.S., Whitney, J.A., Flores, C., Gonzalez, S., Cereijido, M., and Matter, K. (1996). Functional dissociation of paracellular permeability and transepithelial electrical resistance and disruption of the apical-basolateral intramembrane diffusion barrier by expression of a mutant tight junction membrane protein. J Cell Biol *134*, 1031-1049.

Baldys, A., and Raymond, J.R. (2009). Critical role of ESCRT machinery in EGFR recycling. Biochemistry *48*, 9321-9323.

Barczyk, M., Carracedo, S., and Gullberg, D. (2010). Integrins. Cell Tissue Res *339*, 269-280.

Baricault, L., Fransen, J.A., Garcia, M., Sapin, C., Codogno, P., Ginsel, L.A., and Trugnan, G. (1995). Rapid sequestration of DPP IV/CD26 and other cell surface proteins in an autophagic-like compartment in Caco-2 cells treated with forskolin. J Cell Sci *108 ( Pt 5)*, 2109-2121.

Barr, F.A., and Gruneberg, U. (2007). Cytokinesis: placing and making the final cut. Cell *131*, 847-860.

Bazzoni, G., Martinez-Estrada, O.M., Orsenigo, F., Cordenonsi, M., Citi, S., and Dejana, E. (2000). Interaction of junctional adhesion molecule with the tight junction components ZO-1, cingulin, and occludin. J Biol Chem *275*, 20520-20526.

Bennett, N.A., Pattillo, R.A., Lin, R.S., Hsieh, C.Y., Murphy, T., and Lyn, D. (2001). TSG101 expression in gynecological tumors: relationship to cyclin D1, cyclin E, p53 and p16 proteins. Cell Mol Biol (Noisy-le-grand) *47*, 1187-1193.

Ben-Yosef, T., Belyantseva, I.A., Saunders, T.L., Hughes, E.D., Kawamoto, K., Van Itallie, C.M., Beyer, L.A., Halsey, K., Gardner, D.J., Wilcox, E.R., Rasmussen, J., Anderson, J.M., Dolan, D.F., Forge, A., Raphael, Y., Camper, S.A., and Friedman, T.B. (2003). Claudin 14 knockout mice, a model for autosomal recessive deafness DFNB29, are deaf due to cochlear hair cell degeneration. Hum Mol Genet *12*, 2049-2061.

Berlin, I., Schwartz, H., and Nash, P.D. (2010). Regulation of epidermal growth factor receptor ubiquitination and trafficking by the USP8.STAM complex. J Biol Chem *285*, 34909-34921.

Bilder, D. (2004). Epithelial polarity and proliferation control: links from the Drosophila neoplastic tumor suppressors. Genes Dev *18*, 1909-1925.

Bilder, D., and Perrimon, N. (2000). Localization of apical epithelial determinants by the basolateral PDZ protein Scribble. Nature *403*, 676-680.

Bilder, D., Schober, M., and Perrimon, N. (2003). Integrated activity of PDZ protein complexes regulates epithelial polarity. Nat Cell Biol *5*, 53-58.

Bishop, N., Horman, A., and Woodman, P. (2002). Mammalian class E vps proteins recognize ubiquitin and act in the removal of endosomal protein-ubiquitin conjugates. J Cell Biol *157*, 91-101.

Bode, A.M., and Dong, Z. (2007). The functional contrariety of JNK. Mol Carcinog *46*, 591-598.

Bonne, S., Gilbert, B., Hatzfeld, M., Chen, X., Green, K.J., and van Roy, F. (2003). Defining desmosomal plakophilin-3 interactions. J Cell Biol *161*, 403-416.

Bosman, F.T., de Bruine, A., Flohil, C., van der Wurff, A., ten Kate, J., and Dinjens, W.W. (1993). Epithelial-stromal interactions in colon cancer. Int J Dev Biol *37*, 203-211.

Bowers, K., Piper, S.C., Edeling, M.A., Gray, S.R., Owen, D.J., Lehner, P.J., and Luzio, J.P. (2006). Degradation of endocytosed epidermal growth factor and virally ubiquitinated major histocompatibility complex class I is independent of mammalian ESCRTII. J Biol Chem *281*, 5094-5105.

Brennan, K., Offiah, G., McSherry, E.A., and Hopkins, A.M. (2010). Tight junctions: a barrier to the initiation and progression of breast cancer? J Biomed Biotechnol *2010*, 460607.

Brown, P.S., Wang, E., Aroeti, B., Chapin, S.J., Mostov, K.E., and Dunn, K.W. (2000). Definition of distinct compartments in polarized Madin-Darby canine kidney (MDCK) cells for membrane-volume sorting, polarized sorting and apical recycling. Traffic *1*, 124-140.

Bryant, D.M., Datta, A., Rodriguez-Fraticelli, A.E., Peranen, J., Martin-Belmonte, F., and Mostov, K.E. (2010). A molecular network for de novo generation of the apical surface and lumen. Nat Cell Biol *12*, 1035-1045.

Bryant, D.M., and Mostov, K.E. (2008). From cells to organs: building polarized tissue. Nat Rev Mol Cell Biol *9*, 887-901.

Bryant, D.M., and Stow, J.L. (2004). The ins and outs of E-cadherin trafficking. Trends Cell Biol *14*, 427-434.

Busch, C., Hanssen, T.A., Wagener, C., and B, O.B. (2002). Down-regulation of CEACAM1 in human prostate cancer: correlation with loss of cell polarity, increased proliferation rate, and Gleason grade 3 to 4 transition. Hum Pathol *33*, 290-298.

Carlton, J.G., and Martin-Serrano, J. (2007). Parallels between cytokinesis and retroviral budding: a role for the ESCRT machinery. Science *316*, 1908-1912.

Chalmers, A.D., Pambos, M., Mason, J., Lang, S., Wylie, C., and Papalopulu, N. (2005). aPKC, Crumbs3 and Lgl2 control apicobasal polarity in early vertebrate development. Development *132*, 977-986.

Chan, S.W., Lim, C.J., Chen, L., Chong, Y.F., Huang, C., Song, H., and Hong, W. (2011). The Hippo pathway in biological control and cancer development. J Cell Physiol *226*, 928-939.

Chantret, I., Barbat, A., Dussaulx, E., Brattain, M.G., and Zweibaum, A. (1988). Epithelial polarity, villin expression, and enterocytic differentiation of cultured human colon carcinoma cells: a survey of twenty cell lines. Cancer Res *48*, 1936-1942.

Chanut-Delalande, H., Jung, A.C., Baer, M.M., Lin, L., Payre, F., and Affolter, M. (2010). The Hrs/Stam complex acts as a positive and negative regulator of RTK signaling during Drosophila development. PLoS One *5*, e10245.

Chao, Y.C., Pan, S.H., Yang, S.C., Yu, S.L., Che, T.F., Lin, C.W., Tsai, M.S., Chang, G.C., Wu, C.H., Wu, Y.Y., Lee, Y.C., Hong, T.M., and Yang, P.C. (2009). Claudin-1 is a metastasis suppressor and correlates with clinical outcome in lung adenocarcinoma. Am J Respir Crit Care Med *179*, 123-133.

Chen, B.J., and Lamb, R.A. (2008). Mechanisms for enveloped virus budding: can some viruses do without an ESCRT? Virology *372*, 221-232.

Chen, X., Bonne, S., Hatzfeld, M., van Roy, F., and Green, K.J. (2002). Protein binding and functional characterization of plakophilin 2. Evidence for its diverse roles in desmosomes and beta -catenin signaling. J Biol Chem *277*, 10512-10522.

Chiarugi, P., and Giannoni, E. (2008). Anoikis: a necessary death program for anchorage-dependent cells. Biochem Pharmacol *76*, 1352-1364.

Chiba, H., Osanai, M., Murata, M., Kojima, T., and Sawada, N. (2008). Transmembrane proteins of tight junctions. Biochim Biophys Acta *1778*, 588-600.

Citi, S., Sabanay, H., Kendrick-Jones, J., and Geiger, B. (1989). Cingulin: characterization and localization. J Cell Sci *93 ( Pt 1)*, 107-122.

Clague, M.J., and Urbe, S. (2006). Endocytosis: the DUB version. Trends Cell Biol *16*, 551-559.

Coates, J.M., Galante, J.M., and Bold, R.J. (2010). Cancer therapy beyond apoptosis: autophagy and anoikis as mechanisms of cell death. J Surg Res *164*, 301-308.

Coradini, D., Casarsa, C., and Oriana, S. (2011). Epithelial cell polarity and tumorigenesis: new perspectives for cancer detection and treatment. Acta Pharmacol Sin *32*, 552-564.

Cordenonsi, M., D'Atri, F., Hammar, E., Parry, D.A., Kendrick-Jones, J., Shore, D., and Citi, S. (1999). Cingulin contains globular and coiled-coil domains and interacts with ZO-1, ZO-2, ZO-3, and myosin. J Cell Biol *147*, 1569-1582.

Cotter, T.G. (2009). Apoptosis and cancer: the genesis of a research field. Nat Rev Cancer *9*, 501-507.

Cramm-Behrens, C.I., Dienst, M., and Jacob, R. (2008). Apical cargo traverses endosomal compartments on the passage to the cell surface. Traffic *9*, 2206-2220.

Cresawn, K.O., Potter, B.A., Oztan, A., Guerriero, C.J., Ihrke, G., Goldenring, J.R., Apodaca, G., and Weisz, O.A. (2007). Differential involvement of endocytic compartments in the biosynthetic traffic of apical proteins. EMBO J *26*, 3737-3748.

D'Atri, F., and Citi, S. (2001). Cingulin interacts with F-actin in vitro. FEBS Lett *507*, 21-24.

D'Atri, F., Nadalutti, F., and Citi, S. (2002). Evidence for a functional interaction between cingulin and ZO-1 in cultured cells. J Biol Chem *277*, 27757-27764.

Davis, R.J. (2000). Signal transduction by the JNK group of MAP kinases. Cell *103*, 239-252.

De Luca, A., Carotenuto, A., Rachiglio, A., Gallo, M., Maiello, M.R., Aldinucci, D., Pinto, A., and Normanno, N. (2008). The role of the EGFR signaling in tumor microenvironment. J Cell Physiol *214*, 559-567.

Debnath, J., and Brugge, J.S. (2005). Modelling glandular epithelial cancers in three-dimensional cultures. Nat Rev Cancer *5*, 675-688.

Delva, E., Tucker, D.K., and Kowalczyk, A.P. (2009). The desmosome. Cold Spring Harb Perspect Biol *1*, a002543.

Dhawan, P., Singh, A.B., Deane, N.G., No, Y., Shiou, S.R., Schmidt, C., Neff, J., Washington, M.K., and Beauchamp, R.D. (2005). Claudin-1 regulates cellular transformation and metastatic behavior in colon cancer. J Clin Invest *115*, 1765-1776.

Dong, J., Feldmann, G., Huang, J., Wu, S., Zhang, N., Comerford, S.A., Gayyed, M.F., Anders, R.A., Maitra, A., and Pan, D. (2007). Elucidation of a universal size-control mechanism in Drosophila and mammals. Cell *130*, 1120-1133.

Doyotte, A., Russell, M.R., Hopkins, C.R., and Woodman, P.G. (2005). Depletion of TSG101 forms a mammalian "Class E" compartment: a multicisternal early endosome with multiple sorting defects. J Cell Sci *118*, 3003-3017.

Dukes, J.D., Fish, L., Richardson, J.D., Blaikley, E., Burns, S., Caunt, C.J., Chalmers, A.D., and Whitley, P. (2011). Functional ESCRT machinery is required for constitutive recycling of claudin-1 and maintenance of polarity in vertebrate epithelial cells. Mol Biol Cell *22*, 3192-3205.

Dukes, J.D., Richardson, J.D., Simmons, R., and Whitley, P. (2008). A dominant-negative ESCRT-III protein perturbs cytokinesis and trafficking to lysosomes. Biochem J *411*, 233-239.

Dussmann, H., Rehm, M., Kogel, D., and Prehn, J.H. (2003). Outer mitochondrial membrane permeabilization during apoptosis triggers caspase-independent mitochondrial and caspase-dependent plasma membrane potential depolarization: a single-cell analysis. J Cell Sci *116*, 525-536.

Eaton, S., and Simons, K. (1995). Apical, basal, and lateral cues for epithelial polarization. Cell *82*, 5-8.

Eder, A.M., Sui, X., Rosen, D.G., Nolden, L.K., Cheng, K.W., Lahad, J.P., Kango-Singh, M., Lu, K.H., Warneke, C.L., Atkinson, E.N., Bedrosian, I., Keyomarsi, K., Kuo, W.L., Gray, J.W., Yin, J.C., Liu, J., Halder, G., and Mills, G.B. (2005). Atypical PKCiota contributes to poor prognosis through loss of apical-basal polarity and cyclin E overexpression in ovarian cancer. Proc Natl Acad Sci U S A *102*, 12519-12524.

Egeblad, M., and Werb, Z. (2002). New functions for the matrix metalloproteinases in cancer progression. Nat Rev Cancer *2*, 161-174.

Engle, M.J., Goetz, G.S., and Alpers, D.H. (1998). Caco-2 cells express a combination of colonocyte and enterocyte phenotypes. J Cell Physiol *174*, 362-369.

Fader, C.M., and Colombo, M.I. (2009). Autophagy and multivesicular bodies: two closely related partners. Cell Death Differ *16*, 70-78.

Fallon, R.F., and Goodenough, D.A. (1981). Five-hour half-life of mouse liver gap-junction protein. J Cell Biol *90*, 521-526.

Farquhar, M.G., and Palade, G.E. (1963). Junctional complexes in various epithelia. J Cell Biol *17*, 375-412.

Farr, G.A., Hull, M., Mellman, I., and Caplan, M.J. (2009). Membrane proteins follow multiple pathways to the basolateral cell surface in polarized epithelial cells. J Cell Biol *186*, 269-282.

Feigin, M.E., and Muthuswamy, S.K. (2009). Polarity proteins regulate mammalian cell-cell junctions and cancer pathogenesis. Curr Opin Cell Biol *21*, 694-700.

Filimonenko, M., Stuffers, S., Raiborg, C., Yamamoto, A., Malerod, L., Fisher, E.M., Isaacs, A., Brech, A., Stenmark, H., and Simonsen, A. (2007). Functional multivesicular bodies are required for autophagic clearance of protein aggregates associated with neurodegenerative disease. J Cell Biol *179*, 485-500.

Folsch, H., Mattila, P.E., and Weisz, O.A. (2009). Taking the scenic route: biosynthetic traffic to the plasma membrane in polarized epithelial cells. Traffic *10*, 972-981.

Fujii, K., Hurley, J.H., and Freed, E.O. (2007). Beyond Tsg101: the role of Alix in 'ESCRTing' HIV-1. Nat Rev Microbiol *5*, 912-916.

Fujita, H., Yamanaka, M., Imamura, K., Tanaka, Y., Nara, A., Yoshimori, T., Yokota, S., and Himeno, M. (2003). A dominant negative form of the AAA ATPase SKD1/VPS4 impairs membrane trafficking out of endosomal/lysosomal compartments: class E vps phenotype in mammalian cells. J Cell Sci *116*, 401-414.

Furuse, M., Hata, M., Furuse, K., Yoshida, Y., Haratake, A., Sugitani, Y., Noda, T., Kubo, A., and Tsukita, S. (2002). Claudin-based tight junctions are crucial for the mammalian epidermal barrier: a lesson from claudin-1-deficient mice. J Cell Biol *156*, 1099-1111.

Furuse, M., Hirase, T., Itoh, M., Nagafuchi, A., Yonemura, S., and Tsukita, S. (1993). Occludin: a novel integral membrane protein localizing at tight junctions. J Cell Biol *123*, 1777-1788.

Futter, C.E., Gibson, A., Allchin, E.H., Maxwell, S., Ruddock, L.J., Odorizzi, G., Domingo, D., Trowbridge, I.S., and Hopkins, C.R. (1998). In polarized MDCK cells basolateral vesicles arise from clathrin-gamma-adaptin-coated domains on endosomal tubules. J Cell Biol *141*, 611-623.

Galluzzi, L., Zamzami, N., de La Motte Rouge, T., Lemaire, C., Brenner, C., and Kroemer, G. (2007). Methods for the assessment of mitochondrial membrane permeabilization in apoptosis. Apoptosis *12*, 803-813.

Gao, N., and Kaestner, K.H. (2010). Cdx2 regulates endo-lysosomal function and epithelial cell polarity. Genes Dev *24*, 1295-1305.

Garrus, J.E., von Schwedler, U.K., Pornillos, O.W., Morham, S.G., Zavitz, K.H., Wang, H.E., Wettstein, D.A., Stray, K.M., Cote, M., Rich, R.L., Myszka, D.G., and Sundquist, W.I. (2001). Tsg101 and the vacuolar protein sorting pathway are essential for HIV-1 budding. Cell *107*, 55-65.

Gassama-Diagne, A., Yu, W., ter Beest, M., Martin-Belmonte, F., Kierbel, A., Engel, J., and Mostov, K. (2006). Phosphatidylinositol-3,4,5-trisphosphate regulates the formation of the basolateral plasma membrane in epithelial cells. Nat Cell Biol *8*, 963-970.

Genevet, A., and Tapon, N. (2011). The Hippo pathway and apico-basal cell polarity. Biochem J *436*, 213-224.

Georgiadis, A., Tschernutter, M., Bainbridge, J.W., Balaggan, K.S., Mowat, F., West, E.L., Munro, P.M., Thrasher, A.J., Matter, K., Balda, M.S., and Ali, R.R. (2010). The tight junction associated signalling proteins ZO-1 and ZONAB regulate retinal pigment epithelium homeostasis in mice. PLoS One *5*, e15730.

Gibson, A., Futter, C.E., Maxwell, S., Allchin, E.H., Shipman, M., Kraehenbuhl, J.P., Domingo, D., Odorizzi, G., Trowbridge, I.S., and Hopkins, C.R. (1998). Sorting mechanisms regulating membrane protein traffic in the apical transcytotic pathway of polarized MDCK cells. J Cell Biol *143*, 81-94.

Gibson, M.C., and Perrimon, N. (2003). Apicobasal polarization: epithelial form and function. Curr Opin Cell Biol *15*, 747-752.

Gilbert, M.M., Beam, C.K., Robinson, B.S., and Moberg, K.H. (2009). Genetic interactions between the Drosophila tumor suppressor gene ept and the stat92E transcription factor. PLoS One *4*, e7083.

Gilmore, A.P. (2005). Anoikis. Cell Death Differ *12 Suppl 2*, 1473-1477.

Golachowska, M.R., Hoekstra, D., and van, I.S.C. (2010). Recycling endosomes in apical plasma membrane domain formation and epithelial cell polarity. Trends Cell Biol *20*, 618-626.

Gonzalez-Mariscal, L., Tapia, R., and Chamorro, D. (2008). Crosstalk of tight junction components with signaling pathways. Biochim Biophys Acta *1778*, 729-756.

Grabher, C., von Boehmer, H., and Look, A.T. (2006). Notch 1 activation in the molecular pathogenesis of T-cell acute lymphoblastic leukaemia. Nat Rev Cancer *6*, 347-359.

Grandal, M.V., and Madshus, I.H. (2008). Epidermal growth factor receptor and cancer: control of oncogenic signalling by endocytosis. J Cell Mol Med *12*, 1527-1534.

Grasset, E., Pinto, M., Dussaulx, E., Zweibaum, A., and Desjeux, J.F. (1984). Epithelial properties of human colonic carcinoma cell line Caco-2: electrical parameters. Am J Physiol *247*, C260-267.

Guillemot, L., and Citi, S. (2006). Cingulin regulates claudin-2 expression and cell proliferation through the small GTPase RhoA. Mol Biol Cell *17*, 3569-3577.

Guillemot, L., Hammar, E., Kaister, C., Ritz, J., Caille, D., Jond, L., Bauer, C., Meda, P., and Citi, S. (2004). Disruption of the cingulin gene does not prevent tight junction formation but alters gene expression. J Cell Sci *117*, 5245-5256.

Halder, G., and Johnson, R.L. (2011). Hippo signaling: growth control and beyond. Development *138*, 9-22.

Hanahan, D., and Weinberg, R.A. (2000). The hallmarks of cancer. Cell *100*, 57-70.

Hanahan, D., and Weinberg, R.A. (2011). Hallmarks of cancer: the next generation. Cell *144*, 646-674.

Hanson, P.I., Roth, R., Lin, Y., and Heuser, J.E. (2008). Plasma membrane deformation by circular arrays of ESCRT-III protein filaments. J Cell Biol *180*, 389-402.

Hariharan, I.K., and Bilder, D. (2006). Regulation of imaginal disc growth by tumor-suppressor genes in Drosophila. Annu Rev Genet *40*, 335-361.

Herz, H.M., and Bergmann, A. (2009). Genetic analysis of ESCRT function in Drosophila: a tumour model for human Tsg101. Biochem Soc Trans *37*, 204-207.

Herz, H.M., Chen, Z., Scherr, H., Lackey, M., Bolduc, C., and Bergmann, A. (2006). vps25 mosaics display non-autonomous cell survival and overgrowth, and autonomous apoptosis. Development *133*, 1871-1880.

Herz, H.M., Woodfield, S.E., Chen, Z., Bolduc, C., and Bergmann, A. (2009). Common and distinct genetic properties of ESCRT-II components in Drosophila. PLoS One *4*, e4165.

Hierro, A., Sun, J., Rusnak, A.S., Kim, J., Prag, G., Emr, S.D., and Hurley, J.H. (2004). Structure of the ESCRT-II endosomal trafficking complex. Nature *431*, 221-225.

Hoekstra, D., Tyteca, D., and van, I.S.C. (2004). The subapical compartment: a traffic center in membrane polarity development. J Cell Sci *117*, 2183-2192.

Horikoshi, Y., Suzuki, A., Yamanaka, T., Sasaki, K., Mizuno, K., Sawada, H., Yonemura, S., and Ohno, S. (2009). Interaction between PAR-3 and the aPKC-PAR-6 complex is indispensable for apical domain development of epithelial cells. J Cell Sci *122*, 1595-1606.

Hurley, J.H. (2008). ESCRT complexes and the biogenesis of multivesicular bodies. Curr Opin Cell Biol *20*, 4-11.

Hurley, J.H., and Emr, S.D. (2006). The ESCRT complexes: structure and mechanism of a membrane-trafficking network. Annu Rev Biophys Biomol Struct *35*, 277-298.

Ikari, A., Takiguchi, A., Atomi, K., Sato, T., and Sugatani, J. (2011). Decrease in claudin-2 expression enhances cell migration in renal epithelial Madin-Darby canine kidney cells. J Cell Physiol *226*, 1471-1478.

Ikari, A., Takiguchi, A., Atomi, K., and Sugatani, J. (2010). Epidermal growth factor increases clathrin-dependent endocytosis and degradation of claudin-2 protein in MDCK II cells. J Cell Physiol.

Ikeda, H., and Kerppola, T.K. (2008). Lysosomal localization of ubiquitinated Jun requires multiple determinants in a lysine-27-linked polyubiquitin conjugate. Mol Biol Cell *19*, 4588-4601.

Ikenouchi, J., Furuse, M., Furuse, K., Sasaki, H., and Tsukita, S. (2005). Tricellulin constitutes a novel barrier at tricellular contacts of epithelial cells. J Cell Biol *171*, 939-945.

Ikenouchi, J., Sasaki, H., Tsukita, S., and Furuse, M. (2008). Loss of occludin affects tricellular localization of tricellulin. Mol Biol Cell *19*, 4687-4693.

Im, Y.J., Wollert, T., Boura, E., and Hurley, J.H. (2009). Structure and function of the ESCRT-II-III interface in multivesicular body biogenesis. Dev Cell *17*, 234-243.

Ireton, R.C., Davis, M.A., van Hengel, J., Mariner, D.J., Barnes, K., Thoreson, M.A., Anastasiadis, P.Z., Matrisian, L., Bundy, L.M., Sealy, L., Gilbert, B., van Roy, F., and Reynolds, A.B. (2002). A novel role for p120 catenin in E-cadherin function. J Cell Biol *159*, 465-476.

Ivanov, A.I., Nusrat, A., and Parkos, C.A. (2005). Endocytosis of the apical junctional complex: mechanisms and possible roles in regulation of epithelial barriers. Bioessays *27*, 356-365.

Jeanes, A., Smutny, M., Leerberg, J.M., and Yap, A.S. (2009). Phosphatidylinositol 3'-kinase signalling supports cell height in established epithelial monolayers. J Mol Histol *40*, 395-405.

Jekely, G., and Rorth, P. (2003). Hrs mediates downregulation of multiple signalling receptors in Drosophila. EMBO Rep *4*, 1163-1168.

Kallay, L.M., McNickle, A., Brennwald, P.J., Hubbard, A.L., and Braiterman, L.T. (2006). Scribble associates with two polarity proteins, Lgl2 and Vangl2, via distinct molecular domains. J Cell Biochem *99*, 647-664.

Karp, C.M., Tan, T.T., Mathew, R., Nelson, D., Mukherjee, C., Degenhardt, K., Karantza-Wadsworth, V., and White, E. (2008). Role of the polarity determinant crumbs in suppressing mammalian epithelial tumor progression. Cancer Res *68*, 4105-4115.

Katzmann, D.J., Stefan, C.J., Babst, M., and Emr, S.D. (2003). Vps27 recruits ESCRT machinery to endosomes during MVB sorting. J Cell Biol *162*, 413-423.

Kessenbrock, K., Plaks, V., and Werb, Z. (2010). Matrix metalloproteinases: regulators of the tumor microenvironment. Cell *141*, 52-67.

Kim, E.K., and Choi, E.J. (2010). Pathological roles of MAPK signaling pathways in human diseases. Biochim Biophys Acta *1802*, 396-405.

King, K.L., and Cidlowski, J.A. (1998). Cell cycle regulation and apoptosis. Annu Rev Physiol *60*, 601-617.

Klein, G., Langegger, M., Timpl, R., and Ekblom, P. (1988). Role of laminin A chain in the development of epithelial cell polarity. Cell *55*, 331-341.

Knight, A., Hughson, E., Hopkins, C.R., and Cutler, D.F. (1995). Membrane protein trafficking through the common apical endosome compartment of polarized Caco-2 cells. Mol Biol Cell *6*, 597-610.

Knust, E., and Bossinger, O. (2002). Composition and formation of intercellular junctions in epithelial cells. Science *298*, 1955-1959.

Kobielak, A., and Fuchs, E. (2004). Alpha-catenin: at the junction of intercellular adhesion and actin dynamics. Nat Rev Mol Cell Biol *5*, 614-625.

Kohler, K., and Zahraoui, A. (2005). Tight junction: a co-ordinator of cell signalling and membrane trafficking. Biol Cell *97*, 659-665.

Kopfstein, L., and Christofori, G. (2006). Metastasis: cell-autonomous mechanisms versus contributions by the tumor microenvironment. Cell Mol Life Sci *63*, 449-468.

Kostelansky, M.S., Schluter, C., Tam, Y.Y., Lee, S., Ghirlando, R., Beach, B., Conibear, E., and Hurley, J.H. (2007). Molecular architecture and functional model of the complete yeast ESCRT-I heterotetramer. Cell *129*, 485-498.

Kouklis, P.D., Hutton, E., and Fuchs, E. (1994). Making a connection: direct binding between keratin intermediate filaments and desmosomal proteins. J Cell Biol *127*, 1049-1060.

Krahn, M.P., Buckers, J., Kastrup, L., and Wodarz, A. (2010). Formation of a Bazooka-Stardust complex is essential for plasma membrane polarity in epithelia. J Cell Biol *190*, 751-760.

Kramer, F., White, K., Kubbies, M., Swisshelm, K., and Weber, B.H. (2000). Genomic organization of claudin-1 and its assessment in hereditary and sporadic breast cancer. Hum Genet *107*, 249-256.

Krause, G., Winkler, L., Mueller, S.L., Haseloff, R.F., Piontek, J., and Blasig, I.E. (2008). Structure and function of claudins. Biochim Biophys Acta *1778*, 631-645.

Kroemer, G., Galluzzi, L., and Brenner, C. (2007). Mitochondrial membrane permeabilization in cell death. Physiol Rev *87*, 99-163.

Kuphal, S., Wallner, S., Schimanski, C.C., Bataille, F., Hofer, P., Strand, S., Strand, D., and Bosserhoff, A.K. (2006). Expression of Hugl-1 is strongly reduced in malignant melanoma. Oncogene *25*, 103-110.

Lal-Nag, M., and Morin, P.J. (2009). The claudins. Genome Biol *10*, 235.

Laprise, P., Chailler, P., Houde, M., Beaulieu, J.F., Boucher, M.J., and Rivard, N. (2002). Phosphatidylinositol 3-kinase controls human intestinal epithelial cell differentiation by promoting adherens junction assembly and p38 MAPK activation. J Biol Chem *277*, 8226-8234.

Lata, S., Roessle, M., Solomons, J., Jamin, M., Gottlinger, H.G., Svergun, D.I., and Weissenhorn, W. (2008a). Structural basis for autoinhibition of ESCRT-III CHMP3. J Mol Biol *378*, 818-827.

Lata, S., Schoehn, G., Jain, A., Pires, R., Piehler, J., Gottlinger, H.G., and Weissenhorn, W. (2008b). Helical structures of ESCRT-III are disassembled by VPS4. Science *321*, 1354-1357.

Lata, S., Schoehn, G., Solomons, J., Pires, R., Gottlinger, H.G., and Weissenhorn, W. (2009). Structure and function of ESCRT-III. Biochem Soc Trans *37*, 156-160.

Le, T.L., Yap, A.S., and Stow, J.L. (1999). Recycling of E-cadherin: a potential mechanism for regulating cadherin dynamics. J Cell Biol *146*, 219-232.

Lee, J.G., and Kay, E.P. (2006). FGF-2-induced wound healing in corneal endothelial cells requires Cdc42 activation and Rho inactivation through the phosphatidylinositol 3-kinase pathway. Invest Ophthalmol Vis Sci *47*, 1376-1386.

Lee, M.P., and Feinberg, A.P. (1997). Aberrant splicing but not mutations of TSG101 in human breast cancer. Cancer Res *57*, 3131-3134.

Lemmers, C., Michel, D., Lane-Guermonprez, L., Delgrossi, M.H., Medina, E., Arsanto, J.P., and Le Bivic, A. (2004). CRB3 binds directly to Par6 and regulates the morphogenesis of the tight junctions in mammalian epithelial cells. Mol Biol Cell *15*, 1324-1333.

Li, J., Belogortseva, N., Porter, D., and Park, M. (2008). Chmp1A functions as a novel tumor suppressor gene in human embryonic kidney and ductal pancreatic tumor cells. Cell Cycle *7*, 2886-2893.

Li, L., and Cohen, S.N. (1996). Tsg101: a novel tumor susceptibility gene isolated by controlled homozygous functional knockout of allelic loci in mammalian cells. Cell *85*, 319-329.

Li, L., Li, X., Francke, U., and Cohen, S.N. (1997). The TSG101 tumor susceptibility gene is located in chromosome 11 band p15 and is mutated in human breast cancer. Cell *88*, 143-154.

Lisovsky, M., Dresser, K., Baker, S., Fisher, A., Woda, B., Banner, B., and Lauwers, G.Y. (2009). Cell polarity protein Lgl2 is lost or aberrantly localized in gastric dysplasia and adenocarcinoma: an immunohistochemical study. Mod Pathol *22*, 977-984.

Liu, R.T., Huang, C.C., You, H.L., Chou, F.F., Hu, C.C., Chao, F.P., Chen, C.M., and Cheng, J.T. (2002). Overexpression of tumor susceptibility gene TSG101 in human papillary thyroid carcinomas. Oncogene *21*, 4830-4837.

Lloyd, T.E., Atkinson, R., Wu, M.N., Zhou, Y., Pennetta, G., and Bellen, H.J. (2002). Hrs regulates endosome membrane invagination and tyrosine kinase receptor signaling in Drosophila. Cell *108*, 261-269.

Lobert, V.H., Brech, A., Pedersen, N.M., Wesche, J., Oppelt, A., Malerod, L., and Stenmark, H. (2010). Ubiquitination of alpha 5 beta 1 integrin controls fibroblast migration through lysosomal degradation of fibronectin-integrin complexes. Dev Cell *19*, 148-159.

Lobert, V.H., and Stenmark, H. (2011). Cell polarity and migration: emerging role for the endosomal sorting machinery. Physiology (Bethesda) *26*, 171-180.

Lowe, S.W., Cepero, E., and Evan, G. (2004). Intrinsic tumour suppression. Nature *432*, 307-315.

Lu, H., and Bilder, D. (2005). Endocytic control of epithelial polarity and proliferation in Drosophila. Nat Cell Biol *7*, 1232-1239.

Lu, Q., Hope, L.W., Brasch, M., Reinhard, C., and Cohen, S.N. (2003). TSG101 interaction with HRS mediates endosomal trafficking and receptor down-regulation. Proc Natl Acad Sci U S A *100*, 7626-7631.

Malerod, L., Stuffers, S., Brech, A., and Stenmark, H. (2007). Vps22/EAP30 in ESCRT-II mediates endosomal sorting of growth factor and chemokine receptors destined for lysosomal degradation. Traffic *8*, 1617-1629.

Mariano, C., Sasaki, H., Brites, D., and Brito, M.A. (2011). A look at tricellulin and its role in tight junction formation and maintenance. Eur J Cell Biol *90*, 787-796.

Martin, T.A., Mansel, R.E., and Jiang, W.G. (2010). Loss of occludin leads to the progression of human breast cancer. Int J Mol Med *26*, 723-734.

Martin-Belmonte, F., Gassama, A., Datta, A., Yu, W., Rescher, U., Gerke, V., and Mostov, K. (2007). PTEN-mediated apical segregation of phosphoinositides controls epithelial morphogenesis through Cdc42. Cell *128*, 383-397.

Martin-Belmonte, F., and Mostov, K. (2008). Regulation of cell polarity during epithelial morphogenesis. Curr Opin Cell Biol *20*, 227-234.

Martin-Belmonte, F., Yu, W., Rodriguez-Fraticelli, A.E., Ewald, A.J., Werb, Z., Alonso, M.A., and Mostov, K. (2008). Cell-polarity dynamics controls the mechanism of lumen formation in epithelial morphogenesis. Curr Biol *18*, 507-513.

Martinou, J.C., and Youle, R.J. (2011). Mitochondria in apoptosis: Bcl-2 family members and mitochondrial dynamics. Dev Cell *21*, 92-101.

Marzesco, A.M., Dunia, I., Pandjaitan, R., Recouvreur, M., Dauzonne, D., Benedetti, E.L., Louvard, D., and Zahraoui, A. (2002). The small GTPase Rab13 regulates assembly of functional tight junctions in epithelial cells. Mol Biol Cell *13*, 1819-1831.

Matlin, K.S., Haus, B., and Zuk, A. (2003). Integrins in epithelial cell polarity: using antibodies to analyze adhesive function and morphogenesis. Methods *30*, 235-246.

Matsuda, M., Kubo, A., Furuse, M., and Tsukita, S. (2004). A peculiar internalization of claudins, tight junction-specific adhesion molecules, during the intercellular movement of epithelial cells. J Cell Sci *117*, 1247-1257.

Matter, K., and Balda, M.S. (2007). Epithelial tight junctions, gene expression and nucleo-junctional interplay. J Cell Sci *120*, 1505-1511.

McCullough, J., Row, P.E., Lorenzo, O., Doherty, M., Beynon, R., Clague, M.J., and Urbe, S. (2006). Activation of the endosome-associated ubiquitin isopeptidase AMSH by STAM, a component of the multivesicular body-sorting machinery. Curr Biol *16*, 160-165.

McDonald, B., and Martin-Serrano, J. (2008) Regulation of Tsg101 expression by the steadiness box: a role of Tsg101-associated ligase. Mol Biol Cell *19,* 754-763.

Mellman, I., and Nelson, W.J. (2008). Coordinated protein sorting, targeting and distribution in polarized cells. Nat Rev Mol Cell Biol *9*, 833-845.

Meng, R.D., Shelton, C.C., Li, Y.M., Qin, L.X., Notterman, D., Paty, P.B., and Schwartz, G.K. (2009). gamma-Secretase inhibitors abrogate oxaliplatin-induced activation of the Notch-1 signaling pathway in colon cancer cells resulting in enhanced chemosensitivity. Cancer Res *69*, 573-582.

Mineta, K., Yamamoto, Y., Yamazaki, Y., Tanaka, H., Tada, Y., Saito, K., Tamura, A., Igarashi, M., Endo, T., Takeuchi, K., and Tsukita, S. (2011). Predicted expansion of the claudin multigene family. FEBS Lett *585*, 606-612.

Miyamori, H., Takino, T., Kobayashi, Y., Tokai, H., Itoh, Y., Seiki, M., and Sato, H. (2001). Claudin promotes activation of pro-matrix metalloproteinase-2 mediated by membrane-type matrix metalloproteinases. J Biol Chem *276*, 28204-28211.

Miyoshi, J., and Takai, Y. (2005). Molecular perspective on tight-junction assembly and epithelial polarity. Adv Drug Deliv Rev *57*, 815-855.

Mizushima, N., Levine, B., Cuervo, A.M., and Klionsky, D.J. (2008). Autophagy fights disease through cellular self-digestion. Nature *451*, 1069-1075.

Moberg, K.H., Schelble, S., Burdick, S.K., and Hariharan, I.K. (2005). Mutations in erupted, the Drosophila ortholog of mammalian tumor susceptibility gene 101, elicit non-cell-autonomous overgrowth. Dev Cell *9*, 699-710.

Morais-de-Sa, E., Mirouse, V., and St Johnston, D. (2010). aPKC phosphorylation of Bazooka defines the apical/lateral border in Drosophila epithelial cells. Cell *141*, 509-523.

Morimoto, S., Nishimura, N., Terai, T., Manabe, S., Yamamoto, Y., Shinahara, W., Miyake, H., Tashiro, S., Shimada, M., and Sasaki, T. (2005). Rab13 mediates the continuous endocytic recycling of occludin to the cell surface. J Biol Chem *280*, 2220-2228.

Morin, P.J. (2005). Claudin proteins in human cancer: promising new targets for diagnosis and therapy. Cancer Res *65*, 9603-9606.

Morita, E., Sandrin, V., Chung, H.Y., Morham, S.G., Gygi, S.P., Rodesch, C.K., and Sundquist, W.I. (2007). Human ESCRT and ALIX proteins interact with proteins of the midbody and function in cytokinesis. EMBO J *26*, 4215-4227.

Morrison, H.A., Dionne, H., Rusten, T.E., Brech, A., Fisher, W.W., Pfeiffer, B.D., Celniker, S.E., Stenmark, H., and Bilder, D. (2008). Regulation of early endosomal entry by the Drosophila tumor suppressors Rabenosyn and Vps45. Mol Biol Cell *19*, 4167-4176.

Mukherjee, S., Ghosh, R.N., and Maxfield, F.R. (1997). Endocytosis. Physiol Rev *77*, 759-803.

Muller, H.A. (2000). Genetic control of epithelial cell polarity: lessons from Drosophila. Dev Dyn *218*, 52-67.

Murata, M., Kojima, T., Yamamoto, T., Go, M., Takano, K., Osanai, M., Chiba, H., and Sawada, N. (2005). Down-regulation of survival signaling through MAPK and Akt in occludin-deficient mouse hepatocytes in vitro. Exp Cell Res *310*, 140-151.

Murphy, L.O., and Blenis, J. (2006). MAPK signal specificity: the right place at the right time. Trends Biochem Sci *31*, 268-275.

Muto, S., Hata, M., Taniguchi, J., Tsuruoka, S., Moriwaki, K., Saitou, M., Furuse, K., Sasaki, H., Fujimura, A., Imai, M., Kusano, E., Tsukita, S., and Furuse, M. (2010). Claudin-2-deficient mice are defective in the leaky and cation-selective paracellular permeability properties of renal proximal tubules. Proc Natl Acad Sci U S A *107*, 8011-8016.

Nakagawa, S., Maeda, S., and Tsukihara, T. (2010). Structural and functional studies of gap junction channels. Curr Opin Struct Biol *20*, 423-430.

Nakagawa, S., Yano, T., Nakagawa, K., Takizawa, S., Suzuki, Y., Yasugi, T., Huibregtse, J.M., and Taketani, Y. (2004). Analysis of the expression and localisation of a LAP protein, human scribble, in the normal and neoplastic epithelium of uterine cervix. Br J Cancer *90*, 194-199.

Nakayama, Y., Shivas, J.M., Poole, D.S., Squirrell, J.M., Kulkoski, J.M., Schleede, J.B., and Skop, A.R. (2009). Dynamin participates in the maintenance of anterior polarity in the Caenorhabditis elegans embryo. Dev Cell *16*, 889-900.

Nara, A., Mizushima, N., Yamamoto, A., Kabeya, Y., Ohsumi, Y., and Yoshimori, T. (2002). SKD1 AAA ATPase-dependent endosomal transport is involved in autolysosome formation. Cell Struct Funct *27*, 29-37.

Nejsum, L.N., and Nelson, W.J. (2007). A molecular mechanism directly linking E-cadherin adhesion to initiation of epithelial cell surface polarity. J Cell Biol *178*, 323-335.

Nelson, P.J., and Daniel, T.O. (2002). Emerging targets: molecular mechanisms of cell contact-mediated growth control. Kidney Int *61*, S99-105.

Niessen, C.M., and Gottardi, C.J. (2008). Molecular components of the adherens junction. Biochim Biophys Acta *1778*, 562-571.

Nievers, M.G., Schaapveld, R.Q., and Sonnenberg, A. (1999). Biology and function of hemidesmosomes. Matrix Biol *18*, 5-17.

Nitta, T., Hata, M., Gotoh, S., Seo, Y., Sasaki, H., Hashimoto, N., Furuse, M., and Tsukita, S. (2003). Size-selective loosening of the blood-brain barrier in claudin-5-deficient mice. J Cell Biol *161*, 653-660.

Normanno, N., De Luca, A., Bianco, C., Strizzi, L., Mancino, M., Maiello, M.R., Carotenuto, A., De Feo, G., Caponigro, F., and Salomon, D.S. (2006). Epidermal growth factor receptor (EGFR) signaling in cancer. Gene *366*, 2-16.

Oberst, A., Bender, C., and Green, D.R. (2008). Living with death: the evolution of the mitochondrial pathway of apoptosis in animals. Cell Death Differ *15*, 1139-1146.

O'Boyle, J.D., Proctor, M.L., Fong, K.M., Lin, W.M., Miller, D.S., and Muller, C.Y. (1999). Role of TSG101 in uterine cervix cancer. Gynecol Oncol *75*, 401-405.

O'Brien, L.E., Zegers, M.M., and Mostov, K.E. (2002). Opinion: Building epithelial architecture: insights from three-dimensional culture models. Nat Rev Mol Cell Biol *3*, 531-537.

Oh, K.B., Stanton, M.J., West, W.W., Todd, G.L., and Wagner, K.U. (2007). Tsg101 is upregulated in a subset of invasive human breast cancers and its targeted overexpression in transgenic mice reveals weak oncogenic properties for mammary cancer initiation. Oncogene *26*, 5950-5959.

Oh, Y., Proctor, M.L., Fan, Y.H., Su, L.K., Hong, W.K., Fong, K.M., Sekido, Y.S., Gazdar, A.F., Minna, J.D., and Mao, L. (1998). TSG101 is not mutated in lung cancer but a shortened transcript is frequently expressed in small cell lung cancer. Oncogene *17*, 1141-1148.

Ojakian, G.K., and Schwimmer, R. (1994). Regulation of epithelial cell surface polarity reversal by beta 1 integrins. J Cell Sci *107 ( Pt 3)*, 561-576.

Ola, M.S., Nawaz, M., and Ahsan, H. (2011). Role of Bcl-2 family proteins and caspases in the regulation of apoptosis. Mol Cell Biochem *351*, 41-58.

Oliveira, S.S., and Morgado-Diaz, J.A. (2007). Claudins: multifunctional players in epithelial tight junctions and their role in cancer. Cell Mol Life Sci *64*, 17-28.

Oliveira, S.S., Oliveira, I.M., De Souza, W., and Morgado-Diaz, J.A. (2005). Claudins upregulation in human colorectal cancer. FEBS Lett *579*, 6179-6185.

Osanai, M., Murata, M., Chiba, H., Kojima, T., and Sawada, N. (2007). Epigenetic silencing of claudin-6 promotes anchorage-independent growth of breast carcinoma cells. Cancer Sci *98*, 1557-1562.

Ozawa, M., Ringwald, M., and Kemler, R. (1990). Uvomorulin-catenin complex formation is regulated by a specific domain in the cytoplasmic region of the cell adhesion molecule. Proc Natl Acad Sci U S A *87*, 4246-4250.

Paez, J.G., Janne, P.A., Lee, J.C., Tracy, S., Greulich, H., Gabriel, S., Herman, P., Kaye, F.J., Lindeman, N., Boggon, T.J., Naoki, K., Sasaki, H., Fujii, Y., Eck, M.J.,

Sellers, W.R., Johnson, B.E., and Meyerson, M. (2004). EGFR mutations in lung cancer: correlation with clinical response to gefitinib therapy. Science *304*, 1497-1500.

Pasternak, S.H., Bagshaw, R.D., Guiral, M., Zhang, S., Ackerley, C.A., Pak, B.J., Callahan, J.W., and Mahuran, D.J. (2003). Presenilin-1, nicastrin, amyloid precursor protein, and gamma-secretase activity are co-localized in the lysosomal membrane. J Biol Chem *278*, 26687-26694.

Perl, A.K., Wilgenbus, P., Dahl, U., Semb, H., and Christofori, G. (1998). A causal role for E-cadherin in the transition from adenoma to carcinoma. Nature *392*, 190-193.

Pettigrew, C.A., and Cotter, T.G. (2009). Deregulation of cell death (apoptosis): implications for tumor development. Discov Med *8*, 61-63.

Pornillos, O., Alam, S.L., Rich, R.L., Myszka, D.G., Davis, D.R., and Sundquist, W.I. (2002). Structure and functional interactions of the Tsg101 UEV domain. EMBO J *21* 2397-2406.

Raiborg, C., Malerod, L., Pedersen, N.M., and Stenmark, H. (2008). Differential functions of Hrs and ESCRT proteins in endocytic membrane trafficking. Exp Cell Res *314*, 801-813.

Raiborg, C., and Stenmark, H. (2009). The ESCRT machinery in endosomal sorting of ubiquitylated membrane proteins. Nature *458*, 445-452.

Raiborg, C., Wesche, J., Malerod, L., and Stenmark, H. (2006). Flat clathrin coats on endosomes mediate degradative protein sorting by scaffolding Hrs in dynamic microdomains. J Cell Sci *119*, 2414-2424.

Raleigh, D.R., Marchiando, A.M., Zhang, Y., Shen, L., Sasaki, H., Wang, Y., Long, M., and Turner, J.R. (2010). Tight junction-associated MARVEL proteins marveld3, tricellulin, and occludin have distinct but overlapping functions. Mol Biol Cell *21*, 1200-1213.

Raymond, C.K., Howald-Stevenson, I., Vater, C.A., and Stevens, T.H. (1992). Morphological classification of the yeast vacuolar protein sorting mutants: evidence for a prevacuolar compartment in class E vps mutants. Mol Biol Cell *3*, 1389-1402.

Razi, M., and Futter, C.E. (2006). Distinct roles for Tsg101 and Hrs in multivesicular body formation and inward vesiculation. Mol Biol Cell *17*, 3469-3483.

Reedijk, M., Odorcic, S., Chang, L., Zhang, H., Miller, N., McCready, D.R., Lockwood, G., and Egan, S.E. (2005). High-level coexpression of JAG1 and NOTCH1 is observed in human breast cancer and is associated with poor overall survival. Cancer Res *65*, 8530-8537.

Regala, R.P., Weems, C., Jamieson, L., Khoor, A., Edell, E.S., Lohse, C.M., and Fields, A.P. (2005). Atypical protein kinase C iota is an oncogene in human non-small cell lung cancer. Cancer Res *65*, 8905-8911.

Rehder, D., Iden, S., Nasdala, I., Wegener, J., Brickwedde, M.K., Vestweber, D., and Ebnet, K. (2006). Junctional adhesion molecule-a participates in the formation of apico-basal polarity through different domains. Exp Cell Res *312*, 3389-3403.

Resnick, M.B., Konkin, T., Routhier, J., Sabo, E., and Pricolo, V.E. (2005). Claudin-1 is a strong prognostic indicator in stage II colonic cancer: a tissue microarray study. Mod Pathol *18*, 511-518.

Riazuddin, S., Ahmed, Z.M., Fanning, A.S., Lagziel, A., Kitajiri, S., Ramzan, K., Khan, S.N., Chattaraj, P., Friedman, P.L., Anderson, J.M., Belyantseva, I.A., Forge, A., and Friedman, T.B. (2006). Tricellulin is a tight-junction protein necessary for hearing. Am J Hum Genet *79*, 1040-1051.

Rodahl, L.M., Haglund, K., Sem-Jacobsen, C., Wendler, F., Vincent, J.P., Lindmo, K., Rusten, T.E., and Stenmark, H. (2009b). Disruption of Vps4 and JNK function in Drosophila causes tumour growth. PLoS One *4*, e4354.

Rodahl, L.M., Stuffers, S., Lobert, V.H., and Stenmark, H. (2009a). The role of ESCRT proteins in attenuation of cell signalling. Biochem Soc Trans *37*, 137-142.

Roh, M.H., Fan, S., Liu, C.J., and Margolis, B. (2003). The Crumbs3-Pals1 complex participates in the establishment of polarity in mammalian epithelial cells. J Cell Sci *116*, 2895-2906.

Row, P.E., Liu, H., Hayes, S., Welchman, R., Charalabous, P., Hofmann, K., Clague, M.J., Sanderson, C.M., and Urbe, S. (2007). The MIT domain of UBPY constitutes a CHMP binding and endosomal localization signal required for efficient epidermal growth factor receptor degradation. J Biol Chem *282*, 30929-30937.

Roxrud, I., Stenmark, H., and Malerod, L. (2010). ESCRT & Co. Biol Cell *102*, 293-318.

Roy, M., Pear, W.S., and Aster, J.C. (2007). The multifaceted role of Notch in cancer. Curr Opin Genet Dev *17*, 52-59.

Ruland, J., Sirard, C., Elia, A., MacPherson, D., Wakeham, A., Li, L., de la Pompa, J.L., Cohen, S.N., and Mak, T.W. (2001). p53 accumulation, defective cell proliferation, and early embryonic lethality in mice lacking tsg101. Proc Natl Acad Sci U S A *98*, 1859-1864.

Russ, P.K., Pino, C.J., Williams, C.S., Bader, D.M., Haselton, F.R., and Chang, M.S. (2011) Bves modulates tight junction associated signalling. PLoS ONE *6,* 4563.

Rusten, T.E., and Stenmark, H. (2009). How do ESCRT proteins control autophagy? J Cell Sci *122*, 2179-2183.

Rusten, T.E., Vaccari, T., Lindmo, K., Rodahl, L.M., Nezis, I.P., Sem-Jacobsen, C., Wendler, F., Vincent, J.P., Brech, A., Bilder, D., and Stenmark, H. (2007). ESCRTs and Fab1 regulate distinct steps of autophagy. Curr Biol *17*, 1817-1825.

Saitou, M., Furuse, M., Sasaki, H., Schulzke, J.D., Fromm, M., Takano, H., Noda, T., and Tsukita, S. (2000). Complex phenotype of mice lacking occludin, a component of tight junction strands. Mol Biol Cell *11*, 4131-4142.

Sakakibara, A., Furuse, M., Saitou, M., Ando-Akatsuka, Y., and Tsukita, S. (1997). Possible involvement of phosphorylation of occludin in tight junction formation. J Cell Biol *137*, 1393-1401.

Sakata, T., Sakaguchi, H., Tsuda, L., Higashitani, A., Aigaki, T., Matsuno, K., and Hayashi, S. (2004). Drosophila Nedd4 regulates endocytosis of notch and suppresses its ligand-independent activation. Curr Biol *14*, 2228-2236.

Saksena, S., Wahlman, J., Teis, D., Johnson, A.E., and Emr, S.D. (2009). Functional reconstitution of ESCRT-III assembly and disassembly. Cell *136*, 97-109.

Sambuy, Y., De Angelis, I., Ranaldi, G., Scarino, M.L., Stammati, A., and Zucco, F. (2005). The Caco-2 cell line as a model of the intestinal barrier: influence of cell and culture-related factors on Caco-2 cell functional characteristics. Cell Biol Toxicol *21*, 1-26.

Sandy, P., Ventura, A., and Jacks, T. (2005). Mammalian RNAi: a practical guide. Biotechniques *39*, 215-224.

Schimanski, C.C., Schmitz, G., Kashyap, A., Bosserhoff, A.K., Bataille, F., Schafer, S.C., Lehr, H.A., Berger, M.R., Galle, P.R., Strand, S., and Strand, D. (2005). Reduced expression of Hugl-1, the human homologue of Drosophila tumour suppressor gene lgl, contributes to progression of colorectal cancer. Oncogene *24*, 3100-3109.

Schluter, M.A., and Margolis, B. (2009). Apical lumen formation in renal epithelia. J Am Soc Nephrol *20*, 1444-1452.

Schluter, M.A., Pfarr, C.S., Pieczynski, J., Whiteman, E.L., Hurd, T.W., Fan, S., Liu, C.J., and Margolis, B. (2009). Trafficking of Crumbs3 during cytokinesis is crucial for lumen formation. Mol Biol Cell *20*, 4652-4663.

Schoenenberger, C.A., Zuk, A., Kendall, D., and Matlin, K.S. (1991). Multilayering and loss of apical polarity in MDCK cells transformed with viral K-ras. J Cell Biol *112*, 873-889.

Schoenenberger, C.A., Zuk, A., Zinkl, G.M., Kendall, D., and Matlin, K.S. (1994). Integrin expression and localization in normal MDCK cells and transformed MDCK cells lacking apical polarity. J Cell Sci *107 ( Pt 2)*, 527-541.

Shan, G. (2010). RNA interference as a gene knockdown technique. Int J Biochem Cell Biol *42*, 1243-1251.

Shen, L., and Turner, J.R. (2008). Intercellular junctions: actin the PARt. Curr Biol *18*, R1014-1017.

Shin, K., Fogg, V.C., and Margolis, B. (2006). Tight junctions and cell polarity. Annu Rev Cell Dev Biol *22*, 207-235.

Shin, K., Straight, S., and Margolis, B. (2005). PATJ regulates tight junction formation and polarity in mammalian epithelial cells. J Cell Biol *168*, 705-711.

Shivas, J.M., Morrison, H.A., Bilder, D., and Skop, A.R. (2010). Polarity and endocytosis: reciprocal regulation. Trends Cell Biol *20*, 445-452.

Simpson, C.D., Anyiwe, K., and Schimmer, A.D. (2008). Anoikis resistance and tumor metastasis. Cancer Lett *272*, 177-185.

Singh, A.B., and Harris, R.C. (2004). Epidermal growth factor receptor activation differentially regulates claudin expression and enhances transepithelial resistance in Madin-Darby canine kidney cells. J Biol Chem *279*, 3543-3552.

Smith, E.A., and Fuchs, E. (1998). Defining the interactions between intermediate filaments and desmosomes. J Cell Biol *141*, 1229-1241.

Sorkin, A., and von Zastrow, M. (2009). Endocytosis and signalling: intertwining molecular networks. Nat Rev Mol Cell Biol *10*, 609-622.

Sorokin, L., Sonnenberg, A., Aumailley, M., Timpl, R., and Ekblom, P. (1990). Recognition of the laminin E8 cell-binding site by an integrin possessing the alpha 6 subunit is essential for epithelial polarization in developing kidney tubules. J Cell Biol *111*, 1265-1273.

Staehelin, L.A. (1973). Further observations on the fine structure of freeze-cleaved tight junctions. J Cell Sci *13*, 763-786.

Steed, E., Balda, M.S., and Matter, K. (2010). Dynamics and functions of tight junctions. Trends Cell Biol *20*, 142-149.

Steed, E., Rodrigues, N.T., Balda, M.S., and Matter, K. (2009). Identification of MarvelD3 as a tight junction-associated transmembrane protein of the occludin family. BMC Cell Biol *10*, 95.

Steller, H. (2008). Regulation of apoptosis in Drosophila. Cell Death Differ *15*, 1132-1138.

Stevenson, B.R., Siliciano, J.D., Mooseker, M.S., and Goodenough, D.A. (1986). Identification of ZO-1: a high molecular weight polypeptide associated with the tight junction (zonula occludens) in a variety of epithelia. J Cell Biol *103*, 755-766.

Straight, S.W., Shin, K., Fogg, V.C., Fan, S., Liu, C.J., Roh, M., and Margolis, B. (2004). Loss of PALS1 expression leads to tight junction and polarity defects. Mol Biol Cell *15*, 1981-1990.

Stuffers, S., Brech, A., and Stenmark, H. (2009a). ESCRT proteins in physiology and disease. Exp Cell Res *315*, 1619-1626.

Stuffers, S., Sem Wegner, C., Stenmark, H., and Brech, A. (2009b). Multivesicular endosome biogenesis in the absence of ESCRTs. Traffic *10*, 925-937.

Stutzmann, J., Bellissent-Waydelich, A., Fontao, L., Launay, J.F., and Simon-Assmann, P. (2000). Adhesion complexes implicated in intestinal epithelial cell-matrix interactions. Microsc Res Tech *51*, 179-190.

Suzuki, A., Ishiyama, C., Hashiba, K., Shimizu, M., Ebnet, K., and Ohno, S. (2002). aPKC kinase activity is required for the asymmetric differentiation of the premature junctional complex during epithelial cell polarization. J Cell Sci *115*, 3565-3573.

Suzuki, A., and Ohno, S. (2006). The PAR-aPKC system: lessons in polarity. J Cell Sci *119*, 979-987.

Suzuki, A., Yamanaka, T., Hirose, T., Manabe, N., Mizuno, K., Shimizu, M., Akimoto, K., Izumi, Y., Ohnishi, T., and Ohno, S. (2001). Atypical protein kinase C is involved in the evolutionarily conserved par protein complex and plays a critical role in establishing epithelia-specific junctional structures. J Cell Biol *152*, 1183-1196.

Tachibana, K., Nakanishi, H., Mandai, K., Ozaki, K., Ikeda, W., Yamamoto, Y., Nagafuchi, A., Tsukita, S., and Takai, Y. (2000). Two cell adhesion molecules, nectin and cadherin, interact through their cytoplasmic domain-associated proteins. J Cell Biol *150*, 1161-1176.

Taelman, V.F., Dobrowolski, R., Plouhinec, J.L., Fuentealba, L.C., Vorwald, P.P., Gumper, I., Sabatini, D.D., and De Robertis, E.M. (2010). Wnt signaling requires sequestration of glycogen synthase kinase 3 inside multivesicular endosomes. Cell *143*, 1136-1148.

Takahashi, K., Nakanishi, H., Miyahara, M., Mandai, K., Satoh, K., Satoh, A., Nishioka, H., Aoki, J., Nomoto, A., Mizoguchi, A., and Takai, Y. (1999). Nectin/PRR: an immunoglobulin-like cell adhesion molecule recruited to cadherin-based adherens

junctions through interaction with Afadin, a PDZ domain-containing protein. J Cell Biol *145*, 539-549.

Takahashi, S., Iwamoto, N., Sasaki, H., Ohashi, M., Oda, Y., Tsukita, S., and Furuse, M. (2009). The E3 ubiquitin ligase LNX1p80 promotes the removal of claudins from tight junctions in MDCK cells. J Cell Sci *122*, 985-994.

Takehara, M., Nishimura, T., Mima, S., Hoshino, T., and Mizushima, T. (2009). Effect of claudin expression on paracellular permeability, migration and invasion of colonic cancer cells. Biol Pharm Bull *32*, 825-831.

Tamai, K., Tanaka, N., Nara, A., Yamamoto, A., Nakagawa, I., Yoshimori, T., Ueno, Y., Shimosegawa, T., and Sugamura, K. (2007). Role of Hrs in maturation of autophagosomes in mammalian cells. Biochem Biophys Res Commun *360*, 721-727.

Tanaka, N., Kyuuma, M., and Sugamura, K. (2008). Endosomal sorting complex required for transport proteins in cancer pathogenesis, vesicular transport, and non-endosomal functions. Cancer Sci *99*, 1293-1303.

Teis, D., Saksena, S., and Emr, S.D. (2008). Ordered assembly of the ESCRT-III complex on endosomes is required to sequester cargo during MVB formation. Dev Cell *15*, 578-589.

Teo, H., Gill, D.J., Sun, J., Perisic, O., Veprintsev, D.B., Vallis, Y., Emr, S.D., and Williams, R.L. (2006). ESCRT-I core and ESCRT-II GLUE domain structures reveal role for GLUE in linking to ESCRT-I and membranes. Cell *125*, 99-111.

Terry, S.J., Zihni, C., Elbediwy, A., Vitiello, E., Leefa Chong San, I.V., Balda, M.S., and Matter, K. (2011). Spatially restricted activation of RhoA signalling at epithelial junctions by p114RhoGEF drives junction formation and morphogenesis. Nat Cell Biol *13*, 159-166.

Theos, A.C., Truschel, S.T., Tenza, D., Hurbain, I., Harper, D.C., Berson, J.F., Thomas, P.C., Raposo, G., and Marks, M.S. (2006). A lumenal domain-dependent pathway for sorting to intralumenal vesicles of multivesicular endosomes involved in organelle morphogenesis. Dev Cell *10*, 343-354.

Thompson, A., Nessler, R., Wisco, D., Anderson, E., Winckler, B., and Sheff, D. (2007). Recycling endosomes of polarized epithelial cells actively sort apical and basolateral cargos into separate subdomains. Mol Biol Cell *18*, 2687-2697.

Thompson, B.J., Mathieu, J., Sung, H.H., Loeser, E., Rorth, P., and Cohen, S.M. (2005). Tumor suppressor properties of the ESCRT-II complex component Vps25 in Drosophila. Dev Cell *9*, 711-720.

Tokes, A.M., Kulka, J., Paku, S., Szik, A., Paska, C., Novak, P.K., Szilak, L., Kiss, A., Bogi, K., and Schaff, Z. (2005). Claudin-1, -3 and -4 proteins and mRNA expression in benign and malignant breast lesions: a research study. Breast Cancer Res *7*, R296-305.

Torkko, J.M., Manninen, A., Schuck, S., and Simons, K. (2008). Depletion of apical transport proteins perturbs epithelial cyst formation and ciliogenesis. J Cell Sci *121*, 1193-1203.

Toyoshima, M., Tanaka, N., Aoki, J., Tanaka, Y., Murata, K., Kyuuma, M., Kobayashi, H., Ishii, N., Yaegashi, N., and Sugamura, K. (2007). Inhibition of tumor growth and metastasis by depletion of vesicular sorting protein Hrs: its regulatory role on E-cadherin and beta-catenin. Cancer Res *67*, 5162-5171.

Trajkovic, K., Hsu, C., Chiantia, S., Rajendran, L., Wenzel, D., Wieland, F., Schwille, P., Brugger, B., and Simons, M. (2008). Ceramide triggers budding of exosome vesicles into multivesicular endosomes. Science *319*, 1244-1247.

Traweger, A., Fang, D., Liu, Y.C., Stelzhammer, W., Krizbai, I.A., Fresser, F., Bauer, H.C., and Bauer, H. (2002). The tight junction-specific protein occludin is a functional target of the E3 ubiquitin-protein ligase itch. J Biol Chem *277*, 10201-10208.

Treier, M., Staszewski, L.M., and Bohmann, D. (1994). Ubiquitin-dependent c-Jun degradation in vivo is mediated by the delta domain. Cell *78*, 787-798.

Tsuiki, H., Tnani, M., Okamoto, I., Kenyon, L.C., Emlet, D.R., Holgado-Madruga, M., Lanham, I.S., Joynes, C.J., Vo, K.T., and Wong, A.J. (2003). Constitutively active forms of c-Jun NH2-terminal kinase are expressed in primary glial tumors. Cancer Res *63*, 250-255.

Turksen, K., and Troy, T.C. (2011). Junctions gone bad: claudins and loss of the barrier in cancer. Biochim Biophys Acta *1816*, 73-79.

Umeda, K., Ikenouchi, J., Katahira-Tayama, S., Furuse, K., Sasaki, H., Nakayama, M., Matsui, T., Tsukita, S., and Furuse, M. (2006). ZO-1 and ZO-2 independently determine where claudins are polymerized in tight-junction strand formation. Cell *126*, 741-754.

Urbe, S., Sachse, M., Row, P.E., Preisinger, C., Barr, F.A., Strous, G., Klumperman, J., and Clague, M.J. (2003). The UIM domain of Hrs couples receptor sorting to vesicle formation. J Cell Sci *116*, 4169-4179.

Vaccari, T., and Bilder, D. (2005). The Drosophila tumor suppressor vps25 prevents nonautonomous overproliferation by regulating notch trafficking. Dev Cell *9*, 687-698.

Vaccari, T., and Bilder, D. (2009). At the crossroads of polarity, proliferation and apoptosis: the use of Drosophila to unravel the multifaceted role of endocytosis in tumor suppression. Mol Oncol *3*, 354-365.

Vaccari, T., Lu, H., Kanwar, R., Fortini, M.E., and Bilder, D. (2008). Endosomal entry regulates Notch receptor activation in Drosophila melanogaster. J Cell Biol *180*, 755-762.

Vaccari, T., Rusten, T.E., Menut, L., Nezis, I.P., Brech, A., Stenmark, H., and Bilder, D. (2009). Comparative analysis of ESCRT-I, ESCRT-II and ESCRT-III function in Drosophila by efficient isolation of ESCRT mutants. J Cell Sci *122*, 2413-2423.

Van Itallie, C.M., and Anderson, J.M. (2006). Claudins and epithelial paracellular transport. Annu Rev Physiol *68*, 403-429.

Volpe, D.A. (2008). Variability in Caco-2 and MDCK cell-based intestinal permeability assays. J Pharm Sci *97*, 712-725.

Wagner, K.U., Krempler, A., Qi, Y., Park, K., Henry, M.D., Triplett, A.A., Riedlinger, G., Rucker, I.E., and Hennighausen, L. (2003). Tsg101 is essential for cell growth, proliferation, and cell survival of embryonic and adult tissues. Mol Cell Biol *23*, 150-162.

Wang, E., Brown, P.S., Aroeti, B., Chapin, S.J., Mostov, K.E., and Dunn, K.W. (2000). Apical and basolateral endocytic pathways of MDCK cells meet in acidic common endosomes distinct from a nearly-neutral apical recycling endosome. Traffic *1*, 480-493.

Weaver, V.M., Lelievre, S., Lakins, J.N., Chrenek, M.A., Jones, J.C., Giancotti, F., Werb, Z., and Bissell, M.J. (2002). beta4 integrin-dependent formation of polarized three-dimensional architecture confers resistance to apoptosis in normal and malignant mammary epithelium. Cancer Cell *2*, 205-216.

Wegner, C.S., Rodahl, L.M., and Stenmark, H. (2011). ESCRT proteins and cell signalling. Traffic *12*, 1291-1297.

Weisz, O.A., and Rodriguez-Boulan, E. (2009). Apical trafficking in epithelial cells: signals, clusters and motors. J Cell Sci *122*, 4253-4266.

Weston, C.R., and Davis, R.J. (2002). The JNK signal transduction pathway. Curr Opin Genet Dev *12*, 14-21.

Wiley, H.S., and Burke, P.M. (2001). Regulation of receptor tyrosine kinase signaling by endocytic trafficking. Traffic *2*, 12-18.

Williams, R.L., and Urbe, S. (2007). The emerging shape of the ESCRT machinery. Nat Rev Mol Cell Biol *8*, 355-368.

Witcher, L.L., Collins, R., Puttagunta, S., Mechanic, S.E., Munson, M., Gumbiner, B., and Cowin, P. (1996). Desmosomal cadherin binding domains of plakoglobin. J Biol Chem *271*, 10904-10909.

Wittinger, M., Vanhara, P., El-Gazzar, A., Savarese-Brenner, B., Pils, D., Anees, M., Grunt, T.W., Sibilia, M., Holcmann, M., Horvat, R., Schemper, M., Zeillinger, R., Schofer, C., Dolznig, H., Horak, P., and Krainer, M. (2011). hVps37A Status Affects Prognosis and Cetuximab Sensitivity in Ovarian Cancer. Clin Cancer Res *17*, 7816-7827.

Wollert, T., Wunder, C., Lippincott-Schwartz, J., and Hurley, J.H. (2009). Membrane scission by the ESCRT-III complex. Nature *458*, 172-177.

Woodman, P. (2009). ESCRT proteins, endosome organization and mitogenic receptor down-regulation. Biochem Soc Trans *37*, 146-150.

Xu, Z., Liang, L., Wang, H., Li, T., and Zhao, M. (2003). HCRP1, a novel gene that is downregulated in hepatocellular carcinoma, encodes a growth-inhibitory protein. Biochem Biophys Res Commun *311*, 1057-1066.

Yamanaka, T., Horikoshi, Y., Izumi, N., Suzuki, A., Mizuno, K., and Ohno, S. (2006). Lgl mediates apical domain disassembly by suppressing the PAR-3-aPKC-PAR-6 complex to orient apical membrane polarity. J Cell Sci *119*, 2107-2118.

Yang, J., and Weinberg, R.A. (2008). Epithelial-mesenchymal transition: at the crossroads of development and tumor metastasis. Dev Cell *14*, 818-829.

Yin, T., and Green, K.J. (2004). Regulation of desmosome assembly and adhesion. Semin Cell Dev Biol *15*, 665-677.

Yorikawa, C., Shibata, H., Waguri, S., Hatta, K., Horii, M., Katoh, K., Kobayashi, T., Uchiyama, Y., and Maki, M. (2005). Human CHMP6, a myristoylated ESCRT-III protein, interacts directly with an ESCRT-II component EAP20 and regulates endosomal cargo sorting. Biochem J *387*, 17-26.

Yoshimori, T., Yamagata, F., Yamamoto, A., Mizushima, N., Kabeya, Y., Nara, A., Miwako, I., Ohashi, M., Ohsumi, M., and Ohsumi, Y. (2000). The mouse SKD1, a homologue of yeast Vps4p, is required for normal endosomal trafficking and morphology in mammalian cells. Mol Biol Cell *11*, 747-763.

Young, T.W., Rosen, D.G., Mei, F.C., Li, N., Liu, J., Wang, X.F., and Cheng, X. (2007). Up-regulation of tumor susceptibility gene 101 conveys poor prognosis through suppression of p21 expression in ovarian cancer. Clin Cancer Res *13*, 3848-3854.

Yu, A.S., McCarthy, K.M., Francis, S.A., McCormack, J.M., Lai, J., Rogers, R.A., Lynch, R.D., and Schneeberger, E.E. (2005). Knockdown of occludin expression leads to diverse phenotypic alterations in epithelial cells. Am J Physiol Cell Physiol *288*, C1231-1241.

Yu, D., and Turner, J.R. (2008). Stimulus-induced reorganization of tight junction structure: the role of membrane traffic. Biochim Biophys Acta *1778*, 709-716.

Zeng, Q., and Hong, W. (2008). The emerging role of the hippo pathway in cell contact inhibition, organ size control, and cancer development in mammals. Cancer Cell *13*, 188-192.

Zhan, L., Rosenberg, A., Bergami, K.C., Yu, M., Xuan, Z., Jaffe, A.B., Allred, C., and Muthuswamy, S.K. (2008). Deregulation of scribble promotes mammary tumorigenesis and reveals a role for cell polarity in carcinoma. Cell *135*, 865-878.

Zhang, H., Squirrell, J.M., and White, J.G. (2008). RAB-11 permissively regulates spindle alignment by modulating metaphase microtubule dynamics in Caenorhabditis elegans early embryos. Mol Biol Cell *19*, 2553-2565.

Zhu, G., Gilchrist, R., Borley, N., Chng, H.W., Morgan, M., Marshall, J.F., Camplejohn, R.S., Muir, G.H., and Hart, I.R. (2004). Reduction of TSG101 protein has a negative impact on tumor cell growth. Int J Cancer *109*, 541-547.